Compendium of Plant Genomes
Series Editor: Chittaranjan Kole

Takashi Onozaki
Masafumi Yagi *Editors*

The Carnation Genome

Springer

Compendium of Plant Genomes

Series Editor

Chittaranjan Kole, Raja Ramanna Fellow, Government of India, ICAR-National Research Center on Plant Biotechnology, Pusa, New Delhi, India

Whole-genome sequencing is at the cutting edge of life sciences in the new millennium. Since the first genome sequencing of the model plant Arabidopsis thaliana in 2000, whole genomes of about 100 plant species have been sequenced and genome sequences of several other plants are in the pipeline. Research publications on these genome initiatives are scattered on dedicated web sites and in journals with all too brief descriptions. The individual volumes elucidate the background history of the national and international genome initiatives; public and private partners involved; strategies and genomic resources and tools utilized; enumeration on the sequences and their assembly; repetitive sequences; gene annotation and genome duplication. In addition, synteny with other sequences, comparison of gene families and most importantly potential of the genome sequence information for gene pool characterization and genetic improvement of crop plants are described.

Interested in editing a volume on a crop or model plant?
Please contact Prof. C. Kole, Series Editor, at ckoleorg@gmail.com

More information about this series at http://www.springer.com/series/11805

Takashi Onozaki • Masafumi Yagi
Editors

The Carnation Genome

Springer

Editors
Takashi Onozaki
Institute of Vegetable
and Floriculture Science
NARO
Tsukuba, Ibaraki, Japan

Masafumi Yagi
Institute of Vegetable
and Floriculture Science
NARO
Tsukuba, Ibaraki, Japan

ISSN 2199-4781 ISSN 2199-479X (electronic)
Compendium of Plant Genomes
ISBN 978-981-15-8260-8 ISBN 978-981-15-8261-5 (eBook)
https://doi.org/10.1007/978-981-15-8261-5

This Springer imprint is published by the registered company Springer Nature Singapore Pte Ltd.
The registered company address is: 152 Beach Road, #21-01/04 Gateway East, Singapore 189721, Singapore

This book series is dedicated to my wife Phullara and our children Sourav and Devleena

Chittaranjan Kole

Preface to the Series

Genome sequencing has emerged as the leading discipline in the plant sciences coinciding with the start of the new century. For much of the twentieth century, plant geneticists were only successful in delineating putative chromosomal location, function, and changes in genes indirectly through the use of a number of "markers" physically linked to them. These included visible or morphological, cytological, protein, and molecular or DNA markers. Among them, the first DNA marker, the RFLPs, introduced a revolutionary change in plant genetics and breeding in the mid-1980s, mainly because of their infinite number and thus potential to cover maximum chromosomal regions, pheno- typic neutrality, absence of epistasis, and codominant nature. An array of other hybridization-based markers, PCR-based markers, and markers based on both facilitated construction of genetic linkage maps, mapping of genes controlling simply inherited traits, and even gene clusters (QTLs) controlling polygenic traits in a large number of model and crop plants. During this period, a number of new mapping populations beyond F_2 were utilized and a number of computer programs were developed for map construction, mapping of genes, and for mapping of polygenic clusters or QTLs. Molecular markers were also used in the studies of evolution and phylogenetic relationship, genetic diversity, DNA fingerprinting, and map-based cloning. Markers tightly linked to the genes were used in crop improvement employing the so-called marker-assisted selection. These strategies of molecular genetic mapping and molecular breeding made a spectacular impact during the last one and a half decades of the twentieth century. But still they remained "indirect" approaches for elucidation and utilization of plant genomes since much of the chromosomes remained unknown and the complete chemical depiction of them was yet to be unraveled.

Physical mapping of genomes was the obvious consequence that facilitated the development of the "genomic resources" including BAC and YAC libraries to develop physical maps in some plant genomes. Subsequently, integrated genetic–physical maps were also developed in many plants. This led to the concept of structural genomics. Later on, emphasis was laid on EST and transcriptome analysis to decipher the function of the active gene sequences leading to another concept defined as functional genomics. The advent of techniques of bacteriophage gene and DNA sequencing in the 1970s was extended to facilitate sequencing of these genomic resources in the last decade of the twentieth century.

As expected, sequencing of chromosomal regions would have led to too much data to store, characterize, and utilize with the-then available computer software could handle. But the development of information technology made the life of biologists easier by leading to a swift and sweet marriage of biology and informatics, and a new subject was born—bioinformatics.

Thus, the evolution of the concepts, strategies, and tools of sequencing and bioinformatics reinforced the subject of genomics—structural and functional. Today, genome sequencing has traveled much beyond biology and involves biophysics, biochemistry, and bioinformatics!

Thanks to the efforts of both public and private agencies, genome sequencing strategies are evolving very fast, leading to cheaper, quicker, and automated techniques right from clone-by-clone and whole-genome shotgun approaches to a succession of second-generation sequencing methods. The development of software of different generations facilitated this genome sequencing. At the same time, newer concepts and strategies were emerging to handle sequencing of the complex genomes, particularly the polyploids.

It became a reality to chemically—and so directly—define plant genomes, popularly called whole-genome sequencing or simply genome sequencing.

The history of plant genome sequencing will always cite the sequencing of the genome of the model plant Arabidopsis thaliana in 2000 that was followed by sequencing the genome of the crop and model plant rice in 2002. Since then, the number of sequenced genomes of higher plants has been increasing exponentially, mainly due to the development of cheaper and quicker genomic techniques and, most importantly, the development of collaborative platforms such as national and international consortia involving partners from public and/or private agencies.

As I write this preface for the first volume of the new series "Compendium of Plant Genomes," a net search tells me that complete or nearly complete whole-genome sequencing of 45 crop plants, eight crop and model plants, eight model plants, 15 crop progenitors and relatives, and 3 basal plants is accomplished, the majority of which are in the public domain. This means that we nowadays know many of our model and crop plants chemically, i.e., directly, and we may depict them and utilize them precisely better than ever. Genome sequencing has covered all groups of crop plants. Hence, information on the precise depiction of plant genomes and the scope of their utilization are growing rapidly every day. However, the information is scattered in research articles and review papers in journals and dedicated Web pages of the consortia and databases. There is no compilation of plant genomes and the opportunity of using the information in sequence-assisted breeding or further genomic studies. This is the underlying rationale for starting this book series, with each volume dedicated to a particular plant.

Plant genome science has emerged as an important subject in academia, and the present compendium of plant genomes will be highly useful both to students and teaching faculties. Most importantly, research scientists involved in genomics research will have access to systematic deliberations on the plant genomes of their interest. Elucidation of plant genomes is of interest not only for the geneticists and breeders, but also for practitioners of an array of plant science disciplines, such as taxonomy, evolution, cytology,

physiology, pathology, entomology, nematology, crop production, biochemistry, and obviously bioinformatics. It must be mentioned that information regarding each plant genome is ever-growing. The contents of the volumes of this compendium are, therefore, focusing on the basic aspects of the genomes and their utility. They include information on the academic and/or economic importance of the plants, description of their genomes from a molecular genetic and cytogenetic point of view, and the genomic resources developed. Detailed deliberations focus on the background history of the national and international genome initiatives, public and private partners involved, strategies and genomic resources and tools utilized, enumeration on the sequences and their assembly, repetitive sequences, gene annotation, and genome duplication. In addition, synteny with other sequences, comparison of gene families, and, most importantly, the potential of the genome sequence information for gene pool characterization through genotyping by sequencing (GBS) and genetic improvement of crop plants have been described. As expected, there is a lot of variation of these topics in the volumes based on the information available on the crop, model, or reference plants.

I must confess that as the series editor, it has been a daunting task for me to work on such a huge and broad knowledge base that spans so many diverse plant species. However, pioneering scientists with lifetime experience and expertise on the particular crops did excellent jobs editing the respective volumes. I myself have been a small science worker on plant genomes since the mid-1980s and that provided me the opportunity to personally know several stalwarts of plant genomics from all over the globe. Most, if not all, of the volume editors are my longtime friends and colleagues. It has been highly comfortable and enriching for me to work with them on this book series. To be honest, while working on this series I have been and will remain a student first, a science worker second, and a series editor last. And I must express my gratitude to the volume editors and the chapter authors for providing me the opportunity to work with them on this compendium.

I also wish to mention here my thanks and gratitude to the Springer staff, Dr. Christina Eckey and Dr. Jutta Lindenborn in particular, for all their constant and cordial support right from the inception of the idea.

I always had to set aside additional hours to edit books beside my professional and personal commitments—hours I could and should have given to my wife, Phullara, and our kids, Sourav, and Devleena. I must mention that they not only allowed me the freedom to take away those hours from them but also offered their support in the editing job itself. I am really not sure whether my dedication of this compendium to them will suffice to do justice to their sacrifices for the interest of science and the science community.

Kalyani, India Chittaranjan Kole

Preface

Carnation (*Dianthus caryophyllus* L.) is one of the most important ornamental flowers in the world along with chrysanthemum and rose. A very complex hybridization process lies behind the modern carnation cultivars owing to the long history of breeding. The genome of carnation was sequenced by a Japanese research team during the 2013 end. Carnation has been genetically improved over the years and there are various types of flower colors, shapes, patterns, and sizes. The molecular mechanism of anthocyanin synthesis and transposable elements causing the diversity have been well studied. In addition, the breeding and physiological research for improving flower vase life, which is one of the most important traits in ornamentals, have been aggressively carried out in carnation as a model of ethylene susceptible flowers. To improve the selection efficiency, genomic analysis tools including DNA markers and genetic linkage maps have been developed. In carnation, mutant cultivars contributed to the expansion of flower colors and shapes, thus mutation breeding technology such as ion beams irradiation has been developed. Moreover, carnation is a scarce ornamental in which genetic engineering technology has been put into practical use, and the blue-violet genetically modified carnation has been widely distributed in the world. In this book, we summarize the recent progress in carnation genomic research for large-scale transcriptome analysis, draft genome sequence, DNA markers, and genome mapping. We also report the flower color, mutations, flower vase life, interspecific hybridization, fragrance for carnation, and discuss the future prospects in carnation genome researches.

Prof. Chittaranjan Kole, Series Editor of the book series entitled, Compendium of Plant Genomes recommended us to edit a book on *The Carnation Genome* and helped us all along. For publishing this book, we have been supported by Nareshkumar Mani, Praveen Anand, Fumiko Yamaguchi and Yuko Matsumoto of Springer, We are much grateful for the helpful suggestions and encouragements.

Tsukuba, Japan

Takashi Onozaki
Masafumi Yagi

Contents

Contributors

Yutaka Abe Department of Biotechnology and Life Science, Tokyo University of Agriculture and Technology, Koganei, Tokyo, Japan;
Division of Food Additives, Division of Pharmacognosy, Phytochemistry and Narcotics, National Institute of Health Sciences, Kawasaki, Kanagawa, Japan

Steve Chandler School of Applied Sciences, Royal Melbourne Institute of Technology, RMIT University, Bundoora, VIC, Australia

Yoshihiro Hase Takasaki Advanced Radiation Research Institute, National Institutes for Quantum and Radiological Science and Technology (QST), Takasaki, Gunma, Japan

Kaoru Higuchi Department of Biotechnology and Life Science, Tokyo University of Agriculture and Technology, Koganei, Tokyo, Japan

Hideki Hirakawa Facility for Genome Informatics, Kazusa DNA Research Institute, Kisarazu, Chiba, Japan

Makiko Hotta Aichi Agricultural Research Center, Nagakute, Aichi, Japan

Luna Iijima Department of Biotechnology and Life Science, Tokyo University of Agriculture and Technology, Koganei, Tokyo, Japan

Yoshio Itoh Department of Biotechnology and Life Science, Tokyo University of Agriculture and Technology, Koganei, Tokyo, Japan

Kyutaro Kishimoto Institute of Vegetable and Floriculture Science, NARO, Tsukuba, Ibaraki, Japan

Sanae Kishimoto Institute of Vegetable and Floriculture Science, NARO, Tsukuba, Ibaraki, Japan

Yuki Matsuba Department of Biotechnology and Life Science, Tokyo University of Agriculture and Technology, Koganei, Tokyo, Japan;
North American Crop Protection Division, BASF, Durham, NC, USA

Taira Miyahara Department of Biotechnology and Life Science, Tokyo University of Agriculture and Technology, Koganei, Tokyo, Japan; Graduate School of Horticulture, Chiba University, Chiba, Chiba, Japan

Noriko Nakamura Suntory Global Innovation Center Ltd, Soraku-gun, Kyoto, Japan

Masayoshi Nakayama Institute of Vegetable and Floriculture Science, NARO, Tsukuba, Ibaraki, Japan

Yuzo Nishizaki Department of Biotechnology and Life Science, Tokyo University of Agriculture and Technology, Koganei, Tokyo, Japan; Division of Food Additives, Division of Pharmacognosy, Phytochemistry and Narcotics, National Institute of Health Sciences, Kawasaki, Kanagawa, Japan

Mikio Nimura Aichi Agricultural Research Center, Nagakute, Aichi, Japan

Jun Ogata Department of Biotechnology and Life Science, Tokyo University of Agriculture and Technology, Koganei, Tokyo, Japan; Division of Food Additives, Division of Pharmacognosy, Phytochemistry and Narcotics, National Institute of Health Sciences, Kawasaki, Kanagawa, Japan

Akemi Ohmiya Institute of Vegetable and Floriculture Science, NARO, Tsukuba, Ibaraki, Japan

Masachika Okamura Central Laboratories for Key Technologies, Kirin Company, Yokohama, Kanagawa, Japan

Yoshihiro Ozeki Department of Biotechnology and Life Science, Tokyo University of Agriculture and Technology, Koganei, Tokyo, Japan

Nobuhiro Sasaki Department of Biotechnology and Life Science, Tokyo University of Agriculture and Technology, Koganei, Tokyo, Japan; Department of Food and Life Sciences, Toyo University, Ora-gun, Gunma, Japan

Shigeru Satoh Faculty of Agriculture, Ryukoku University, Otsu, Shiga, Japan

Yukiko Shinbo Suntory Global Innovation Center Ltd, Soraku-gun, Kyoto, Japan

Akane Suzuki-Wagner Department of Biotechnology and Life Science, Tokyo University of Agriculture and Technology, Koganei, Tokyo, Japan

Takamasa Suzuki Department of Biological Chemistry, College of Bioscience and Biotechnology, Chubu University, Kasugai, Aichi, Japan

Yoshikazu Tanaka Suntory Global Innovation Center Ltd, Soraku-gun, Kyoto, Japan

Koji Tanase Institute of Vegetable and Floriculture Science, NARO, Tsukuba, Ibaraki, Japan

Takashi Tsujimoto Department of Biotechnology and Life Science, Tokyo University of Agriculture and Technology, Koganei, Tokyo, Japan

Masafumi Yagi Institute of Vegetable and Floriculture Science, NARO, Tsukuba, Ibaraki, Japan

Abbreviations

2,4-PDCA	2,4-pyridinedicarboxylic acid
3-PCA	3-pyridinecarboxylic acid
4CL	4-coumarate:CoA ligase
AA5GT	Acyl-glucose dependent anthocyanin 3-*O*-glucoside 5-glucosyltransferase
AARC	Aichi Agricultural Research Center
ACC	1-aminocyclopropane-1-carboxylate
ACO	ACC oxidase
ACS	ACC synthase
AFLP	Amplified fragment length polymorphism
AHCT	Anthocyanin *O*-hydroxycinnamoyltransferase
ALA	5-aminolevulinic acid
AMalT	Malyl-glucose dependent anthocyanin acyltransferase
ANS	Anthocyanidin synthase
APM	Amiprophos-methyl
AVI	Anthocyanic vacuolar inclusion
BAMT	Benzoic acid carboxyl methyltransferase
BEAT	Benzylalcohol *O*-acetyltransferase
bHLH	Basic helix-loop-helix
BSMT	Benzoic acid/salicylic acid methyltransferase
C4H	Cinnamate 4-hydroxylase
CAO	Chlorophyllide *a* oxygenase
CARACC3	Carnation ACS 3
CARAO1	Carnation ACO 1
CARAS1	Carnation AC*S* 1
CAS	Caffeine synthase
CBW	Carnation bacterial wilt
CCDs	Carotenoid cleavage dioxygenases
cDNA	Complimentary DNA
CHGT	UDP-glucose dependent chalcone glucosyltransferase
CHI	Chalcone isomerase
CHS	Chalcone synthase
CHYB	Carotenoid β-ring hydroxylase
CML37	Calmodulin-like protein 37
COL16	Constans-like 16
CP	Cysteine proteinase

CRTISO	Carotenoid isomerase
CWP	Cerise Westpearl
DAT	Deacetylvindoline 4-*O*-acetultransferase
DB	Database
DD	Differential display
ddRAD-Seq	Double digest restriction site–associated DNA sequencing
DFR	Dihydroflavonol 4-redulctase
DMAPP	Dimethylallyldiphosphate
DREB3	Dehydration-responsive element binding protein 3
EBGs	Early anthocyanin biosynthetic genes
ER	Ethylene receptor
EST	Expressed sequence tag
F3'5'H	Flavonoid 3',5'-hydroxylase
F3H	Flavone 3-hydroxylase
FONS	Fully-open and non-senescent
GA	Gibberellic acid
GGPP	Geranylgeranyl diphosphate
GH1	Glucoside hydrolase family 1
GMO	Genetically modified organism
GO	Gene ontology
GST	Glutathione *S*-transferases
GT1	Family 1 glucosyltransferases
GWAS	Genome-wide association study
HCAR	7-hydroxymethyl-chlorophyll *a* reductase
HCBT	Anthranilate *N*-hydroxycinnamoyl/benzoyltransferase
HPLC	High-performance liquid chromatography
IAMT	Indole acetic acid methyltransferase
InDels	Insertions and deletions
INSDC	International Nucleotide Sequence Database Collaboration
IPI	IPP isomerase
IPP	Isopentenyl diphosphate
JMTs	Jasmonic acid carboxyl methyltransferases
KOG	Eukaryotic Orthologous Groups
LBG	Late biosynthetic gene
LCYB	Lycopene β-cyclase
LCYE	Lycopene ε-cyclase
LG	Linkage group
LOD	Logarithm of odds
LPB	Light Pink Barbara
LR	Left border
LTR	Long terminal repeat
MAS	Marker-assisted selection
MATE	Multidrug and toxic compound extrusion
MEP	Methylerythritol 4-phosphate
MgPMT	Mg-protoporphyrin IX methyltransferase
MP	Mate-pair
MVA	Mevalonate
NARO	National Agriculture and Food Research Organization

NGS	Next-generation sequencer/ next-generation sequencing
NIVFS	Institute of Vegetable and Floriculture Science, NARO
NOL	NYC1-like
NSY	Neoxanthin synthase
NYC1	Non-yellow coloring 1
ODS	Octadecylsilane
OMT	*O*-methyl transferase
ORF	Open reading frame
PAL1	Phenylalanine ammonia-lyase 1
PaO	Pheophorbide *a* oxygenase
PDCA	Pyridinedicarboxylic acid
PDS	Phytoene desaturase
PE	Paired-end
PGDBj	Plant Genome Database of Japan
PPH	Pheophytinase
PSY	Phytoene synthase
PYP1	Pale yellow petal 1
QTL	Quantitative trait locus
RAD	Restriction site–associated DNA
RAD-seq	RAD-sequencing
RAPD	Random amplified polymorphic DNA
RB	Right border
RCC	Red chlorophyll catabolite
RCCR	RCC reductase
RFLP	Restriction fragment length polymorphism
RNA-i	RNA-interference
RNA-seq	RNA-sequence
ROS	Reactive oxygen species
SAGE	Serial analysis of gene expression
SAM	*S*-adenosyl-l-methionine
SAMT	Salicylic acid carboxyl methyltransferase
SAT	1-*O*-sinapoyl-β-glucose:anthocyanin sinapoyltransferase
SCPL	Serine carboxypeptidase-like
SE	Single-end
SGR	*Stay-green*
SMT	1-*O*-sinapoyl-β-glucose:L-malate sinapoyltransferase
SNP	Single nucleotide polymorphism
SR	Senescence-related
SS1	Sucrose synthase 1
SSH	Suppression subtractive hybridization
SSR	Simple-sequence repeat
SST	1-*O*-sinapoyl-β-glucose:1-*O*-sinapoyl-β-glucose sinapoyltransferase
STP4	Sugar transport protein 4
STS	Sequence-tagged site
STS	Silver thiosulfate
SVs	Structural variants
T-DNA	Transfer-DNA

TE	Transposable element
THC	Tetrahydroxychalcone
TLC	Thin-layer chromatography
TPM	Transcripts per million
UA3GT	UDP-glucose dependent anthocyanin 3-O-glucosyltransferase
UGT	UDP-glucose dependent glycosyltransferase
VDE	Violaxanthin de-epoxidase
XES	Xanthophyll esterase
XET	Xyloglucan endotransglucosylase
XG	Xyloglucan
XGO	Xyloglucan oligosaccharide
XTH	Xyloglucan endotransglucosylase/hydrolase
ZDS	ζ-carotene desaturase
ZEP	Zeaxanthin epoxidase
Z-ISO	ζ-carotene isomerase

Draft Genome Sequence

1

Hideki Hirakawa

Abstract

The genome sequences of various kinds of plant species, such as cereals, vegetables, fruits, and flowers, have been determined. The genome sequence of carnation (*Dianthus caryophyllus*) cultivar 'Francesco' was first determined as a floricultural crop using next-generation sequencing data obtained by Illumina HiSeq and 454 GS FLX+ platforms. The genome size of the carnation was estimated as 638.7 Mb. The draft genome sequence DCA_r1.0 was determined by a combination of three kinds of *de novo* assemblers. The total and N50 lengths of the draft genome sequence were 568,887,315 bp and 60,737 bp, respectively. Of 56,382 transcripts identified by the gene prediction, 43,491 were determined to be genes without transposable elements. The genes were annotated by similarity searches against the UniProtKB/TrEMBL, TAIR10, and RAP-DB databases and by domain searches against the InterPro database. The genes were mapped onto the KEGG pathways and classified into gene ontology (GO) groups and EuKaryotic Orthologous Groups (KOG) of proteins. The genome data are available from the Carnation DB (https://plant1.kazusa.or.jp/carnation/). The 496 DNA markers of carnation, including 491 SSR markers, have been released from the Plant Genome DataBase Japan (PGDBj) (http://pgdbj.jp). As genome data and DNA markers accumulate, studies of the molecular genetics of carnation would be promoted, and molecular breeding would be made more effective.

1.1 Introduction

The genome sequence of *Arabidopsis thaliana* was first determined in 2000 as a model plant by an international collaboration (Arabidopsis Genome Initiative 2000). After that, the genome sequences of plant species were determined for rice (*Oryza sativa*) in 2002 (International Rice Genome Sequencing Project 2005), poplar (*Populus trichocarpa*) in 2006 (Tuskan et al. 2006), *Lotus japonicus* in 2006 (Sato et al. 2008), and so on. These genome sequences were determined by using a Sanger sequencer, such as ABI3730xl (Applied Biosystems, Foster City, CA, USA). In 2009, the genome sequence of cucumber (*Cucumis sativus*) (Huang et al. 2009) was determined by a combination of Sanger and Illumina platforms (Illumina) known as Next-Generation Sequencers (NGSs). The genome sequence of wild strawberry (*Fragaria vesca*) was determined by a combination of Sanger, 454,

H. Hirakawa (✉)
Facility for Genome Informatics, Kazusa DNA Research Institute, 2-6-7 Kazusakamatari, Kisarazu 292-0818, Chiba, Japan
e-mail: hh@kazusa.or.jp

T. Onozaki and M. Yagi (eds.), *The Carnation Genome*, Compendium of Plant Genomes,
https://doi.org/10.1007/978-981-15-8261-5_1

and Illumina sequencers (Roche Diagnostics, Basel, Switzerland). In 2014, the genome sequence of carnation (*Dianthus caryophyllus*) cultivar 'Francesco' was first determined as a floricultural crop using 454 and Illumina sequencers (Yagi et al. 2014b). The 'Francesco' is a red Mediterranean standard-type cultivar, which is a leading cultivar in Japan. Carnation has a diploid genome structure and 30 chromosomes (2n = 2x = 30). According to the C-value database (https://cvalues.science.kew.org/search), the genome size of *D. caryophyllus* cultivar 'Master' is estimated as 686 Mb. The genome sequencing of *D. caryophyllus* was performed to understand its genetic systems and to apply them to molecular breeding. In this section, a study of the genome sequencing of carnation performed in 2014 is described. The sequencing of the chloroplast of carnation was also conducted by two other research groups, and their works are described here. Finally, the databases related to carnation are described.

1.2 Genome Assembly of Carnation

1.2.1 Genome Sequencing

The genome sequence of cultivar 'Francesco' was determined by Yagi et al. (2014a). The single-end (SE) reads (accession: DRX012628, total reads: 5.9 M, total length: 3.9 Gb, average length: 663 bases), and paired-end (PE) reads with 4 kb insert size (DRX012629, total reads: 1.3 M, total length: 589 Mb, average length: 436 bases) were sequenced by a 454 GS FLX+ sequencer (Roche Diagnostics). The PE reads with insert sizes 180 bp (DRX012624, total reads: 763.2 M, total length: 152.6 Gb) and 500 bp (DRX012625, total reads: 638.7 M, total length: 127.7 Gb) and MP reads with insert sizes 3 kb (DRX012626, total reads: 221.3 M, total length: 44.3 Gb) and 5 kb (DRX012627, total reads: 237.7 M, total length: 47.5 Gb) were sequenced by a HiSeq 1000 platform (Illumina). These obtained reads were applied to the *de novo* genome assembly.

1.2.2 Estimation of Genome Size

The heterozygosity of the 'Francesco' genome was investigated based on the *k*-mer frequency analysis using the Illumina PE reads with insert size 500 bp. The *k*-mer frequency obtained using the PE reads by Jellyfish (Marçais and Kingsford 2011) is shown in Fig. 1.1. There are two clear peaks, indicating that the heterozygosity of the genome sequence of 'Francesco' is high. The genome size was estimated as 638.7 Mb with a multiplicity of 168 of the *k*-mer frequency plot. The heterozygosity rate was calculated as 1.12% by GenomeScope (Vurture et al. 2017).

1.2.3 Genome Assembly

The *de novo* genome assembly of 'Francesco' was conducted using the whole-genome shotgun reads sequenced by the combination of 454 GS FLX+ (Roche Diagnostics) and Illumina HiSeq 1000 platforms (Illumina). The strategy of the genome assembly is shown in Fig. 1.2. The '454 reads' sequenced by the 454 GS FLX+ platform were assembled *de novo* by Newbler 2.6 (Roche Diagnostics), and the resultant contigs were called '454 contigs'. The total and N50 lengths of the '454-contigs' were 384 Mb and 2.6 kb, respectively. The Illumina 'PE reads' with insert size 500 bp were assembled *de novo* by SOAPdenovo2 v2.23 (Li et al. 2010), and 'SOAP-contigs' were constructed. The total and N50 lengths of the 'SOAP-contigs' were 283 Mb and 1.6 kb, respectively. In parallel, the 'PE reads' were assembled by FERMI v1.1 (Li 2012), and the resultant contigs were called 'FERMI-contigs'. The total and N50 lengths of FERMI-contigs were 334 Mb and 2.1 kb, respectively. The 'PE reads' with insert size 180 bp were connected at both ends of the reads to construct the overlapping fragments (OFs). The OFs, PE reads with insert size 500 bp, and MP reads with insert sizes 3 and 5 kb were applied to the *de novo* assembly by ALLPATHS-LG v45879 (Gnerre et al. 2011), and the resultant contigs were called 'ALLPATHS-scafs'. The

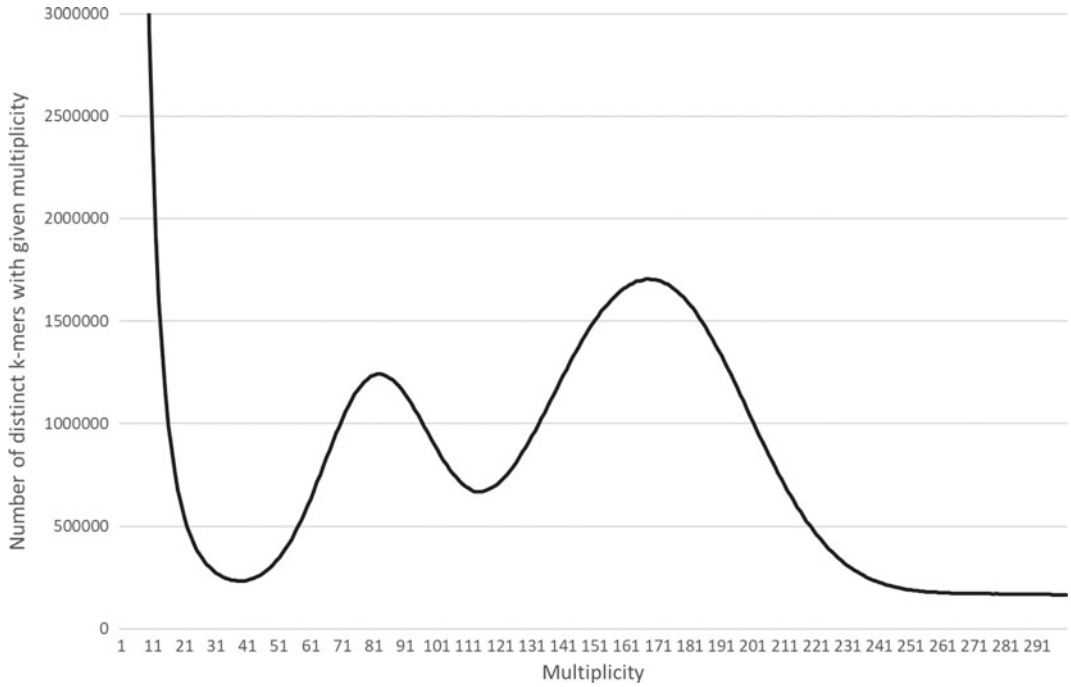

Fig. 1.1 *K*-mer frequency distribution plot of the carnation cultivar 'Francesco'. The *k*-mer distribution was calculated by Jellyfish with *k*-mer size 17

total and N50 lengths of the 'ALLPATHS-scafs' were 369 Mb and 69.7 kb, respectively. The '454-contigs', 'SOAP-contigs', and 'FERMI-contigs' that were 500 bp or longer were merged by GAM-NGS (Vicedomini et al. 2013), and the resultant contigs were called 'Merged-contigs'. The 'Merged-contigs' and 'ALLPATHS-scafs' $\geq$ 500 bp were further merged by excluding the redundant sequences, and the resultant sequences were called 'Merged ALLPATHS-scafs'. The 'Merged ALLPATHS-scafs' were connected by the MP reads using SSPACE v2.0 (Boetzer et al. 2011), and 'Super-scaffolds' were constructed. The gaps in the 'Super-scaffolds' were closed using the PE reads by GapCloser (https://soap.genomics.org.cn). Finally, the scaffolds longer than 200 bp were selected as a draft sequence, DCA_r1.0.

The statistics of the genome sequences are summarized in Table 1.1. The 89,083 contigs and 16,350 scaffolds are available from GenBank under accession numbers BAUD01000001-BAUD01089083 and DF340864-DF357213, respectively (BioProject ID: PRJDB1491). The 16,350 scaffolds consisted of 60,345 contigs. The 45,088 scaffolds including the 16,350 scaffolds and 28,738 contigs were selected and named DCA_r1.0. The total and N50 lengths of the DCA_r1.0 were 568,887,315 bp and 60,737 bp, respectively. The maximum length of DCA_r1.0 was 1,287,144 bp, and the G+C content was 36.4%. These sequence data are available from the 'Carnation DB' described in Sect. 1.3.

The completeness of the DCA_r1.0 was confirmed by using CEGMA v2.4 (Parra et al. 2007) and BUSCO v3.0.2 (Seppey et al. 2019). Of the 248 core eukaryotic genes defined by CEGMA, 96% were found in DCA_r1.0. The BUSCO analysis revealed that 96.3% (single-copy (S): 71.1%, duplicated (D): 25.2%) of the 1,375 BUSCOs (Embryophyta dataset in odb10) were conserved

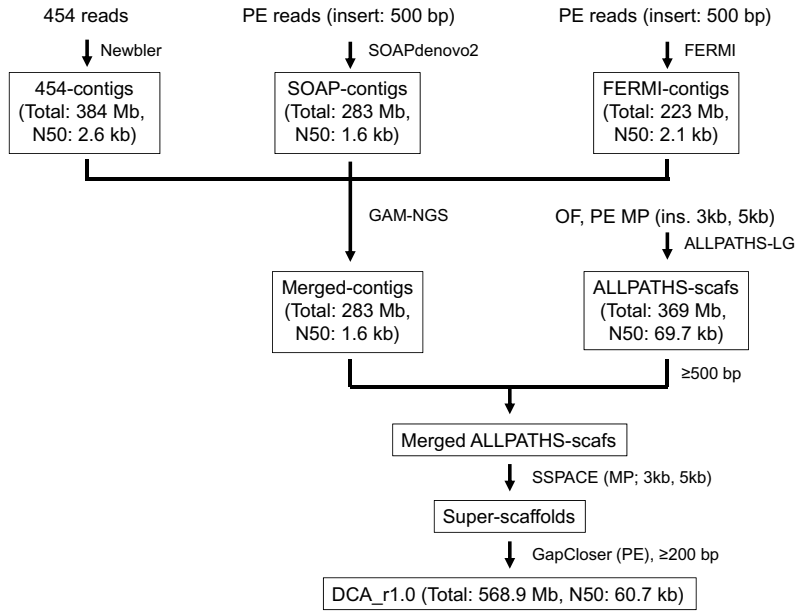

Fig. 1.2 Strategy for *de novo* genome assembly. Initially, the *de novo* genome assemblers, Newbler, SOAPdenovo2, FERMI, and ALLPATHS-LG were applied. The '454-contigs', 'SOAP-contigs', 'FERMI-contigs' were merged. The 'Merged-contigs' and 'ALLPATHS-scafs' were further merged. The 'Merged ALLPATHS-LG' were connected by SSPACE using the mate-pairs. The gaps in the 'Super-scaffolds' were closed by GapCloser. Finally, DCA_r1.0 was constructed

completely (complete (C)), 0.8% were fragmented (F), and 2.9% were missing (M).

1.2.4 Repetitive Sequences

The repetitive sequences in DCA_r1.0 were searched in two steps. First, the repetitive sequences were searched by RepeatScout v1.0.5 (Price et al. 2005) and Piler v1.0 (Edgar and Myers 2005). The repetitive sequences were searched against the Swiss-Prot database (https://www.uniprot.org) by BLASTX, and the sequences having similarities were excluded as coding genes. Next, the resultant repetitive sequences detected by RepeatScout and the known repetitive sequences registered in Repbase (Jurka 1998) were identified by RepeatMasker (https://www.repeatmasker.org). The percentages of interspersed repeats classified into LTR, LINE, and SINE in class I were 7.3%, 0.7%, and 0.01%, respectively, and the percentage of DNA elements placed in class II was 0.9%. The percentage of unclassified repeats was 20.0%. In total, the repetitive sequences accounted for 33% of the DCA_r1.0. Comparison of the repetitive sequences among carnation, *Arabidopsis thaliana*, *Brassica rapa*, potato, tomato, cotton, soybean, sweet orange, rice, foxtail millet, and sorghum revealed that the percentage of LTR was lowest in carnation. The percentages of unclassified repetitive elements were higher among these plant species.

1.2.5 Gene Prediction

The cDNA sequences obtained by Sanger (FY382825-FY405424) and 454 GS FLX + platforms (FX296474-FX334317) were mapped onto DCA_r1.0, and the genes were predicted by using PASA ver. R20130605p1 (Haas et al. 2003). The 300 genes containing complete coding regions predicted by PASA were applied to construct a training set used for *ab initio* prediction using Augustus v2.7 (Keller et al. 2011).

Table 1.1 Statistics of the genome and gene sequences of carnation cultivar 'Francesco'

		GenBank		Carnation genome database		
		Genome		Genome	CDS	
		Cotings (BAUD01000001-BAUD01089083)	Scaffolds (DF340864-DF357213)	DCA_r1.0	DCA_r1.0_cds	DCA_r1.0_cds (woTE)
Total	Number of sequences	89,083	16,350	45,088	56,382	43,491
	Total length (bases)	500,258,142	513,619,466	568,887,315	65.687,037	47,801,775
	Average length (bases)	5,616	31,414	12,617	1,165	1,099
	Max length (bases)	363,056	1,287,144	1,287,144	15,186	15,186
	Min length (bases)	20	1,106	200	9	9
	N50 length (bases)	16,727	70,988	60,737	1,491	1,422
	A	159,495,405	142,468,238	159,496,650	17,799,166	12,808,174
	T	158,834,741	141,881,165	158,835,938	17,253,266	12,649,964
	G	90,863,546	80,889,614	90,864,080	16,593,632	12,185,728
	C	91,047,352	80,961,618	91,047,826	14,034,370	10,154,633
	n	0	0	18,154,037	0	0
	N	17,098	67,418,831	50,488,784	6,603	3,276
	Others	0	0	0	0	0
	G+C%	36.4	36.3	36.4	46.6	46.7
≥ 500b	Number of sequences	85,190	16,350	45,059	44,853	33,397
	Total length (bases)	499,422,881	513,619,466	568,873,924	61,608,654	44,249,070
	Average length (bases)	5,862	31,414	12,625	1,374	1,325
≥ 1 kb	Number of sequences	63,980	13,637	30,716	26,864	19,378
	Total length (bases)	488,722,870	513,619,466	558,517,605	48,328,851	33,965,673
	Average length (bases)	7,561	16,350	18,183	1,799	1,753
≥ 5 kb	Number of sequences	22,801	13,637	15,363	276	200
	Total length (bases)	393,679,258	503,954,037	526,383,760	1,728,363	1,279,416
	Average length (bases)	17,266	36,955	34,263	6,262	6,397

The cDNA sequences were also mapped by using BLAT v34 (Kent 2002) to generate a hint file used for Augustus. As a result, 10,519 and 99,418 transcripts were respectively predicted by PASA and Augustus, and they were merged into 56,382 transcripts. Of these, 42,047 transcripts had significant similarities to the UniProtKB/TrEMBL database (https://www.uniprot.org), and 12,871 transcripts had similarities to transposable elements (TEs). Next the predicted transcripts consisting of a single exon were excluded. Finally, 43,266 protein-coding genes were selected. The BUSCO v3 analysis of the 43,491 transcripts were C: 86.7% (S: 65.8%, D: 20.9%), F: 5.3%, M: 8.0%. On the other hand, 1050, 13, 92, and 143 genes for tRNA, rRNA, snoRNA, and miRNA were respectively identified in DCA_r1.0 (Yagi et al. 2014a).

1.2.6 Gene Annotation

As described above, the predicted genes were searched against the protein sequences of the UniProtKB/TrEMBL database (https://www.uniprot.org). In addition, the genes were searched against the protein sequences of *Arabidopsis* and rice, respectively, obtained from TAIR10 (https://www.arabidopsis.org) and RAP-DB (https://rapdb.dna.affrc.go.jp). The domain searches were conducted against InterPro (https://www.ebi.ac.uk/interpro/) using InterProScan (Jones et al. 2014). These functional annotations can be browsed at the Carnation DB described in Sect. 1.3.1. The genes were classified into KOG (NCBI's EuKaryotic Orthologous Groups of proteins) (Tatusov et al. 2003) and compared among carnation, *A. thaliana*, and *O. sativa*. In carnation, the genes classified into KOG Q (secondary metabolites biosynthesis, transport, and catabolism) were relatively high. The genes were mapped onto Gene Ontology (GO) (https://geneontology.org) using GOslim (https://www.geneontology.org/page/go-slim-and-subset-guide) and compared among carnation, *A. thaliana*, and *O. sativa*. In carnation, the genes classified into 'nucleobase, nucleotide and nucleic acid metabolic process (Biological Process; BP)', 'cell wall (Cellular Component; CC)', and 'transferase activity (Molecular Function; MF)' were relatively high in number. The genes were mapped onto the KEGG metabolic pathways (https://www.genome.jp/kegg/pathway.html) by BLAST searches against the GENES database (https://www.genome.jp/kegg/genes.html) with an E-value cutoff of 1E-10, length coverage $\geq 25\%$, and identity $\geq 50\%$. The genes on the KEGG pathways were compared among carnation, *B. vulgaris* (sugar beet), *A. thaliana*, and *O. sativa*, revealing that the pathways mapped only in carnation were 'Pentose phosphate pathway', 'Galactose metabolism', 'Ether lipid metabolism', 'Alanine, aspartate and glutamate metabolism', 'Glycine, serine and threonine metabolism', 'Cysteine and methionine metabolism', 'Metabolism of xenobiotics by cytochrome P450′, and others. In the paper related to the genome sequencing of carnation, the genes related to 'phenylpropanoid biosynthesis pathway', 'betalain synthesis', 'chlorophyll & carotenoid synthesis', 'disease resistance', 'ethylene metabolism', 'carbohydrate metabolism & cell wall modification during flower opening', and 'floral scent' were listed (Yagi et al. 2014a).

1.3 Complete Chloroplast Genome Sequences

The chloroplast genome sequences of carnation were determined in 2018 (Chen et al. 2018) and 2019 (Li et al. 2019a). Chloroplast genome sequences are widely used for genetic engineering or the development of molecular markers and for the improvement of industrial applications. In this section, the chloroplast genome sequences reported by two other groups are described.

1.3.1 Cultivar Developed at Central South University of Forestry and Technology

The chloroplast genome sequence of carnation was determined by Chen et al. (2018). The cultivar was planted in the experimental yard of Central South University of Forestry and Technology (Changsha, China). The Illumina PE reads sequenced by the HiSeq 2500 platform (Illumina) were assembled by SPAdes v3.9.0 (Bankevich et al. 2012). The length of the genome sequence was 147,604 bp. The genome sequence was released under accession number NC_039650.1 (BioProject: PRJNA496193). The genome sequence encodes 83 genes, and the total length is 77,487 bp. Ten protein-coding genes (*rps16*, *atpF*, *rpoC1*, *petB*, *petD*, *rpl16*, *ndhB*, *ndhA*, *ycf1*, *ndhB*) were applied to phylogenetic analysis among 22 plant species classified into 14 genera (*Akebia*, *Allium*, *Mesembryanthemum*, *Portulaca*, *Talinum*, *Cistanthe*, *Chenopodium*, *Haloxylon*, *Bienertia*, *Salicornia*, *Colobanthus*, *Dianthus*, *Silene*, *Lychnis*), and the authors indicated that carnation (*D. callyophyllus*) was close to *D. longicalyx*.

1.3.2 Cultivar 'Francesco'

The chloroplast genome sequence of the cultivar 'Francesco' was determined by Li et al. (2019a). The Illumina PE reads obtained from NCBI (Accession: DRR014087) were trimmed and mapped onto the complete chloroplast genome sequence of *D. longicalyx* (KM668208.1 (total length: 149,539 bp)) by using CLC Genomics Workbench v7.01 (https://www.clcbio.com) and Ray v2.3.1 (Boisvert et al. 2010). The length of the chloroplast genome sequence of 'Francesco' is 149,595 bp. The genome sequence encodes 112 unique genes including 78 protein-coding, 4 tRNA, and 30 tRNA genes.

1.4 Databases

1.4.1 Carnation DB

The genome data of cultivar 'Francesco' was released from the Carnation DB (https://plant1.kazusa.or.jp/carnation/). The top page of the database is shown in Fig. 1.3. The navigation bar on that page has four tabs: HOME, BLAST, LIST, and DOWNLOAD. On the HOME page, keyword searches against the top hits of the BLAST searches against UniProtKB/TrEMBL, TAIR10 (*Arabidopsis*), and RAP-DB (rice) are available. Users can extract a sequence by inputting the start and end positions from the draft genome sequence (DCA_r1.0). The sequence can be converted into reverse complement. On the BLAST page, BLAST searches against DCA_r1.0, repetitive sequences, gene sequences, gene sequences excluding transposable elements (TEs), translated gene sequences, and translated genes excluding transposable elements are available. On the LIST page, the functional annotation of the genes, the number of exons, gene id, the top hits against UniProtKB/TrEMBL, TAIR10, and RAP-DB, repetitive sequences, gene sequences, translated gene sequences, and draft genome sequences (DCA_r1.0) are available. On the DOWNLOAD page, the manual of this database, draft genome sequence (DCA_r1.0), gene sets (nucleotide genes, translated genes, annotations of TEs, BLAST search results against TAIR10 and RAP-DB), noncoding RNAs (miRNA, rRNA, snoRNA, tRNA), and repetitive sequences (fasta file, repeat list) are available.

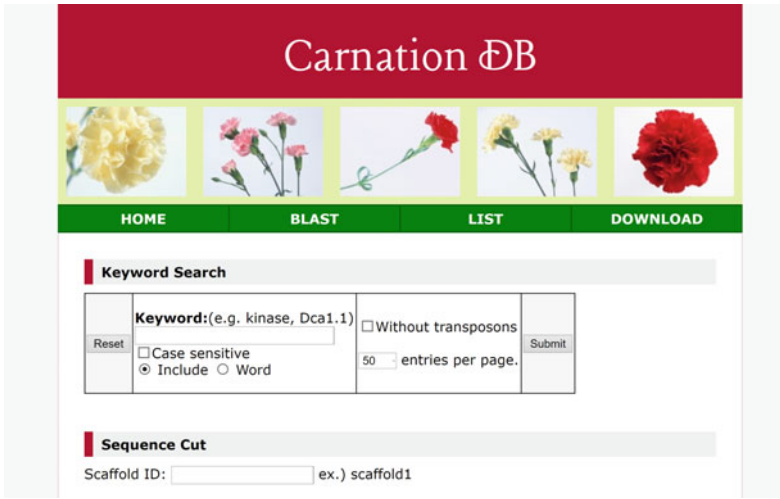

Fig. 1.3 Top page of the Carnation DB

1.4.2 Plant Genome Database of Japan (PGDBj)

Thus far, the genome sequences of approximately 400 kinds of plant genome sequences have been released. The genome data have been published from public databases such as GenBank/EMBL/DDBJ or from databases released from research groups. Therefore, many databases are widely distributed and thus difficult to search for. To solve this problem, an integrated database, the Plant Genome Database of Japan (PGDBj) (http://pgdbj.jp) was established at Kazusa DNA Research Institute in 2011 (Asamizu et al. 2014; Nakaya et al. 2017). Currently, the DNA markers of 65 species, QTL information on 45 species, orthologous genes among 40 Viridiplantae and 213 Cyanobacteria, plant resources of approximately 900 citrus species and 6 non-citrus species have been released. In carnation, 496 DNA markers including 491 SSR markers and STS markers were released. For example, the information on marker CES0230 of carnation is summarized as follows: 'Scientific name': *Dianthus caryophyllus*, 'Family name': *Caryophyllaceae*, 'Marker name': CES0230, 'Marker type': SSR, 'Primer seq (fwd)': TGGTGGTGATGATGAGAGGA, 'Primer seq (rv)': TCTCAACAACACGTGCAACA, 'Population': 85–11 x 'Pretty Favvare', 'LG (linkage group)': LG_085P_4, 'Chr (chromosome)': NA, 'Linked trait or Linked gene': CBW (carnation bacterial wilt resistance), 'Trait type': 3 (stress trait), 'DOI or PMD': 10.1186/1471–2164-14–734. When the marker 'CES0230' is selected, detailed information will be shown, such as 'PCR condition': '94C_5min −> (94C_30s −> 56C_90s −> 72C_90s) × 30 −> (94C_30s −> 53C_90s −> 72C_90s) × 8 −> 72C_10min', 'map name': 85–11 x 'Pretty Favvare', 'Population type': F2, 'Linkage group': LG_085P_4, 'Map position (cM)': 43.5. Thus far, DNA markers and QTL information from the literature for various kinds of plant species have been curated. The PGDBj helps researchers efficiently obtain genomic information, including markers, for carnation.

1.5 Conclusion

Short- and long-read sequencers have been developed so far. Illumina has released the iSeq 100/MiniSeq/MiSeq/NextSeq/NovaSeq platforms (https://www.illumina.com) as short-read type sequencers, while Pacific Biosciences has released the PacBio RSII/Sequel/SequelII platforms (https://www.pacb.com) and Oxford Nanopore has released the MinION/GridION/PromethION (https://nanoporetech.com) platforms as long-read type sequencers. The genome sequence of azuki bean (*Vigna angularis*) was first determined using PacBio long-read data

(Sakai et al. 2015). A genetic linkage map covering 969.6 cM has been constructed using 412 SSR loci for the '85P' population of carnation (Yagi et al. 2014a). A linkage map consisting of 15 LGs covering 971.5 cM has also been constructed by using 285 SSR markers and 2,119 ddRAD-Seq markers for the F_2 mapping population (n = 93), the parental F_1 line (11A04-72), and the grandparents (806-46b and Mizuki) (Yagi et al. 2017). Genetic linkage maps constructed based on DNA markers or ddRAD-Seq data are useful for constructing genome sequences at the pseudomolecule level (Shirasawa et al. 2017). NRGene (https://www.nrgene.com) is an Israeli company that has developed a *de novo* genome assembler, DeNovoMAGIC™ (https://www.nrgene.com/solutions/denovomagic/). This program uses Illumina PE, MP reads, and 10 × Genomics linked-reads, which can assemble at the pseudomolecule level by using only short-read data. It can be applied to high heterozygosity genomes and polyploid genomes with phased genome sequences. Currently, the genome sequences of emmer (Avni et al. 2017), maize (Springer et al. 2018), wheat (hexaploid; International Wheat Genome Sequencing Consortium 2018), blueberry (tetraploid; Colle et al. 2019), strawberry (octoploid; Edger et al. 2019), *Gossypium barbadense* and *Gossypium hirsutum* (Hu et al. 2019), and soybean (Valliyodan et al. 2019) have been determined by NRGene. On the other hand, novel technologies for constructing DNA libraries with long insert sizes have been developed. BioNano Genomics has released the Saphyr genome mapping system (https://bionanogenomics.com/products/saphyr/) based on an optical mapping method. By using this method, contigs or scaffolds can be ordered and connected. The insert size of a DNA library made by this technology ranges up to 1 M bases. This method can be used to detect structural variants (SVs) including indels, repetitive sequences, inversions, and translocations. An ultra-long-range library construction method has also been developed. Dovetail Genomics (https://dovetailgenomics.com) developed the Chicago® library and the Hi-Rise™ assembler. In general, the library size of the paired-end (PE) and mate-pair (MP) of Illumina reads is respectively from ∼500 bp and 3 to 20 kb, but the insert size of the Chicago® library covers several tens of kb in length. Phase Genomics (https://phasegenomics.com) has released the Hi-C library and Proximo™ assembler. The insert size of this library covers several tens of Mb in length. These technologies for constructing libraries with ultra-long range are used to connect contigs or scaffolds for assembly at the pseudomolecule or chromosome level. LACHESIS (Burton et al. 2013), SALSA (Ghurye et al. 2019), and ALLHiC (Zhang et al. 2019) are freely available assemblers for Hi-C data. From now on, the genome sequences of various kinds of plant species would be determined on the chromosome scale by using these ultra-long-range libraries. Thus far, the genome sequences of floricultural plant species have been published for orchid (*Phalaenopsis equestris* (Cai et al. 2015)), *Primula veris* (Nowak et al. 2015), dendribium (*Dendrobium officinale* (Yan et al. 2015)), petunia (*Petunia axillaris* and *P. inflata* (Bombarely et al. 2016)), morning glory (*Ipomoea nil*) (Hoshino et al. 2016), roses (*Rosa roxburghii* (Lu et al. 2016), *Rosa multiflora* (Nakamura et al. 2018), *Rosa chinensis* (Raymond et al. 2018, Hibrand Saint-Oyant et al. 2018), *Rosa lucieae* (Jeon and Kim, 2019), *Rosa hybrida* (Qi et al. 2018), chrysanthemum (*Chrysanthemum nankingense* (Song et al. 2018), *C. setisuspe* (Hirakawa et al. 2019)), snapdragon (*Antirrhinum majus* (Li et al. 2019b)). As described above, the genome sequence of carnation has been determined at the draft level. The sequence could be determined at the pseudomolecule level by using the current technologies described above. When the chromosome-scale genome sequence of carnation is determined, studies of molecular genetics and more efficient molecular breeding can be performed.

References

Arabidopsis Genome Initiative (2000) Analysis of the genome sequence of the flowering plant *Arabidopsis thaliana*. Nature 408:796–815

Asamizu E, Ichihara H, Nakaya A, Nakamura Y, Hirakawa H, Ishii T, Tamura T, Fukami-Kobayashi K, Nakajima Y, Tabata S (2014) Plant genome database Japan (PGDBj): a portal website for the integration of plant genome-related databases. Plant Cell Physiol 55:e8

Avni R, Nave M, Barad O, Baruch K, Twardziok SO, Gundlach H, Hale I, Mascher M, Spannagl M, Wiebe K, Jordan KW, Golan G, Deek J, Ben-Zvi B, Ben-Zvi G, Himmelbach A, MacLachlan RP, Sharpe AG, Fritz A, Ben-David R, Budak H, Fahima T, Korol A, Faris JD, Hernandez A, Mikel MA, Levy AA, Steffenson B, Maccaferri M, Tuberosa R, Cattivelli L, Faccioli P, Ceriotti A, Kashkush K, Pourkheirandish M, Komatsuda T, Eilam T, Sela H, Sharon A, Ohad N, Chamovitz DA, Mayer KFX, Stein N, Ronen G, Peleg Z, Pozniak CJ, Akhunov ED, Distelfeld A (2017) Wild emmer genome architecture and diversity elucidate wheat evolution and domestication. Science 357:93–97

Bankevich A, Nurk S, Antipov D, Gurevich AA, Dvorkin M, Kulikov AS, Lesin VM, Nikolenko SI, Pham S, Prjibelski AD, Pyshkin AV, Sirotkin AV, Vyahhi N, Tesler G, Alekseyev MA, Pevzner PA (2012) SPAdes: a new genome assembly algorithm and its applications to single-cell sequencing. J Comput Biol 19:455–477

Boetzer M, Henkel CV, Jansen HJ, Butler D, Pirovano W (2011) Scaffolding pre-assembled contigs using SSPACE. Bioinformatics 27:578–579

Boisvert S, Laviolette F, Corbeil J (2010) Ray: simultaneous assembly of reads from a mix of high-throughput sequencing technologies. J Comput Biol 17:1519–1533

Bombarely A, Moser M, Amrad A, Bao M, Bapaume L, Barry CS, Bliek M, Boersma MR, Borghi L, Bruggmann R, Bucher M, D'Agostino N, Davies K, Druege U, Dudareva N, Egea-Cortines M, Delledonne M, Fernandez-Pozo N, Franken P, Grandont L, Heslop-Harrison JS, Hintzsche J, Johns M, Koes R, Lv X, Lyons E, Malla D, Martinoia E, Mattson NS, Morel P, Mueller LA, Muhlemann J, Nouri E, Passeri V, Pezzotti M, Qi Q, Reinhardt D, Rich M, Richert-Pöggeler KR, Robbins TP, Schatz MC, Schranz ME, Schuurink RC, Schwarzacher T, Spelt K, Tang H, Urbanus SL, Vandenbussche M, Vijverberg K, Villarino GH, Warner RM, Weiss J, Yue Z, Zethof J, Quattrocchio F, Sims TL, Kuhlemeier C (2016) Insight into the evolution of the Solanaceae from the parental genomes of *Petunia hybrida*. Nat Plants 2:16074

Burton JN, Adey A, Patwardhan RP, Qiu R, Kitzman JO, Shendure J (2013) Chromosome-scale scaffolding of de novo genome assemblies based on chromatin interactions. Nat Biotechnol 31:1119–1125

Cai J, Liu X, Vanneste K, Proost S, Tsai WC, Liu KW, Chen LJ, He Y, Xu Q, Bian C, Zheng Z, Sun F, Liu W, Hsiao YY, Pan ZJ, Hsu CC, Yang YP, Hsu YC, Chuang YC, Dievart A, Dufayard JF, Xu X, Wang JY, Wang J, Xiao XJ, Zhao XM, Du R, Zhang GQ, Wang M, Su YY, Xie GC, Liu GH, Li LQ, Huang LQ, Luo YB, Chen HH, Van de Peer Y, Liu ZJ (2015) The genome sequence of the orchid *Phalaenopsis equestris*. Nat Genet 47:65–72

Chen S, Xu Z, Zhao Y, Zhong X, Li C, Yang G (2018) Structural characteristic and phylogenetic analysis of the complete chloroplast genome of *Dianthus Caryophyllus*. Mitochondrial DNA Part B 3:1131–1132

Colle M, Leisner CP, Wai CM, Ou S, Bird KA, Wang J, Wisecaver JH, Yocca AE, Alger EI, Tang H, Xiong Z, Callow P, Ben-Zvi G, Brodt A, Baruch K, Swale T, Shiue L, Song GQ, Childs KL, Schilmiller A, Vorsa N, Buell CR, VanBuren R, Jiang N, Edger PP (2019) Haplotype-phased genome and evolution of phytonutrient pathways of tetraploid blueberry. Gigascience 8(pii):giz012

Edger PP, Poorten TJ, VanBuren R, Hardigan MA, Colle M, McKain MR, Smith RD, Teresi SJ, Nelson ADL, Wai CM, Alger EI, Bird KA, Yocca AE, Pumplin N, Ou S, Ben-Zvi G, Brodt A, Baruch K, Swale T, Shiue L, Acharya CB, Cole GS, Mower JP, Childs KL, Jiang N, Lyons E, Freeling M, Puzey JR, Knapp SJ (2019) Origin and evolution of the octoploid strawberry genome. Nat Genet 51:541–547

Edgar RC, Myers EW (2005) PILER: identification and classification of genomic repeats. Bioinform Suppl 1: i152-158

Ghurye J, Rhie A, Walenz BP, Schmitt A, Selvaraj S, Pop M, Phillippy AM, Koren S (2019) Integrating Hi-C links with assembly graphs for chromosome-scale assembly. Plos Comput Biol 15:e1007273

Gnerre S, Maccallum I, Przybylski D, Ribeiro FJ, Burton JN, Walker BJ, Sharpe T, Hall G, Shea TP, Sykes S, Berlin AM, Aird D, Costello M, Daza R, Williams L, Nicol R, Gnirke A, Nusbaum C, Lander ES, Jaffe DB (2011) High-quality draft assemblies of mammalian genomes from massively parallel sequence data. Proc Natl Acad Sci USA 108:1513–1518

Haas BJ, Delcher AL, Mount SM, Wortman JR, Smith RK Jr, Hannick LI, Maiti R, Ronning CM, Rusch DB, Town CD, Salzberg SL, White O (2003) Improving the Arabidopsis genome annotation using maximal transcript alignment assemblies. Nucleic Acids Res 31:5654–5666

Hibrand Saint-Oyant L, Ruttink T, Hamama L, Kirov I, Lakhwani D, Zhou NN, Bourke PM, Daccord N, Leus L, Schulz D, Van de Geest H, Hesselink T, Van Laere K, Debray K, Balzergue S, Thouroude T, Chastellier A, Jeauffre J, Voisine L, Gaillard S, Borm TJA, Arens P, Voorrips RE, Maliepaard C, Neu E, Linde M, Le Paslier MC, Bérard A, Bounon R,

Clotault J, Choisne N, Quesneville H, Kawamura K, Aubourg S, Sakr S, Smulders MJM, Schijlen E, Bucher E, Debener T, De Riek J, Foucher F (2018) A high-quality genome sequence of *Rosa chinensis* to elucidate ornamental traits. Nat Plants 4:473–484

Hirakawa H, Sumitomo K, Hisamatsu T, Nagano S, Shirasawa K, Higuchi Y, Kusaba M, Koshioka M, Nakano Y, Yagi M, Yamaguchi H, Taniguchi K, Nakano M, Isobe SN (2019) De novo whole-genome assembly in *Chrysanthemum seticuspe*, a model species of Chrysanthemums, and its application to genetic and gene discovery analysis. DNA Res 26:195–203

Hoshino A, Jayakumar V, Nitasaka E, Toyoda A, Noguchi H, Itoh T, Shin-I T, Minakuchi Y, Koda Y, Nagano AJ, Yasugi M, Honjo MN, Kudoh H, Seki M, Kamiya A, Shiraki T, Carninci P, Asamizu E, Nishide H, Tanaka S, Park KI, Morita Y, Yokoyama K, Uchiyama I, Tanaka Y, Tabata S, Shinozaki K, Hayashizaki Y, Kohara Y, Suzuki Y, Sugano S, Fujiyama A, Iida S, Sakakibara Y (2016) Genome sequence and analysis of the Japanese morning glory *Ipomoea nil*. Nat Commun 7:13295

Hu Y, Chen J, Fang L, Zhang Z, Ma W, Niu Y, Ju L, Deng J, Zhao T, Lian J, Baruch K, Fang D, Liu X, Ruan YL, Rahman MU, Han J, Wang K, Wang Q, Wu H, Mei G, Zang Y, Han Z, Xu C, Shen W, Yang D, Si Z, Dai F, Zou L, Huang F, Bai Y, Zhang Y, Brodt A, Ben-Hamo H, Zhu X, Zhou B, Guan X, Zhu S, Chen X, Zhang T (2019) *Gossypium barbadense* and *Gossypium hirsutum* genomes provide insights into the origin and evolution of allotetraploid cotton. Nat Genet 51:739–748

Huang S, Li R, Zhang Z, Li L, Gu X, Fan W, Lucas WJ, Wang X, Xie B, Ni P, Ren Y, Zhu H, Li J, Lin K, Jin W, Fei Z, Li G, Staub J, Kilian A, van der Vossen EA, Wu Y, Guo J, He J, Jia Z, Ren Y, Tian G, Lu Y, Ruan J, Qian W, Wang M, Huang Q, Li B, Xuan Z, Cao J, Asan, Wu Z, Zhang J, Cai Q, Bai Y, Zhao B, Han Y, Li Y, Li X, Wang S, Shi Q, Liu S, Cho WK, Kim JY, Xu Y, Heller-Uszynska K, Miao H, Cheng Z, Zhang S, Wu J, Yang Y, Kang H, Li M, Liang H, Ren X, Shi Z, Wen M, Jian M, Yang H, Zhang G, Yang Z, Chen R, Liu S, Li J, Ma L, Liu H, Zhou Y, Zhao J, Fang X, Li G, Fang L, Li Y, Liu D, Zheng H, Zhang Y, Qin N, Li Z, Yang G, Yang S, Bolund L, Kristiansen K, Zheng H, Li S, Zhang X, Yang H, Wang J, Sun R, Zhang B, Jiang S, Wang J, Du Y, Li S (2009) The genome of the cucumber, *Cucumis sativus* L. Nat Genet 41:1275–1281

International Rice Genome Sequencing Project (2005) The map-based sequence of the rice genome. Nature 436:793–800

International Wheat Genome Sequencing Consortium (IWGSC) (2018) Shifting the limits in wheat research and breeding using a fully annotated reference genome. Science 361:eaar7191

Jeon JH, Kim SC (2019) Comparative analysis of the complete chloroplast genome sequences of three closely related East-Asian wild roses (Rosa sect. Synstylae; Rosaceae). Genes (Basel). 10:E23

Jones P, Binns D, Chang HY, Fraser M, Li W, McAnulla C, McWilliam H, Maslen J, Mitchell A, Nuka G, Pesseat S, Quinn AF, Sangrador-Vegas A, Scheremetjew M, Yong SY, Lopez R, Hunter S (2014) InterProScan 5: genome-scale protein function classification. Bioinformatics 30:1236–1240

Jurka J (1998) Repeats in genomic DNA: mining and meaning. Curr Opin Struct Biol 8:333–337

Keller O, Kollmar M, Stanke M, Waack S (2011) A novel hybrid gene prediction method employing protein multiple sequence alignments. Bioinformatics 27:757–763

Kent WJ (2002) BLAT–the BLAST-like alignment tool. Genome Res 12:656–664

Li H (2012) Exploring single-sample SNP and INDEL calling with whole-genome de novo assembly. Bioinformatics 28:1838–1844

Li G, Tembrock LR, Wu Z, Liu F (2019a) Complete chloroplast genome of carnation (Caryophyllaceae: *Dianthus caryophyllus* L.). Mitochondrial DNA Part B 4:1463–1464

Li M, Zhang D, Gao Q, Luo Y, Zhang H, Ma B, Chen C, Whibley A, Zhang Y, Cao Y, Li Q, Guo H, Li J, Song Y, Zhang Y, Copsey L, Li Y, Li X, Qi M, Wang J, Chen Y, Wang D, Zhao J, Liu G, Wu B, Yu L, Xu C, Li J, Zhao S, Zhang Y, Hu S, Liang C, Yin Y, Coen E, Xue Y (2019b) Genome structure and evolution of *Antirrhinum majus* L. Nat Plants 5:174–183

Li R, Zhu H, Ruan J, Qian W, Fang X, Shi Z, Li Y, Li S, Shan G, Kristiansen K, Li S, Yang H, Wang J, Wang J (2010) De novo assembly of human genomes with massively parallel short read sequencing. Genome Res 20:265–272

Lu M, An H, Li L (2016) Genome Survey Sequencing for the Characterization of the genetic background of *Rosa roxburghii* Tratt and leaf ascorbate metabolism genes. PLoS ONE 11:e0147530

Marçais G, Kingsford C (2011) A fast, lock-free approach for efficient parallel counting of occurrences of k-mers. Bioinformatics 27:764–770

Nakamura N, Hirakawa H, Sato S, Otagaki S, Matsumoto S, Tabata S, Tanaka Y (2018) Genome structure of *Rosa multiflora*, a wild ancestor of cultivated roses. DNA Res 25:113–121

Nakaya A, Ichihara H, Asamizu E, Shirasawa S, Nakamura Y, Tabata S, Hirakawa H (2017) Plant genome database Japan (PGDBj). Methods Mol Biol 1533:45–77

Nowak MD, Russo G, Schlapbach R, Huu CN, Lenhard M, Conti E (2015) The draft genome of *Primula veris* yields insights into the molecular basis of heterostyly. Genome Biol 16:12

Parra G, Bradnam K, Korf I (2007) CEGMA: a pipeline to accurately annotate core genes in eukaryotic genomes. Bioinformatics 23:1061–1067

Price AL, Jones NC, Pevzner PA (2005) De novo identification of repeat families in large genomes. Bioinform Suppl 1:i351-358

Qi W, Chen X, Fang P, Shi S, Li J, Liu X, Cao X, Zhao N, Hao H, Li Y, Han Y, Zhang Z (2018) Genomic and transcriptomic sequencing of *Rosa hybrida* provides microsatellite markers for breeding, flower trait improvement and taxonomy studies. BMC Plant Biol 18:119

Raymond O, Gouzy J, Just J, Badouin H, Verdenaud M, Lemainque A, Vergne P, Moja S, Choisne N, Pont C, Carrère S, Caissard JC, Couloux A, Cottret L, Aury JM, Szécsi J, Latrasse D, Madoui MA, François L, Fu X, Yang SH, Dubois A, Piola F, Larrieu A, Perez M, Labadie K, Perrier L, Govetto B, Labrousse Y, Villand P, Bardoux C, Boltz V, Lopez-Roques C, Heitzler P, Vernoux T, Vandenbussche M, Quesneville H, Boualem A, Bendahmane A, Liu C, Le Bris M, Salse J, Baudino S, Benhamed M, Wincker P, Bendahmane M (2018) The Rosa genome provides new insights into the domestication of modern roses. Nat Genet 50:772–777

Sakai H, Naito K, Ogiso-Tanaka E, Takahashi Y, Iseki K, Muto C, Satou K, Teruya K, Shiroma A, Shimoji M, Hirano T, Itoh T, Kaga A, Tomooka N (2015) The power of single molecule real-time sequencing technology in the de novo assembly of a eukaryotic genome. Sci Rep 5:16780

Sato S, Nakamura Y, Kaneko T, Asamizu E, Kato T, Nakao M, Sasamoto S, Watanabe A, Ono A, Kawashima K, Fujishiro T, Katoh M, Kohara M, Kishida Y, Minami C, Nakayama S, Nakazaki N, Shimizu Y, Shinpo S, Takahashi C, Wada T, Yamada M, Ohmido N, Hayashi M, Fukui K, Baba T, Nakamichi T, Mori H, Tabata S (2008) Genome structure of the legume, *Lotus japonicus*. DNA Res 15:227–239

Seppey M, Manni M, Zdobnov EM (2019) BUSCO: Assessing genome assembly and annotation completeness. Methods Mol Biol 1962:227–245

Shirasawa K, Isuzugawa K, Ikenaga M, Saito Y, Yamamoto T, Hirakawa H, Isobe S (2017) The genome sequence of sweet cherry (*Prunus avium*) for use in genomics-assisted breeding. DNA Res 24:499–508

Song C, Liu Y, Song A, Dong G, Zhao H, Sun W, Ramakrishnan S, Wang Y, Wang S, Li T, Niu Y, Jiang J, Dong B, Xia Y, Chen S, Hu Z, Chen F, Chen S (2018) The *Chrysanthemum nankingense* genome provides insights into the evolution and diversification of Chrysanthemum flowers and medicinal traits. Mol Plant 11:1482–1491

Springer NM, Anderson SN, Andorf CM, Ahern KR, Bai F, Barad O, Barbazuk WB, Bass HW, Baruch K, Ben-Zvi G, Buckler ES, Bukowski R, Campbell MS, Cannon EKS, Chomet P, Dawe RK, Davenport R, Dooner HK, Du LH, Du C, Easterling KA, Gault C, Guan JC, Hunter CT, Jander G, Jiao Y, Koch KE, Kol G, Köllner TG, Kudo T, Li Q, Lu F, Mayfield-Jones D, Mei W, McCarty DR, Noshay JM, Portwood JL 2nd, Ronen G, Settles AM, Shem-Tov D, Shi J, Soifer I, Stein JC, Stitzer MC, Suzuki M, Vera DL, Vollbrecht E, Vrebalov JT, Ware D, Wei S, Wimalanathan K, Woodhouse MR, Xiong W, Brutnell TP (2018) The maize W22 genome provides a foundation for functional genomics and transposon biology. Nat Genet 50:1282–1288

Tatusov RL, Fedorova ND, Jackson JD, Jacobs AR, Kiryutin B, Koonin EV, Krylov DM, Mazumder R, Mekhedov SL, Nikolskaya AN, Rao BS, Smirnov S, Sverdlov AV, Vasudevan S, Wolf YI, Yin JJ, Natale DA (2003) The COG database: an updated version includes eukaryotes. BMC Bioinformatics 4:41

Tuskan GA, Difazio S, Jansson S, Bohlmann J, Grigoriev I, Hellsten U, Putnam N, Ralph S, Rombauts S, Salamov A, Schein J, Sterck L, Aerts A, Bhalerao RR, Bhalerao RP, Blaudez D, Boerjan W, Brun A, Brunner A, Busov V, Campbell M, Carlson J, Chalot M, Chapman J, Chen GL, Cooper D, Coutinho PM, Couturier J, Covert S, Cronk Q, Cunningham R, Davis J, Degroeve S, Déjardin A, Depamphilis C, Detter J, Dirks B, Dubchak I, Duplessis S, Ehlting J, Ellis B, Gendler K, Goodstein D, Gribskov M, Grimwood J, Groover A, Gunter L, Hamberger B, Heinze B, Helariutta Y, Henrissat B, Holligan D, Holt R, Huang W, Islam-Faridi N, Jones S, Jones-Rhoades M, Jorgensen R, Joshi C, Kangasjärvi J, Karlsson J, Kelleher C, Kirkpatrick R, Kirst M, Kohler A, Kalluri U, Larimer F, Leebens-Mack J, Leplé JC, Locascio P, Lou Y, Lucas S, Martin F, Montanini B, Napoli C, Nelson DR, Nelson C, Nieminen K, Nilsson O, Pereda V, Peter G, Philippe R, Pilate G, Poliakov A, Razumovskaya J, Richardson P, Rinaldi C, Ritland K, Rouzé P, Ryaboy D, Schmutz J, Schrader J, Segerman B, Shin H, Siddiqui A, Sterky F, Terry A, Tsai CJ, Uberbacher E, Unneberg P, Vahala J, Wall K, Wessler S, Yang G, Yin T, Douglas C, Marra M, Sandberg G, Van de Peer Y, Rokhsar D (2006) The genome of black cottonwood, *Populus trichocarpa* (Torr. & Gray). Science 313:1596–1604

Valliyodan B, Cannon SB, Bayer PE, Shu S, Brown AV, Ren L, Jenkins J, Chung CY, Chan TF, Daum CG, Plott C, Hastie A, Baruch K, Barry KW, Huang W, Patil G, Varshney RK, Hu H, Batley J, Yuan Y, Song Q, Stupar RM, Goodstein DM, Stacey G, Lam HM, Jackson SA, Schmutz J, Grimwood J, Edwards D, Nguyen HT (2019) Construction and comparison of three reference-quality genome assemblies for soybean. Plant J 100:1066–1082

Vicedomini R, Vezzi F, Scalabrin S, Arvestad L, Policriti A (2013) GAM-NGS: genomic assemblies merger for next generation sequencing. BMC Bioinform Suppl 7:S6

Vurture GW, Sedlazeck FJ, Nattestad M, Underwood CJ, Fang H, Gurtowski J, Schatz MC (2017)

GenomeScope: fast reference-free genome profiling from short reads. Bioinformatics 33:2202–2204

Yagi M, Yamamoto T, Isobe S, Hirakawa H, Tabata S, Tanase K, Yamaguchi H, Onozaki T (2014a) Construction of a reference genetic linkage map for carnation (*Dianthus caryophyllus* L.). BMC Genomics 14:734

Yagi M, Kosugi S, Hirakawa H, Ohmiya A, Tanase K, Harada T, Kishimoto K, Nakayama M, Ichimura K, Onozaki T, Yamaguchi H, Sasaki N, Miyahara T, Nishizaki Y, Ozeki Y, Nakamura N, Suzuki T, Tanaka Y, Sato S, Shirasawa K, Isobe S, Miyamura Y, Watanabe A, Nakayama S, Kishida Y, Kohara M, Tabata S (2014b) Sequence analysis of the genome of carnation (*Dianthus caryophyllus* L.). DNA Res 2:231–241

Yagi M, Shirasawa K, Waki T, Kume T, Isobe S, Tanase K, Yamaguchi H (2017) Construction of an SSR and RAD marker-based genetic linkage map for carnation (*Dianthus caryophyllus* L.). Plant Mol Biol Rep 35:110–117

Yan L, Wang X, Liu H, Tian Y, Lian J, Yang R, Hao S, Wang X, Yang S, Li Q, Qi S, Kui L, Okpekum M, Ma X, Zhang J, Ding Z, Zhang G, Wang W, Dong Y, Sheng J (2015) The genome of *Dendrobium officinale* illuminates the biology of the important traditional Chinese orchid herb. Mol Plant 8:922–934

Zhang X, Zhang S, Zhao Q, Ming R, Tang H (2019) Assembly of allele-aware, chromosomal-scale autopolyploid genomes based on Hi-C data. Nat Plants 5:833–845

Transcriptome Analysis in Carnation

2

Koji Tanase

Abstract

The transcriptome is a collection of all the transcribed RNAs in a particular cell, tissue, or organ. Transcriptome analysis using differential gene expression analyses, microarrays, and RNA-sequences (RNA-seq) provides useful biological information that allows the identification of candidate mRNAs associated with biological function and understanding the interactions among the multiple components and the expressed markers associated with the traits of interest. Technological advances in the biological investigation have enabled the transcriptome analysis in crops, including carnation, on a tremendous scale. We performed transcriptome analysis in carnation to enhance our understanding of the regulation of the transcripts by constructing a large-scale expressed sequence tag (EST) database based on next-generation sequencing (NGS). We identified a few differentially expressed genes responsible for the flower color metabolism by microarray analysis. In some studies, transcriptome analysis using RNA-seq is also performed to identify the differential gene expression in interesting traits. This review summarizes the strategies used for transcriptome analyses in plants as well as the findings with regard to the important traits that have been achieved through the transcriptome analyses in carnation researches.

2.1 Introduction

Virtually, mRNAs can serve various biological functions, including the segregation of cell-fate determinants, maintenance of homeostasis, and the response to external stimuli. A certain amount of mRNA is preferentially transcribed from the specific part of DNA in a particular kind of cell, tissue, or organ representing only a small percentage of the whole genome. Nevertheless, the characterization of a transcriptome to identify the mRNAs involved in a particular biological function or phenotype is rather laborious.

The typical approaches to gene identification are protein characterization, peptide sequence determination, and identification of the corresponding mRNA and genome DNA sequences. Recently, differential gene expression analyses, expressed sequence tags (ESTs), large scale gene expression profiling (transcriptome), and associated informatics technologies have been utilized in life science including plant sciences (Fig. 2.1, Dunwell et al. 2001). These approaches take advantage of their general versatility for characterizing large numbers of nucleic acid

K. Tanase (✉)
Institute of Vegetable and Floriculture Science, NARO, Tsukuba 305-0852, Ibaraki, Japan
e-mail: tanase@affrc.go.jp

T. Onozaki and M. Yagi (eds.), *The Carnation Genome*, Compendium of Plant Genomes,
https://doi.org/10.1007/978-981-15-8261-5_2

sequences, and the expanding collection of nucleic acid sequence data from diverse taxa. Transcriptome analysis, which allows the identification of candidate mRNAs and expressed markers associated with the traits of interest, and understanding the interactions among multiple components, has been described as transcriptomics. Moreover, these data have been also utilized to accurately determine the intron/exon structure and to identify splicing variants as well as 5′- and 3′-untranslated sequences, which are difficult to predict from the automated annotations of the whole-genome sequence. The identification of genes that control the economically important traits will provide the basis for advances in the genetic improvement of crop species.

2.2 Gene Expression Analysis

Technology utilization has played an important role in understanding the complex regulation of the transcripts, like the precocious technique of quantitative detection of specific mRNA levels, northern blotting (Alwine et al. 1978). In this technique, RNA mixture from sample cells was separated according to their sizes using gel electrophoresis and then transferred onto a blotting membrane. Specific RNA bands can be detected by hybridization with DNA or RNA probes labeled with a radioactive atom or a fluorescent dye. Although northern blotting is an effectual technique for the detection of transcript variants of genes, it has disadvantages, such as the requirement of large amounts of RNA, difficulty in detection using multiple probes, and relatively low sensitivity, implying that low-level transcripts may be overlooked (Streit et al. 2008). Another method of gene expression analysis, the quantitative real-time PCR has become a major approach for measuring the expression of target genes (Unamba et al. 2015). In real-time PCR, a specific target sequence in a sample, which is the complementary DNA converted from RNA, is amplified and the amplification progress is monitored using fluorescent reporters (Valasek and Repa 2005). It reduces the required quantity of RNA and has become an ordinary method for measuring the expression of target genes. In northern blotting and real-time PCR methods, identification of sequence data of the target genes is a prerequisite for the analysis of their expression, and it is hard to implement the measurement of the expression of hundreds of known genes at a particular time.

Detection transcripts of unknown genes which express in different cell and tissues is accomplished in some differential gene expression analyses, such as Suppression Subtractive Hybridization (SSH), Differential Display (DD), cDNA-amplified fragment length polymorphism

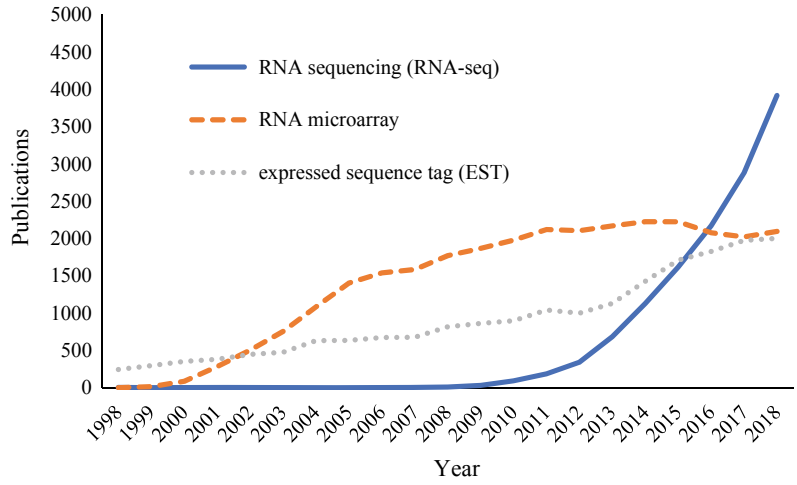

Fig. 2.1 Transcriptomics method use over two decades. Publications referring to RNA sequencing, RNA microarray and expressed sequence tag were surveyed by Medline trend: automated yearly statistics of PubMed results for any query (https://dan.corlan.net/medline-trend.html)

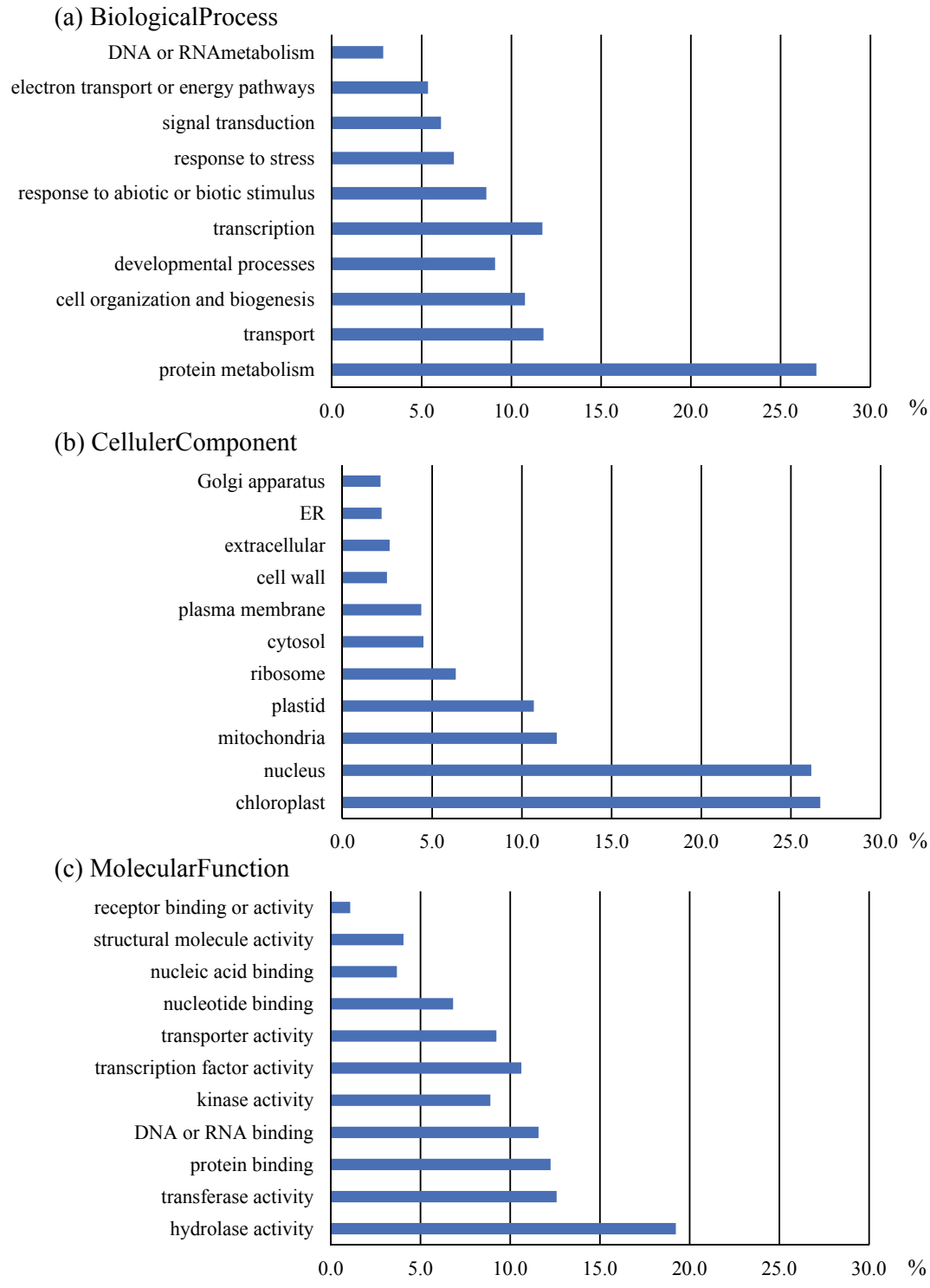

Fig. 2.2 Classification of carnation ESTs into functional category according to *Arabidopsis* Gene Ontology. **a** Biological Process, **b** Cellular Component, **c** Molecular Function. This figure was modified from a previous publication (Tanase et al. 2012)

(cDNA-AFLP), and Serial Analysis of Gene Expression (SAGE). The SSH relies on hybridization, relative to control, to separate differentially expressed genes among the sequences taken from a sample. Transcripts from the sample with no sequence homology with the transcripts from the control are separated from the pool as differentially expressed (Diatchenko et al. 1999). The SSH has been used in many studies in plant responses to stress, hormone, and pathogenicity responses in plants (Goswami et al. 2006; Guo et al. 2013; Kong et al. 2005; Nguyen et al. 2009).

Differential display methodology is a PCR-based technique that identify the differentially expression genes between two or more samples. The transcribed cDNAs are amplified with a set of arbitrary primers that anneal to the 3′ oligo dT and/or to the arbitrary primers previously used in the conversion step (Liang and Pardee 1992; Welsh et al. 1992). The PCR products are separated on a gel, and the differentially expressed sample and control bands are visualized, extracted, and sequenced. There are several studies on the identification of the differentially expressed genes in plants using DD; for example, gene family of 1 aminocyclopropane-1-carboxylate oxidase (ACO) the key enzyme involved in the synthesis of plant hormone ethylene, are differentially regulated during fruit ripening and senescence in tomato (Barry et al. 1996), specific genes coding enzymes of the biosynthetic pathway of anthocyanin (Saito et al. 1999), genes differentially expressed in flower transition and development (Yu and Goh 2000; Yung et al. 1999), and phytochrome A regulated genes (Kuno et al. 2000).

The cDNA-AFLP, an AFLP-based transcript profiling method (Vos et al. 1995; Vuylsteke et al. 2007), involves the reverse transcription of mRNA into double-stranded cDNA, followed by restriction digestion, ligation of specific adapters, and fractionation of this mixture of cDNA fragments into smaller subsets by selective PCR amplification. Differences in gene expression levels of samples are reflected as different band intensities on gels. The differentially expressed genes can be identified by direct sequencing of the re-amplified cDNA-AFLP tags purified from the gels. The cDNA-AFLP has been used in studies on plant responses to hormone and pathogenicity responses in plants (Colling et al. 2013; Durrant et al. 2000).

Serial analysis of gene expression (SAGE) detect and quantify mRNA in a sample of interest by using small tags that correspond to fragments of those transcripts. In SAGE, mRNA is converted to cDNA followed by restriction digestion. Fragments of cDNA are attached to tags, amplified in a bacterial host, and then sequenced. The frequency of appearance of a specific sequence tag determines the relative abundance of the transcript in that sample. SAGE is one of the most useful techniques among the differential gene expression analyses but the SAGE is rarely used in the plant research (Dunwell et al. 2001; Lee and Lee 2003). Though differential gene expression analyses can identify the differentially expressed genes and enrich rare transcripts to facilitate the identification of novel genes, most plant scientists seem to be interested in large-scale gene expression studies using Microarray methodologies and RNA-sequence (RNA-seq) for transcriptome by next-generation sequencing (NGS).

Microarray and RNA-seq enable massive transcriptome profiling and comprehension of the complex behavior of transcriptome toward developmental cues and external stimuli. Microarray provides the profiling about the expression level of mRNA in the form of signal intensity generated by their hybridization with the complementary probes and allows the simultaneous analysis of thousands of genes, and the identification of both their presence and differential expression (Kuo et al. 2002). The primary type of microarray was reported in 1995 using the model plant, *Arabidopsis* (Schena et al. 1995) and the microarray format based on the whole genome was also establish using *Arabidopsis* in 2000 (Zhu and Wang 2000). The initial studies were performed mostly on *Arabidopsis*, but soon the technology was utilized in other plants, like rice (Ma et al. 2005). The microarray approach for transcriptome profiling is currently used in the

designing of DNA chips, protocols for hybridization, and analysis tools. In addition, the cost of microarray is relatively low, and DNA chips prepared from genome sequences of major crops such as *Arabidopsis*, tobacco, rice, soybean, tomato, and barley are available in some biotechnology companies. The results of microarray profiling can be accessed from public databases, like the Gene Expression Omnibus at NCBI. Microarray has several disadvantages; the biggest disadvantage is that only previously defined gene sequences can be analyzed by DNA chips. Therefore, microarray for transcriptome profiling is limited by the availability of existing EST collections and/or genome sequence data.

RNA-seq, which is currently the most popular method for transcriptome analysis, has already been employed in many studies on model plants and non-model plant species, including horticulture crops (Agarwal et al. 2014). The major steps involved in RNA-Seq are as follows: RNA extraction and library construction, sequencing of the library on an NGS platform, and analysis using bioinformatics tools. RNA-seq based expression is assessed by the numerical frequency of a sequence in the library. The advantage of RNA-seq in the analysis of transcriptomes of plants with no reference genome, without detection limit, detection of novel transcripts, assessment of low abundance transcripts, detection of non-coding RNAs, and analysis of mutations such as single nucleotide polymorphisms (SNPs) and InDels. However, it has limitations; detection of the larger transcripts is easier than smaller ones. The analysis can be complex if paralogs, splice variants, and gene fusions are present. There are few examples of both microarray and RNA-seq analysis using the same RNA sample, especially horticulture crops, but some studies in *Arabidopsis* and maize reported that both the technologies revealed a similar overview of the transcriptome (Bhargava et al. 2013; Sekhon et al. 2013). The integrated data from both microarray and RNA-seq analysis will increase our understanding of the plant transcriptome.

2.2.1 Transcriptome Analysis in Carnation

The first large-scale transcriptome analysis of carnation was reported by Hoeberichts et al. (2007). In this study, the differential gene expression profiling on senescence of carnation petals was analyzed using cDNA microarrays. The RNA was isolated from the petals of cut carnation flowers, and then a subtraction was performed using RNA from stem tissue for the construction of a cDNA library containing predominantly flower-specific and senescence-specific genes. The DNA sequencing was performed by the Sanger method, and 2,224 DNA fragments were deposited on the glass slides for microarray. After hybridization and evaluation of the signal quality, signal data from 1,664 DNA fragments were available for the expression analysis. Approximately 65% of all transcripts showed a large oscillation through the experimental period (Hoeberichts, 2007). Seven senescence-associated genes, 1-aminocyclopropane-1-carboxylic acid oxidase (*ACO1* = *CARAO1*; (tenHave and Woltering 1997)), 1-aminocyclopropane-1-carboxylic acid synthase (*ACS1* = *CARACC3*; (Park et al. 1992)), *ACS2* (=*CARAS1*; (Henskens et al. 1994)), *SR5* (Itzhaki et al. 1994; Verlinden et al. 2002), *SR8* (Meyer et al. 1991), *SR12* (Raghothama et al. 1991), and *S*-adenosylmethionine (SAM) synthetase (Woodson et al. 1992) which had been included as control in the microarray showed signal levels similar to the previously published data. This study showed that many transcription factors, such as EIN3-like (EIL) transcription factor, MYB-like DNA binding protein, zinc finger transcription factor, MYC-type transcription factor, MADS-box gene, and NAC transcription factor were up-regulated and prevented the induction of the gene expression by sucrose and STS. The authors inferred that the EIL transcription factor plays an important role for regulation of ethylene production. They also showed that these sequences, involved in the process of programmed cell death, remobilization, and defense mechanisms, were up-regulated.

2.2.2 Transcriptome Analysis Using RNA-Seq in Carnation

To increase our understanding of the regulation of the transcripts in carnation, we performed a transcriptome analysis for the first time by constructing a large-scale EST database based on NGS (Tanase et al. 2012). A normalized cDNA library and 3′-UTR library preparation of mRNA extracted from the aerial part of carnation were sequenced using a Roche 454 GS FLX sequencer. A total of 1,162,126 high-quality reads was obtained and assembled into 300,740 unigenes, consisting of 37,844 contigs and 262,896 singlets. The contigs averaged 605nt in length, and they ranged from 117 to 3,850 nt in length. The sequences of these contigs were searched against an *Arabidopsis* gene database, and 61.8% of them (23,380 contigs) had at least one hit using BLASTX. These data showed as sufficiently high-quality EST data sets in comparison with those of other non-model plants, which were sequenced by the 454 GS FLX sequencer. These data were also utilized to generate whole-genome datasets in carnation (Yagi et al. 2014). The contigs were annotated with Gene Ontology (GO) and were found to cover a vast range of GO categories. The proportions of genes assigned to each GO category (A: Biological Process, B: Cellular Component and C: Molecular Function) were very similar to those found in the genome annotation of *Arabidopsis*. The most common assignments in the Biological Process category were protein metabolism (27%), those in the Cellular Component were chloroplast (27%) and nucleus (26%), and those in the Molecular Function were hydrolase activity (19%) (Fig. 2.1). We focused on gene discovery in the areas of flower color and ethylene biosynthesis. Transcripts were identified for almost every gene involved in chlorophyll metabolism, carotenoid metabolism, anthocyanin biosynthesis, and ethylene biosynthesis in flowers. In chlorophyll and carotenoid metabolism, we clarified the key steps in chlorophyll accumulation and carotenoid accumulation by oligonucleotide microarray and real-time PCR (Ohmiya et al. 2013, 2014; Tanase et al. 2012). In chlorophyll metabolism, expression of the genes related to chlorophyll biosynthesis in pale-green petals was higher than those in non-green petals. The expression of the genes involved in chlorophyll degradation was almost similar in the pale-green and non-green petals. The difference in chlorophyll content between non-green and pale-green petals might be due to the different levels of chlorophyll biosynthesis in carnation. In carotenoid metabolism, genes encoding phytoene synthase and lycopene ε-cyclase were differentially expressed between the petals and leaves, thus low rates of carotenoid biosynthesis caused low levels of carotenoids in carnation petals. These data present a basis for further molecular and genetic studies on chlorophyll accumulation and carotenoid accumulation in carnation petals.

Recently, transcriptome analysis using RNA-seq was highlighted in differential gene expression analysis. In carnation, RNA-seq was also performed for the transcriptome analysis of some physiological attributes. A study of carnation plants subjected to heat stress revealed many differentially expressed genes through RNA-seq (Wan et al. 2015). In the study, a non-normalized cDNA library was constructed using mixed mRNA extracted from leaf tissues subjected to various heat stress treatments and was sequenced on the Illumina Hiseq2000 platform. A total of 45,604,882 paired-end reads was obtained and assembled into 99,255 contigs, which averaged 1,053 nt. RNA from samples treated with heat stress and control plants were sequenced for transcript profiling, and then, the numbers of reads were analyzed for the identification of the differentially expressed genes under heat shock. A total of 2,482 genes showed significantly altered expression levels due to heat stress, and some genes, including heat shock proteins, transcription factors, ROS-related genes, and signal transduction factors, were highly differentially expressed.

In adventitious root formation, transcriptome analysis using RNA-seq identified differentially expressed genes between stem cutting and auxin-induced in two lines (Villacorta-Martin et al. 2015). Several genes associated with Aux/IAA proteins, sucrose degradation enzymes such as

invertase and sucrose synthase, cyclins, kinesin, and histone variants showed differential expression after planting.

In a study of vase life and flower type in carnation, 500 genotypes were tested for transcriptome analysis using RNA-seq (Boxriker et al. 2017). Four samples of RNA combinations consisting of two types of vase life (normal and long life), and two types with flower size (standard and mini type flower) were separately sequenced using Illumina HiSeq 2500. Additionally, a combination of RNA-seq and massive analysis of cDNA ends were used for transcriptome analysis. As a result, these technologies produced better results with an average contig length of 1,258 nt along with their annotation. The vase life and flower type in the differentially expressed genes were analyzed using GO annotation. The GO terms associated with vase life included proteasome assembly, response to toxic substances, response to misfolded proteins, response of metal ion, and gluconeogenesis. In addition, GO terms associated with senescence were analyzed in detailed, followed by the identification of the ethylene transcription factors (*ERF1A* and *ERF8*), stress-associated transcripts (gibberellic acid (GA) insensitive mutant protein, dehydration-responsive element binding protein (*DREB3*), and calmodulin-like protein (*CML37*), GA associated transcripts, transcripts responsible for the stomata closure and the turgor pressure, transcripts associated with auxin and metabolism of carbohydrate (glycosyltransferase, sugar transport protein (*STP4*), and sucrose synthase (*SS1*)). In the analysis of carnation type, GO terms, such as secondary metabolic process, toxin catabolic process, negative regulation of translation, and dicarboxylic acid biosynthetic process, were identified.

As described above, numerous transcriptome data according to carnation have been accumulated through some studies. Increase of information on the transcriptome level is crucial for developing the research on the physiological aspects and economically important character of carnation. In addition, further studies will focus on the functional characterization of genes for the elucidation of the differentially expressed genes.

2.3 Conclusion

Transcriptome analysis is an effective and efficient strategy for the study of the biological mechanisms because it allows the detection of genes and the elucidation of molecular functions related to physiological events, signal transduction, primary and secondary metabolism, defense mechanisms, and stress response. Various methodologies and strategies that can be applied for the identification of differentially expressed genes, but the choice of methodology and/or strategy is determined by the available technology plus the cost and the limitations of the analysis. In the study of carnation, the methodologies and strategies used for the transcriptome analysis were limited, but transcriptome analysis, especially NGS technology will be increasingly used in the carnation study with an improvement in the optimization protocols and reduction of cost. This will enable better exploration of the carnation and a greater understanding of the mechanisms underlying the processes of gene expression and physiological responses, in addition to creation of the genomic resources for marker-assisted breeding.

References

Agarwal P, Parida SK, Mahto A, Das S, Mathew IE, Malik N, Tyagi AK (2014) Expanding frontiers in plant transcriptomics in aid of functional genomics and molecular breeding. Biotechnol J 9:1480–1492

Alwine JC, Kemp DJ, Stark GR (1978) Method for detection of specific RNAs in agarose gels by transfer to diazobenzyloxymethyl-paper and hybridization with DNA probes. Proc Natl Acad Sci USA 74:5350–5354

Barry CS, Blume B, Bouzayen M, Cooper W, Hamilton AJ, Grierson D (1996) Differential expression of the 1-aminocyclopropane-1-carboxylate oxidase gene family of tomato. Plant J 9:525–535

Bhargava A, Clabaugh I, To JP, Maxwell BB, Chiang YH, Schaller GE, Loraine A, Kieber JJ (2013) Identification of Cytokinin-Responsive Genes Using

Microarray Meta-Analysis and RNA-Seq in Arabidopsis. Plant Physiol 162:272–294

Boxriker M, Boehm R, Krezdorn N, Rotter B, Piepho HP (2017) Comparative transcriptome analysis of vase life and carnation type in *Dianthus caryophyllus* L. Sci Hortic 217:61–72

Colling J, Pollier J, Makunga NP, Goossens A (2013) cDNA-AFLP-based transcript profiling for genome-wide expression analysis of jasmonate-treated plants and plant cultures. Methods Mol Biol 1011:287–303

Diatchenko L, Lukyanov S, Lau YFC, Siebert PD (1999) Suppression subtractive hybridization: A versatile method for identifying differentially expressed genes. Methods Enzymol 303:349–380

Dunwell JM, Moya-Leon MA, Herrera R (2001) Transcriptome analysis and crop improvement (a review). Biol Res 34:153–164

Durrant WE, Rowland O, Piedras P, Hammond-Kosack KE, Jones JDG (2000) cDNA-AFLP reveals a striking overlap in race-specific resistance and wound response gene expression profiles. Plant Cell 12:963–977

Goswami RS, Xu JR, Trail F, Hilburn K, Kistler HC (2006) Genomic analysis of host-pathogen interaction between *Fusarium graminearum* and wheat during early stages of disease development. Microbiology 152:1877–1890

Guo, W. L., R. G. Chen, Z. H. Gong, Y. X. Yin and D. W. Li (2013) Suppression subtractive hybridization analysis of genes regulated by application of exogenous abscisic acid in pepper plant (*Capsicum annuum* L.) Leaves under Chilling Stress. Plos One 8.

Henskens JAM, Rouwendal GJA, Tenhave A, Woltering EJ (1994) Molecular-cloning of 2 different acc synthase pcr fragments in carnation flowers and organ-specific expression of the corresponding genes. Plant Mol Biol 26:453–458

Hoeberichts FA, van Doorn WG, Vorst O, van Wordragen MF (2007) Sucrose prevents up-regulation of senescence-associated genes in carnation petals. J Exp Bot 58:2873–2885

Itzhaki H, Maxson JM, Woodson WR (1994) An Ethylene-responsive enhancer element is involved in the senescence-related expression of the carnation glutathione-s-transferase (GST1) gene. Proc Natl Acad Sci USA 91:8925–8929

Kong L, Anderson JM, Ohm HW (2005) Induction of wheat defense and stress-related genes in response to *Fusarium graminearum*. Genome 48:29–40

Kuno N, Muramatsu T, Hamazato F, Furuya M (2000) Identification by large-scale screening of phytochrome-regulated genes in etiolated seedlings of *Arabidopsis* using a fluorescent differential display technique. Plant Physiol 122:15–24

Kuo WP, Jenssen TK, Butte AJ, Ohno-Machado L, Kohane IS (2002) Analysis of matched mRNA measurements from two different microarray technologies. Bioinformatics 18:405–412

Lee JY, Lee DH (2003) Use of serial analysis of gene expression technology to reveal changes in gene expression in *Arabidopsis* pollen undergoing cold stress. Plant Physiol 132:517–529

Liang P, Pardee AB (1992) Differential display of eukaryotic messanger RNA by means of the polymerase chain reaction. Science 257:967–971

Ma LG, Chen C, Liu XG, Jiao YL, Su N, Li L, Wang XF, Cao ML, Sun N, Zhang XQ, Bao JY, Li J, Pedersen S, Bolund L, Zhao HY, Yuan LP, Wong GKS, Wang J, Deng XW, Wang J (2005) A microarray analysis of the rice transcriptome and its comparison to *Arabidopsis*. Genome Res 15:1274–1283

Meyer RC, Goldsbrough PB, Woodson WR (1991) An ethylene-responsive flower senescence-related gene from carnation encodes a protein homologous to glutathione s-transferases. Plant Mol Biol 17:277–281

Nguyen HT, Leipner J, Stamp P, Guerra-Peraza O (2009) Low temperature stress in maize (*Zea mays* L.) induces genes involved in photosynthesis and signal transduction as studied by suppression subtractive hybridization. Plant Physiol Biochem. 47:116–122

Ohmiya A, Tanase K, Hirashima M, Yamamizo C, Yagi M (2013) Analysis of carotenogenic gene expression in petals and leaves of carnation (*Dianthus caryophyllus* L.). Plant Breed 132:423–429

Ohmiya, A., M. Hirashima, M. Yagi, K. Tanase and C. Yamamizo (2014) Identification of genes associated with chlorophyll accumulation in flower petals. Plos One 9. https://doi.org/10.1371/journal.pone.0113738

Park KY, Drory A, Woodson WR (1992) Molecular cloning of an 1-aminocyclopropane-1-carboxylate synthase from senescing carnation flower petals. Plant Mol Biol 18:377–386

Raghothama KG, Lawton KA, Goldsbrough PB, Woodson WR (1991) Characterization of an ethylene-regulated flower senescence-related gene from carnation. Plant Mol Biol 17:61–71

Saito K, Kobayashi M, Gong ZZ, Tanaka Y, Yamazaki M (1999) Direct evidence for anthocyanidin synthase as a 2-oxoglutarate-dependent oxygenase: molecular cloning and functional expression of cDNA from a red forma of *Perilla frutescens*. Plant J 17:181–189

Schena M, Shalon D, Davis RW, Brown PO (1995) Quantitative monitoring of gene-expression patterns with a complementary-DNA microarray. Science 270:467–470

Sekhon, R. S., R. Briskine, C. N. Hirsch, C. L. Myers, N. M. Springer, C. R. Buell, N. de Leon and S. M. Kaeppler (2013) Maize Gene atlas developed by RNA sequencing and comparative evaluation of transcriptomes based on RNA sequencing and microarrays. Plos One 8. https://doi.org/10.1371/journal.pone.0061005

Streit S, Michalski CW, Erkan M, Kleeff J, Friess H (2008) Northern blot analysis for detection and quantification of RNA in pancreatic cancer cells and tissues. Nature Protocol 4:37–43

Tanase, K., C. Nishitani, H. Hirakawa, S. Isobe, S. Tabata, A. Ohmiya and T. Onozaki (2012) Transcriptome analysis of carnation (*Dianthus caryophyllus* L.)

based on next-generation sequencing technology. BMC Genomics 13. https://doi.org/https://doi.org/10.1186/1471-2164-13-292

tenHave A, Woltering EJ (1997) Ethylene biosynthetic genes are differentially expressed during carnation (*Dianthus caryophyllus* L.) flower senescence. Plant Mol Biol 34:89–97

Unamba, CIN, Nag A, Sharma RK (2015) Next generation sequencing technologies: the doorway to the unexplored genomics of non-model plants. Front Plant Sci 6. 10.3389/fpls.2015.01074

Valasek MA, Repa JJ (2005) The power of real-time PCR. Adv Physiol Educ 29:151–159

Verlinden S, Boatright J, Woodson WR (2002) Changes in ethylene responsiveness of senescence-related genes during carnation flower development. Physiol Plant 116:503–511

Villacorta-Martin C, Sanchez-Garcia AB, Villanova J, Cano A, van de Rhee M, de Haan J, Acosta M, Passarinho P, Perez-Perez JM (2015) Gene expression profiling during adventitious root formation in carnation stem cuttings. BMC Genomics 16. 10.1186/s12864-015-2003-5

Vos P, Hogers R, Bleeker M, Reijans M, Vandelee T, Hornes M, Frijters A, Pot J, Peleman J, Kuiper M, Zabeau M (1995) Aflp—a new technique for DNA-fingerprinting. Nucleic Acids Res 23:4407–4414

Vuylsteke M, Peleman JD, van Eijk MJ (2007) AFLP-based transcript profiling (cDNA-AFLP) for genome-wide expression analysis. Nat Protoc 2:1399–1413

Wan XL, Zhou Q, Wang, YY, Wang WE, Bao MZ, Zhang JW (2015) Identification of heat-responsive genes in carnation (*Dianthus caryophyllus* L.) by RNA-seq. Front Plant Sci 6

Welsh J, Chada K, Dalal SS, Cheng R, Ralph D, Mcclelland M (1992) Arbitrarily primed PCR fingerprinting of RNA. Nucleic Acids Res 20:4965–4970

Woodson WR, Park KY, Drory A, Larsen PB, Wang H (1992) Expression of ethylene biosynthetic-pathway transcripts in senescing carnation flowers. Plant Physiol 99:526–532

Yagi M, Kosugi S, Hirakawa H, Ohmiya A, Tanase K, Harada T, Kishimoto K, Nakayama M, Ichimura K, Onozaki T, Yamaguchi H, Sasaki N, Miyahara T, Nishizaki Y, Ozeki Y, Nakamura N, Suzuki T, Tanaka Y, Sato S, Shirasawa K, Isobe S, Miyamura Y, Watanabe A, Nakayama S, Kishida Y, Kohara M, Tabata S (2014) Sequence analysis of the genome of carnation (*Dianthus caryophyllus* L.). DNA Res 21:231–241

Yu H, Goh CJ (2000) Identification and characterization of three orchid MADS-box genes of the AP1/AGL9 subfamily during floral transition. Plant Physiol 123:1325–1336

Yung MH, Schaffer R, Putterill J (1999) Identification of genes expressed during early *Arabidopsis* carpel development by mRNA differential display: characterisation of ATCEL2, a novel endo-1,4-beta-D-glucanase gene. Plant J 17:203–208

Zhu T, Wang X (2000) Large-scale profiling of the *Arabidopsis* transcriptome. Plant Physiol 124:1472–1476

3 Construction of Linkage Maps and Development of Useful DNA Markers for Carnation Breeding

Masafumi Yagi

Abstract

Although many carnation cultivars are already grown, demand from growers and consumers for new cultivars is high. To increase the efficiency of breeding, DNA markers have been used in various agronomic crops. However, DNA markers for breeding are scarce in ornamental plants, including carnations. In the past decade, in order to improve selection efficiency for breeding bacterial wilt (CBW)-resistant carnations, tightly linked DNA markers and simple-sequence repeat-based genetic linkage maps have been developed. The CBW-resistant standard-type cultivar 'Karen Rouge' and spray-type cultivar 'Momokaren' were bred by DNA marker-assisted selection. Additionally, the development of next-generation sequencing technology has made the development of DNA markers and high-density linkage maps more cost-effective and efficient. In this chapter, linkage maps and useful markers developed for carnation breeding are summarized.

3.1 Introduction

The carnation (*Dianthus caryophyllus* L.) is a cut flower that belongs to the family Caryophyllaceae. Carnations are one of the most important ornamental flowers, together with roses and chrysanthemums. More than 30,000 carnation cultivars have been developed worldwide (Ince and Karaca 2015), many with attractive characteristics such as unusual flower colors or forms, large flowers, a pleasant fragrance, high flower yield, resistance to disease, and longer vase life (Onozaki 2018). In current carnation breeding, elite cultivars are crossed and selected, and prominent cultivars are propagated vegetatively. These methods are dependent upon breeders' observations.

Plant genomes have been extensively studied using molecular techniques; for example, DNA markers to detect genetic variation at the DNA level have been developed. Marker-assisted selection (MAS), a method that uses DNA markers closely linked to relevant traits, shows great promise as a means of boosting the efficiency of the carnation breeding process. MAS enables accurate selection regardless of environmental factors, even at the seedling stage. It has been used in various crop breeding programs, and many commercial cultivars have been developed as a result (Francia et al. 2005; Xu and Crouch 2008). In ornamental breeding programs, genomic techniques such as MAS are not widely

M. Yagi (✉)
Institute of Vegetable and Floriculture Science, NARO, 2-1 Fujimoto, Tsukuba 305-0852, Ibaraki, Japan
e-mail: myagi@affrc.go.jp

T. Onozaki and M. Yagi (eds.), *The Carnation Genome*, Compendium of Plant Genomes,
https://doi.org/10.1007/978-981-15-8261-5_3

available, despite expectations (De Riek and Debener 2010; Yagi 2013, 2015; Smulders et al. 2019). In this chapter, the construction of linkage maps and the development of DNA markers in carnations will be summarized, with reference mainly to our study. The development of the bacterial wilt (CBW)-resistant carnation cultivars 'Karen Rouge' and 'Momokaren' by MAS will also be introduced.

3.2 Construction of Genetic Linkage Maps in Carnations

The construction of genetic linkage maps is a key step that serves several purposes in studies of genome structure, map-based cloning of agriculturally valuable genes, and mapping of quantitative trait loci (QTL). The linkage maps reported in carnations to date are listed in Table 3.1.

3.2.1 Randomly Amplified Polymorphic DNA (RAPD) Marker-Based Linkage Map

To map the genetic loci involved in resistance to CBW derived from wild *D. capitatus* Balbis ex DC. ssp. *andrzejowskianus* Zapal, the first molecular linkage map was constructed using 134 progeny (NP population) derived from a cross between 'Carnation Nou No. 1′ and 'Pretty Favvare', a susceptible cultivar (Yagi et al. 2006a). 'Carnation Nou No. 1′ is the F_1 line of a cross between a highly resistant wild species, *D. capitatus* ssp. *andrzejowskianus*, and carnation 'Super Gold' (Onozaki et al. 2002), and is used as breeding material to produce highly resistant progeny. To construct the linkage map, RAPD analysis was first conducted. RAPD markers can quickly generate a large number of polymorphisms, produce a large number of scorable loci per single assay, and generally give a broad coverage of the genome (Staub et al. 1996). A total of 1161 arbitrary primers were screened in the RAPD reaction using DNA isolated from parental lines; of these, 137 showed polymorphism between parents.

Smulders et al. (2000, 2003) had previously reported 16 simple-sequence repeat (SSR) markers in *Dianthus*, nine of which were polymorphic in our mapping population. The 137 RAPD and 9 SSR markers identified 16 linkage groups (LGs) covering 605.0 cM. This genetic linkage map revealed that the LGs in carnations differ from the haploid number (x = 15) and exposed the presence of several minor LGs.

3.2.2 SSR Marker-Based Linkage Map

Generally, RAPD does not require the nucleotide sequence information of target plants. However, since RAPD markers are anonymous, it is

Table 3.1 Summary of reports for the construction of the linkage map for carnation

Year	Cross combination (population name)	Population type	Number of linkage groups	Number of mapped loci	Map length (cM)	Marker types	Authors
2006	'Carnation Nou No. 1' and 'Pretty Favvare' (NP)	F_1 (n = 134)	16	146	605.0	RAPD, SSR	Yagi et al.
2012	line 85–11 and 'Pretty Favvare' (85P)	F_2 (n = 90)	16	178	843.6	SSR	Yagi et al.
2013	line 85–11 and 'Pretty Favvare' (85P) 'Carnation Nou No. 1' and 'Pretty Favvare' (NP)	F_2 (n = 91) F_1 (n = 94)	17 15	412 348	969.6 978.3	SSR RAPD, SSR	Yagi et al.
2017	line 806-46b and 'Mizuki' (72L)	F_2 (n = 93)	15	2404	971.5	SSR, SNP	Yagi et al.

difficult to compare or to combine genetic maps produced using this method. A single SSR is comprised of tandem arrays of 2–5 bp monomeric repeat units (Staub et al. 1996), but because of their abundance throughout the genome and co-dominant expression (Morgante and Olivieri 1993), they are useful for transferring data to other segregating populations. We constructed an SSR-based genetic linkage map using a mapping population produced from line 85–11 and 'Pretty Favvare'. Line 85–11 is a breeding line that exhibits CBW resistance and long vase life. Lines with resistance derived from *D. capitatus* ssp. *andrzejowskianus* were not used as breeding materials for line 85–11. We hoped that line 85–11 would therefore represent a new source of CBW resistance. In our study, 90 F_2 populations (85P population) were used for analysis. We developed SSR markers based on SSR-enriched genomic libraries and conducted expressed sequence tag (EST) analysis (Yagi et al. 2012). We constructed SSR-enriched genomic libraries from 'Francesco' leaves. A total of 5,856 randomly selected clones were sequenced: 1,848 from the CA motif library; 1,848 from the GA motif library; 1,848 from the ATG motif library; and 312 from the TAGA motif library. Then, SSRs $\geq$15 nucleotides in length, which contained all possible combinations of di-, tri-, and tetranucleotide repeats, were identified from the sequences. We developed a total of 1,634 di-, tri-, and tetra-SSR primer pairs, 539 of which were chosen at random for testing to identify markers that showed polymorphisms between the parental line 85–11 and 'Pretty Favvare'. Ultimately, we detected 59 polymorphic SSR markers in our mapping population. We also analyzed 11,616 and 3,936 cDNA clones randomly selected from the cDNA libraries of young plants and flower buds, respectively, of 'Francesco'. We identified 2,689 di-, tri-, and tetranucleotide SSRs of 15 bp or more in the non-redundant EST sequences. A total of 109 markers were confirmed as reproducible single-locus polymorphisms by means of fluorescent fragment analysis. A further 10 markers from previous reports (Smulders et al. 2002, 2003; Kimura et al. 2009) and EST sequences registered in the NCBI database were also mapped. This revealed a total of 178 SSR markers that showed single-locus polymorphisms in our mapping population. Of these, 68 were genomic SSR markers and the other 110 were EST-SSR markers. Linkage analysis with a minimum LOD score of 5.0 revealed 16 LGs. The map covered 843.6 cM with an average distance of 6.5 cM between two loci, although it was not saturated.

3.2.3 Construction of a Reference Linkage Map

Production of a high-density genetic map would be useful for breeding purposes and genetic research. Yagi et al. (2013) refined the SSR-based genetic linkage map to include 412 SSR loci covering 978.3 cM, adding 234 new SSR markers derived from genomic SSR libraries and transcriptome analysis (Tanase et al. 2012) via next-generation sequencing (NGS).

Tanase et al. (2012) obtained 1,417,410 sequences from 454 sequencing, leaving a total of 485,507 unique sequences after cleaning, clustering, and assembly. A search for di-, tri-, tetra-, and pentanucleotide repeats identified a total of 17,362 potential SSRs in 14,291 unigenes, and 4,177 SSR primer pairs were designed. Of 897 SSR primers that included di- and trinucleotide SSR motifs, 107 produced amplicons that were polymorphic (Yagi et al. 2013). Additionally, 62 and 65 novel markers derived from the previously developed SSR-enriched genomic libraries and EST analysis, respectively, were also mapped. Linkage analysis with a minimum LOD score of 7.0 revealed 17 LGs. We also updated the RAPD-based linkage map for the NP population. By adding 192 SSR, 8 RAPD, and 2 sequence-tagged site (STS) loci, the RAPD-based genetic linkage map was refined to include 15 LGs consisting of 348 loci covering 978.3 cM.

Comparison of the 85P and NP linkage maps revealed that the positions of SSR loci mapped to both LGs were conserved between LGs. These results indicated that four of the five minor LGs

identified in the 85P population could be consolidated into two LGs. Consequently, the number of LGs for the 85P population corresponded to the basic carnation chromosomal number (x = 15). The improved genetic linkage maps have many SSR markers that showed co-dominant inheritance and are comprehensively available in carnations. As it included many more markers, the 85P population linkage map will serve as a genetic reference for carnations and other members of the genus *Dianthus*, and should be useful for mapping QTLs associated with various traits and for improving carnation breeding programs.

3.2.4 Higher-Density Linkage Map

Linkage maps with more markers are of greater value for genetic analysis. To develop a higher-density genetic linkage map, we tried to challenge a cost-effective method for SNP detection, double digest restriction site-associated DNA sequencing (ddRAD-Seq), based on the protocol developed by Shirasawa et al. (2016) (Yagi et al. 2017).

We used 93 F_2 progenies (72L population) of the carnation breeding line 806-46b and 'Mizuki' for map construction. First, 412 SSR markers (282 EST and 130 genomic) mapped on the 85P linkage map (Yagi et al. 2013) were screened; thus, we mapped 161 markers. Screening of 1248 newly developed SSR primer pairs with trinucleotide SSR motifs derived from RNA-Seq analysis (Tanase et al. 2012) revealed 129 SSR markers with polymorphisms in this study.

Next, we conducted ddRAD-Seq analysis. A total of 289.01 million paired-end reads for the 96 samples (3.01 million paired-end reads on average) were obtained from a single flow cell lane on an Illumina HiSeq2000. After trimming low-quality data and adapter sequences, 94% of 2.97 million high-quality reads for each line were successfully mapped onto the carnation reference genome sequence to detect 121,044 SNP candidates. After selecting SNP loci heterozygous in the F_1 generation with both alleles also present in the grandparents (806-46b and Mizuki), we obtained 2454 SNPs that were segregated in the F_2 population. Linkage analysis identified a high-density linkage map based on a combination of SSR and SNP markers developed by ddRAD-Seq. A total of 2404 markers (285 SSR and 2119 SNP) were assigned to 15 LGs spanning 971.5 cM, with an average marker interval of 0.4 cM (Yagi et al. 2017). Comparative analysis between a reference linkage map (Yagi et al. 2013) and the high-density linkage map demonstrated that the marker positions and alignments showed good collinearity. The marker density (marker/cM) was 2.5, which was greater than that of the previous map (0.42; Yagi et al. 2013).

3.3 Development of a Useful DNA Marker

The purpose of linkage maps is to identify loci for important traits and linked DNA markers. Tightly linked DNA markers can make breeding faster and more efficient. Known DNA markers linked to important traits are unfortunately scarce in carnations, but the availability of a high-density linkage map and genome sequence will accelerate the development of very precise DNA markers. The reported DNA markers linked to important traits in carnations are listed in Table 3.2.

3.3.1 CBW Resistance Derived from *D. capitatus*

CBW, caused by *Burkholderia caryophylli* (Burkholder) Yabuuchi, Kasako, Oyaizu, Yano, Hotta, Hashimoto, Ezaki, and Arakawa, is one of the most damaging diseases affecting carnation cultivation in Japan. It causes serious crop losses, especially in summer. *Burkholderia caryophylli* also infects *Limonium sinuatum* Mill. (Jones and Engelhard 1984) and *Eustoma grandiflorum* (Furuya et al. 2000). First found in Washington, USA, in 1941 (Jones 1941), CBW has since expanded into European countries. The main symptoms are sudden wilting, vascular discoloration, and root rot. The disease is difficult to

Table 3.2 Useful markers for carnation breeding

Year	Traits	Marker type	Authors
1997	Single flower	RAPD, STS	Scovel et al.
2004	Major QTL for carnation bacterial wilt (CBW) resistance derived from *Dianthus capitatus* ssp. *andrezejowskianus*	RAPD, STS	Onozaki et al.
2006	Single flower type derived from *D. capitatus* ssp. *andrezejowskianus*	RAPD, STS	Onozaki et al.
2012	QTL for CBW resistance from line 85–11	SSR	Yagi et al.
2013	Double flower	SSR	Yagi et al.
2020	QTL for flowering time	SNP, Indel	Yagi et al.

control because the pathogen infects the roots, colonizes the vascular system, and produces no external symptoms (Onozaki 2006). In 1988, NIVFS initiated a breeding program for CBW resistance.

Onozaki et al. screened 277 cultivars and 70 wild *Dianthus* accessions to identify species resistant to CBW. There were no highly resistant cultivars at that time (Onozaki et al. 1999a), although Onozaki et al. (1999b) finally found a highly resistant wild species, *D. capitatus* ssp. *andrzejowskianus*. Subsequently, Onozaki et al. (2002) succeeded in introducing resistance from *D. capitatus* ssp. *andrzejowskianus* into carnation cultivars and produced a new CBW-resistant line, 'Carnation Nou No. 1′. However, this line has traits that make it unsuitable for cut flower use, such as small flowers and short stems. To remove only the unwanted characteristics derived from *D. capitatus* ssp. *andrzejowskianus* and retain resistance, repeated crossing and selection for resistance to CBW was conducted.

The cut-root-soaking method used to select progeny that were resistant to CBW took more than 3 months, and screening the large quantities of data produced was a labor-intensive task. First, Onozaki (2004) tried to develop a linked marker for bulked segregant analysis. A total of 505 RAPD primers were screened; 8 of these, identified by bulked segregant analysis, were thought to be linked to a major CBW resistance gene. QTL analysis was performed using the partially constructed linkage map. Of the markers identified, WG44-1050 had the greatest effect on resistance to bacterial wilt. WG44-1050 (hereafter referred to as STS-WG44) was successfully converted to a single band.

The major disadvantage of the RAPD technique is its low reproducibility (Debener 2002). Further, the RAPD technique is highly sensitive to reaction conditions (Scovel et al. 1998), and there are differences in amplification level among PCR machines from various manufacturers. STS markers are PCR-based markers generated by a pair of primers (about 20 bases long) designed according to known DNA sequences (Olson et al. 1989).

QTL analysis performed using the updated NP linkage map, identified one major and one minor QTL in LG NP_4 (LOD = 22.1) and LG NP_13 (LOD = 2.8), respectively. We named the major QTL *Cbw1* (CBW resistance locus 1) and the minor QTL *Cbw2*. The nearest marker to *Cbw1* was STS-WG44, in agreement with previous results (Onozaki et al. 2004; Yagi et al. 2006a). There were no other significant QTLs with an LOD score above 2.7, which was the minimum LOD score after 1000 permutation tests; hence, *Cbw3*, which had a low LOD score of 2.3 in our previous study (Yagi et al. 2006a),

was not included in the revised map. This may be a result of differences in the number and orientation of markers on linkage maps, or among analysis software (MAPMAKER vs. WinQTL Cartographer).

To evaluate the utility of these markers for developing resistant lines, the presence of the identified markers was investigated in backcross lines strongly resistant to CBW (Yagi et al. 2006b). The STS-WG44 marker, which is the marker nearest *Cbw1*, was present in all lines up to the BC_4 generation. However, OQ12, a marker in LG NP_13 linked to a QTL with a minor effect on resistance, was found only in the F_1 generation. Furthermore, its incidence declined in successive generations and was totally absent in the BC_4 generation. The other markers located in LG NP_3 have not been tested before now. This result demonstrates the efficacy of the STS-WG44 marker in selecting resistant plants.

To ascertain whether STS-WG44 could also be used in actual breeding, disease incidence in relation to the presence of this marker was investigated in a total of 98 lines derived from crosses between susceptible and resistant backcross lines (Yagi et al. 2006b). Investigation of disease incidence in these 98 lines by the root-soaking inoculation method revealed a mean disease incidence ranging from 0 to 100%, showing a large segregation for resistance. The mean disease incidence was 28.5% in the 64 lines carrying STS-WG44 and 91.1% in the 34 lines lacking STS-WG44, revealing a significant difference of 62.6% depending on the presence or absence of STS-WG44 (Fig. 3.1). These findings suggest that STS-WG44 is a selective marker that facilitates the selection of highly resistant plants for practical breeding.

By showing how STS-WG44 could be used as a selection marker to select for low mean disease incidence and strong CBW resistance, this study demonstrated the potential for MAS in the breeding of carnations.

3.3.2 Breeding of 'Karen Rouge' by MAS

In 2010, using both traditional disease screening and MAS, Yagi et al. (2010) developed a new red standard-type cultivar, 'Karen Rouge' (Fig. 3.2). This cultivar had both high bacterial wilt resistance and other traits desirable for ornamental use. Many bacterial wilt resistant lines in early breeding populations had undesirable characteristics, such as a low number of petals, dark flower color, or non-rigid stems, which were assumed to be derived from the wild species. Repeated crossing with more desirable cultivars gradually improved these unwanted characteristics in later generations (Fig. 3.2). In 2004, MAS with the STS-WG44 marker was initiated. To the best of our knowledge, 'Karen Rouge' is the first carnation cultivar produced using MAS technology. The mean disease incidence in 'Karen Rouge' was 7.1%, ranging from 0.0 to 19.0% across six tests. In these tests, the susceptible carnation cultivars began to wilt 20 days after inoculation and most plants were dead within 49 days. Conversely, however, most of the 'Karen Rouge' plants survived the entire 91-day test. In addition to high CBW resistance, 'Karen Rouge' also showed high flower quality and adequate flower yields for commercial production.

NIVFS have collaborated with Nagasaki prefecture to breed CBW-resistant carnations since 2009. Finally, in 2018, Nagasaki prefecture and NIVFS announced the name of a new highly resistant carnation cultivar: 'Momokaren' (Figs. 3.3, 3.4, Takebe et al. 2020). 'Momokaren' is the first CBW-resistant spray-type cultivar and is the progeny of 'Karen Rouge' and 'Daisuki', which are the original pink carnation cultivars bred by Nagasaki prefecture. MAS using STS-WG44 markers was conducted in the breeding process. This shows that the combination of breeding material and DNA markers improve breeding efficiency and speed up the production of new cultivars.

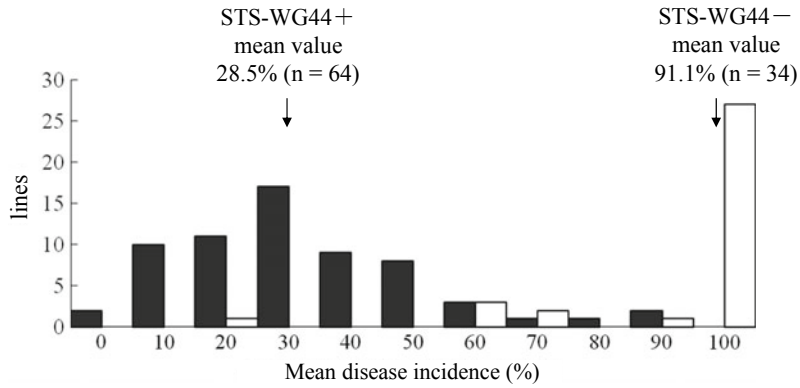

Fig. 3.1 Relationship between the presence of the STS-WG44 marker and the incidence of bacterial wilt in a practical carnation breeding population

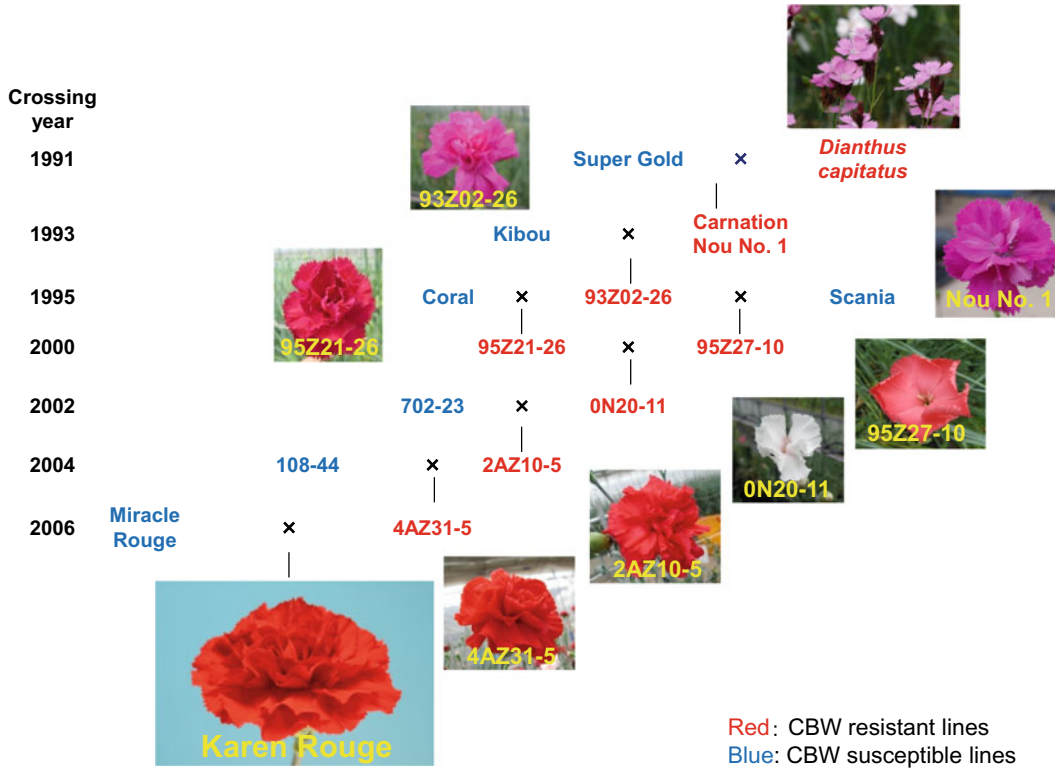

Fig. 3.2 Breeding process of "Karen Rouge"

3.3.3 CBW Resistance from Line 85–11

During breeding for improved flower longevity, Yagi et al. (2012) unexpectedly identified line 85–11, which exhibited a significant level of CBW resistance not derived from *D. capitatus* ssp. *andrzejowskianus*. To develop markers linked to the CBW resistance of line 85–11, Yagi et al. (2012) constructed an SSR-based genetic linkage map using F_2 populations of line 85–11 and a susceptible cultivar ('Pretty Favvare').

Fig. 3.3 Bacterial wilt-resistant carnation cultivar 'Momokaren'

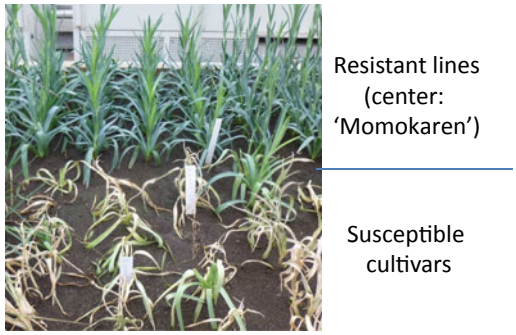

Fig. 3.4 Bacterial wilt-resistance test in carnations 35 days after inoculation

A new carnation map was constructed that included 178 SSRs in 16 LGs covering 843.6 cM (Yagi et al. 2012). QTL analysis for CBW resistance revealed only one QTL in LG 85P_4 (*Cbw4*), with two tightly linked SSR markers identified adjacent to the *Cbw4* locus: CES2643 and CES1161 (Fig. 3.5).

Interestingly, comparative analysis of CBW resistance loci between LG 85P_4 (*Cbw4*) and LG NP_4 (*Cbw1*) using SSR markers revealed nearly identical positions in both LGs (Fig. 3.6). We expected the *Cbw4* derived from line 85–11 was the origin of resistance; however, its position on the map was almost same as that of *Cbw1*. The CBW resistance of line 85–11 depended upon the conditions of the test for resistance and the resistance of the progeny of line 85–11 was not as high as expected (unpublished data). As such, we concluded that *D. capitatus* ssp. *andrzejowskianus* is better breeding material than line 85–11. However, whether or not the resistant gene located on the same locus is truly the same gene is an interesting question. Isolation of the gene responsible for *Cbw1* and *Cbw4* is a future goal.

3.3.4 Mapping of Flower Color

Carnation flowers exhibit various colors and patterns. The flower pigments in carnations are anthocyanin glucosides derived from pelargonidin and cyanidin, and flavonol derivatives based on kaempferol and quercetin (Nakayama et al. 2000). The metabolism of these and other flavonoids has been well studied in carnation flowers (Itoh et al. 2002; Mato et al. 2000; Matsuba et al. 2010). Using a population segregated for CBW resistance, Yagi et al. (2013) identified two QTLs governing anthocyanin content in flower petals: carnation anthocyanin pigmentation loci1 (*Cap1*) and 2 (*Cap2*) in LGs NP_4 and 10, respectively. *Cbw1* was located in the same LG as *Cap1*. In the course of breeding 'Karen Rouge', many resistant lines in the initial breeding populations were observed to have purplish flowers (Fig. 3.2). This phenomenon may be attributed to linkage between the major resistance gene and the QTL for anthocyanin pigmentation. Future mapping of genes involved in anthocyanin biosynthesis may reveal whether any of these genes correspond to the identified QTL and lead to the development of useful DNA markers for flower color.

3.3.5 Doubleness

Doubleness is an important breeding target in ornamental plants. Flowers of wild *Dianthus* have five petals. During domestication and selection, carnation flowers with more than five petals, called "double flower" cultivars, have been selected. A simultaneous increase in the number of petals and other floral organs is commonly observed in floricultural plants, including not only carnations but also petunias and garden balsam (Nishijima 2012). Each floral organ in double flowers is fully functional.

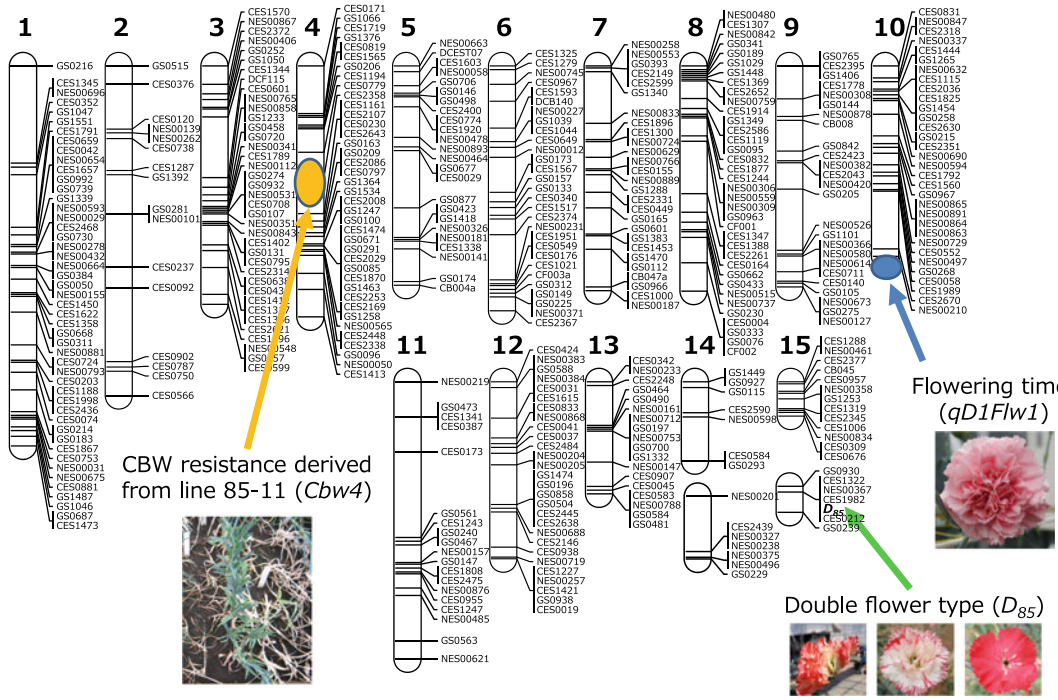

Fig. 3.5 Reference linkage map of 412 SSR markers in 85P population and mapped traits in carnations

However, very little is known about the genetics of doubleness in carnations (Conners 1913; Saunders 1917). Saunders (1917) suggested that the carnation flower phenotype was a monogenic trait and named the locus involved 'D', whereby the recessive homozygote allele (dd) is the single flower type, the heterozygote (Dd) is double, and the dominant homozygote (DD) is super double.

Scovel et al. (1998) developed RAPD and RFLP markers linked to the single flower locus *d*. Onozaki et al. (2006) identified a single flower locus (*d*) in LG NP_15 of the NP population and DNA markers linked to a recessive gene controlling single flower type derived from *D. capitatus* ssp. *andrzejowskianus*. Using the 85P mapping population, Yagi et al. (2014b) located the D_{85} locus for flower type (double or single) in LG 85P_15-2 and identified four co-segregating SSR markers (Fig. 3.5). They concluded that among the four markers, CES1982 and CES0212 were linked to the D_{85} locus, and the 176 bp allele of CES1982 and the 269 bp allele of CES0212 were tightly linked to the dominant *D* allele responsible for the double flower phenotype. Co-dominant markers were linked to doubleness (*D*) to easily discriminate between DD and Dd.

In roses, the locus controlling the simple versus double corolla phenotype, referred to as *Blfo* or *d6*, has been identified through genetic mapping studies in LG3 (Crespel et al. 2002; Debener and Mattiesch 1999; Smulders et al. 2019), Hibrand Saint-Oyant et al. (2018). identified a rose APETALA2/TOE homologue within the QTL region in LG3 as the most likely candidate gene for the major regulator of petal number in roses; silencing it decreased the number of petals. It was proposed that insertion of a TE in the intron is responsible for transcription of a messenger RNA without an miR172 binding site, leading to deregulation of the APETALA2/TOE homologue (François et al. 2018; Gattolin et al. 2018). A similar mechanism was proposed in *Camellia* (Li et al. 2017), and the results suggest that a similar mechanism also occurs in carnations. In carnations, as a result of expanding 85P mapping population to 543 progenies from 121 progenies, all progenies were

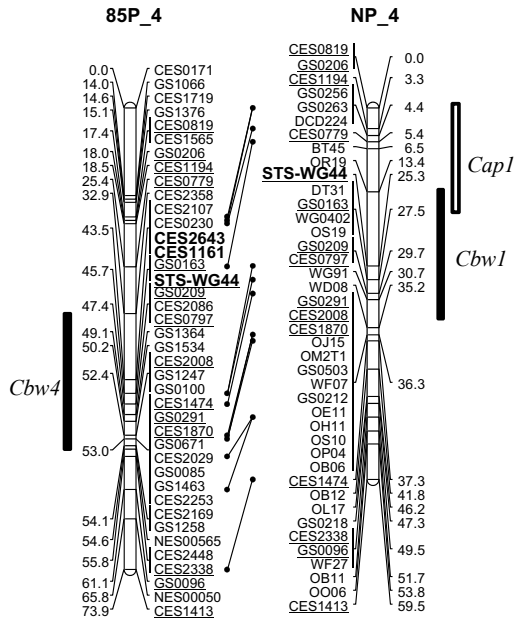

Fig. 3.6 Genetic map of the genomic region containing major QTLs for carnation bacterial wilt resistances (*Cbw4* and *Cbw1*). Marker names and map distances (cM) are shown on opposite sides of each linkage group. *Cap1* is one of the QTLs governing carnation anthocyanin pigmentation. Markers located on both maps are underlined and connected by lines

identical between the genotypes of CES0212 and the flower type (single or double); however, but one progeny showed double flower despite having the 'dd' genotype (single flower type) at the CES1982 locus. This result revealed that the CES0212 locus is more tightly linked to the D_{85} locus compared with the CES1982 locus (Yagi et al. 2015). The search for the sequence of CES0212 marker to carnation genome DB (Yagi et al. 2014a) identified the scaffold 2131; moreover, the sequence of CES0212 was found to be a part of the Dca21029.1 gene (Fig. 3.7). Surprisingly, searching the neighboring genes of the Dca21029.1 gene identified Dca21030.1, which is annotated to the AP2 homologous gene (Fig. 3.7) (Yagi et al. 2015). Subsequently, we determined 6292 bp of the genome sequence surrounding Dca21030.1, including the promoter and 3′ sequence in the single flower 'Pretty Favvare'. Some insertions or deletions and SNPs were identified between the double flower 'Francesco' and the single flower 'Pretty Favvare'. Moreover, large differences were identified at the regulation site of miRNA 172 of this gene: 1019 bp insertion sequence was found in the double flower 'Francesco' genome (Fig. 3.8a). To confirm the insertion in double flower cultivars, we developed primer set to detect the insertion (Fig. 3.8a). Approximately 613-bp sequences including insertions (using primer-1 and -2) were commonly observed in double flowers (Fig. 3.8b). Approximately 1716-bp sequences were commonly observed in double flowers and 700-bp sequences were commonly observed in single flowers (Fig. 3.8b). 'Nora' and 'Barbara' were supposed to be heterozygous at this locus (Fig. 3.8b). These results suggested that such large insertion sequences are present only in double flower cultivars and are absent in single-flower cultivars or *Dianthus* (Fig. 3.8). We confirmed that that of >30 the tested cultivars, all double cultivars commonly had such large insertion sequences (data not shown). Until now, there was no direct evidence for the origin of doubleness in carnations owing to such insertions; the results of this study suggest that the mutation of *AP2* is related to doubleness even in carnations.

3.3.6 Flowering Time

There are large differences in flowering times among carnation cultivars. Carnations are quantitatively long-day plants that flower fastest when exposed to light for long periods, but they can initiate flowering and flower when the days are short given more time (Holly and Baker 1991). Generally, long-day treatment accelerates flowering and retards secondary shoot development, but the effect is highly dependent on the genotype of the carnation cultivar in question (Sparnaaij et al. 1990).

The genetic architecture and molecular pathways controlling flowering time are well-described in model systems such as *Arabidopsis thaliana* and are becoming clearer for important agronomic crops (Blümel et al. 2015; Putterill and Varkonyi-Gasic 2016). However,

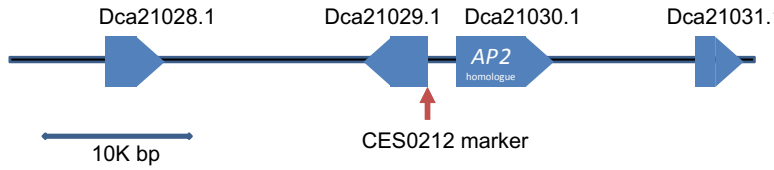

Fig. 3.7 Genomic structure of scaffold2131 including CES0212 marker tightly linked to double flower

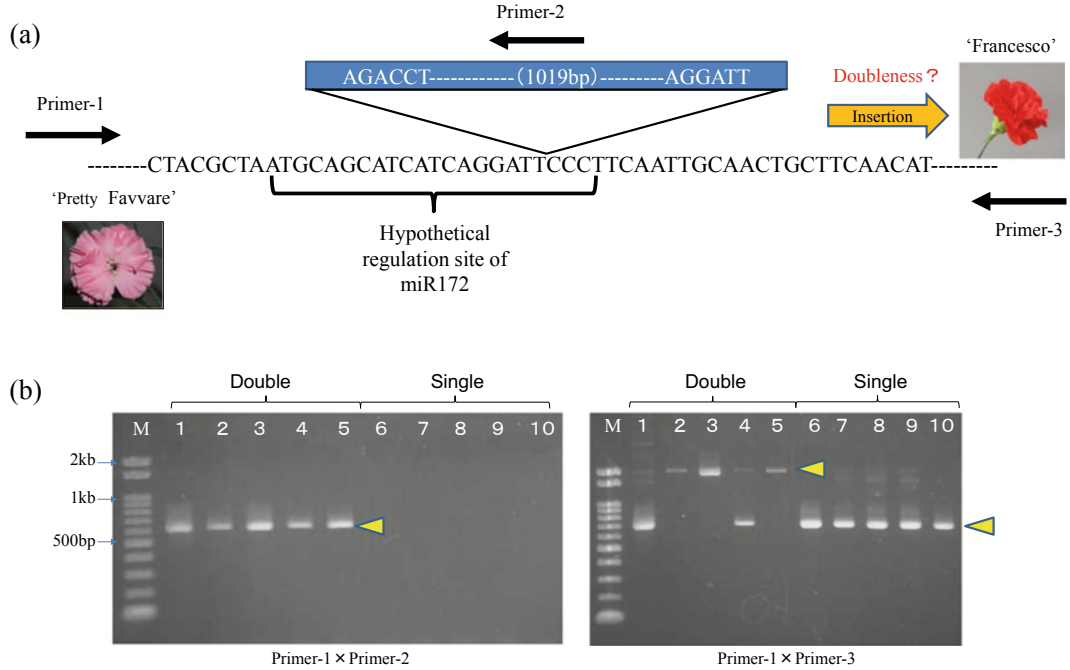

Fig. 3.8 Genomic structure of the miR172 regulation site of Dca21030.1 gene of 'Pretty Favvare' and 'Francesco' (**a**), and the figures of amplified PCR fragments in those regions using double and single flower cultivars (**b**). **a** Primer sequence are primer-1 (5′TTGTCGCTGACCAAGAAGTG 3′, named as DoubleSingle1-F), primer-2 (5′GTTGTCTTCGGGTTCGAGTG3′, Double2-R), and primer-3 (5′AGCGACCAAGTGACCAAAAC3′, Single2-R), respectively. **b** M: 100 bp ladder, 1: 'Nora', 2: 'Francesco', 3: 'Excerea', 4: 'Barbara', 5: 'Komachi', 6: 'Pretty Favvare', 7: 'Youkihi', 8: 'Sonnet Sailor', 9: 'Sonnet Miho', 10: *Dianthus capitatus* ssp. *andrzejowskianus* (1–5: double flowers, 6–10 single flowers). Targeted amplicons are indicated by arrow heads

the genetic basis for flowering time in carnations is still poorly understood.

We conducted QTL analysis for flowering time using two previously developed mapping populations (85P and 72L) (Yagi et al. 2020). We developed a DNA marker that was linked to the major QTL for flowering time and validated its effectiveness in a different population. Thus, a common QTL for flowering time was detected in LG 10, even though two different mapping populations over different years were used in the analysis. We found no other QTL above the threshold LOD value in the permutation tests. We named the common QTL for D1Flw (the first flower opening day) detected in LG 10 *qD1Flw1* (Fig. 3.5). We developed a qD1Flw1-sc43-4 marker in the neighboring scaffold. qD1Flw1-sc43-4 markers were developed based on sequence differences between mapping parents as the marker that sandwiched the deleted regions to detect polymorphisms. To evaluate the effectiveness of the DNA marker in another

population, we developed F_1 progeny by crossing late-flowering 'Light Pink Barbara' and early-flowering 'Kaneainou 1 go' (Hotta et al. 2016). There was a difference of 47.2 d in flowering time between lines that carried the 'Light Pink Barbara' allele and those that did not. This result implies that the qD1Flw1-sc43-4 marker could be valuable for distinguishing flowering times in other carnation populations.

We are identifying the gene or genes responsible for flowering time and searching unidentified QTL for flowering time. This works will contribute to our understanding of the control of and overall mechanism of flowering in carnations.

3.4 The Future of Carnation Genomics and Genetics

We developed DNA markers and related genomic analysis tools for use in carnation breeding. In early research, the construction of linkage maps took years; however, the birth of NGS technology has shortened this time, and today only around ten days are required to construct high-density genetic linkage maps. The cost of NGS analysis has also been decreasing year by year. Thus, SNP detection from whole-genome resequencing of mapping populations is a realistic alternative to partial genome analysis methods such as RAD-Seq. There are a lot of important breeding targets in carnations, such as flower longevity and *Fusarium* resistance. Efficient construction of linkage maps will contribute useful DNA markers to breeding programs. Although the structure of populations derived from narrow genetic backgrounds must be checked, genome-wide association study (GWAS) analysis, which is independent of particular crossing populations, will be effective in carnation genomic studies. It is said that more than 30,000 carnation cultivars have been produced, and various types of flowers exist. GWAS analysis has been attempted in some other ornamental plants, such as the rose. High-density SNP arrays and GWAS analysis has successfully identified regions associated with anthochyanin and carotenoids (Schulz et al. 2016), and the capacity of leaf petioles for direct shoot regeneration (Nguyen et al. 2017). In hexaploid chrysanthemums, also attempted at inflorescence trait (Chong et al. 2019) and waterlogging stress (Su et al. 2019). To successfully identify DNA markers by GWAS analysis, each trait must be precisely evaluated. Moreover, more precise genome sequences will also be needed. Currently, the available carnation genome is highly fragmented (45,088 scaffolds; Yagi et al. 2014a). At least in the early stages, construction of pseudomolecules and sequencing of heterozygous regions is necessary for future genomic studies in carnations.

Acknowledgements This work was partially supported by the JSPS KAKENHI (grant no. 26850022 and 17K07654). I sincerely thank the Japanese Society for Horticultural Science (JSHS) for Fig. 3.1 from Yagi et al. (2006b) and Fig. 3.6 from Yagi et al. (2015). Fig. 3.3 was kindly provided by Shouichi Takebe, Nagasaki Prefecture.

References

Blümel M, Dally N, Jung C (2015) Flowering time regulation in crops—what did we learn from Arabidopsis? Curr Opin Biotechnol 32:121–129. https://doi.org/10.1016/j.copbio.2014.11.023

Chong X, Su J, Wang F et al (2019) Identification of favorable SNP alleles and candidate genes responsible for inflorescence-related traits via GWAS in chrysanthemum. Plant Mol Biol 99:407–420. https://doi.org/10.1007/s11103-019-00826-w

Conners CH (1913) Multiplication of floral parts in the carnation. Am Soc Hort Sci 10:93–99

Crespel L, Chirollet M, Durel CE et al (2002) Mapping of qualitative and quantitative phenotypic traits in *Rosa* using AFLP markers. Theor Appl Genet 105:1207–1214. https://doi.org/10.1007/s00122-002-1102-2

Debener T, Mattiesch L (1999) Construction of a genetic linkage map for roses using RAPD and AFLP markers. Theor Appl Genet 99:891–899. https://doi.org/10.1007/s001220051310

De Riek J, Debener T (2010) Present use of molecular markers in ornamental breeding. Acta Hort 855:77–83

Debener T (2002) Molecular markers as a tool for analyses of genetic relatedness and selection in ornamentals. In: Vainstein A (ed) Breeding for ornamentals: classical and molecular approaches. Kluwer Academic Publishers, Dordrecht, pp 329–345

Francia E, Tacconi G, Crosatti C et al (2005) Marker assisted selection in crop plants. Plant Cell Tiss Organ Cult 82:317–342. https://doi.org/10.1007/s11240-005-2387-z

François L, Verdenaud M, Fu X et al (2018) A miR172 target-deficient AP2-like gene correlates with the double flower phenotype in roses. Sci Rep 8:12912. https://doi.org/10.1038/s41598-018-30918-4

Furuya N, Masunaga T, Khan AA et al (2000) Bacterial wilt of Russell Prairie gentian caused by *Burkholderia caryophylli*. J Gen Plant Pathol 66:316–322. https://doi.org/10.1007/PL00012971

Gattolin S, Cirilli M, Pacheco I et al (2018) Deletion of the miR172 target site in a TOE-type gene is a strong candidate variant for dominant double-flower trait in Rosaceae. Plant J 96:358–371. https://doi.org/10.1111/tpj.14036|

Hibrand Saint-Oyant L, Ruttink T, Hamama L et al (2018) A high-quality genome sequence of *Rosa chinensis* to elucidate ornamental traits. Nat Plants 4:473–484. https://doi.org/10.1038/s41477-018-0166-1

Holly WD, Baker R (1991) Carnation production II. Kendall/Hunt, Iowa

Hotta M, Hattori H, Hirano T et al (2016) Breeding and characteristics of spray type carnation 'Kaneainou 1 go' with long vase life. Res Bull Aichi Agric Res Ctr 48:63–71 (In Japanese with English summary)

Ince AG, Karaca M (2015) Td-DAMD-PCR assays for fingerprinting of commercial carnations Turk. J Biol 39:290–298. https://doi.org/10.3906/biy-1407-66

Itoh Y, Higeta D, Suzuki A et al (2002) Excision of transposable elements from the chalcone isomerase and dihydroflavonol 4-reductase genes may contribute to the variegation of the yellow-flowered carnation (*Dianthus caryophyllus*). Plant Cell Physiol 43:578–585. https://doi.org/10.1093/pcp/pcf065

Jones LK (1941) Bacterial wilt of carnation. Phytopathology 31:199

Jones JB, Engelhard AW (1984) Crown and leaf rot of statice incited by a bacterium resembling *Pseudomonas caryophylli*. Plant Dis 68:338–340

Kimura T, Yagi M, Nishitani C et al (2009) Development of SSR markers in carnation (*Dianthus caryophyllus*). J Japan Soc Hort Sci 78:115–123. https://doi.org/10.2503/jjshs1.78.115

Li X, Li J, Fan Z et al (2017) Global gene expression defines faded whorl specification of double flower domestication in *Camellia*. Sci Rep 7:3197. https://doi.org/10.1038/s41598-017-03575-2

Mato M, Onozaki T, Ozeki Y et al (2000) Flavonoid biosynthesis in white-flowered Sim carnations (*Dianthus caryophyllus*). Sci Hortic 84:333–347. https://doi.org/10.1016/S0304-4238(99)00140-5

Matsuba Y, Sasaki N, Tera M et al (2010) A novel glucosylation reaction on anthocyanins catalyzed by acyl-glucose-dependent glucosyltransferase in the petals of carnation and delphinium. Plant Cell 22:3374–3389. https://doi.org/10.1105/tpc.110.077487

Morgante M, Olivieri AM (1993) PCR-amplified microsatellites as markers in plant genetics. Plant J 3:175–182. https://doi.org/10.1046/j.1365-313X.1993.t01-9-00999.x

Nakayama M, Koshioka M, Yoshida H et al (2000) Cyclic malyl anthocyanins in *Dianthus caryophyllus*. Phytochemistry 55:937–939. https://doi.org/10.1016/S0031-9422(00)00263-6

Nishijima T (2012) Larger flower size: molecular basis and role of cytokinin. J Japan Soc Hort Sci 81:129–139. https://doi.org/10.2503/jjshs1.81.129

Nguyen THN, Schulz D, Winkelmann T et al (2017) Genetic dissection of adventitious shoot regeneration in roses by employing genome-wide association studies. Plant Cell Rep 36:1493–1505. https://doi.org/10.1007/s00299-017-2170-8

Olson M, Hood L, Cantor C et al (1989) A common language for physical mapping of the human genome. Science 245:1434–1435. https://doi.org/10.1126/science.2781285

Onozaki T (2006) Carnation. Horticulture in Japan 2006. Japan Soc Hor Sci (ed) pp 223–230

Onozaki T (2018) Dianthus. In: Van Huylenbroeck J (ed) Ornamental Crops. Springer Nature Germany, pp 349–381. https://doi.org/10.1007/978-3-319-90698-0_15

Onozaki T, Yamaguchi T, Himeno M et al (1999a) Evaluation of 277 carnation cultivars for resistance to bacterial wilt (*Pseudomonas caryophylli*). J Japan Soc Hort Sci 68:546–550. https://doi.org/10.2503/jjshs.68.546

Onozaki T, Yamaguchi T, Himeno M et al (1999b) Evaluation of wild *Dianthus* accessions for resistance to bacterial wilt (*Pseudomonas caryophylli*). J Japan Soc Hort Sci 68:974–978. https://doi.org/10.2503/jjshs.68.974

Onozaki T, Ikeda H, Yamaguchi T et al (2002) 'Carantion Nou No. 1', a carnation breeding line resistant to bacterial wilt (*Burkholderia caryophylli*). Hort Res (Japan) 1:13–16 (In Japanese with English summary). https://doi.org/10.2503/hrj.1.13

Onozaki T, Tanikawa N, Taneya M et al (2004) A RAPD-derived STS marker is linked to a bacterial wilt (*Burkholderia caryophylli*) resistance gene in carnation. Euphytica 138:255–262. https://doi.org/10.1023/B:EUPH.0000047099.48469.3c

Onozaki T, Yoshinari T, Yoshimura T et al (2006) DNA markers linked to a recessive gene controlling single flower type derived from a wild species, *Dianthus capitatus* ssp. *andrzejowskianus*. Hort Res (Japan) 5:363–367 (In Japanese with English summary). https://doi.org/10.2503/hrj.5.363

Putterill J, Varkonyi-Gasic E (2016) FT and florigen long-distance flowering control in plants. Curr Opin Plant Biol 33:77–82. https://doi.org/10.1016/j.pbi.2016.06.008

Saunders ER (1917) Studies in the inheritance of doubleness in flowers, II. Meconopsis. Althaea Dianthus J Genet 6:165–184. https://doi.org/10.1007/BF02983260

Schulz DF, Schott RT, Voorrips RE et al (2016) Genome-wide association analysis of the anthocyanin and

carotenoid contents of rose petals. Front Plant Sci 7:1798. https://doi.org/10.3389/fpls.2016.01798

Scovel G, Ben-Meir H, Ovadis M et al (1998) RAPD and RFLP markers tightly linked to the locus controlling carnation (*Dianthus caryophyllus*) flower type. Theor Appl Genet 96:117–122. https://doi.org/10.1007/s001220050717

Shirasawa K, Hirakawa H, Isobe S (2016) Analytical workflow of double-digest restriction site-associated DNA sequencing based on empirical and *in silico* optimization in tomato. DNA Res 23:145–153. https://doi.org/10.1093/dnares/dsw004

Smulders MJM, Rus-Kortekaas W, Vosman B (2000) Microsatellite markers useful throughout the genus *Dianthus*. Genome 43:208–210. https://doi.org/10.1139/g99-089

Smulders MJM, Noordijk Y, Rus-Kortekaas W et al (2003) Microsatellite genotyping of carnation varieties. Theor Appl Genet 106:1191–1195. https://doi.org/10.1007/s00122-002-1166-z

Smulders MJM, Arens P, Bourke PM et al (2019) In the name of the rose: a roadmap for rose research in the genome era. Hort Res 6:65. https://doi.org/10.1038/s41438-019-0156-0

Sparnaaij LD, Demmink JF, Koehorst-van Putten HJJ (1990) Variation between genotypes of carnation (*Dianthus caryophyllus* cultivars and interspecific hybrids) in time of flowering and response to long days. I. Variation in yield distribution. Euphytica 50:35–42. https://doi.org/10.1007/BF00023158

Staub JE, Serquen FC, Gupta M (1996) Genetic markers, map construction, and their application in plant breeding. HortScience 31:729–741

Su J, Zhang F, Chong X et al (2019) Genome-wide association study identifies favorable SNP alleles and candidate genes for waterlogging tolerance in chrysanthemums. Hort Res 6:21. https://doi.org/10.1038/s41438-018-0101-7

Takebe S, Watarikawa Y, Uematsu K et al (2020) Breeding of new spray-type carnation cultivars 'Hohoemi' and 'Momokaren'. Res Bull Nagasaki Agric Res Ctr 10:1–15 (In Japanese with English summary)

Tanase K, Nishitani C, Hirakawa H et al (2012) Transcriptome analysis of carnation (*Dianthus caryophyllus* L.) based on next-generation sequencing technology. BMC Genom 13:292. https://doi.org/10.1186/1471-2164-13-292

Xu Y, Crouch JH (2008) Marker-assisted selection in plant breeding: from publications to practice. Crop Sci 48:391–407. https://doi.org/10.2135/cropsci2007.04.0191

Yagi M (2013) Application of DNA markers for breeding carnations resistant to bacterial wilt. JARQ 47:29–35. https://doi.org/10.6090/jarq.47.29

Yagi M (2015) Recent progress in genomic analysis of ornamental plants, with a focus on carnation. Hort J 84:3–13. https://doi.org/10.2503/hortj.MI-IR01

Yagi M, Onozaki T, Taneya M et al (2006a) Construction of a genetic linkage map for the carnation by using RAPD and SSR markers and mapping quantitative trait loci (QTL) for resistance to bacterial wilt caused by *Burkholderia caryophylli*. J Japan Soc Hort Sci 75:166–172. https://doi.org/10.2503/jjshs.75.166

Yagi M, Onozaki T, Tanikawa N et al (2006b) Molecular marker assisted selection in breeding for resistance to bacterial wilt in carnation (*Dianthus caryophyllus* L.). Hort Res (Japan) 5:241–245 (In Japanese with English summary). https://doi.org/10.2503/hrj.5.241

Yagi M, Onozaki T, Ikeda H et al (2010) Breeding process and characteristics of carnation 'Karen Rouge' with resistance to bacterial wilt. Bull Natl Inst Flor Sci 10:1–10 (In Japanese with English summary)

Yagi M, Kimura T, Yamamoto T et al (2012) QTL analysis for resistance to bacterial wilt (*Burkholderia caryophylli*) in carnation (*Dianthus caryophyllus*) using an SSR-based genetic linkage map. Mol Breed 30:495–509. https://doi.org/10.1007/s11032-011-9639-x

Yagi M, Yamamoto T, Isobe S et al (2013) Construction of a reference genetic linkage map for carnation *(Dianthus caryophyllus* L.). BMC Genomics 14:734. https://doi.org/https://doi.org/10.1186/1471-2164-14-734

Yagi M, Kosugi S, Hirakawa H et al (2014a) Sequence analysis of the genome of carnation (*Dianthus caryophyllus* L.). DNA Res 21:231–241. https://doi.org/10.1093/dnares/dst053

Yagi M, Yamamoto T, Isobe S et al (2014b) Identification of tightly linked SSR markers for flower type in carnation (*Dianthus caryophyllus* L.). Euphytica 198:175–183. https://doi.org/10.1007/s10681-014-1090-8

Yagi M, Fujiwara S, Yamaguchi H (2015) Sequence analysis of *AP2* ortholog linked to flower type locus in carnation (*Dianthus caryophyllus* L.). Hort Res (Japan) 14(Suppl. 2):516 (In Japanese)

Yagi M, Shirasawa K, Waki T et al (2017) Construction of an SSR and RAD marker-based genetic linkage map for carnation (*Dianthus caryophyllus* L.). Plant Mol Biol Rep 35:110–117. https://doi.org/10.1007/s11105-016-1010-2

Yagi M, Shirasawa K, Hirakawa H et al (2020) QTL analysis for flowering time in carnation (*Dianthus caryophyllus* L.). Sci Hortic 262:109053. https://doi.org/10.1016/j.scienta.2019.109053

Recent Topics on Flower Opening and Senescence in Cut Carnation Flowers

4

Shigeru Satoh

Abstract

This chapter describes recent topics on flower opening and senescence of carnation flowers, highlighting new chemicals found to promote flower opening in carnation flowers, and the allelic nature of two variants (*DcACS1a* and *DcACS1b*) of a senescence-related 1-aminocyclopropane-1-carboxylate (ACC) synthase gene (*DcACS1*). Xyloglucan oligosaccharides (XGO) accelerated flower opening in some cultivars of spray-type carnation, suggesting the involvement of xyloglucan metabolism in petal cells undergoing cell expansion leading to petal growth. Isomers of pyridinedicarboxylic acid (PDCA), especially 2,3- and 2,4-pyridinedicarboxylic acids, accelerated flower opening in spray-type carnation, and eventually 3-pyridinecarboxylic acid, the most simple analog of PDCA, was highest in the acceleration of flower opening. ACC synthase gene *DcACS1,* the key gene acting in ethylene production in senescing carnation petals had two variants, *DcACS1a* and *DcACS1b*. Some carnation cultivars had only *DcACS1a*, and others *DcACS1a* and *DcACS1b*. A recent search revealed two carnation cultivars, 'Skyline' and 'Scarlett Plus', which had only *DcACS1b*, suggesting that *DcACS1a* and *DcACS1b* are present as alleles.

4.1 Introduction

This chapter describes our recent findings on chemicals which accelerate flower opening, eventually leading to the extension of vase life in some carnation flowers, and the allelic nature of two variants of a senescence-related carnation 1-aminocylopropane-1-carboxylate synthase gene. The vase life of cut carnation flowers is determined by the sum of the period for flower opening and that for flower senescence. Acceleration of flower opening followed by retardation of flower senescence would surely prolong the vase life of the flowers. There are many chemicals which have been used to retard the senescence of carnation flowers by inhibiting the synthesis and/or action of ethylene (Satoh et al. 2014). Whereas, to our best knowledge, no chemicals which accelerate the opening of carnation flower were not practically used previously. Therefore, we started to search for the chemicals which accelerate flower opening and help extend the vase life of the flowers. Our work to discover such the chemicals revealed xyloglucan oligosaccharide mixture (XGO) (Satoh et al. 2013) and isomers of pyridine-*di/mono*-carboxylic acids (Satoh et al. 2014, Satoh and Nomura 2019, Sugiyama and Satoh 2015). XGO is a mixture of enzymatic hydrolysis products of xyloglucan, a constituent of cell wall

S. Satoh (✉)
Faculty of Agriculture, Ryukoku University, Otsu 520-2194, Shiga, Japan
e-mail: jxymp688@yahoo.co.jp

T. Onozaki and M. Yagi (eds.), *The Carnation Genome*, Compendium of Plant Genomes,
https://doi.org/10.1007/978-981-15-8261-5_4

of dicot plants, and was shown to promote flower opening in some carnation cultivars. Its mechanism of action was suggested to participate in the process of cell wall loosening and promote petal cell expansion, and eventually leading to flower opening of carnation flowers. Vlad et al. (2010) were the first to report that 2,4-pyridinedi carboxylic acid (2,4-PDCA) inhibited ethylene production in detached flowers of 'White Sim' carnation and delayed senescence of the flowers. Then, Satoh et al. (2014) observed that 2,4-PDCA prolonged the vase life of cut flowers of spray-type carnation, by acceleration of flower opening in addition to delayed senescence of fully open flowers. The promotion of flower opening was caused by many isomers of pyridine-di/mono-carboxylic acids, although their mechanism of action has not been uncovered yet.

Senescence in carnation flowers is characterized by autocatalytic ethylene production from petals and subsequent wilting of the petals. A large amount of ethylene is synthesized several days after full opening of the flower during natural senescence (Woodson et al. 1992), or several hours after compatible pollination (Larsen et al. 1995; Nichols 1977; Nichols et al. 1983) or treatment with exogenous ethylene (ten Have and Woltering 1997; Wang and Woodson 1989). A substantial portion of ethylene comes from the petals of the flower. The increased ethylene production accelerates in-rolling of petals resulting in wilting of the flower.

Ethylene is synthesized in carnation petals, as well as in other plant tissues, via the following pathway: L-methionine → *S*-adenosyl-L-methionine (AdoMet) → 1-aminocyclopropane-1-carboxylate (ACC) → ethylene. The conversion of AdoMet to ACC is a rate-limiting step in ethylene biosynthesis and is catalyzed by ACC synthase (ACS) (Yang and Hoffman 1984). Three cDNAs coding for ACC synthase (*DcACS1*, *DcACS2*, and *DcACS3*) were cloned from carnation plants, suggesting that ACC synthase genes form a family in the plants, and tissue-specific or chemical-induced expression of mRNA has been studied (Jones 2003, Jones and Woodson 1999, ten Have and Woltering 1997).

DcACS1 is mainly responsible for autocatalytic ethylene production in carnation petals (Jones 2003, Jones and Woodson 1999, Satoh 2011, Shibuya and Ichimura 2010, ten Have and Woltering 1997); *DcACS1* showed ethylene-enhanced expression in petals (Jones 2003, Jones and Woodson 1999, ten Have and Woltering 1997), and carnation lines transformed with *DcACS1* transgenes showed suppressed ethylene production in flowers (Iwazaki et al. 2004).

About a decade ago genomic *DcACS1* gene was found to have two forms (variants), *DcACS1a* and *DcACS1b*, in which the sizes and nucleotide sequences of introns were different (Harada et al. 2011a). These two genes were suspected to make alleles of *DcACS1* gene, but this was not confirmed until recently.

4.2 Promotion by a Xyloglucan Oligosaccharide Mixture of Flower Opening in Carnation

Flower opening involves elongation, expansion, and outward bending of petals, which result from the enlargement of petal cells (Evans and Reid 1988; Kenis et al. 1985; Koning 1984). Cell-wall extensibility may be a growth-limiting factor for petal expansion (Yamada et al. 2009). An apoplastic enzyme, xyloglucan endotransglycosylase/hydrolase (XTH) is considered to be involved in cell-wall loosening in dicot plants (Carpita and McCann 2000). XTH catalyzes the transglycosylation of xyloglucan, which results in cleaving and reattachment among xyloglucan chains [xyloglucan endotransglycosylase (XET) activity], and realignment of the xyloglucan chain in different strata when newly synthesized xyloglucans are incorporated (Fry et al. 1992; Nishitani and Tominaga 1992; Vissenberg et al. 2000). By disturbing or inhibiting the cell-wall metabolism in the growing petals of opening flowers with an excess amount of xyloglucan oligosaccharides (XGO), the flower-opening process might be affected, resulting in a modified display time of the flowers.

A mixture of xyloglucan oligosaccharides (XGO) was prepared from xyloglucan (XG) of tamarind seed gum by digestion with *Aspergillus* XG-specific xyloglucanase and subsequent purification by ethanol fractionation. The XGO mixture contained XG7, XG8, and XG9 (Fig. 4.1) at the ratio of 1: 4: 5, which was almost identical to the literature value of constituent subunits ratio of 1.2: 3.8: 5.

The effect of XGO on flower opening was examined in several carnation cultivars. For example, cut buds, of cultivars 'Pure Red', 'Lillian' and 'Collin' were treated continuously with 1% XGO for 10 days. Figure 4.2 shows the time of flower opening over a period of 10 days and flowering profiles at 5 days ('Pure Red' and 'Collin') and 6 days ('Lillian') after the start of the experiment. XGO treatment promoted flower opening in 'Pure Red' and 'Lillian'. In 'Pure Red' carnation, the stimulation of flower opening was significant even one day after the start of treatment. Flower opening of 'Lillian' carnation was also promoted, but less than that of 'Pure Red' carnation. XGO treatment did not affect flower opening of 'Collin' carnation (Fig. 4.2) and 'Light Pink Barbara (LPB)' and 'Mule' carnations (data not shown). The reason why the XGO's effect varies among carnation cultivars has not been clarified yet.

The proposed mechanism of xyloglucan oligosaccharide on promotion of flower opening is as follows. Xyloglucan endotransglycosylase (XET) activity of XTH catalyzes the transglycosylation of xyloglucan, in which one chain of xyloglucan is cleaved and reattached to the non-reducing end of another xyloglucan chain (Fig. 4.3; Fry et al. 1992; Nishitani and Tominaga 1992; Vissenberg et al. 2000). Exogenously applied XGO might act as a substrate for XET, that is, an acceptor molecule of cleaved xyloglucan polymers (Fig. 4.3). Since XGO was not anchored to cellulose microfibrils, the formation of XGO-xyloglucan polymer complexes would cause more enhanced slippage of cellulose microfibrils, which was led by turgor in cells, resulting in the promoted expansion growth of petal cells.

Carnation plants have at least four genomic genes encoding xyloglucan endotransglycosylase/hydrolase (XTH) (*DcXTH1-DcXTH4*) (Harada et al. 2011b; Yagi et al. 2014). Harada et al. (2011b) suggested that two XTH genes (*DcXTH2* and *3*) are associated with petal growth and development during flower opening. It is interesting to investigate the in vivo and in vitro action of XGO on XTH enzymes.

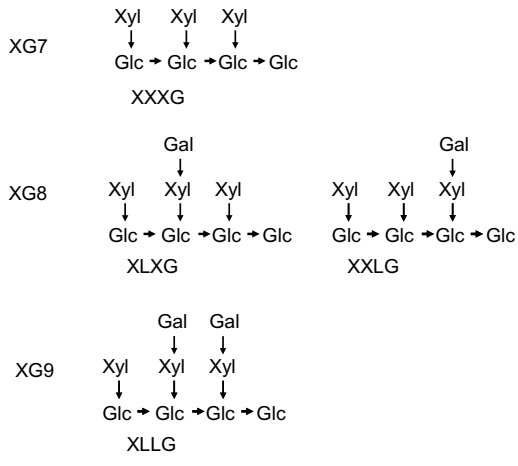

Fig. 4.1 Structures of XG7, XG8, and XG9 prepared from tamarind seed gum. Conventional abbreviations for respective XG oligosaccharides (XGO) are shown below the structure

4.3 Acceleration by Pyridinecarboxylic Acid Isomers of Flower Opening in Spray-Type Carnation

4.3.1 Acceleration of Flower Opening by Treatment with 2,4-Pyridinedicarboxylic Acid

Vlad et al. (2010) demonstrated that 2,4-pyridinedicarboxylic acid (2,4-PDCA) inhibited ethylene production in detached flowers of 'White Sim', a standard-type carnation which has one flower on a stem, and delayed senescence of the flowers. They suggested that 2,4-PDCA inhibited the activity of ACC oxidase by acting as a structural analog of ascorbate. Later, Satoh

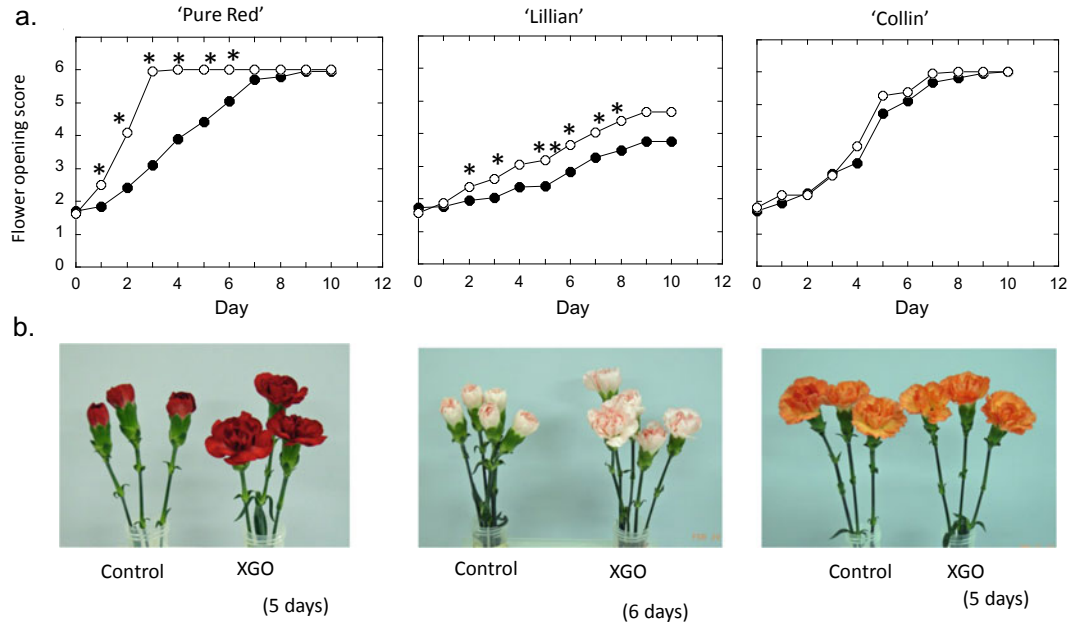

Fig. 4.2 Effects of 1% XGO on flower opening in 'Pure Red', 'Lillian', and 'Collin' carnation. **a** Time course of flower opening after treatment with 1% XGO (○) or with water (●). **b** Flower-opening profiles for respective cultivars at given days after the start of treatment. Data are the means of three replications, each with 6 or 7 flowers. * and ** show significant difference by Mann–Whitney's U-test at $P < 0.05$ and $P < 0.01$, respectively, on each day The flower-opening score was determined by separating flower opening profile into 6 stages according to Harada et al. (2011a): score 1, petals just emerged from buds; score 2, petals elongated vertically; score 3, petal clusters expanded; score 4, outer petals start to reflex (bend outwards); score 5, outer petals have reflexed; score 6, fully open flower with outer petals at right angles to the stem

et al. (2014, 2016) examined 2,4-PDCA action on ethylene production and senescence in 'LPB' carnation. Interestingly, they demonstrated the acceleration of flower opening by 2,4-PDCA as well as 2,3-pyridinedicarboxylic acid (2,3-PDCA) in the flowers, in addition to retardation of their senescence, resulting in prolonged display time. Eventually, 3-pyridinecarboxylic acid (3-PCA), the simplest analog of pyridinecarboxylic acid, was found to promote most markedly the flower opening of cut spray-type carnation. This section will describe the effects of the pyridinecarboxylic acid analogs on flower opening in cut spray-type carnation.

Usually, the time of flower opening and the vase life of carnation flower are determined by observing onset of flower opening and senescence, *i.e.*, in-rolling of petal margin leading to wilting of whole petals. This method has been used successfully for a standard type of carnation flower with only one flower per stalk (stem). However, in spray-type carnation flowers, which have a main stalk with several offshoots, each having one or two flowers at their tips, the time of flower opening and the vase life of the flowers are determined differently, since the onset of flower opening and senescence varies depending on each floret. Satoh et al. (2005, 2014) developed a method to determine the 'time to flower opening' and 'vase life', for characterizing flower opening profiles in cut spray-type carnation flowers. This newly developed method is demonstrated in the following with 'LPB' flowers treated with 2,4-PDCA.

Figure 4.4 shows the percentage of fully open and non-senescent (FONS) flowers of cut 'LPB' flowers treated with various concentrations of 2,4-PDCA (Sugiyama and Satoh 2015).

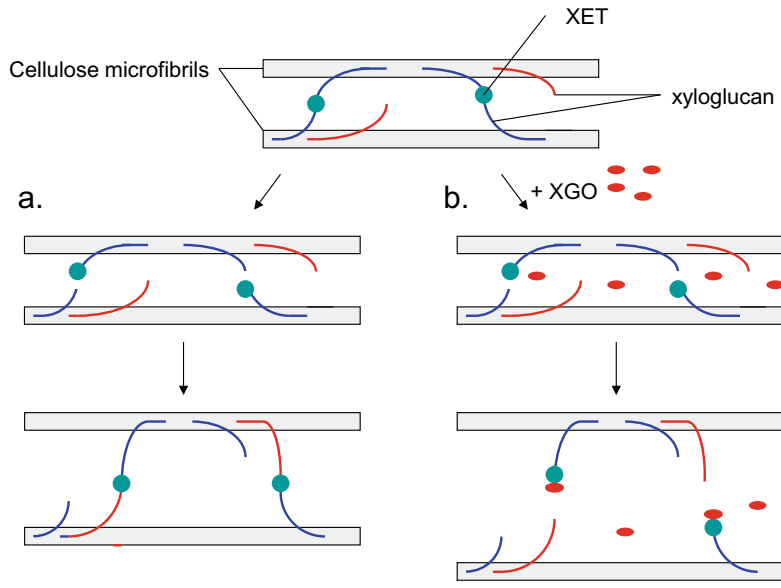

Fig. 4.3 Possible action mechanism of XGO on the promotion of flower opening in carnation. The drawing was made according to the figure shown in a textbook (Biochemistry and Molecular Biology of Plants, 2.38; Carpita and McCann 2000) with necessary modification. **a** During the ordinate process of petal cell growth, XET catalyzes cleavage and reattachment among xyloglucan chains, resulting in transient slippage of cellulosic microfibrils. **b** When XGO was present in excess, cleaved xyloglucan polymers were transferred to unanchored XGO, causing more enhanced slippage of cellulose microfibrils, eventually promoting flower opening

The percentage of FONS flowers was calculated from the proportion of those flowers to the total number of initial flower buds (25 buds per 5 flowers). The time to flower opening is the time in days from the start of experiment until the percentage of open flowers reached 40%. The vase life of spray-type carnation flowers was the period during which 40% or more were fully open and non-senescent (Satoh et al. 2005, 2014). The treatment with 0.3, 1 and 2 mM 2,4-PDCA tended to shorten the time to flower opening; that is, 4.3, 3.3 and 3.8 days, respectively, as compared to 4.4 days in the control, although the difference was significant only with treatment at 1 mM by Steel's multiple range test ($P < 0.05$). The results suggested that 2,4-PDCA accelerates flower bud opening. The vase life was significantly lengthened by treatment with 2,4-PDCA, attaining 53, 111, and 135% increases at 0.3, 1, and 2 mM 2,4-PDCA, respectively, as compared with the control (Satoh et al. 2014).

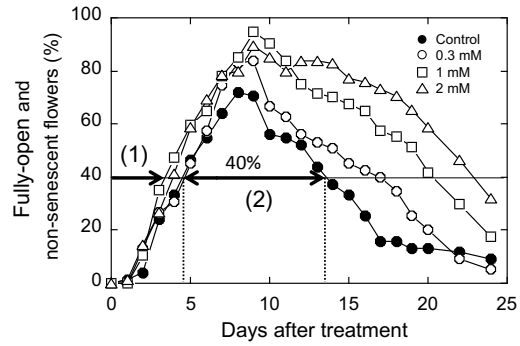

Fig. 4.4 Evaluation of flower opening by determining the time to flower opening and the duration of vase life in cut flowers of 'Light Pink Barbara' carnation treated continuously with different concentrations of 2,4-PDCA. This figure was adapted from Fig. 4.2 in Sugiyama and Satoh (2015). The percentage of fully open and non-senescent (FONS) flowers was calculated from the proportion of those flowers to the total number of initial flower buds (25 buds per 5 flowers). The time to flower opening (1) is the time in days from the start of experiment until the percentage of open flowers reached 40%. The display time of the flowers (2) is the duration when the percentage of FONS flowers was 40% or more

4.3.2 Acceleration by Various Pyridinedicarboxylic Acid Isomers of Flower Opening in Spray-Type Carnation

Pryridinedicarboxylic acids (PDCAs) have six isomers as shown in Fig. 4.5. Figure 4.6 shows the flower opening and senescing profiles of the flowers of 'LPB' carnation treated with 2,3-, 2,4-, 2,5-, and 3,4-PDCAs at 2 mM, which were chosen as typical specimens out of 3 replicates 0, 3, and 10 days after the start of the experiment. On day 3, there were more open pink flowers among the flowers treated with PDCAs, especially with 2,3- and 2,4-PDCAs, than in the control. These observations indicated that treatment with PDCAs accelerated flower opening compared with that in the untreated control flowers, and the acceleration effect was greatest with 2,3-PDCA among the PDCAs. On day 10, the control flowers remained as a mixture of buds, open flowers, and senesced flowers. The senesced flowers showed in-rolling and wilting of petals, typical symptoms of senescence in response to ethylene. On the other hand, almost all of the flowers treated with PDCAs were fully open with non-wilted and turgid petals. At the later stage, the PDCA-treated flowers withered with browning at the petal margins, as well as with jumbled, but turgid, fading petals, as reported previously (Satoh et al. 2014), or lost their vase lives by the breaking of flower stems.

Table 4.1 summarizes the effects of various PDCA isomers at 2 mM on the time to flower opening and the vase life of cut 'LPB' flowers. The control (H_2O) flowers reached the stage of flower opening (40%) on day 9.0. The treatment with all the PDCA isomers promoted flower opening by shortening the time to flower opening. The time to flower opening was the shortest (4.0 days) for 2,3-PDCA and 2,4-PDCA, followed by 2,5-PDCA and 3,5-PDCA (both, 4.7 days), then 2,6-PDCA and 3,4-PDCA. Four of the PDCA analogs (2,3-, 2,4-, 3,4-, and 3,5-PDCA) significantly lengthened the vase life compared with that of the control (8.3 days); the vase lives varied from 14.7 to 15.5 days.

A representative PDCA isomer 2,4-PDCA promoted flower opening of spray-type carnation cultivars, 'Barbara', 'Beam Cherry', 'Candle', 'Collin', 'Rascal Green', 'Scarlett Ostera', and 'Mule', as well as 'LPB'. Treatment of 'LPB' flowers for the initial 24 h with 2,4-PDCA at 5 and 10 mM was almost as effective as the continuous treatment with the chemical at 2 mM (Satoh et al. 2016).

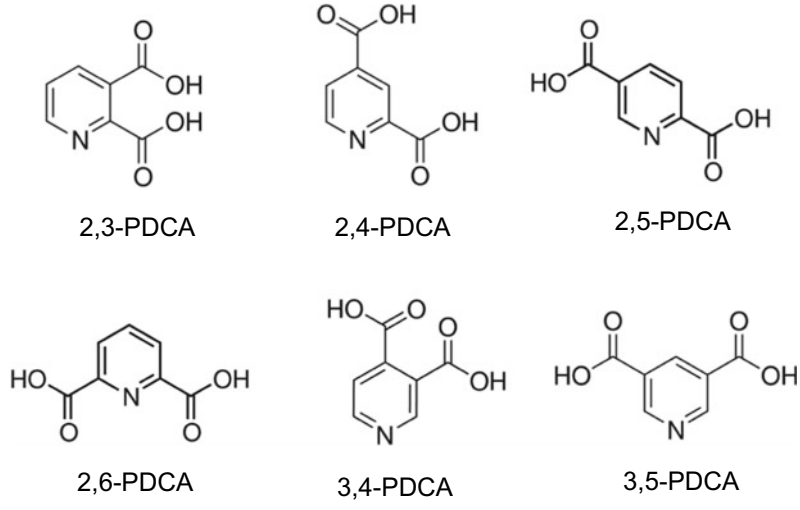

Fig. 4.5 Structures of pyridinedicarboxylic acid isomers (PDCAs). Drawings of the chemical structures were taken from HP of Sigma-Aldrich Co. LLC.

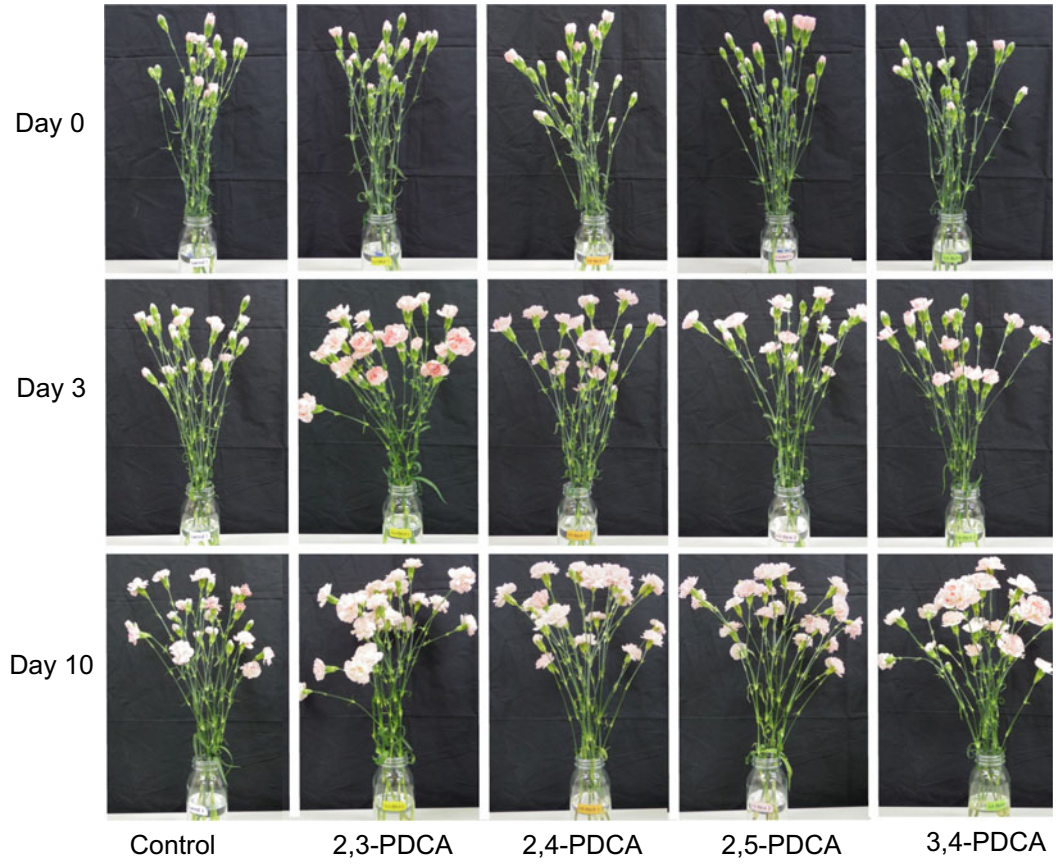

Fig. 4.6 Flower-opening and -senescing profiles of cut 'Light Pink Barbara' flowers treated with 2,3-, 2,4-, 2,5-, or 3,4-PDCA at 2 mM or water (control). Typical profiles for each treatment out of 3 replicates were chosen for 0, 3, and 10 days after the start of the experiment

Table 4.1 Effects of PDCA isomers at 2 mM on the time to flower opening and the vase life of cut spray-type 'Light Pink Barbara' carnation flowers

Chemicals	Time to flower opening (days)	Vase life (days)
Control (H_2O)	9.0±1.0	8.3±1.9
2,3-PDCA	4.0[a] ± 0.0	14.7[a] ± 0.3
2,4-PDCA	4.0[a]± 0.6	14.7[a] ± 1.7
2,5-PDCA	4.7[a]± 0.3	13.0±2.1
2,6-PDCA	5.3[a] ± 0.3	9.3±1.5
3,4-PDCA	5.7[a] ± 0.3	14.7[a] ± 2.4
3,5-PDCA	4.7[a] ± 0.7	15.5[a] ± 1.2

Data are the mean ± SE of 3 replicates, each with 5 flower stems with 5 florets (buds) on a stem

[a]Shows a significant difference from the control in each column by Dunnett's multiple range test ($P < 0.05$)

4.3.3 Acceleration by 3-pyridinecarboxylic Acid (3-PCA) of Flower Opening in Spray-Type Carnation

The treatment of pyridinecarboxylic acids (PCAs) revealed that 3-pyridinecarboxylic acid (3-PCA) and its derivative, 3-PCA amide, were most active in accelerating flower opening of cut 'LPB' flowers (Satoh and Nomura 2019). Figure 4.7 shows the changes in the percentage of FONS flowers of 'LPB' carnations that were treated on the first day with PCA and PDCA analogs at 5 mM, then left in water for another 29 days.

3-PCA and 3-PCA amide markedly promoted the opening of cut 'LPB' flowers and reduced the days to flower opening (Fig. 4.7a). It is possible that 3-PCA amide can be easily converted to 3-PCA, an expected active form, or vice versa. 2-PCA and 4-PCA also accelerated flower opening, but their effects were weaker than those of 3-PCA and 3-PCA amide. Moreover, the promotive effects of 3-PCA and 3-PCA amide were stronger than that of 2,3-PDCA, 2,4-PDCA, and

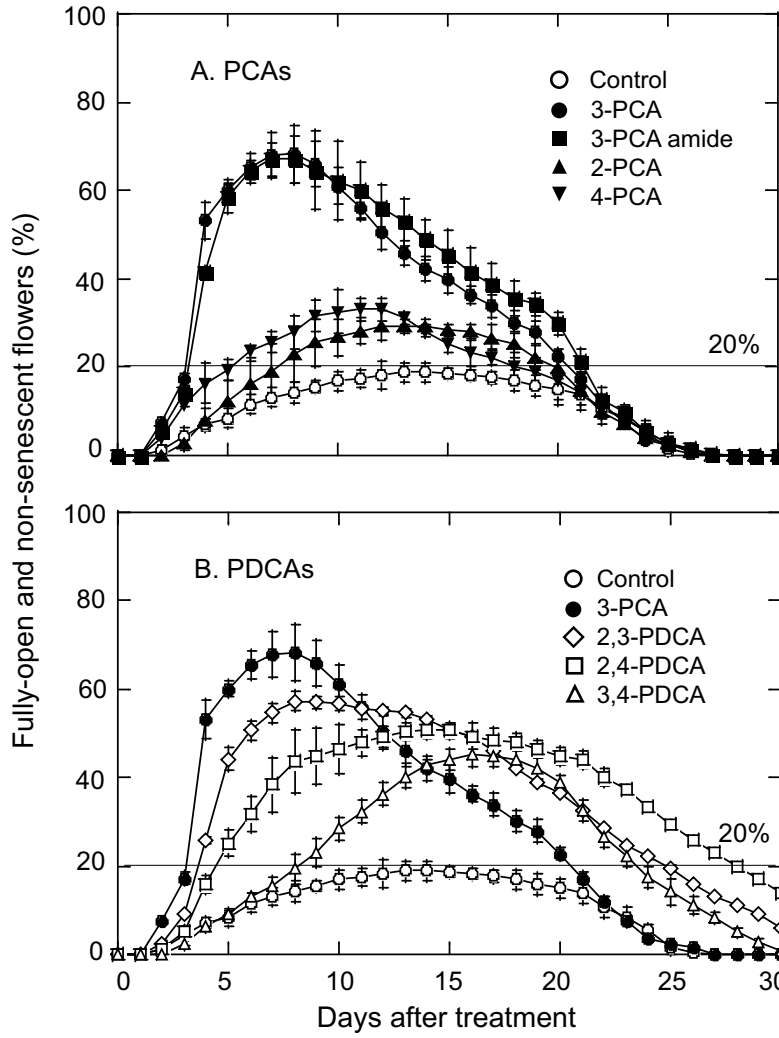

Fig. 4.7 Changes in the percentage of fully open and non-senescent 'Light Pink Barbara' flowers treated with or without pyridinecarboxylic acids (PCAs) (**a**) and pyridinedicarboxylic acids (PDCAs) (**b**) analogs at 5 mM for one day then kept in water until day 30. Data show the mean ± SE of three replicates, each with 25 flower buds. Data for the control and 3-PCA treatment are shown in both figures for comparison.

Table 4.2 Effects of PCA and PDCA isomers on the time to flower opening and the vase life of 'Light Pink Barbara' carnation flowers

Chemicals	Time to flower opening (days)	Vase life (days)
Control	(8.5[a])	(15.9[a])
2-PCA	6.8 ± 0.3	12.2 ± 0.5
3-PCA	3.1 ± 0.2	18.4 ± 1.1
3-PCA amide	3.1 ± 0.3	18.5 ± 1.7
4-PCA	4.0 ± 0.7	15.8 ± 3.4
2,3-PDCA	4.2 ± 0.6	16.6 ± 5.7
2,4-PDCA	(4.4[a])	(23.5[a])
3,4-PDCA	(8.4[b])	(14.5[a])

Data are the mean ± SE of 3 experiments, each with 3 replicates with 5 flower stems (25 buds in total) when the least display values for the flowers treated with respective chemicals surpassed 20%. However, if this was not the case, values from only one experiment ([a]) or the mean of two experiments ([b]) are shown in parentheses for reference. The threshold value of 20% was used because of low flowering vigor of a used flower sample as explained by Sugiyama and Satoh (2015)

3,4-PDCA (Sugiyama and Satoh 2015). Table 4.2 summarizes the days to flower opening and the vase life of the flowers as affected by the treatment with PCA and PDCA isomers, which were determined in three experiments including that shown in Fig. 4.7. Flower opening was earliest in the flowers treated with 3-PCA and 3-PCA amide (3.1 days), followed by 4-PCA (4.0 days), 2,3-PDCA (4.2 days), and 2-PCA (6.8 days) in this order. Among the PCA analogs, 3-PCA was more effective than 4-PCA and 2-PCA in promoting flower opening. These finding suggested that the carboxyl group at position 3 of the pyridine ring is needed for the promotion of flower opening.

4.4 Allelic Nature of Two Forms (Variants) of DcACS1 Gene, DcACS1a, and DcACS1b

4.4.1 Genomic DNA Structure of a Carnation ACS Gene, DcACS1

DcACS1 was found to be mainly responsible for autocatalytic ethylene production in carnation petals (Jones 2003, Jones and Woodson 1999, Satoh 2011, Shibuya and Ichimura, 2010, ten Have and Woltering 1997), and the genomic DNA structure of *DcACS1* was determined by genomic PCR (Harada et al. 2011a). Interestingly, in the genome of 'LPB' carnation, two distinct nucleotide sequences, so-called variants, were found and were designated *DcACS1a* and *DcACS1b*. The former corresponded to a cDNA coding for the carnation *DcACS1* which was first cloned as *CARACC3* from 'White Sim' carnation (Park et al. 1992), and later confirmed by Henskens et al. (1994). The latter was a novel gene (Fig. 4.8a). Both *DcACS1a* and *DcACS1b* have five exons and four introns. These two genes (variants) had almost identical nucleotide sequences in exons, but not in some introns and 3′-UTR (Fig. 4.8b). Previous genomic PCR analysis of 32 carnation cultivars showed that 25 cultivars have only *DcACS1a* and seven cultivars have both *DcACS1a* and *DcACS1b*; that is, cultivars such as 'White Sim', 'Scania', 'Nora', and so on had only *DcACS1a*, whereas others such as 'LPB', 'Tanga', 'Kibo', and so on had both *DcACS1a* and *DcACS1b* (Table 4.3).

4.4.2 Allelic Nature of DcACS1a and DcACS1b Genes

There are two variants of *DcACS1* gene, *DcACS1a* and *DcACS1b*, which could be alleles of *DcACS1* gene. A search for carnation cultivars which are homozygotes of the *DcACS1b* gene was not successful (Harada et al. 2011a).

a.

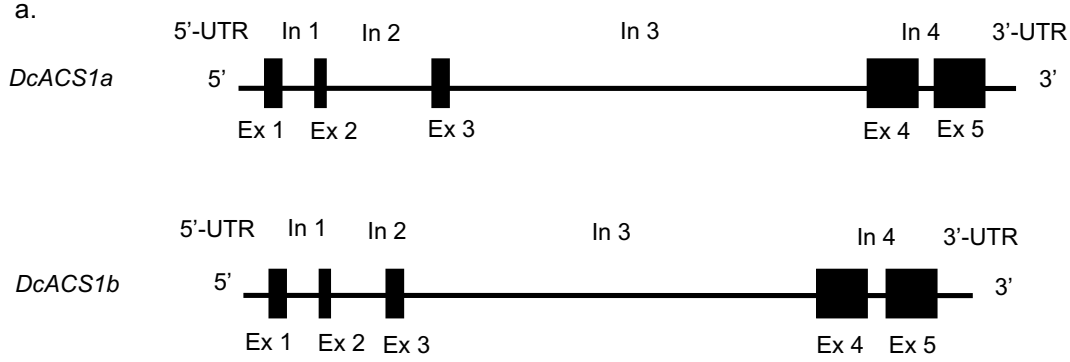

b.

Region	5'-UTR	Exon 1	Intron 1	Exon 2	Intron 2	Exon 3	Intron 3	Exon 4	Intron 4	Exon 5	3'-UTR
DcACS1a	168*	174	217	132	769	161	2962	558	119	529	248
DcACS1b	166	174	296	132	445	161	2891	558	119	511	225
Identity (%)	87.5	100	69.6	100	56.4	100	65.6	99.5	100	94.7	55.8

* Sizes are in nucleotide number.

Fig. 4.8 Genomic structures (**a**) and sizes (**b**) in nucleotide number of five exons, four introns, 3′-UTR, and 5′-UTR of *DcACS1a* and *DcACS1b*

Table 4.3 Classification of 40 carnation cultivars by genomic PCR fragments of *DcACS1*

Cultivars harboring DcACS1a/DcACS1a			
Apollo	Candy	Chinera	Coral
Delphi	Eternal Green	Francesco	Killer
Kirk*	Lester	Light Cream Candle	Miracle Rouge
Miracle Symphony	Nora	Northland	Orange Range
Pallas	Peter	Pure Red	Scania
Tobias	Toy*	Uconn Sim	White Lucena
White Sim	William Sim	Yosooi	
Cultivars harboring DcACS1a/DcACS1b			
Barullo*	Beam Cherry	Carnet*	Cherry Tessino*
Fuji	Kibo	Light Pink Barbara	Scarlett Ostera*
Seto no Hatsushimo	Snow Crown Pink	Tanga	
Cultivars harboring DcACS1b/DcACS1b			
Scarlett Plus*	Skyline*		

In this table, eight cultivars (with an asterisk) were newly added to the previously shown 32 cultivars (Harada et al. 2011a)

However, very recently, genomic PCR analysis revealed two carnation cultivars 'Skyline' and 'Scarlett Plus', which had only the *DcACS1b* gene, suggesting these cultivars are homozygotes of the *DcACS1b* gene (Satoh et al. 2020). Furthermore, analysis of the gene structure of a

hybrid carnation between ordinal carnation and wild pink provided further evidence of the allelic nature of *DcACS1a* and *DcASC1b* genes (Satoh et al. 2020). Table 4.3 summarizes carnation cultivars thought to be homozygotes of *DcACS1a* or *DcACS1b*, and heterozygotes of both genes. In the table, eight cultivars were added to the 32 cultivars examined previously (Harada et al. 2011a). Analysis of transcript accumulation revealed that both *DcACS1a* and *DcACS1b* are expressed at a similar level in senescing petals of 'LPB' carnation, suggesting that *DcACS1a* and *DcACS1b* are codominant genes (Harada et al. 2011a).

Genomic ACC synthase genes, homologous to carnation *DcACS1* gene, were present as variants in other two *Dianthus* species; six variants in *D. petraeus* and seven variants in *D. superbus* var. *longicalycinus* (Satoh et al. 2011). All 13 sequenced homologous *ACS1* genes had five exons and four introns, similar to *DcACS1* genes in carnation. The exons had similar nucleotide sequences and consequently similar deduced amino-acid sequences. Satoh et al. (2011) suggested the possible origin of two variants (now alleles), *DcACS1a* and *DcACS1b*, by studying the intron structure in *DcACS1* homologous genes of *Dianthus* species. They suggested that (1) the variation in intron structure between two variants of carnation *DcACS1* is reminiscent of the variation that occurred universally in *Dianthus* species, (2) *DcACS1a* is probably a gene intrinsic to carnation, and (3) *DcACS1b* was acquired from another, as yet unknown, *Dianthus* species, in the course of breeding modern carnation cultivars. The present findings suggest that variants of *DcACS1* homologous genes in other *Dianthus* species are also alleles in the specific species; for example, *DsACS1a* and *DsACS1b* in *D. superbus* var. *longicalcinus* are also alleles in *Dianthus* species.

References

Carpita N, McCann M (2000) The cell wall. In: Buchanan BB, Gruissem W, Jones RL (eds) Biochemistry and molecular biology of plants. Am Soc Plant Physiol, Rockville, pp 52–108

Evans RY, Reid MS (1988) Changes in carbohydrates and osmotic potential during rhythmic expansion of rose petals. J Am Soc Hort Sci 113:884–888

Fry SC, Smith RC, Renwick KF et al (1992) Xyloglucan endotransglycosylase, a new wall-loosening enzyme activity from plants. Biochem J 15:821–828

Harada T, Murakoshi Y, Torii Y et al (2011a) Analysis of genomic DNA of *DcACS1*, a 1-aminocyclopropane-1-carboxylate synthase gene, expressed in senescing petals of carnation (*Dianthus caryophyllus*) and its orthologous genes in *D. superbus* var. *longicalycinus*. Plant Cell Rep 30:519–527

Harada T, Torii Y, Morita S et al (2011b) Cloning, characterization, and expression of xyloglucan endotransglucosylase/hydrolase and expansin genes associated with petal growth and development during carnation flower opening. J Exp Bot 62:815–823

Henskens JAM, Rouwendal GJA, ten Have A et al (1994) Molecular cloning of two different ACC synthase PCR fragments in carnation flowers and organ specific expression of the corresponding genes. Plant Mol Biol 26:453–458

Iwazaki Y, Kosugi Y, Waki K et al (2004) Generation and ethylene production of transgenic carnations harboring ACC synthase cDNA in sense or antisense orientation. J Appl Hort 6:67–71

Jones ML (2003) Ethylene biosynthetic genes are differentially regulated by ethylene and ACC in carnation styles. Plant Growth Regul 40:129–138

Jones ML, Woodson WR (1999) Differential expression of three members of the 1-aminocyclopropane-1-carboxylate synthase gene family in carnation. Plant Physiol 119:755–764

Kenis JD, Silvente ST, Trippi VS (1985) Nitrogen metabolite and senescence-associated change during growth of carnation flowers. Physiol Plant 65:455–459

Koning RE (1984) The role of plant hormones in the growth of the corolla of *Gaillardia grandiflora* (Asteraceae) ray flowers. Am J Bot 71:1–8

Larsen PB, Ashworth EN, Jones ML et al (1995) Pollination-induced ethylene in carnation (Role of pollen tube growth and sexual compatibility). Plant Physiol 108:1405–1412

Nichols R (1977) Sites of ethylene production in the pollinated and unpollinated senescing carnation

(*Dianthus caryophyllus*) inflorescence. Planta 135:155–159

Nichols R, Bufler G, Mor Y et al (1983) Changes in ethylene production and 1-aminocyclopropane-1-carboxylic acid content of pollinated carnation flowers. J Plant Growth Regul 2:1–8

Nishitani K, Tominaga R (1992) Endo-xyloglucan transferase, a novel class of glycosyltransferase that catalyzes transfer as a segments of xyloglucan molecule to another xyloglucan molecule. J Biol Chem 267:21058–21064

Park KY, Drory A, Woodson WR (1992) Molecular cloning of an 1-aminocyclopropane-1-carboxylate synthase from senescing carnation flower petals. Plant Mol Biol 18:377–386

Satoh S (2011) Ethylene production and petal wilting during senescence of cut carnation (*Dianthus caryophyllus*) flowers and prolonging their vase life by genetic transformation. J Jpn Soc Hort Sci 80:127–135

Satoh S, Kosugi Y, Sugiyama S et al (2014) 2,4-Pyridinedicarboxylic acid prolongs the vase life of cut flowers of spray carnations. J Jpn Soc Hort Sci 83:72–80

Satoh S, Meng N, Harada T et al (2011) Possible origin of two variants of a carnation 1-aminocyclopropane-1-carboxylate synthase gene, DcACS1a and DcACS1b, as suggested by intron structure in homologous genes in Dianthus species. J Jpn Soc Hort Sci 80:443–451

Satoh S, Nomura Y (2019) Promotion of flower opening of spray-type carnation cut flowers by 3-pyridinecarboxylic acid, a simple analog of pyridinedicarboxylic acids (PDCAs) including 2,3- and 2,4-PDCAs. Hort J 88:293–298

Satoh S, Nomura Y, Kosugi Y et al (2020) Allelic nature of two carnation variants 1-aminocyclopropane-1-carboxylate (ACC) synthase genes, *DcACS1a* and *DcACS1b*. Hort J 89:311–318

Satoh S, Nomura Y, Morita S et al (2016) Further characterization of the action of pyridinecarboxylic acids: multifunctional flower care agents for cut flowers of spray-type carnation. J Appl Hort 18:3–6

Satoh S, Nukui H, Inokuma T (2005) A method for determining the vase life of cut spray carnation flowers. J Appl Hort 7:8–10

Satoh S, Tateishi A, Sugiyama S (2013) Preparation of a xyloglucan oligosaccharide mixture from tamarind seed gum and its promotive action on flower opening in carnation cultivars. J Jpn Soc Hort Sci 82:270-276

Shibuya K, Ichimura K (2010) Depression of autocatalytic ethylene production by high-temperature treatment in carnation flowers. J Jpn Soc Hort Sci 79:97–102

Sugiyama S, Satoh S (2015) Pyridinedicarboxylic acids prolong the vase life of cut flowers of spray-type 'Light Pink Barbara' carnation by accelerating flower opening in addition to an already-known action of retarding senescence. Hort J 84:172–177

ten Have A, Woltering EJ (1997) Ethylene biosynthetic genes are differentially expressed during carnation (*Dianthus caryophyllus* L.) flower senescence. Plant Mol Biol 34:89–97

Vissenberg K, Martinez-Vilchez IM et al (2000) In vivo colocalization of xyloglucan endotransglycosylase activity and its donor substrate in the elongation zone of *Arabidopsis* roots. Plant Cell 12:1229–1237

Vlad F, Tiainen P, Owen C et al (2010) Characterization of two carnation petal prolyl 4 hydroxylases. Physiol Plant 140:199–207

Wang H, Woodson WR (1989) Reversible inhibition of ethylene action and interruption of petal senescence in carnation flowers by norbornadiene. Plant Physiol 89:434–438

Woodson WR, Park KY, Drory A et al (1992) Expression of ethylene biosynthetic pathway transcripts in senescing carnation flowers. Plant Physiol 99:526–532

Yamada K, Takahashi R, Fujitani C et al (2009) Cell wall extensibility and effect of cell-wall-loosening proteins during rose flower opening. J Jpn Soc Hort Sci 78:242–251

Yagi M, Kosugi S, Hirakawa H et al (2014) Sequence analysis of the genome of carnation (*Dianathus caryophyllus* L.). DNA Res 21:231–241

Yang SF, Hoffman N (1984) Ethylene biosynthesis and its regulation in higher plants. Ann Rev Plant Physiol 35:155–189

Cross-Breeding for Flower Vase Life and Their Molecular Mechanism

5

Koji Tanase

Abstract

Carnation (*Dianthus caryophyllus* L.) is the major floricultural crop in Japan and also worldwide. The vase life of cut ornamental flowers, including carnations, is an important trait determining their quality and consumers' preference. Studies aimed at improving the vase life of carnation flowers has been began in 1992 using conventional cross-breeding techniques at the Institute of Vegetable and Floriculture Science, NARO. We repeatedly crossed and selected promising offspring with long vase life for seven generations. The two developed cultivars, 'Miracle Rouge' and 'Miracle Symphony' with genetically determined long vase lives, were released. In these cultivars, ethylene production was prevented by suppression of the ethylene-related genes, *DcACS1*, *DcACS2,* and *DcACO1*. Line 532–6 showed an ultra-long vase life averaging 30 days (approximately fivefold that of the normal cultivar, 'White Sim'). In line 532–6, genes such as *DcCPIn* and *DcCP1*, which regulate programmed cell death apart from genes related to ethylene were suppressed, and the plant showed extremely low ethylene production. In addition, we found line 806-46b with two characteristics: an ultra-long vase life and low ethylene sensitivity. This chapter provides an overview of information on the breeding of carnation cultivars with genetically long vase life, and of the outcomes relating to the molecular bases of the long vase life trait.

5.1 Introduction

Carnation (*Dianthus caryophyllus* L.) is one of the major floricultural crops worldwide. Carnation varieties are divided into three categories (standard, spray, and pot carnation) based on the plant form, flower size and flower shape, with the both the standard and spray types used for cut flowers. The main breeding criteria for improving cut carnations flowers are yield, appearance, flower color, flower size, plant form, disease tolerance, and flower vase life. The vase life of cut flowers is an economically valuable trait that influences consumer satisfaction, transportability, and the storage period (Onozaki 2018). Most consumers expect cut flower to have a long vase life.

Carnation is a typical ethylene-sensitive flower that has been studied as a model of ethylene-induced flower senescence. Carnation flowers show a climacteric-like rise in ethylene production, accompanied by petal in-rolling (inward rolling or rolling-in) (Fig. 5.1a), a typical senescence signal in carnation flowers in the senescence stage (Abeles et al. 1992; Borochov

K. Tanase (✉)
Institute of Vegetable and Floriculture Science, NARO, Tsukuba, Ibaraki 305-8519, Japan
e-mail: tanase@affrc.go.jp

T. Onozaki and M. Yagi (eds.), *The Carnation Genome*, Compendium of Plant Genomes,
https://doi.org/10.1007/978-981-15-8261-5_5

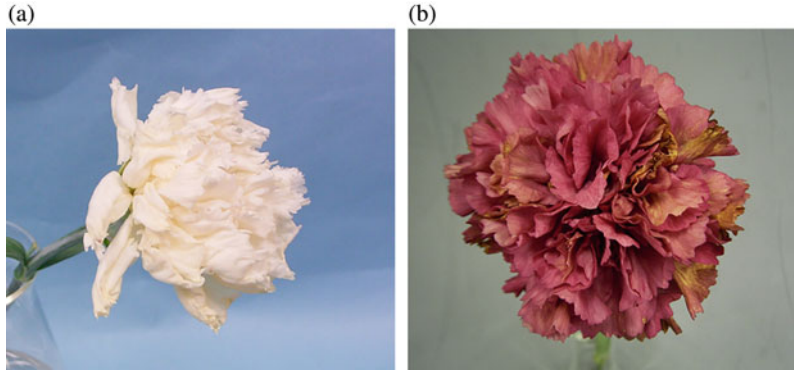

Fig. 5.1 Carnation flowers at senescence stage. **a** Flower of 'White Sim' which is normal life was at 7 days after harvest. Flower that senesced naturally showed petal in-rolling. **b** Flower of 'Miracle Rouge' which is long vase life was at 25 days after harvest. Flower that senesced naturally showed petal browning but did not show petal in-rolling

and Woodson 1989; Halevy and Mayak 1981; Reid and Wu 1992; Wang and Woodson 1989; Woltering and vanDoorn 1988). Additionally, exposure of fully open carnation flowers to ethylene induces autocatalytic ethylene production and wilting in petals of a short time (Halevy and Mayak 1981). Thus, ethylene is an important determinant of carnation vase life. Cut carnation flowers or normal cultivars generally senesce within approximately 7 days, furthermore their vase life can be extended by treatment with post-harvest chemicals. Some post-harvest chemicals prolong vase life; aminooxyacetic acid (Fujino et al. 1980), aminoethoxyvinyl glycine (Baker et al. 1977), and α-aminoisobutyric acid (Onozaki et al. 1998) are inhibitors of ethylene production. Silver thiosulfate (STS) (Veen 1979), 2,5-norbornadiene (Sisler et al. 1983) and 1-methylcyclopropene (Serek et al. 1995) are inhibitors of ethylene action. STS is widely used but potentially causes environmental contamination from waste STS solution (Scariot et al. 2014). Additionally, chemical treatment after harvesting burden farmers by increasing labor time. Genetic approach for improving vase life is attractive because the cultivars would require no or less chemical treatment. A research breeding program was started by the NARO Institute of Vegetable and Floriculture Science in 1992 to improve the vase life of carnation flowers through conventional breeding techniques (Onozaki, 2018). This review reports achievements in the breeding and molecular mechanisms of carnations to extend their vase life.

5.1.1 Cross-Breeding for Long Vase Life Cultivars

According to the complex trait of vase life, few studies were conducted to achieve flower longevity before the 1990s (Onozaki 2018). But carnation cultivars and lines with highly variable ethylene production and sensitivity associated with vase life are valuable in the studies of ethylene-related processes and improving of vase life (Wu et al. 1991a). Examples of flowers with low ethylene production are 'Killer' (Serrano et al. 1991), 'Sandra' (Wu et al. 1991a; b), 'Sandrosa' (Mayak and Tirosh 1993), line 87-37G-2 and line 81–2 (Brandt and Woodson 1992), 'White Candle' (Nukui et al. 2004), 'Miracle Rouge' and 'Miracle Symphony' (Onozaki et al. 2006a; b), line 006–13 and line 62–2" (Onozaki et al. 2001, 2006b; Tanase et al. 2013), and line 532–6 (Tanase et al. 2015; Onozaki et al. 2011). In contrast to cultivars with low ethylene production, the flowers of some other long vase life cultivars such as 'Chinera' (Reid and Wu 1992; Woltering et al. 1993), 'Epomeo' (Woltering et al. 1993), line 902-48a, line 234-43S, and line 234-36S (Onozaki et al. 2008) appear to have relatively low

sensitivity to ethylene. And line 799 (Brandt and Woodson, 1992) and line 806-46b (Onozaki et al. 2015) seem to have both low ethylene production and low ethylene sensitivity.

Genetic improvement has been studied to produce cultivars with improved vase life without the requirement for STS treatment (Onozaki et al. 2006a). Six commercial standard cultivars (four Mediterranean-type cultivars (‘Pallas’, ‘Sandrosa’, 'Candy', and 'Tanga') and two American 'Sim'-type cultivars ('White Sim' and 'Scania') with large difference in vase life were used as initial materials in this program.

In the breeding process, lines selected as having a long vase life in each generation were used as the parents of the next generation (Onozaki et al. 2001, 2011, 2006a). Vase life was evaluated under standard environmental conditions (23 °C, 70% relative humidity, 12-h photoperiod) to reduce post-harvest non-genetic variation from the start of the program. Crossing and selection resulted in large alterations in the vase life of each generation, and particularly in low ethylene production in many lines (Onozaki et al. 2001). The mean vase life increased from 7.4 days in the 1st generation to 15.9 days in the 7th generation. The resulting cultivars ‘Miracle Rouge’ and ‘Miracle Symphony’ were released in 2005. Thus, many carnation lines with genetically long vase lives were developed using conventional cross-breeding techniques (Onozaki et al. 2006a).

The flowers of ‘Miracle Rouge’ and ‘Miracle Symphony’ produced low levels of ethylene (Onozaki et al. 2006a). The plant hormone ethylene regulates many important growth and development processes, such as flower senescence, in numerous plant species. The ethylene biosynthetic pathway can be summarized as follows: methionine → *S*-adenosylmethionine (AdoMet) 1-aminocyclopropane-1-carboxylate (ACC) → ethylene (Kende 1993). The conversion of AdoMet to ACC is catalyzed by ACC synthase (ACS), and ethylene is produced from ACC by ACC oxidase (ACO) (Yang and Hoffman 1984). The catalytic reactions involving ACS and ACO are generally considered to be rate-limiting in ethylene biosynthesis. Both enzymes are well-characterized and the several genes encoding them have been cloned in carnation. Increased ethylene production is associated with increased expression of the ACS and ACO genes (Park et al. 1992; Henskens et al. 1994; Jones and Woodson 1999; Wang and Woodson 1991; Woodson et al. 1992). Three ACC synthase genes (*DcACS1* (previously named as CARACC3), *DcACS2*, and *DcACS3*) and one ACC oxidase gene (*DcACO1* (previously named as pSR120)) have been identified in carnation (Woodson et al. 1992; Jones and Woodson 1999).

5.1.2 Molecular Mechanism of Long Vase Life Carnation

Previous studies have been conducted to examine the mechanisms of downregulation of ethylene production in carnation with long vase lives by evaluating the expression of ethylene-related genes. In cultivars with a normal vase life (control), flower such as ‘White Sim’ and ‘Francesco’, the increase in ethylene production was associated with a dramatic increase in the expression of *DcACS1*, *DcACS2,* and *DcACO1* (Wang and Woodson 1991; Park et al. 1992; Tanase et al. 2008). Reaching peak expression of them, then the climacteric-like ethylene production was observed and the flower senesced with the petal in-rolling.

In long vase life cultivar 'Miracle Rouge' and 'Miracle Symphony', the expression of *DcACS1*, *DcACS2*, and *DcACO1* was strongly suppressed in the gynoecium and petals during senescence, resulting in extremely low ethylene production (Tanase et al. 2008). Therefore, neither cultivars show the climacteric-like ethylene production and petal in-rolling, but they senesced with browning from the petal edge over time (Onozaki et al. 2001, 2006b; Tanase et al. 2008,2013). Lines 006–13 and 62–2, which were developed during the research breeding program to prolong vase life, showed suppression of the ACS and ACO genes, and both lines senesced in the same manner as 'Miracle Rouge' and 'Miracle Symphony' (Tanase et al. 2013). All were progeny of the long vase life cultivar 'Sandrosa', and thus the low ethylene trait related to suppression of

DcACS1, *DcACS2*, and *DcACO1*appears to be heritable.

The spray type carnation cultivar 'White Candle' had a long vase life flowers with the repressed ethylene production (Nukui et al. 2004). Expression of *DcACO1* was detected in senescing flowers, whereas *DcACS* genes expression was not detected. These results indicate that the suppression of *DcACS* genes is associated with the low ethylene production in 'White Candle'. Furthermore, we confirmed the different manners of suppressing ethylene production, ACC, the intermediate of ethylene biosynthesis, was used to long vase life cultivars and line, 'Miracle Rouge', line 006–13, 'Sandrosa', 'White Candle', and normal life (control) 'White Sim' flowers (Fig. 5.2). ACC treatment shortened the vase lives of 'White Candle' and 'White Sim', but not those of 'Miracle Rouge' line 006–13 and 'Sandrosa', indicating the *DcACO1* is a key step in distinguishing between the groups of long vase life carnation. Therefore, suppression of ethylene production was separated into two groups based on expression of *DcACS* and *DcACO*; *DcACS1*, *DcACS2*, and *DcACO1* are suppressed in the flower type of 'Miracle Rouge' and 'Miracle Symphony', and *DcACS* genes is suppressed in that of 'White Candle'.

Fig. 5.2 Flowers of carnation after 12 h of ACC treatment. ACC (1 mM) solution was treated 3 h to the flowers of long vase life ('Miracle Rouge', line 006–13, 'Sandrosa' and 'White Candle') and normal life (control) flower ('White Sim') from left to right. After treatment, flowers moved to distilled water and monitored the inrolling of petals hourly

5.1.3 Ultra-Long Vase Life Cultivars

The 7th-generation line 532–6 showed the longest vase lives of any cultivar ever bred with means of 32.7 days and 27.8 days in 2007 and 2008, respectively, which was defined as an "ultra-long vase life". (Onozaki et al. 2011). The petals of the other long vase life cultivars started browning from the edges, and then slowly desiccated and faded (Fig. 5.1b). However, line 532–6 showed no browning, and instead slowly desiccated and wrinkled.

Normal vase life cultivars, such as 'White Sim' and 'Francesco', senesce by petal inrolling and rapid wilting, which are characteristics typical of ethylene-dependent senescence (Iwazaki et al. 2004; Otsu et al. 2007; Satoh et al. 2011). However, 'Sandrosa', our selected cultivars 'Miracle Rouge' and 'Miracle Symphony' which low ethylene production at senescence, did not exhibit petal in-rolling at senescence, and instead faded and turned brown from the petal edges. Otsu et al. (2007) named this process "ethylene-independent senescence". Line 532–6 showed another senescence pattern, characterized by a lack of petal browning. This indicates that the ultra-long vase lifeline 532–6 not only has extremely low ethylene production, but also expresses some genes that regulate programmed cell death (Tanase et al. 2015).

Petal wilting is regarded as the degradation of cellular components, which induces cell death (van Doorn and Woltering 2004). This process is regulated by hydrolytic enzymes, such as lipases [Lip (Hong et al. 2000; Kim et al. 1999a)], cysteine proteinases [CPs (Jones et al. 1995)], and their regulator, a cysteine proteinase (CP) inhibitor [CPIn (Kim et al. 1999b; Sugawara et al. 2002)]. Many of these senescence-related (SR) genes have been cloned from petals and their expression patterns were studied in

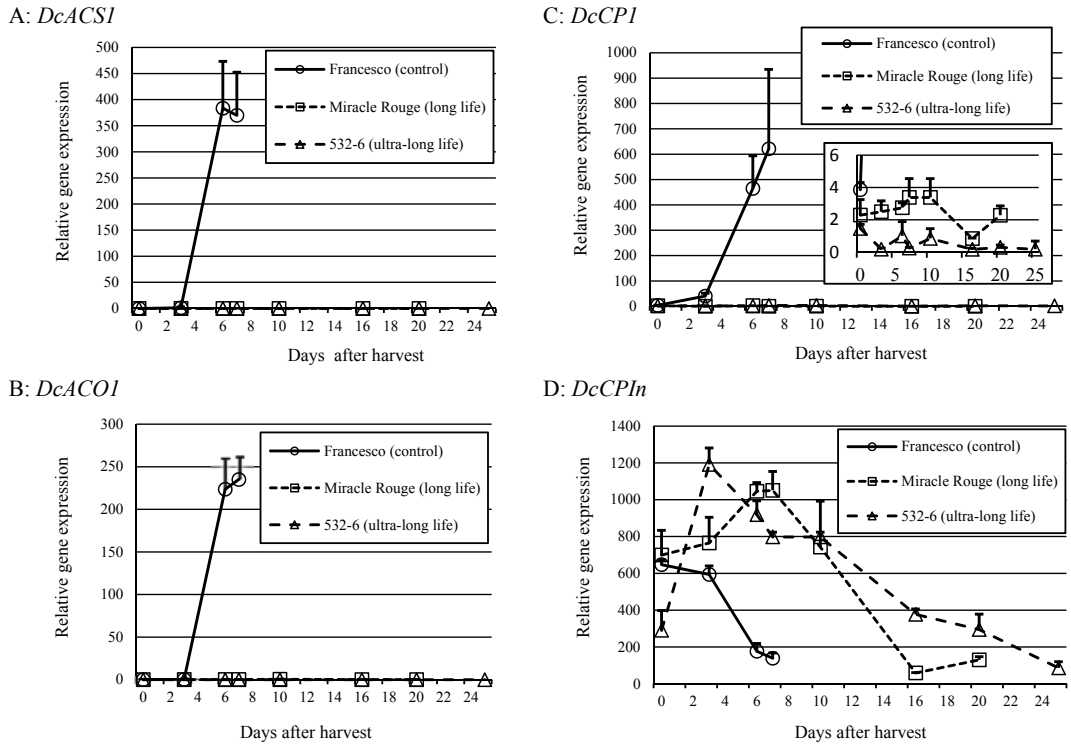

Fig. 5.3 Transcript levels of *DcACS1* (**a**), *DcACO1* (**b**), *DcCP1* (**c**), and *DcCPIn* (**d**) in petals during flower senescence. Petals of 'Francesco' (control), 'Miracle Rouge' (long life flower), and line 532–6 (ultra-long life flower) were used for expression analysis

carnation. In the normal life cultivar (control), the transcript levels of the CP gene [*DcCP1*; previously named as pDCCP1 (Jones et al. 1995)], β-galactosidase gene [*DcbGal*; previously described as SR12 (Lawton et al. 1989)], glutathione-*S*-transferase (*DcGST1*) gene, and lipase (*DcLip*) gene are up-regulated during flower senescence and by endogenous ethylene treatment (Hong et al. 2000, Kim et al. 1999a, Verlinden et al. 2002), whereas the *DcCPIn* transcript level is down-regulated under these condition (Sugawara et al. 2002; Tanase et al. 2013). In addition, we compared the levels of SR genes between long vase life, 'Miracle Rouge' and ultra-long vase life, line 532–6 (Fig. 5.3). Most SR genes were expressed at similar levels between these flowers, whereas the *DcCPIn* and *DcCP1* showed different expression patterns. The extended vase life of 'Miracle Rouge' and line 532–6 compared to in normal flowers depends on the reduced levels of ethylene biosynthetic gene expression and senescence-related genes; the difference between 'Miracle Rouge' and line 532–6 may be related to *DcCPIn* and *DcCP1*.

5.1.4 Genetic Variation in Ethylene Sensitivity

In carnation, the exogenous ethylene response of flowers is accompanied by autocatalytic ethylene production and petal in-rolling. It is also responsible for the rapid and coordinated senescence of petals. Ethylene sensitivity is the time to the beginning of petal in-rolling. Generally, ethylene sensitivity has important effects on flower longevity in carnation. As cut carnation flowers are often exposed to ethylene during shipping and selling condition, cultivars with

insensitive or low sensitivity to ethylene are needed. Our research and other studies revealed that the time to the beginning of petal in-rolling after exposure of exogenous ethylene differed among cultivars and lines; thus, ethylene sensitivity differed. The optimum concentration of exogenous ethylene was 10 μL L^{-1}, and a time-lapse video recording system was used to measure the time to the beginning of petal in-rolling for sensitivity evaluation (Onozaki et al. 2004). Line 64–54, 3rd-generation line, showed lower ethylene sensitivity than the cultivars. In normal cultivars such as 'White Sim' and 'Nora' petal in-rolling rapidly occurred approximately 7–8 h after treatment. In line 64–54, the response time was approximately 20 h thus, this line was less sensitive to ethylene. Line 64–54 is the progeny of 'Candy' and 'Sandrosa'. 'Sandrosa' is sensitive to ethylene, with a response time of 6.2 h, whereas 'Candy' has a response time of 11.6 h and is significantly less sensitive than 'Sandrosa' (Onozaki et al. 2004). The genes conferring low ethylene sensitivity supposed to be derived from 'Candy'. Woltering et al. (1993) showed that reduced ethylene sensitivity is heritable, and thus it is possible to breed ethylene-insensitive or less-sensitive lines with long vase lives through conventional cross-breeding.

Genetic studies have defined the key elements mediating the response to ethylene using the model plant, *Arabidopsis* (Wang et al. 2002). Ethylene is detected by members of the ethylene receptor (ER) family which are the starting point for ethylene signaling in plants. ERs are homologous to bacterial two-component histidine kinases which are involved in sensing environmental changes. Five ERs exist in *Arabidopsis*: ETR1, ETR2, ERS1, ERS2, and EIN4 (Chang et al. 1993; Hua et al. 1995; Hua and Meyerowitz 1998; Sakai et al. 1998). In carnation, the ER genes *DcETR1*, *DcERS1*, and *DcERS2* have been cloned, but *DcERS1* mRNA was not detected in flowers (Nagata et al. 2000; Shibuya et al. 2002). In addition to ERs, many ethylene signal components, such as CTR1, EIN2, EIN3, and EIN3-like (EIL), have been studied in many plant species. CTR1 negatively regulates signaling events downstream of ERs (Kieber et al. 1993). EIN3 and EILs are nuclear-localized transcription factors that appear to play important roles in regulating genes with an ethylene-responsive element in the promoter region (Solano et al. 1998). In carnation, three EILs (DcEIL1/2, DcEIL3, and DcEIL4) may regulate ethylene response factors and SR genes. Particularly, DcEIL3 may play an essential role during flower senescence by regulating senescence-related genes (Iordachescu and Verlinden 2005). The components up to EILs were defined as primary signal, and those downstream of EILs were defined as secondary signals in carnation flower (Verlinden et al. 2002).

The molecular mechanism ethylene sensitivity is poorly understood in carnation. Flowers of 'Chinera' and 'Epomeo' are considerably less sensitive to ethylene than that of 'White Sim', but the number of ERs and affinity of ethylene for ERs are similar in 'Chinera' and 'White Sim' (Woltering et al. 1993; Wu et al. 1991a). The pot carnation cultivars 'Orange Duo' and 'Lemon Soft' flowers are considered to have lower ethylene sensitivity compared to 'Ariel' (Tanase and Onozaki 2016). Expression of ER genes and EIL genes which are ethylene signal components showed only slight differences in these cultivars. Therefore, the low sensitivity to ethylene in some cultivars may be regulated by a factor other than receptors and *EIL*s in ethylene signal transduction pathway.

5.1.5 Ultra-Long Vase Life Line with Low Ethylene Sensitivity

To screen lines with both extremely long vase lives and low sensitivity to ethylene, we repeatedly crossed and selected promising progeny for three generations from 2003 to 2010. In 2010, line 806-46b, which showed both an ultra-long vase life and low ethylene sensitivity, was found among 50 progenies derived from a cross between lines 606-65S and 609-63S (Onozaki et al. 2015). The mean vase life of line 806-46b was 27.1 days which is 4.4-fold longer than that of the normal cultivar 'White Sim'. Lines 532–6

and 806-46b showed an ultra-long vase life but different sensitivity to exogenous ethylene. The response time of line 806-46b to 10 μL L^{-1} ethylene was 21.8 h, whereas that of 532–6 was 6.2 h, which is nearly the same as that of normal cultivar 'White Sim' (Onozaki et al. 2011, 2015). Although line 532–6 has an ultra-long vase life and low level of ethylene production at senescence, it is sensitive to exogenous ethylene. In contrast, line 806-46b with an ultra-long vase life showed low ethylene sensitivity. These results demonstrate that lines with both an extremely long vase life and ethylene resistance can be bred using conventional cross-breeding techniques. The genetic mechanisms underlying low ethylene sensitivity in line 806-46b are poorly understood. To increase our understanding of transcript regulation in carnation, we constructed a large-scale expression sequence tag database based on next-generation sequencing (Tanase et al. 2012). A previous study reported long vase life-related transcripts of carnation determined RNA-seq (Boxriker et al. 2017). Further studies will improve the understanding of the mechanisms of ethylene sensitivity related to flower vase life in carnation.

5.2 Conclusions

The breeding of cultivars with genetically long vase life is an efficient approach to satisfying consumers' quality expectations. Two cultivars, 'Miracle Rouge' and 'Miracle Symphony', have a genetically determined long vase life of approximately 20 days and were released in 2005. Two lines, 532–6 and 806-46b, with an ultra-long vase life of over 27 days were also developed (Onozaki et al. 2006a, 2011, 2015). Ethylene regulates flower senescence in carnation and is suppressed in long vase life cultivars. Ethylene production is suppressed by repression of the induction of ACC synthase and ACC oxidase genes. Although ethylene is involved in many aspects of plant growth and development, these cultivars can be propagated and cultivated without harmful effects.

More recently, expressed sequence tags, large-scale transcriptome analysis, DNA markers, and whole genome sequences have been used to study flower vase life in carnation. These studies have clarified the control of ethylene biosynthesis, perception, and signal transduction in carnation. Understanding the genetic control of these physiological traits and linkage of these physiological characteristics to molecular markers on the genome, as well as the gene(s) underlying these traits, have great potential for use in carnation breeding.

Acknowledgements I thank Dr. Onozaki, Dr. Yagi, and Dr. Ichimura of Institute of Vegetable and Floriculture Science, NARO, and Prof. Satoh of Ryukoku University for giving valuable advice and support on study the molecular analysis in the long vase life carnation. I thank Prof. Shibata of the University of Tokyo for giving an opportunity to the research of the long vase life carnation.

References

Abeles FB, Morgan PW, Saltveit ME Jr (1992) Ethylene in plant biology, 2nd edn. Academic Press, Inc., New York

Baker JE, Wang CY, Lieberman M, Hardenburg R (1977) Delay of senescence in carnations by a rhizobitoxine analog and sodium benzoate. HortScience 12:38–39

Borochov A, Woodson WR (1989) Physiology and biochemistry of flower petal senescence. Hort Rev 11:15–43

Boxriker M, Boehm R, Krezdorn N, Rotter B, Piepho HP (2017) Comparative transcriptome analysis of vase life and carnation type in *Dianthus caryophyllus* L. Sci Hort 217:61–72. https://doi.org/10.1016/j.scienta.2017.01.015

Brandt AS, Woodson WR (1992) Variation in flower senescence and ethylene biosynthesis among carnations. HortScience 27:1100–1102

Chang C, Kwok SF, Bleecker A, Meyerowitz E (1993) *Arabidopsis* ethylene-response gene *ETR1*: similarity of product to two-component regulators. Science 262:539–544

Fujino DW, Reid MS, Yang SF (1980) Effects of aminooxyacetic acid on postharvest characteristics of carnation. Acta Hortic 113:59–64

Halevy AH, Mayak S (1981) Senescence and postharvest physiology of cut flowers, Part 2. Hort Rev 3:59–143

Henskens JAM, Rouwendal GJA, Tenhave A, Woltering EJ (1994) Molecular-cloning of 2 different ACC synthase PCR fragments in carnation flowers and organ-specific expression of the corresponding genes. Plant Mol Biol 26:453–458

Hong YW, Wang TW, Hudak KA, Schade F, Froese CD, Thompson JE (2000) An ethylene-induced cDNA encoding a lipase expressed at the onset of senescence. Proc Natl Acad Sci USA 97:8717–8722

Hua J, Chang C, Sun Q, Meyerowitz EM (1995) Ethylene-insensitivity conferred by *Arabidopsis* ERS gene. Science 269:1712–1714

Hua J, Meyerowitz EM (1998) Ethylene responses are negatively regulated by a receptor gene family in *Arabidopsis thaliana*. Cell 94:261–271

Iordachescu M, Verlinden S (2005) Transcriptional regulation of three EIN3-like genes of carnation (*Dianthus caryophyllus* L. cv. Improved White Sim) during flower development and upon wounding, pollination, and ethylene exposure. J Exp Bot 56:2011–2018

Iwazaki Y, Kosugi Y, Waki K, Yoshioka T, Satoh S (2004) Generation and ethylene production of transgenic carnations harboring ACC synthase cDNA in sense or antisense orientation. J Appl Hort 6:67–71

Jones ML, Larsen PB, Woodson WR (1995) Ethylene-regulated expression of a carnation cysteine proteinase during flower petal senescence. Plant Mol Biol 28:505–512

Jones ML, Woodson WR (1999) Differential expression of three members of the 1-aminocyclopropane-1-carboxylate synthase gene family in carnation. Plant Physiol 119:755–764

Kende H (1993) Ethylene biosynthesis. Ann Rev Plant Physiol Plant Mol Biol 44:283–307

Kieber JJ, Rothenberg M, Roman G, Feldmann KA, Ecker JR (1993) CTR1, a negative regulator of the ethylene response pathway in *Arabidopsis*, encodes a member of the raf family of protein kinases. Cell 72:427–441

Kim JY, Chung YS, Ok SH, Lee SG, Chung WI, Kim IY, Shin JS (1999a) Characterization of the full-length sequences of phospholipase A(2) induced during flower development. Biochim Biophys Acta-Gene Struct Exp 1489:389–392

Kim JY, Chung YS, Paek KH, Park YI, Kim JK, Yu SN, Oh BJ, Shin JS (1999b) Isolation and characterization of a cDNA encoding the cysteine proteinase inhibitor, induced upon flower maturation in carnation using suppression subtractive hybridization. Mol Cells 9:392–397

Lawton KA, Huang B, Goldsbrough PB, Woodson WR (1989) Molecular-cloning and characterization of senescence-related genes from carnation flower petals. Plant Physiol 90:690–696

Mayak S, Tirosh T (1993) Unusual ethylene-related behavior in senescing flowers of the carnation Sandrosa. Physiol Plant 88:420–426

Nagata M, Tanikawa N, Onozaki T, Mori H (2000) Ethylene receptor gene (ETR) homolog from carnation. J Jpn Soc Hort Sci 69(Suppl. 1):407

Nukui H, Kudo S, Yamashita A, Satoh S (2004) Repressed ethylene production in the gynoecium of long-lasting flowers of the carnation 'White Candle': role of the gynoecium in carnation flower senescence. J Exp Bot 55:641–650

Onozaki T (2018) Breeding of carnations (*Dianthus caryophyllus* L.) for long vase life. Breed Sci 68:3–13. https://doi.org/10.1270/jsbbs.17091

Onozaki T, Ikeda H, Shibata M (2004) Video evaluation of ethylene sensitivity after anthesis in carnation (*Dianthus caryophyllus* L.) flowers. Sci Hort 99:187–197

Onozaki T, Ikeda H, Shibata M, Yagi M, Yamaguchi T, Amano M (2006a) Breeding and characteristics of carnation norin No.1 'Miracle Rouge' and No2. 'Miracle Symphony' with long vase life. Bull Nat Inst Floric Sci 5:1–16

Onozaki T, Ikeda H, Yamaguchi T (1998) Effect of calcium nitrate addition to (alpha)-aminoisobutyric acid (AIB) on the prolongation of the vase life of cut carnation flowers. J Jpn Soc Hort Sci 67:198–203

Onozaki T, Ikeda H, Yamaguchi T (2001) Genetic improvement of vase life of carnation flowers by crossing and selection. Sci Hort 87:107–120

Onozaki T, Tanikawa N, Yagi M, Ikeda H, Sumitomo K, Shibata M (2006b) Breeding of carnations (*Dianthus caryophyllus* L.) for long vase life and rapid decrease in ethylene sensitivity of flowers after anthesis. J Jpn Soc Hort Sci 75:256–263

Onozaki T, Yagi M, Shibata M (2008) Selection of ethyleneresistant carnations (*Dianthus caryophyllus* L.) by video recording system and their response to ethylene. Sci Hortic 116:205–212

Onozaki T, Yagi M, Tanase K (2015) Selection of carnation line 806–46b with both ultra-long vase life and ethylene resistance. Hort J 84:58–68. https://doi.org/10.2503/hortj.MI-011

Onozaki T, Yagi M, Tanase K, Shibata M (2011) Crossing and selections for six generations based on flower vase life to create lines with ethylene resistance or ultra-long vase life in carnation (*Dianthus caryophyllus* L.). J Jpn Soc Hort Sci 80:486–498

Otsu S, Satoh S, Kosugi Y (2007) Expression of senescence related genes in carnation petals undergoing wilting and fading. Acta Hort 763:283–287

Park KY, Drory A, Woodson WR (1992) Molecular cloning of an 1-aminocyclopropane-1-carboxylate synthase from senescing carnation flower petals. Plant Mol Biol 18:377–386

Reid MS, Wu MJ (1992) Ethylene and flower senescence. Plant Growth Regul 11:37–43

Sakai H, Hua J, Chen QG, Chang C, Medrano LJ, Bleecker AB, Meyerowitz EM (1998) ETR2 is an ETR1-like gene involved in ethylene signaling in *Arabidopsis*. Proc Natl Acad Sci USA 95:5812–5817

Satoh S, Meng N, Harada T, Nomura Y, Kawarada M, Morita S (2011) Possible origin of two variants of a carnation 1-aminocyclopropane-1-carboxylate synthase gene, *DcACS1a* and *DcACS1b*, as suggested by intron structure in homologous genes in *Dianthus* species. J Jpn Soc Hort Sci 80:443–451

Scariot V, Paradiso R, Rogers H, De Pascale S (2014) Ethylene control in cut flowers: classical and innovative approaches. Postharvest Biol Tech 97:83–92. https://doi.org/10.1016/j.postharvbio.2014.06.010

Serek M, Tamari G, Sisler EC (1995) Inhibition of ethylene-induced cellular senescence symptoms by 1-methylcyclopropene, a new inhibitor of ethylene action. Physiol Plant 94:229–232

Serrano M, Riquelme F, Romojaro F (1991) Ethylene and polyamine metabolism in climacteric and nonclimacteric carnation flowers. HortScience 26:894–896

Shibuya K, Nagata M, Tanikawa N, Yoshioka T, Hashiba T, Satoh S (2002) Comparison of mRNA levels of three ethylene receptors in senescing flowers of carnation (*Dianthus caryophyllus* L.). J Exp Bot 53:399–406

Sisler EC, Reid MS, Fujino DW (1983) Investigation of the mode of action of ethylene in carnation senescence. Acta Hortic 141:229–234

Solano R, Stepanova A, Chao Q, Ecker JR (1998) Nuclear events in ethylene signaling: a transcriptional cascade mediated by ethylene-insensitive3 and ethylene-response-factor1. Genes Dev 12:3703–3714

Sugawara H, Shibuya K, Yoshioka T, Hashiba T, Satoh S (2002) Is a cysteine proteinase inhibitor involved in the regulation of petal wilting in senescing carnation (*Dianthus caryophyllus* L.) flowers? J Exp Bot 53:407–413

Tanase K, Nishitani C, Hirakawa H, Isobe S, Tabata S, Ohmiya A, Onozaki T (2012) Transcriptome analysis of carnation (*Dianthus caryophyllus* L.) based on next-generation sequencing technology. BMC Genomics 13. https://doi.org/10.1186/1471-2164-13-292.

Tanase K, Onozaki T (2016) Regulation of ethylene-and senescence-related genes in pot carnation flowers during flower senescence. Hort J 85:254–263. https://doi.org/10.2503/hortj.MI-093

Tanase K, Onozaki T, Satoh S, Shibata M, Ichimura K (2008) Differential expression levels of ethylene biosynthetic pathway genes during senescence of long-lived carnation cultivars. Postharvest Biol Technol 47:210–217. https://doi.org/10.1016/j.postharvbio.2007.06.023

Tanase K, Otsu S, Satoh S, Onozaki T (2013) Expression and regulation of senescence-related genes in carnation flowers with low ethylene production during senescence. J Jpn Soc Hort Sci 82:179–187. https://doi.org/10.2503/jjshs1.82.179

Tanase K, Otsu S, Satoh S, Onozaki T (2015) Expression levels of ethylene biosynthetic genes and senescence-related genes in carnation (*Dianthus caryophyllus* L.) with ultra-long-life flowers. Sci Hort 183:31–38. https://doi.org/10.1016/j.scienta.2014.11.025

van Doorn WG, Woltering EJ (2004) Senescence and programmed cell death: substance or semantics? J Exp Bot 55:2147–2153

Veen H (1979) Effects of silver on ethylene synthesis and action in cut carnations. Planta 145:467–470. https://doi.org/10.1007/Bf00380101

Verlinden S, Boatright J, Woodson WR (2002) Changes in ethylene responsiveness of senescence-related genes during carnation flower development. Physiol Plant 116:503–511

Wang H, Woodson WR (1989) Reversible Inhibition of ethylene action and interruption of petal senescence in carnation flowers by norbornadiene. Plant Physiol 89:434–438

Wang H, Woodson WR (1991) A flower senescence-related messenger-RNA from carnation shares sequence similarity with fruit ripening-related messenger-rnas involved in ethylene biosynthesis. Plant Physiol 96:1000–1001

Wang KL, Li H, Ecker JR (2002) Ethylene biosynthesis and signaling networks. Plant Cell 14(Suppl):S131-151

Woltering EJ, Somhorst D, Debeer CA (1993) Roles of ethylene production and sensitivity in senescence of carnation flower (*Dianthus caryophyllus*) cultivars White Sim, Chinera and Epomeo. J Plant Physiol 141:329–335

Woltering EJ, vanDoorn WG (1988) Role of ethylene in senescence of petals—Morphological and taxonomical relationship. J Exp Bot 39:1605–1616

Woodson WR, Park KY, Drory A, Larsen PB, Wang H (1992) Expression of ethylene biosynthetic-pathway transcripts in senescing carnation flowers. Plant Physiol 99:526–532. https://doi.org/10.1104/pp.99.2.526

Wu MJ, Vandoorn WG, Reid MS (1991a) Variation in the senescence of carnation (*Dianthus Caryophyllus* L.) cultivars.1. Comparison of flower life, respiration and ethylene biosynthesis. Scientia Hort 48:99–107

Wu MJ, Zacarias L, Reid MS (1991b) Variation in the senescence of carnation (*Dianthus-caryophyllus* L) cultivars 2. Comparison of sensitivity to exogenous ethylene and of ethylene binding. Scientia Hort 48:109–116

Yang SF, Hoffman NE (1984) Ethylene biosynthesis and its regulation in higher plants. Annu Rev Plant Physiol 35:155–189

6 Flower Pigments Responsible for Cyanic, Yellow, and Cream-White Coloration in Carnation

Masayoshi Nakayama

Abstract

Carnation (*Dianthus caryophyllus* L.) has four kinds of major anthocyanin pigments: pelargonidin 3-*O*-malyl-glucoside; pelargonidin 3-*O*, 5-*O*-cyclic malyl-diglucoside; cyanidin 3-*O*-malyl-glucoside; and cyanidin 3-*O*, 5-*O*-cyclic malyl-diglucoside. Acylation of anthocyanins by malic acid and formation of cyclic anthocyanin structures by binding sugar moieties through an organic acid are specific to *Dianthus* species. Each carnation cultivar's flowers contain a single major anthocyanin, which dictates the characteristic coloration—vermilion, pink, dark-red, or red–purple. The anthocyanins can be distinguished based on absorption spectra, or by R_f values, coloration, and fluorescence in thin-layer-chromatography analysis. The pigment responsible for deep yellow coloration of carnation flowers is chalcone 2′-*O*-glucoside. Flower images under blue light are used to discriminate between chalcone 2′-*O*-glucoside and yellow carotenoid. Two flavones—apigenin 6-*C*-, 8-*C*-diglucoside, and apigenin 6-*C*-glucoside-7-*O*-malyl-glucoside—have been identified in carnation flowers; the latter is a co-pigment to a new anthocyanin in a transgenic blue-purple carnation. Six flavonols—kaempferol 3-*O*-rhamnosyl-(1–2)-glucoside, kaempferol 3-*O*-glucosyl-(1–2)-glucoside, kaempferol 3-*O*-rhamnosyl-(1–6)-glucoside, kaempferol 3-*O*-glucosyl-(1–2)-[rhamnosyl-(1–6)]-glucoside and its malyl ester, and kaempferol 3-*O*-rhamnosyl-(1–2)-[rhamnosyl-(1–6)]-glucoside—have been identified as responsible pigments for cream-white coloration. Images under ultraviolet light are used to estimate the flavonol levels in cream-white and white flowers. Representative coloration patterns of carnation cultivars are presented with microscopic images of the coloration borders.

6.1 Introduction

The flower colorations of major carnation cultivars are cyanic, yellow, cream-white, and white. The pigments responsible for these colorations are flavonoids, which are biosynthetically related polar aromatic compounds. Anthocyanins are a group of flavonoids that express cyanic coloration including red, red–purple, blue-purple, and blue due to their resonance structure absorbing visible light. Other types of flavonoids are chalcones, flavones, and flavonols. Chalcones are a yellow pigment, and flavones and flavonols are pale-yellow pigments; they are responsible for the yellow and cream-white coloration of flowers, including carnation flowers.

M. Nakayama (✉)
Institute of Vegetable and Floriculture Science, (NARO), Tsukuba, Ibaraki 305-8519, Japan
e-mail: nakayosi@affrc.go.jp

T. Onozaki and M. Yagi (eds.), *The Carnation Genome*, Compendium of Plant Genomes,
https://doi.org/10.1007/978-981-15-8261-5_6

The biosynthetic relationship between anthocyanins and the other flavonoids is shown in Fig. 6.1. They are biosynthesized from one phenylalanine and three malonyl CoA molecules. The chromophore of an anthocyanin (i.e., the part responsible for the color) is named an "anthocyanidin". Anthocyanidins are composed of A-, B-, and C-rings: the A- and C-rings are dicyclic aromatic rings containing nine carbons and one oxygen derived from the side chain of phenylalanine and three malonyl CoA; the B-ring is a monocyclic aromatic ring containing six carbons derived from the aromatic ring of phenylalanine. Anthocyanidins conjugated with sugars are called anthocyanins; these sugars are often conjugated with organic acids. Flavones and flavonols are also conjugated with sugars and organic acids in a similar manner. In Chap. 6, the structural characteristics, physicochemical properties, and contributions to flower coloration of carnation anthocyanins and flavonoids are explained.

6.2 Anthocyanins, Pigments Responsible for Cyanic Coloration

Like in many other floricultural plants, the pigments responsible for cyanic coloration of carnation flowers are anthocyanins. The major anthocyanins contained in flowers of common carnation cultivars are the following four compounds: pelargonidin 3-*O*-malyl-glucoside (3-*O*-glucosyl pelargonidin 6″-*O*-4-malate) (Terahara et al. 1986; Terahara and Yamaguchi 1986) [(1), Fig. 6.2a]; pelargonidin 3-*O*, 5-*O*-cyclic malyl-diglucoside (3, 5-di-*O*-glucosyl pelargonidin 6″-*O*-4, 6‴-*O*-1-cyclic malate) (Nakayama et al. 2000) [(2), Fig. 6.2a]; cyanidin 3-*O*-malyl-glucoside (3-*O*-glucosyl cyanidin 6″-*O*-4-malate) (Terahara et al. 1986; Terahara and Yamaguchi 1986) [(3), Fig. 6.2a]; and cyanidin 3-*O*, 5-*O*-cyclic malyl-diglucoside (3, 5-di-*O*-glucosyl cyanidin 6″-*O*-4, 6‴-*O*-1-cyclic malate) (Bloor 1998) [(4), Fig. 6.2a]. All of these are anthocyanins specifically detected in *Dianthus* species including carnation.

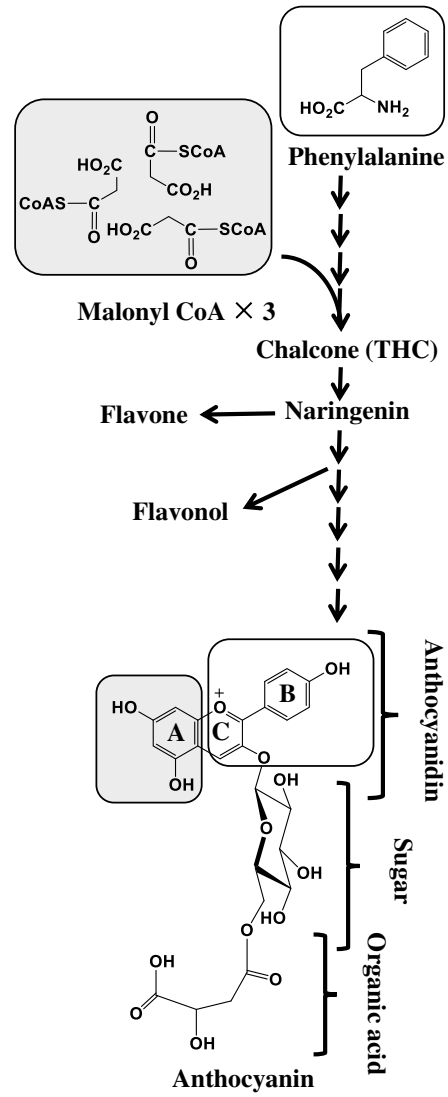

Fig. 6.1 Biosynthetic relationship between anthocyanins and flavonoids. The anthocyanidin, sugar, and organic acid moieties that comprise anthocyanin are indicated by vertical writing. In the anthocyanidin structure, the parts derived from phenylalanine and malonyl CoA are indicated by white and gray boxes, respectively. The letters A, B, and C denote the name of each ring

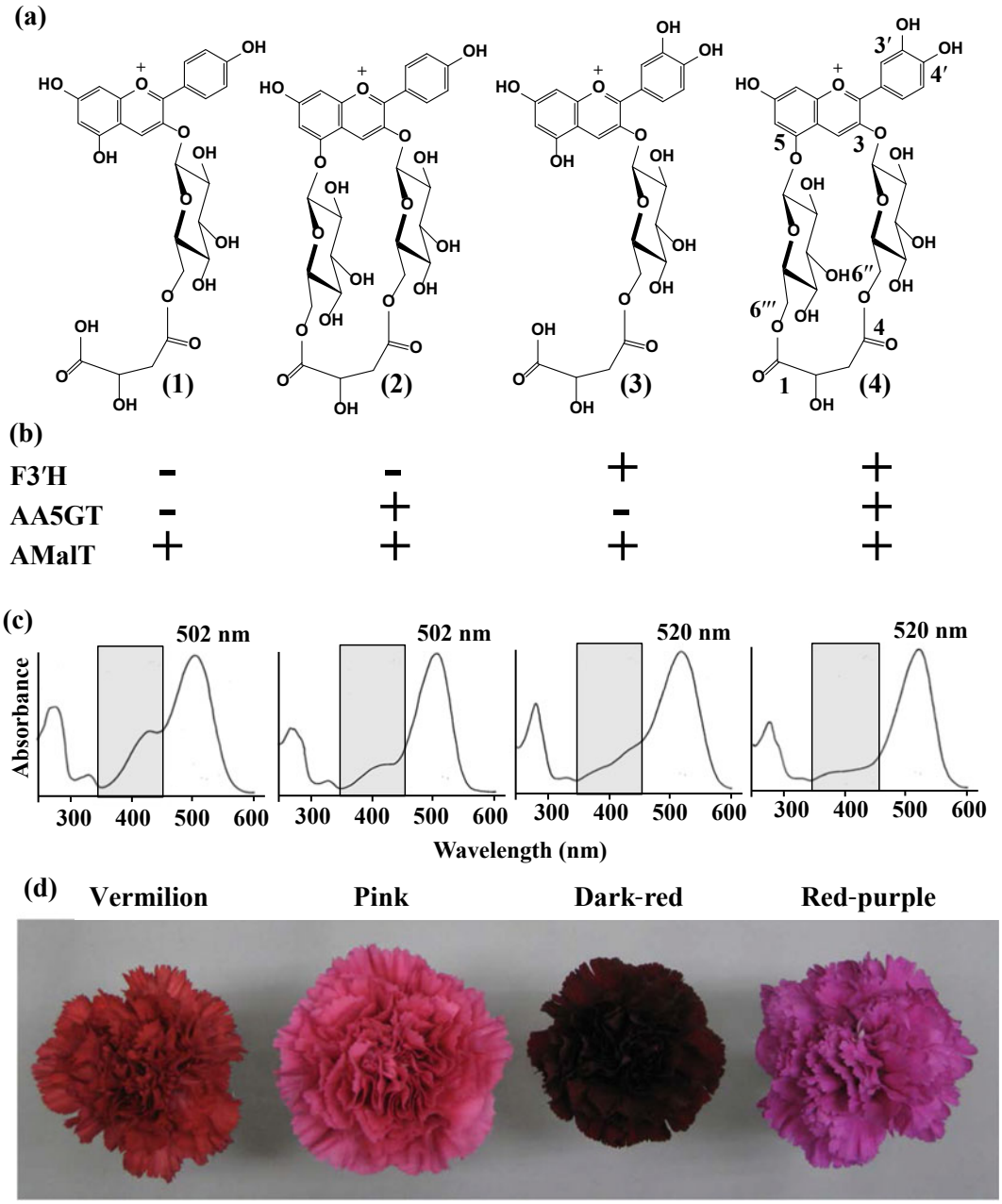

Fig. 6.2 Structures and properties of major anthocyanins in carnation flowers. **a** Structures of the anthocyanins: pelargonidin 3-*O*-malyl-glucoside (1); pelargonidin 3-*O*, 5-*O*-cyclic malyl-diglucoside (2); cyanidin 3-*O*-malyl-glucoside (3); and cyanidin 3-*O*, 5-*O*-cyclic malyl-diglucoside (4). **b** Enzymes required to synthesize each anthocyanin: + and - mean that the enzyme activity and inactivity, respectively, are required. **c** Absorption spectrum of each anthocyanin. Numbers indicate λ_{max}. Gray boxes indicate 350–450 nm wavelengths. **d** Representative carnation flowers containing a single major anthocyanin. All data in (**b**) to (**d**) refer to the anthocyanins presented directly above in (**a**)

6.2.1 Characteristics of Anthocyanidins

The anthocyanidin of the first two carnation anthocyanins listed above is pelargonidin [(1) and (2)], and that of the second two anthocyanins is cyanidin [(3) and (4)]. Pelargonidin has one hydroxy group at the 4′-position in the B-ring, while cyanidin has an additional hydroxy group at the 3′-position in the B-ring. Delphinidin-type

anthocyanidin has an additional hydroxy group at the 5′-position in the B-ring; it is found in transgenic cultivars but not in natural cultivars (Fukui et al. 2003). Peonidin-, petunidin-, and malvidin-type anthocyanidins have methylated hydroxy groups at the 3′- and/or 5′- positions in the B-ring; they are not found in carnation cultivars.

The enzyme that regulates the biosynthesis of cyanidin-type anthocyanins is flavonoid 3′-hydroxylase (F3′H) (Spribille and Forkmann 1982). The *F3′H* gene of carnation has been isolated and sequenced (Momose et al. 2013). In cultivars without active F3′H, the anthocyanidin is hydroxylated at only the 4′-position in the B-ring, resulting in biosynthesis of pelargonidin (Fig. 6.2b). In cultivars with active F3′H, the anthocyanidin is additionally hydroxylated at the 3′-position, resulting in biosynthesis of cyanidin.

6.2.2 Characteristics of Conjugated Sugars

The only sugar conjugated in carnation anthocyanins is glucose. In carnation, one glucose binds at the 3-hydroxy group in the C-ring of the anthocyanidin [(1) and (3)], or additional glucoses bind at the 5-hydroxy group in the A-ring of the anthocyanidin [(2) and (4)] in a glycosidic bond manner.

The enzyme that catalyzes the binding of glucose at the 5-position of the anthocyanidin is acyl-glucose-dependent anthocyanin 5-*O*-glucosyltransferase (AA5GT). The *AA5GT* gene of carnation has been isolated and sequenced (Matsuba et al. 2010; Nishizaki et al. 2011). In cultivars without active AA5GT, glucose binds only at the 3-hydroxy group of the anthocyanidin, resulting in biosynthesis of anthocyanidin 3-glucosides [(1) and (3)] (Fig. 6.2b). In cultivars with active AA5GT, an additional glucose binds at the 5-hydroxy group of the anthocyanidin, resulting in biosynthesis of anthocyanidin 3, 5-diglucosides [(2) and (4)].

6.2.3 Characteristics of Acylated Organic Acid

All carnation anthocyanins are acylated by malic acid alone. To my knowledge, anthocyanins acylated by malic acid are specific to *Dianthus* species. The enzyme catalyzing acylation of all anthocyanins in carnation is 1-*O*-malylglucose: pelargonidin 3-*O*-glucose-6″-*O*-malyltransferase (AMalT) (Abe et al. 2008). Active AMalT operates in flowers of common carnation cultivars (Fig. 6.2b).

In carnation, all glucoses bound at the 3-hydroxy group and/or 5-hydroxy group of the anthocyanin are acylated [(1) to (4)]. The 6″-hydroxy group of glucose binding at the 3-hydroxy group of the anthocyanidin is acylated by the 4-position carboxyl group of malic acid [(1) to (4)]. In addition, in anthocyanins with two glucose moieties [(2) and (4)], the 6‴-hydroxy group of glucose binding at the 5-hydroxy group of the anthocyanidin is acylated by the 1-position carboxyl group of the same malic acid molecule. As a result, the glucoses bound at the 3- and 5-positions of these anthocyanins are bridged through a malic acid. Anthocyanins possessing such bridged architecture are specific to *Dianthus* species including carnation. In summary, the distinctive characteristics of *Dianthus* anthocyanins are acylation by malic acid and the bridged architecture.

In carnation cultivars without active AMalT, acylation cannot be carried out and non-acylated anthocyanins composed of only anthocyanidin and glucose are synthesized (Okamura et al. 2013). The non-acylated anthocyanins are insoluble and become a granular precipitate in the vacuoles of petal cells and express characteristic metallic coloration in carnation flowers. ‘Ekstasis’ is a representative metallic coloration cultivar that is commercially available. These properties of non-acylated anthocyanins are peculiar to carnation; for instance, pelargonidin 3, 5-diglucoside and cyanidin 3, 5-diglucoside, which are de-acylated derivatives of anthocyanin (2) and (4), respectively, are soluble and, therefore, do not become a granular precipitate in rose (*Rosa hybrida*) petals.

6.2.4 Physicochemical Properties

The absorption spectrum of each of the anthocyanins [(1) to (4)] in Fig. 6.2a is shown in the corresponding order in Fig. 6.2c. These spectra were recorded after anthocyanin separation on an on-line high-performance liquid chromatography (HPLC) system equipped with an octadecylsilane (ODS) column in a phosphoric acid–acetonitrile–acetic acid–water mixture as mobile solvent (Nakayama et al. 2000). The pelargonidin-type anthocyanins [(1) and (2)] have the same maximum absorption wavelength (λ_{max}) of 502 nm, which is in the visible light spectrum, but pelargonidin 3-*O*-malyl-glucoside (1) has higher absorption than pelargonidin 3-*O*, 5-*O*-cyclic malyl-diglucoside (2) at 350–450 nm. The cyanidin-type anthocyanins [(3) and (4)] have the same λ_{max} value of 520 nm, but cyanidin 3-*O*-malyl-glucoside (3) has a higher absorption than cyanidin 3-*O*, 5-*O*-cyclic malyl-diglucoside (4) at 350–450 nm. Thus, the four anthocyanins in carnation flowers can be distinguished by their absorption spectra. It is noted that it may be difficult to clearly distinguish carnation anthocyanins only based on retention times under the conditions of the above HPLC analysis. The two pelargonidin-type anthocyanins have similar retention times to each other; the two cyanidin-type anthocyanins have longer retention times than the pelargonidin-type anthocyanins but have similar retention times to each other.

To determine the anthocyanin in a carnation cultivar with less time and cost than required for HPLC analysis, I recommend thin-layer chromatography (TLC) analyses using cellulose as the matrix and 10% acetic acid or *n*-butanol–acetic acid–water (4:1:2 v/v/v) as the developing solvent. Cyanidin 3-*O*-galactoside [(5), Fig. 6.3a] can be used as a standard for comparison because it is a major anthocyanin of red skin in apple (Duncan and Dustman 1936), and is available all year round. Results of TLC analysis of carnation anthocyanins [(1) to (4)] and the standard (5) are shown in Fig. 6.3b. R_f values obtained with 10% acetic acid as the solvent were 0.20, 0.57, 0.11, 0.50, and 0.13 for the carnation anthocyanins (1) to (4) and the standard (5), respectively. Thus, the R_f values for mono-glucosyl–type anthocyanins [(1), (3), and (5)] were less than those for di-glucosyl–type anthocyanins [(2) and (4)].

TLC spots of pelargonidin-type anthocyanins [(1) and (2)] showed similar orange coloration to each other, while those of cyanidin-type anthocyanins [(3) to (5)] showed similar red–purple coloration to each other (Fig. 6.3b). Furthermore, anthocyanins whose 5-hydroxy group of anthocyanidin is glycosylated [(2) and (4)] fluoresce under ultraviolet light (Fig. 6.3c). Pelargonidin 3-*O*, 5-*O*-cyclic malyl-diglucoside (2) shows strong orange fluorescence, while cyanidin 3-*O*, 5-*O*-cyclic malyl-diglucoside (4) shows weak red fluorescence. Note that the R_f values obtained with *n*-butanol–acetic acid–water mixture [4:1:2 (v/v/v)] were 0.39, 0.51, 0.24, 0.41, and 0.23 for the carnation anthocyanins (1) to (4) and the standard (5), respectively. In summary, the four anthocyanins in carnation can be easily distinguished by TLC based on a combination of R_f value, spot coloration, and fluorescence.

6.2.5 Cyanic Flower Coloration and Anthocyanins

Many plants contain several kinds of anthocyanins in a petal. However, it is thought that *Dianthus* species including carnation contain almost exclusively one kind of anthocyanin in the petals of a single cultivar (Yamaguchi, personal communication). This characteristic seems specific to *Dianthus* species. There is a strong correlation between cyanic flower coloration and the major anthocyanin: the flower cultivars containing pelargonidin 3-*O*-malyl-glucoside, pelargonidin 3-*O*, 5-*O*-cyclic malyl-diglucoside, cyanidin 3-*O*-malyl-glucoside, and cyanidin 3-*O*, 5-*O*-cyclic malyl-diglucoside [(1) to (4)] as the major anthocyanin express vermillion, pink, dark-red, and red–purple coloration, respectively (Fig. 6.2d). Therefore, we can infer the kind of major anthocyanin in a cultivar on the basis of its flower coloration. This means that cyanic coloration of carnation flowers is determined by the activities of F3′H and AA5GT (Fig. 6.2b).

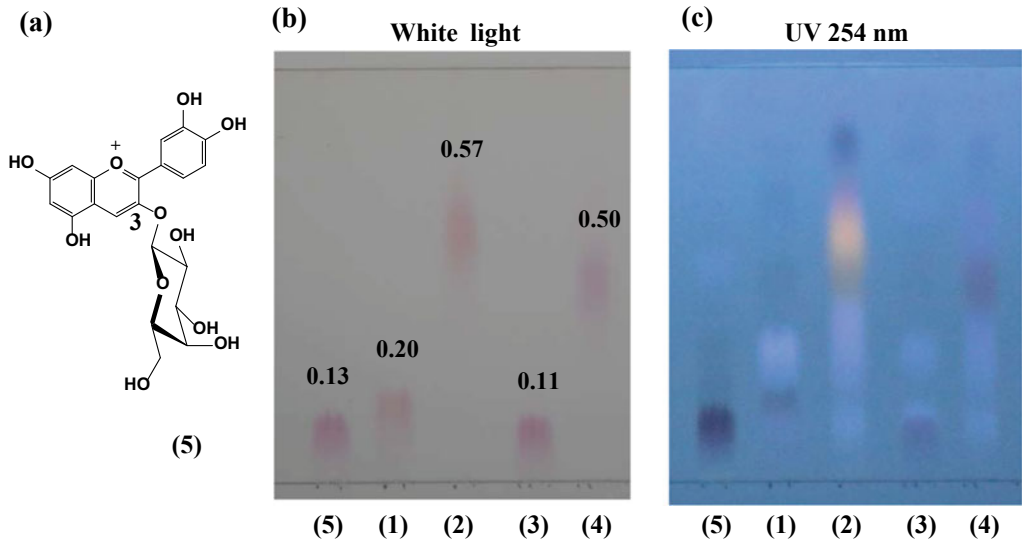

Fig. 6.3 Cellulose thin-layer chromatography (TLC) of the major anthocyanins. **a** Structure of cyanidin 3-*O*-galactoside (5); TLC developed with 10% acetic acid observed under white light (**b**) and ultraviolet light at 254 nm (**c**). Numbers in parentheses are those of the anthocyanins in Fig. 6.2a. The R_f value of each anthocyanin is displayed on the TLC image. Brightness was increased to make the images similar to those seen with the naked eye

A disadvantage of the simple composition of anthocyanins in carnation is that it limits the coloration diversity of carnation flowers.

6.3 Chalcone Glycoside, Pigment Responsible for Yellow Coloration

The pigment responsible for the yellow coloration of carnation flowers is chalcone 2′-*O*-glucoside (isosalipurposide) (Harborne 1966; Yoshida et al. 2004) [(6), Fig. 6.4a]. Expression of yellow coloration due to this pigment is reported for the genera *Helichrysum* (Hänsel et al. 1960), *Cyclamen* (Miyajima et al. 1991), and *Corylopsis* (Iwashina et al. 2009). It is generally known that deep yellow coloration of many kinds of flowers is due to carotenoids, which belong to a different molecular group from anthocyanins and flavonoids; lutein [(7), Fig. 6.4a] is a representative yellow carotenoid.

6.3.1 Characteristics of Aglycone

The aglycone of chalcone 2′-*O*-glucoside is 4, 2′, 4′, 6′-tetrahydroxychalcone (THC) (6). THC is a common biosynthetic precursor of anthocyanins and other flavonoids including flavones and flavonols (Fig. 6.1). THC is composed of an aromatic A-ring derived from three malonyl CoA, an aromatic B-ring derived from the aromatic ring of phenylalanine, and a three carbons' chain derived from the side chain of phenylalanine. The biosynthesis of THC is catalyzed by chalcone synthase. The aromatic C-ring, which anthocyanin and other flavonoids possess, is not synthesized at this stage.

6.3.2 Characteristics of Conjugated Sugar

The only type of sugar conjugated to THC is glucose (6). The activity of chalcone isomerase (CHI), which catalyzes the conversion of THC to

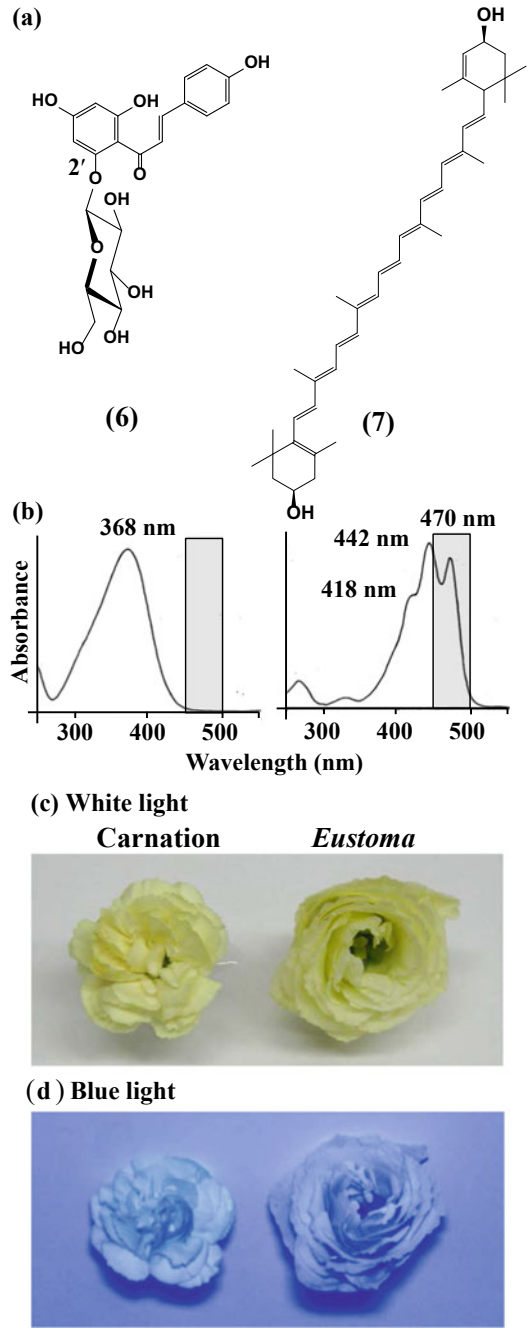

Fig. 6.4 Structure and properties of major yellow pigments in carnation flowers. **a** Structures of chalcone 2′-*O*-glucoside (6) and lutein (7). **b** Absorption spectra of chalcone 2′-*O*-glucoside (left) and lutein (right). Numbers indicate λ_{max}. Gray boxes indicate 450–500 nm wavelengths of blue light. **c**, **d** Yellow carnation flowers and yellow *Eustoma* flowers are shown under white light (**c**) and blue light (**d**). Brightness was increased to make the images similar to those seen with the naked eye

colorless naringenin (Fig. 6.1), must be repressed to allow biosynthesis of chalcone 2′-*O*-glucoside (Itoh et al. 2002; Miyahara et al. 2018). When CHI is repressed, THC is glycosylated at the 2′-hydroxy group by a UDP-glucose-dependent glucosyltransferase reaction and then chalcone 2′-*O*-glucoside accumulates, expressing visible yellow color in petal cells.

6.3.3 Characteristics of Conjugated Organic Acid

Chalcone 2′-*O*-glucoside (6) does not have a conjugated organic acid.

6.3.4 Physicochemical Properties

Chalcone 2′-*O*-glucoside (6) has λ_{max} of 368 nm, which is in the ultraviolet light spectrum (Fig. 6.4b). In contrast to chalcone 2′-*O*-glucoside (6), yellow carotenoid pigments have a fundamentally different structure and λ_{max} in the blue light range (ca. 400–500 nm) of the visible light spectrum; e.g., lutein (7) has λ_{max} of 418, 442, and 470 nm. Yellow coloration is generated by absorption of blue light. Chalcone 2′-*O*-glucoside (6) absorbs this part of the spectrum to a lower extent than yellow carotenoid pigments, and, therefore, chalcone 2′-*O*-glucoside (6) is a yellow pigment with lower coloration density than yellow carotenoid pigments.

6.3.5 Yellow Flower Coloration and Chalcone 2′-*O*-Glucoside

In general, chalcone 2′-*O*-glucoside–derived flower shows as pale-yellow coloration while yellow carotenoid–derived flower, e.g., some cultivars of *Chrysanthemum morifolium* (chrysanthemum; Kishimoto et al. 2004;), shows deep yellow coloration. Although a yellow coloration of *Eustoma* flower is derived from yellow carotenoids including lutein (7), it shows pale-yellow coloration like carnation flowers

(Fig. 6.4c) (Nakayama et al. 2006). As described in Sect. 6.3.4, carotenoids can absorb blue light wavelengths better than chalcone 2′-*O*-glucoside (6). Because of this property, yellow *Eustoma* flowers show darker images than yellow carnation flowers under blue light (Fig. 6.4d). Thus, imaging under blue light, with yellow carnation and *Eustoma* flowers as references, is an easy and non-destructive method to evaluate the responsible pigment (flavonoid vs. carotenoid) in pale-yellow flowers.

6.4 Flavones, Co-Pigments Responsible for Blue-Purple Coloration

The flavones contained in carnation flowers are apigenin 6-*C*-, 8-*C*-diglucoside (vicenin-2; Fukui et al. 2003) [(8), Fig. 6.5a] and apigenin 6-*C*-glucoside-7-*O*-malyl-glucoside (6-*C*-glucosyl, 7-*O*-glucosyl apigenin 6″-*O*-4-malate; Galeotti et al. 2008a) [(9), Fig. 6.5a]. The compound (9) is specifically detected in carnation.

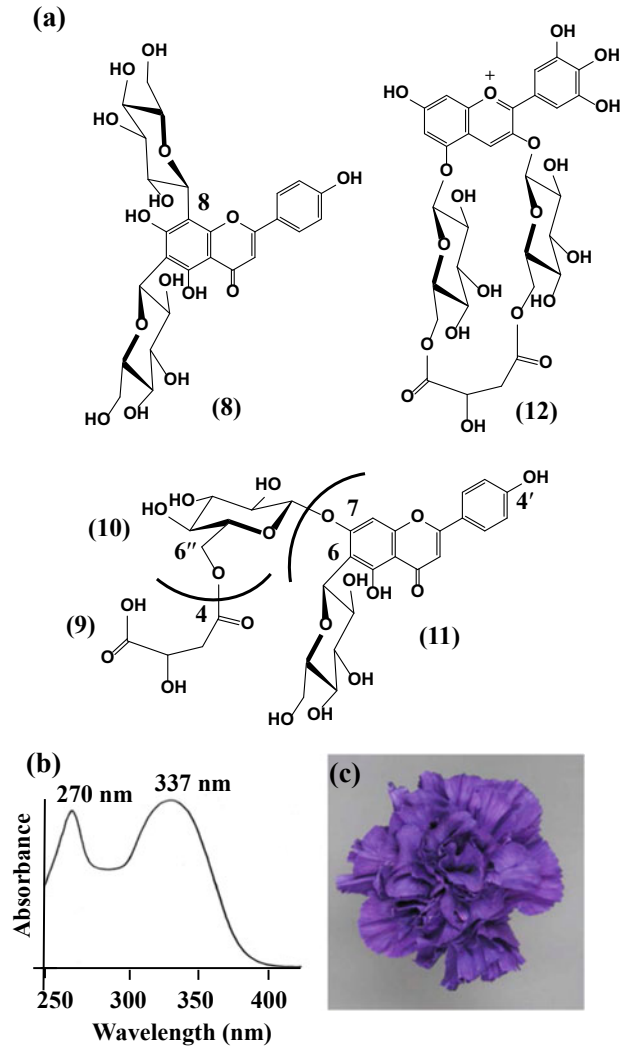

Fig. 6.5 Structures and properties of flavones detected in carnation flowers. **a** Structures of flavones: apigenin 6-*C*-, 8-*C*-diglucoside (8); apigenin 6-*C*-glucoside-7-*O*-malyl-glucoside (9); saponarin (10); isovitexin (11); and an anthocyanin in a transgenic blue-purple carnation flower, delphinidin 3-*O*, 5-*O*-cyclic malyl-diglucoside (12). **b** Absorption spectrum of isovitexin. Numbers indicate λ_{max}. **c** Flower of the transgenic blue-purple carnation

6.4.1 Characteristics of Aglycone

The only type of aglycone in carnation flower flavones is apigenin, which has one hydroxy group at the 4′-position in the B-ring [(8) and (9)]. Aglycones possessing additional hydroxy groups in the B-ring (e.g., luteolin) or methylated hydroxy groups in the B-ring (e.g., acacetin) have not been detected in flowers of carnation cultivars.

6.4.2 Characteristics of Conjugated Sugars

The only type of sugar conjugated in carnation flower flavones is glucose [(8) and (9)]. In both flavones, glucose binds at the 6-position of apigenin by *C*-glycosylation. Another glucose binds at the 8-position by *C*-glycosylation (8) or at the 7-position by *O*-glycosylation (9).

6.4.3 Characteristics of Conjugated Organic Acid

The only type of organic acid conjugated in the carnation flower flavone is malic acid (9). As in the case of anthocyanins, flavone acylated by malic acid is specific to carnation.

6.4.4 Physicochemical Properties

It is generally understood that the absorption spectra of flavones are much more affected by the aglycone than by the conjugated sugars or aliphatic acids. Therefore, apigenin 6-*C*-glucoside-7-*O*-malyl-glucoside (9) likely has a similar absorption spectrum to its derivative lacking the malyl acid, saponarin (apigenin 6-*C*-glucoside-7-*O*-glucoside [(10), Fig. 6.5a]). Vicenin-2 (8) and saponarin (10) are glucose addition derivatives of isovitexin (apigenin 6-*C*-glucoside [(11), Fig. 6.5a]). These flavones [(8), (10) and (11)] have similar λ_{max} values to each other: vicenin-2 (8), 273 nm and 338 nm (Xie et al. 2003); saponarin (10), 272 nm and 335 (Sakamoto 1969); and isovitexin (11), 270 nm and 337 nm. This suggests that the absorption spectra of these four flavones [(8) to (11)] likely resemble each other. Here, I present the absorption spectrum of isovitexin (11) as representative of the spectra of flavones [(8) to (11)] (Fig. 6.5b). The spectrum shows little absorption in the blue light range of the visible spectrum, so the color of flavones [(8) to (11)] is cream-white, which is less dense than the yellow color of chalcone 2′-*O*-glucoside (6).

6.4.5 Blue-Purple Transgenic Flower Coloration and Flavones

Apigenin 6-*C*-glucoside-7-*O*-malyl-glucoside (8) was detected in the blue-purple petals of transgenic carnation (Fig. 6.5c), in which a delphinidin-based anthocyanin (delphinidin 3-*O*, 5-*O*-cyclic malyl-diglucoside [(12), Fig. 6.5a]) accumulates due to the expression of F3′5′H (Fukui et al. 2003). A co-pigment is a colorless compound that makes the color of the corresponding anthocyanin bluer. Apigenin 6-*C*-glucoside-7-*O*-malyl-glucoside (8) contributes to expression of blue-purple coloration as a co-pigment to the delphinidin-type anthocyanin (12).

6.5 Flavonols, Pigments Responsible for Cream-White Coloration

Flavonols contained in carnation flowers are kaempferol 3-*O*-rhamnosyl-(1–2)-glucoside (kaempferol 3-*O*-neohesperidoside) (Iwashina et al. 2010) [(13), Fig. 6.6a]; kaempferol 3-*O*-glucosyl-(1–2)-glucoside (kaempferol 3-*O*-sophoroside) (Iwashina et al. 2010) [(14), Fig. 6.6a]; kaempferol 3-*O*-rhamnosyl-(1–6)-glucoside (kaempferol 3-*O*-rutinoside) (Galeotti et al. 2008a) [(15), Fig. 6.6a]; kaempferol 3-*O*-glucosyl-(1–2)-[rhamnosyl-(1–6)]-glucoside (Fukui et al. 2003, Galeotti et al. 2008a, Iwashina et al. 2010) [(16), Fig. 6.6a]; kaempferol 3-*O*-(6-malyl-glucosyl)-(1–2)-[rhamnosyl-(1–6)]-glucoside [(17), Fig. 6.6a] (Fukui et al. 2003); and kaempferol 3-*O*-rhamnosyl-(1–2)-[rhamnosyl-(1–6)]-glucoside [(18), Fig. 6.6a] (Ozeki, personal

communication). Flavonols (17) and (18) are specifically detected in carnation.

6.5.1 Characteristics of Aglycone

The only type of aglycone in the carnation flower flavonols is kaempferol [(13) to (18)]. Like apigenin, kaempferol has one hydroxy group at the 4′-position in the B-ring. Aglycones possessing additional hydroxy groups in the B-ring (e.g., quercetin and myricetin) or methylated hydroxy groups in the B-ring (e.g., isorhamnetin) have not been detected in flowers of carnation cultivars.

6.5.2 Characteristics of Conjugated Sugars

The only types of sugar conjugated in the carnation flower flavonols are glucose and/or rhamnose [(13) to (18)]. In all flavonols, glucose binds at the 3-hydroxy group of kaempferol in a glycosidic bond manner. The glucose is further bound at the 2″-hydroxy group by rhamnose [(13) and (18)], glucose [(14), (16), (17)], or none (15), and/or at the 6″-hydroxy group by rhamnose [(15) to (18)] or none [(13) and (14)] in a glycosidic bond manner.

6.5.3 Characteristics of the Conjugated Organic Acid

The only type of organic acid conjugated in carnation flower flavonols is malic acid (17). Like anthocyanins and flavone, flavonols acylated by malic acid are specific to carnation.

6.5.4 Physicochemical Properties

The absorption spectrum of kaempferol 3-*O*-rhamnosyl-(1–2)-glucoside (13) is shown in Fig. 6.6b. This spectrum is the same as those of two other carnation flower flavanols [(14) and (15)] (Iwashina et al. 2010). As in the case of flavones, it is generally understood that the absorption spectra of flavonols are affected much more by the aglycone than by the conjugated sugars or aliphatic acids. This suggests that the absorption spectrum of flavonol (13) likely resembles those of other flavonols [(16) to (18)]. The absorption spectrum (Fig. 6.6b) has λ_{max} of 267 and 345 nm, which are both in the ultraviolet spectrum, and a little absorption in the blue range of the visible light spectrum, so that color of flavonols [(13) to (18)] is cream-white, which is less dense than the yellow coloration of chalcone 2′-*O*-glucoside (6).

6.5.5 *Cream-White Flower Coloration and Flavonols*

Flavonol content affects the coloration of flowers: flowers containing more flavanols are cream-white, while those containing less flavanols are pure-white (Onozaki et al. 1999). In Fig. 6.6c, various carnation cultivars are presented. Among them, flowers (***a***–***c***) contain flavonols at a similar middle level, flower (***d***) contains flavonols at the lowest level, and flower (***e***) contains flavonols at the highest level (Iwashina et al. 2010). Consistent with the previous report (Onozaki et al. 1999), flowers (***a***–***c***) are cream-white and flower (***d***) is pure-white. However, flower (***e***) is not cream-white but pure-white, even though it contains the highest content of flavonols. The contradictory results indicate that there remains an unknown mechanism of white coloration in carnation flowers.

Flavonols strongly absorb ultraviolet light at around 365 nm. In white or cream-white flowers, there is a strong inverse relationship between flavonol content and the brightness of the image under ultraviolet light at 365 nm in dark conditions (Fukuta et al. 2005). This relationship holds for carnation flowers: flower (***d***) with the lowest flavanol content has the brightest image, while flower (***e***) with the highest flavanol content has a dark image like flowers (***a***–***c***) (Fig. 6.6d). We can use this method to select carnation cultivars with very low flavanol content.

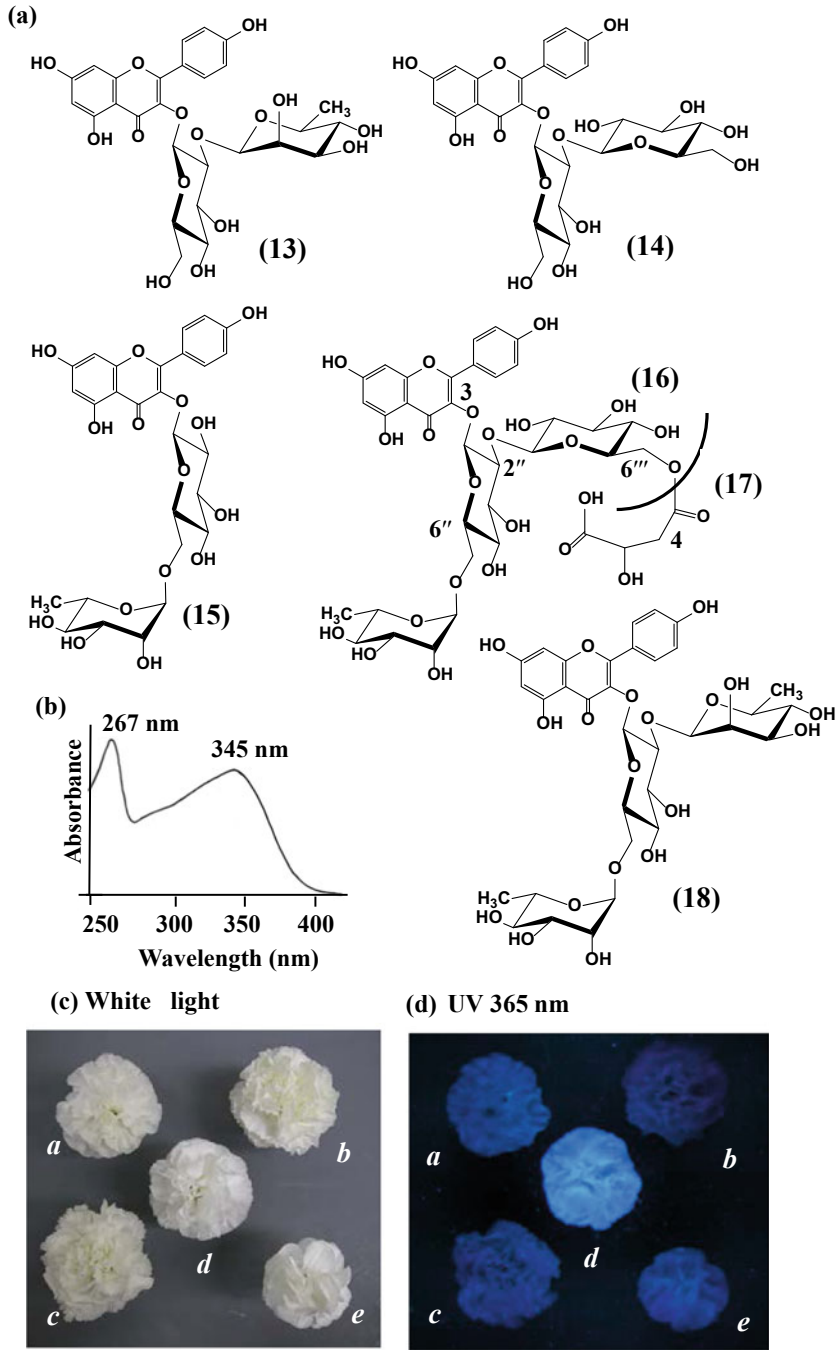

Fig. 6.6 Structures and properties of flavonols detected in carnation flowers. **a** Structures of flavonols: kaempferol 3-*O*-rhamnosyl-(1–2)-glucoside (13); kaempferol 3-*O*-glucosyl-(1–2)-glucoside (14); kaempferol 3-*O*-rhamnosyl-(1–6)-glucoside (15); kaempferol 3-*O*-glucosyl-(1–2)-[rhamnosyl-(1–6)]-glucoside (16); kaempferol 3-*O*-(6″-malyl-glucosyl)-(1–2)-[rhamnosyl-(1–6)]-glucoside (17); and kaempferol 3-*O*- rhamnosyl-(1–2)-[rhamnosyl-(1–6)]-glucoside (18). **b** Absorption spectrum of (13). Numbers indicate λ_{max}. **c**, **d** Cream-white and white carnation flowers under white light (**c**) and ultraviolet light at 365 nm (**d**). Cultivar or line names are as follows: ***a*** 'Annabelle'; ***b*** 'Milky Way'; ***c*** 'BD2398'; ***d*** 'MB3', and ***e*** 'Bridal White'

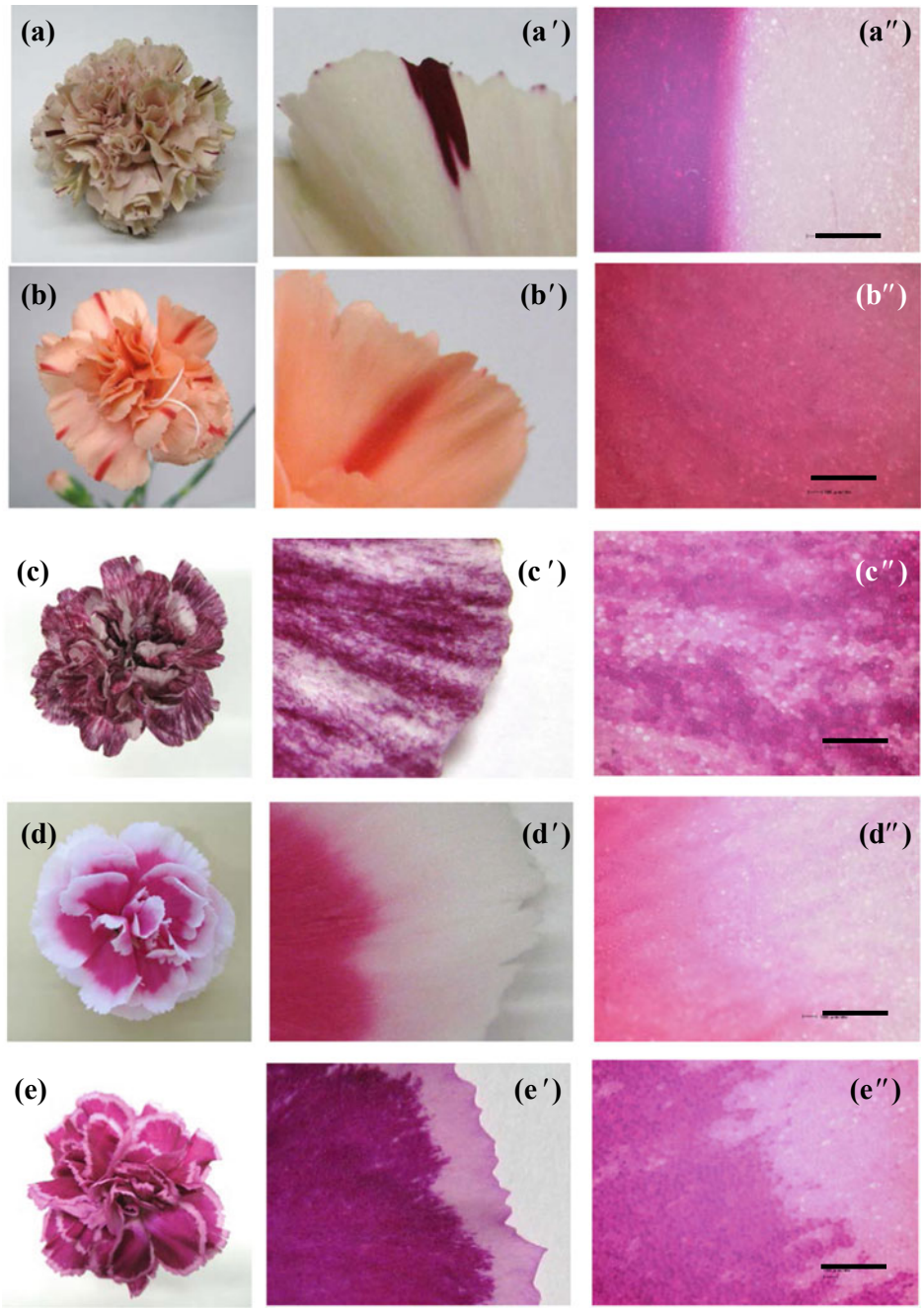

Fig. 6.7 Flower color patterns in common carnation cultivars. **a** spotted (clearer border), **b** spotted (unclear border), **c** splash spotted, **d** marginal picotee (unclear border), **e** marginal picotee (clearer border), **f** colored-edge picotee (narrow and clear border), **g** colored-edge picotee (wide and clearer border), **h** colored-edge picotee (unclear border), **i** colored-edge picotee with spotted stripes, and **j** wider stripe with spotted stripes. Single- and double-primed letters indicate enlarged and microscopic images of the coloration border of the flowers, respectively. **k** The ring-like coloration pattern, which appears in the flowers of some other *Dianthus* species. Single- and double-primed letters indicate microscopic images of the inner and outer sides of the coloration border of the flowers, respectively. Bars indicate 0.5 mm. Brightness was increased to make the images similar to those seen with the naked eye

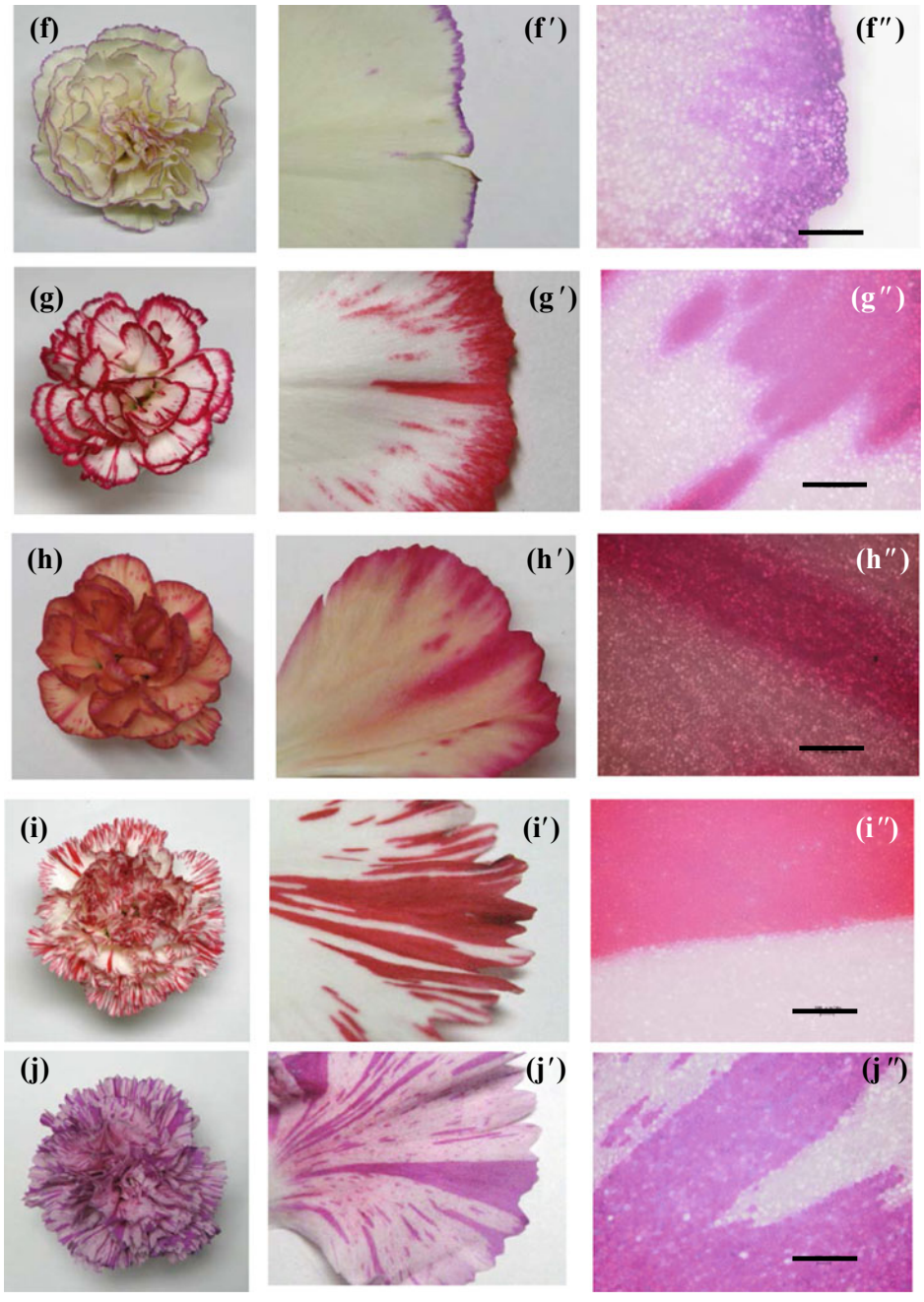

Fig. 6.7 (continued)

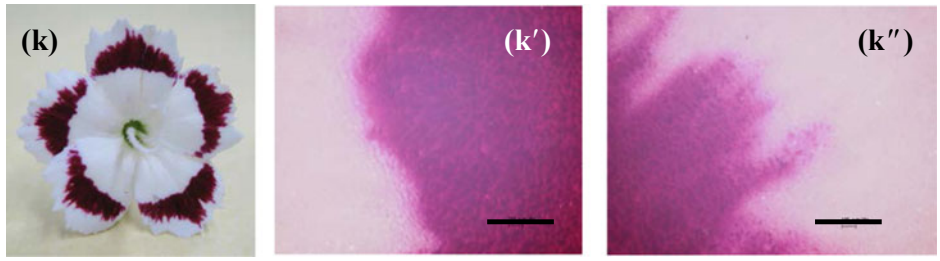

Fig. 6.7 (continued)

6.6 Flower Color Patterns

Some carnation cultivars have various kinds of cyanic flower color patterns. These patterns are generated by spatially specific regulation of anthocyanin biosynthesis. Representative flower color patterns of carnation, named here (a) to (j), are shown in Fig. 6.7. In general, patterns possessing borders with gradual coloration density changes may be underlaid by post-transcriptional gene silencing, while patterns with borders that display abrupt changes in coloration density may be due to transposon excision. Therefore, I introduce flower color patterns with microscopic images of their coloration borders (Fig. 6.7).

In spotted patterns (a) and (b), numerous deeper-colored parts appear near the edge of the petals. Pattern (a) has a clear coloration border compared with pattern (b) [see (a′) and (b′)]. The spotted stripe patterns are vertically and partially colored in petals along the direction of cell division in petal tissue differentiation. Japanese morning glory (*Pharbitis nil*) has coloration patterns caused by transposon excision (Inagaki et al. 1994). These patterns have clear borders composed of cells of drastically different color densities. However, patterns (a) and (b) have coloration borders composed of cells whose coloration density gradually changes, with the gradient being much more gradual in pattern (b) than pattern (a) [see (a″) and (b″)]. Therefore, a mechanism other than transposon excision likely generates the spotted patterns of (a) and (b).

In splash spotted pattern (c), numerous tiny coloration parts randomly appear on the whole petal. The coloration border of the splash spotted pattern (c) is also composed of cells whose coloration density gradually changes [see (c′) and (c″)]. Sweet pea (*Lathyrus odoratus*) has a similar coloration pattern, which is generated by cooperation of two genes belonging to different alleles (Punnett 1936, 1940, note that the pattern is presented as “flake-variegated pattern” in these papers). Yagishita et al. (2018) confirmed that this cooperation operates in modern sweet pea cultivars grown in Japan. A similar mechanism might operate in the generation of splash spotted pattern (c) in carnation.

Different from the above stripe patterns [(a) to (c)], the picotee-type patterns [(d) to (h)] are horizontal in petals (i.e., across the direction of the cell division). Marginal white picotee pattern (d) is composed of marginal white parts and basal colored parts. Pattern (d) has an unclear coloration border [see (d′)]. A marginal white picotee pattern like pattern (d) appears in some *Petunia* cultivars (Saito et al. 2006). In *Petunia*, this pattern is generated by marginal position–specific post-transcriptional gene silencing of *chalcone synthase* genes (Morita et al. 2012; Ban et al. 2019). The *Petunia* marginal white picotee pattern shows an unclear coloration border composed of cells whose coloration density gradually decreases from the center to the margin of the petals (Saito et al. 2007). The carnation marginal white picotee pattern (d) shows similar cell coloration density changes to the *Petunia* marginal white picotee pattern. The similarities

between the carnation and *Petunia* marginal white picotee patterns suggest that post-transcriptional gene silencing of anthocyanin biosynthetic genes possibly operates in carnation pattern (d) as well [see (d″)].

The picotee pattern (e) has a clearer coloration border than the marginal white picotee pattern (d) [see (d′) and (e′)]. The change in the cells' coloration density is more drastic and the deeper-colored cells at the border are arranged in a disordered line [see (e″)]. Therefore, the generation mechanism for picotee pattern (e) may differ from that for marginal white picotee pattern (d).

Unlike picotee patterns (e) and (d), the colored-edge picotee patterns [(f) to (h)] have combinations of colored marginal parts and white basal parts. Although the widths of the colored edges are different between patterns (f) and (g), the coloration borders of both these patterns are clear [see (f′) and (g′)] and are composed of cells whose coloration density gradually changes to a similar degree [see (f″) and (g″)]. Therefore, the patterns (f) and (g) are likely generated by the same mechanism.

The other colored-edge picotee pattern (h) has an unclear border compared with colored-edge picotee patterns (f) and (g) [see (f′) to (h′)]. The change of cell coloration density of (h) is more gradual (h″) than that of (f) or (g) [see (f″) to (h″)]. Therefore, the mechanism that generates pattern (h) may differ from the one that generates patterns (f) and (g).

Pattern (I) possesses the characteristics of both spotted stripes (a) and the colored-edge picotee pattern (g); condensed spotted stripes appear mainly at the petal edge. This pattern has the property of clear coloration borders composed of cells with vastly different coloration densities; the coloration density changes at most over a span of a few cells [see (i′) and (i″)]. This suggests that pattern (i) is neither a variation of the spotted stripe pattern (a) nor the colored-edge picotee pattern (g), both in which the coloration density gradually changes.

Pattern (j) is a wider stripe pattern with many tiny stripes whose appearance is not restricted to the petal edges. Like pattern (i), pattern (j) also possesses clear coloration borders composed of cells with vastly different coloration densities [see (j′) and (j″)]. Therefore, the generation mechanism of patterns (i) and (j) is likely different from those of the patterns previously presented [(a) to (h)].

Some other *Dianthus* species have flower coloration patterns that are not found in carnation cultivars. One is the ring-like coloration pattern (k), that is, coloration borders occur at both the inner and outer sides. Both the inner [see (k′)] and outer [see (k″)] borders are composed of cells whose coloration density gradually changes.

6.7 Flavonoids Detected in Tissues Other than Flowers

Flavonoids detected in leafy shoots and roots of carnation are reported in Curir et al. (1996, 2001, and 2005) and Galeotti et al. (2008b): kaempferol 7-*O*-rhamnosyl-(1–2)-glucoside [(19), Fig. 6.8], kaempferol 3-*O*-glucosyl-(1–2)-glucosyl-(1–2)-[rhamnosyl-(1–6)]-glucoside [(20), Fig. 6.8], quercetin 3-*O*-rhamnoside [(21), Fig. 6.8], and myricetin 3-*O*-rhamnoside [(22), Fig. 6.8]. These flavonoids are all flavonols that have been detected as compounds possessing antifungal activity against *Fusarium oxysporum* f. sp. *dianthi*. In flavonol (19), glucose binds at the 7-hydroxy group, not the 3-hydroxy group, of kaempferol. Flavonol (20) is a tetra-glucoside of kaempferol and has the highest number of conjugated sugars among carnation flavonoids. The aglycons of flavonols (21) and (22) are not kaempferol but quercetin and myricetin, respectively, and the only type of sugar conjugated to the aglycone is rhamnose.

6.8 Analytical Techniques and Conditions

It is thought that anthocyanins and flavonoids are more stable in acidic conditions than in alkaline or neutral conditions; even so, malyl esters of these anthocyanins and flavonoids are unstable. Anthocyanins that have lost the malyl ester

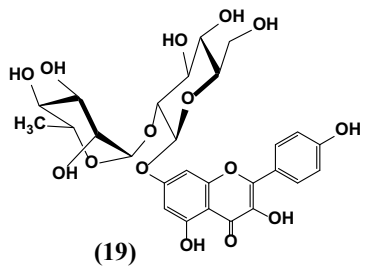

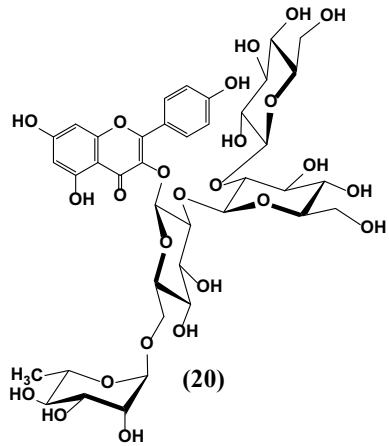

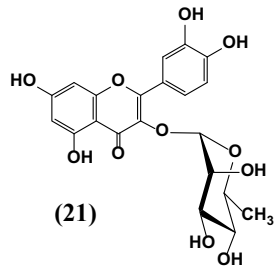

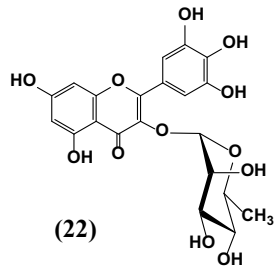

Fig. 6.8 Structures of flavonols detected in carnation leafy shoots and/or roots. Structures of flavonols: kaempferol 7-*O*-rhamnosyl-(1–2)-glucoside (19); kaempferol 3-*O*-glucosyl-(1–2)-glucosyl-(1–2)-[rhamnosyl-(1–6)]-glucoside (20); quercetin 3-*O*-rhamnoside (21); and myricetin 3-*O*-rhamnoside (22)

and/or changed to an open cyclic structure by hydrolysis can often be detected in carnation flower extracts. The hydrolysis is prompted in HCl and other mineral acid solutions. To prevent the hydrolysis, anthocyanins and flavonoids should be extracted by using ca. 10% acetic acid or formic acid solution, and analysis should be carried out soon after the extraction.

In HPLC analysis, ODS columns are generally used to separate anthocyanins and flavonoids. Example conditions of mine are as follows. Solvent is pumped at 0.8 mL/min into an Inertsil ODS-2 column (4.6 mm diameter × 250 mm length) (GL Science, Tokyo, Japan) combined with an Inertsil ODS-2 guard column (GL Science) at 40 °C. Solvents are mixed in a linear gradient of 20%–100% solvent B (1.5% phosphoric acid, 20% acetonitrile, 25% acetic acid) in solvent A (1.5% phosphoric acid) for 40 min. Eluted compounds are detected online based on absorption spectra recorded by a photodiode array detector (GL Science).

TLC does not require specialized equipment, and results can be obtained in a few hours. A 200 mm × 200 mm cellulose TLC glass plate (Merck, Darmstadt, Germany) is cut to a suitable size. Samples are developed for 70 mm on the TLC by solvent. Anthocyanins can be detected by naked-eye observation as red spots. It is difficult to detect spots of flavonoids by the naked eye because the depth of yellow coloration of flavonoids, even chalcone 2′-*O*-glucoside, is not enough. However, flavonoids are easily detected as dark spots under ultraviolet light at 365 nm and 254 nm in dark conditions (Fig. 6.3c). TLC is recommended as a simple and low-cost method for anthocyanin and flavonoid analyses. As described in Sect. 6.2.4, apple skin red pigment anthocyanin is useful as a standard compound to compare R_f values and coloration of spots.

Although anthocyanins (1) and (2) have similar absorption spectra to each other (Fig. 6.2c), flowers containing these anthocyanins express different colorations (Fig. 6.2d). A similar

phenomenon is found for anthocyanins (3) and (4). These phenomena raise the possibility that co-pigments are involved in coloration of non-transgenic carnation flowers, as is observed in the transgenic carnation flowers described in Sect. 6.4.5. The cross-TLC method was developed to enable simultaneous separation and mixture of compounds (Shimizu-Yumoto et al. 2012). This method has been used to detect co-pigments in crude petal extracts. The sample is slantingly cross-loaded on the TLC plate. After the plate is developed, an altered color at a point in the anthocyanin line indicates the presence of co-pigment(s) at that point. Using this method, we detected co-pigments operating in pink sweet pea (Shimizu-Yumoto et al. 2012) and blue chrysanthemum (Noda et al. 2017). The cross-TLC method is expected to be a useful technique to detect co-pigments in carnation flowers as well.

Acknowledgements I thank Dr. Yamaguchi of Minami-Kyusyu University and Dr. Ozeki of Tokyo University of Agriculture and Technology for giving valuable advice on anthocyanin–flavonoid research over a long period, and I thank Dr. Koshioka of Nihon University and Dr. Shibata of the University of Tokyo for providing the opportunity to do anthocyanin–flavonoid research. It is my enjoyment to see Mt. Tsukuba (Fig. 6.9a)—the symbol of Tsukuba city in which my institute resides—whose bimodal summit resembles the absorption spectrum of flavonols (Fig. 6.9b).

Appendix

Some contents of Chap. 6 allude to those of other chapters. Genes involved in biosynthesis of anthocyanins and flavonoids including chalcone 2′-glucoside and transposons generating these flower color mutations are described in Chap. 8 by Dr. Y. Ozeki. Breeding of transgenic carnations with blue-purple flowers due to biosynthesis of a novel anthocyanin is described in Chap. 10 by Dr. Y. Tanaka. Peculiar metallic coloration of flowers due to anthocyanin not acylated with malic acid is described in Chap. 9 by Dr. M. Okamura.

In the long history of carnation breeding history, spontaneous and bud sport mutations have been used to increase the coloration diversity. For further information, I recommend referring to a paper of Morimoto et al. (2019) where genes responsible for the bud mutations in a frequently mutable carnation line are reported (Fig. 6.9).

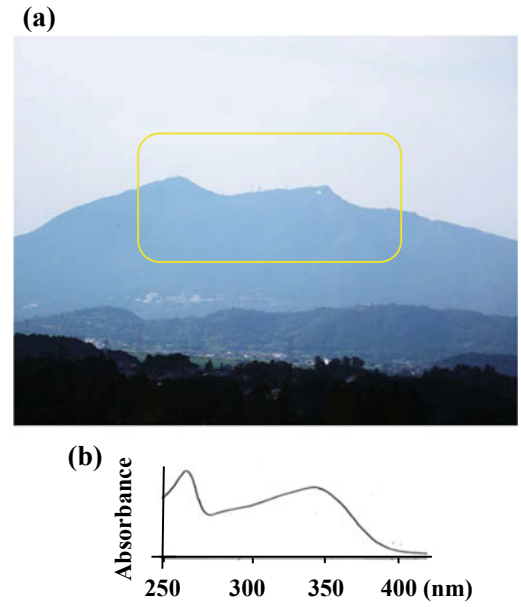

Fig. 6.9 Resemblance of shapes of a ridge and a spectrum. **a** A picture of Mt. Tsukuba. **b** A typical absorption spectrum of kaempferol type flavonols

References

Abe Y, Tera Y, Sasaki N, Okamura M, Umemoto M, Momose M, Kawahara N, Kamakura H, Goda Y, Nagasawa K, Ozeki Y (2008) Detection of 1-*O*-malylglucose: pelargonidin 3-*O*-glucose-6″-*O*-malyltransferase activity in carnation (*Dianthus caryophyllus*). Biochem Biophys Res Commun 373(4):473–477. https://doi.org/10.1016/j.bbrc.2008.04.153

Ban Y, Morita M, Ogawa M, Higashi K, Nakatsuka T, Nishihara M, Nakayama M (2019) Inhibition of post-transcriptional gene silencing of *chalcone synthase* genes in petunia picotee petals by fluacrypyrim. J Exp Bot 70 (5):1513–1523. https://doi.org/10.1093/jxb/erz009

Bloor SJ (1998) A macrocyclic anthocyanin from red/mauve carnation flowers. Phytochemistry 49 (1):225–228. https://doi.org/10.1016/S0031-9422(97)01051-0

Curir P, Marchesini A, Danieli B, Mariani F (1996) 3-Hydroxyacetophenone in carnation is a phytoanticipin active against *Fusarium oxysporum* f. sp. *dianthi*.

Phytochemistry 41(2):447–450. https://doi.org/10.1016/0031-9422(95)00603-6

Curir P, Dolci M, Lanzotti V, Taglialatela-Scafati O (2001) Kaempferol triglycoside: a factor of resistance of carnation (*Dianthus caryophyllus*) to *Fusarium oxysporum* f. sp. *dianthi*. Phytochemistry 56(7):717–721. https://doi.org/10.1016/S0031-9422(00)00488-X

Curir P, Dolci M, Galeotti F (2005) A phytoalexin-like flavonol involved in the carnation (*Dianthus caryophyllus*)-*Fusarium oxysporum* f. sp. *dianthi* pathosystem. J Phytopathol 153(2):103–111. https://doi.org/10.1111/j.1439-0434.2004.00916.x

Duncan IJ, Dustman RB (1936) The anthocyanin pigment of the Winesap apple. J Am Chem Soc 58(9):1511–1514. https://doi.org/10.1021/ja01300a001

Fukui Y, Tanaka Y, Kusumi T, Iwashita T, Nomoto K (2003) A rationale for the shift in colour towards blue in transgenic carnation flowers expressing the flavonoid 3′,5′-hydroxylase gene. Phytochemistry 63(1):15–23. https://doi.org/10.1016/S0031-9422(02)00684-2

Fukuta N, Miyasaka M, Saito R, Kuchitsu K, Nakayama M (2005) The relationship between characteristics of optical image under UV light and flavonoid content in acyanic petals of *Eustoma grandiflorum* (In Japanese). Hort Res 4(2):147–151. https://doi.org/10.2503/hrj.4.147

Galeotti F, Barile E, Lanzotti V, Dolci M, Curir P (2008) Quantification of major flavonoids in carnation tissues (*Dianthus caryophyllus*) as a tool for cultivar discrimination. Z Naturforsch C 63(3–4):161–168. https://doi.org/10.1515/znc-2008-3-401

Galeotti F, Barile E, Curir P, Dolci M, Lanzotti V (2008) Flavonoids from carnation (*Dianthus caryophyllus*) and their antifungal activity. Phytochem Lett 1(1):44–48. https://doi.org/10.1016/j.phytol.2007.10.001

Hänsel H, Pinkewitz G, Langhammer L, Heise D (1960) Das gelbe Pigment der Flores Stoechados. Arch Pharm 293(5):485–489. https://doi.org/10.1002/ardp.19602930504

Harborne JB (1966) Comparative biochemistry of flavonoids-I. Distribution of chalcone and aurone pigments in plants. Phytochemistry 5(1):111–115. https://doi.org/10.1016/S0031-9422(00)85088-8

Inagaki Y, Hisatomi Y, Suzuki T, Kasahara K, Iida S (1994) Isolation of a Suppressor-Mutator/Enhancer-like transposable element, *Tpnl,* from Japanese morning glory bearing variegated flowers. Plant Cell 6:375–383. https://doi.org/10.1105/tpc.6.3.375

Itoh Y, Higeta D, Suzuki A, Yoshida H, Ozeki Y (2002) Excision of transposable elements from the chalcone isomerase and dihydroflavonol 4-reductase genes may contribute to the variegation of the yellow-flowered carnation (*Dianthus caryophyllus*). Plant Cell Physiol 43(5):578–585. https://doi.org/10.1093/pcp/pcf065

Iwashina T, Takemura T, Nishino T (2009) Chalcone glycoside in the flowers of six *Corylopsis* species as yellow pigment. J Jpn Soc Hort Sci 78(4):485–490. https://doi.org/10.2503/jjshs1.78.485

Iwashina T, Yamaguchi M, Nakayama M, Onozaki T, Yoshida Y, Kawanobu S, Ono H, Okamura M (2010) Kaempferol glycosides in the flowers of carnation and their contribution to the creamy white flower color. Nat Prod Commun 5(12):1903–1906. https://doi.org/10.1177/1934578X1000501213

Kishimoto S, Maoka T, Nakayama M, Ohmiya A (2004) Carotenoid composition in petals of chrysanthemum (*Dendranthema grandiflorum* (Ramat,) Kitamura). Phytochemistry 65(20):2781–2787. https://doi.org/10.1016/j.phytochem.2004.08.038

Matsuba Y, Sasaki N, Tera M, Okamura M, Abe Y, Okamoto E, Nakamura H, Funabashi H, Takatsu M, Saito M, Maysuoka H, Nagasawa K, Ozeki Y (2010) A novel glucosylation reaction on anthocyanins catalyzed by acyl-glucose-dependent glucosyltransferase in the petals of carnation and delphinium. Plant Cell 22 (10):3374–3389. https://doi.org/10.1105/tpc.110.077487

Miyahara T, Sugishita N, Ishida-Dei M, Okamoto E, Kouno T, Cano EA, Sasaki N, Watanabe A, Tasaki K, Nishihara M, Ozeki Y (2018) Carnation *I* locus contains two chalcone isomerase genes involved in orange flower coloration. Breed Sci 68(4):481–487. https://doi.org/10.1270/jsbbs.18029

Miyajima I, Maehara T, Kage T, Fujieda K (1991) Identification of the main agent causing yellow color of yellow flowered cyclamen mutant. J Jpn Soc Hort Sci 60(2):409–414. https://doi.org/10.2503/jjshs.60.409

Momose M, Nakayama M, Itoh Y, Umemoto M, Toguri T, Ozeki Y (2013) An active *hAT* transposable element causing bud mutation of carnation by insertion into the flavonoid 3′-hydroxylase gene. Mol Genet Genomics 288(3–4):175–184. https://doi.org/10.1007/s00438-013-0742-z

Morimoto H, Narumi-Kawasaki T, Takamura T, Fukai S (2019) Analysis of flower color variation in carnation (*Dianthus caryophyllus* L.) cultivars derived from continuous bud mutations. J Jpn Soc Hort Sci 88 (1):116–128. https://doi.org/10.2503/hortj.UTD-007

Morita Y, Saito R, Ban Y, Tanikawa N, Kuchitsu K, Ando T, Yoshikawa M, Habu Y, Ozeki Y, Nakayama M (2012) Tandemly arranged chalcone synthase A genes contribute to the spatially regulated expression of siRNA and the natural bicolor floral phenotype in *Petunia hybrida*. Plant J 70(5):739–749. https://doi.org/10.1111/j.1365-313X.2012.04908.x

Nakayama M, Koshioka M, Yoshida H, Kan Y, Fukui Y, Koike A, Yamaguchi M (2000) Cyclic malyl anthocyanins in *Dianthus caryophyllus*. Phytochemistry 55 (8):937–939. https://doi.org/10.1016/S0031-9422(00)00263-6

Nakayama M, Miyasaka M, Maoka T, Yagi M, Fukuta N (2006) A carotenoid-derived yellow *Eustoma* screened under blue and ultraviolet lights. J Jpn Soc Hort Sci 75 (2):161–165. https://doi.org/10.2503/jjshs.75.161

Nishizaki Y, Matsuba Y, Okamoto E, Okamura M, Ozeki Y, Sasaki N (2011) Structure of the acyl-glucose-dependent anthocyanin 5-*O*-glucosyltransferase gene in carnations and its disruption by transposable elements in some varieties. Mol Genet Genomics 286(5–6):383–394. https://doi.org/10.1007/s00438-011-0655-7

Noda N, Yoshioka S, Kishimoto S, Nakayama M, Douzono M, Tanaka Y, Aida R (2017) Generation of blue chrysanthemums by anthocyanin B-ring hydroxylation and glucosylation and its coloration mechanism. Sci Adv 3(7):e1602785. https://doi.org/10.1126/sciadv.1602785

Okamura M, Nakayama M, Umemoto N, Cano EA, Hase Y, Nishizaki Y, Sasaki N, Ozeki Y (2013) Crossbreeding of a metallic color carnation and diversification of the peculiar coloration by ion-beam irradiation. Euphytica 191(1):45–56. https://doi.org/10.1007/s10681-012-0859-x

Onozaki T, Mato M, Shibata M, Ikeda H (1999) Differences in flower color and pigment composition among white carnation (*Dianthus caryophyllus* L.) cultivars. Scientia Hort 82(1–2):103–111. https://doi.org/10.1016/S0304-4238(99)00040-0

Punnett (1936) The flaked sweet pea. J Genet 32:171–177. https://link.springer.com/content/pdf/10.1007%2FBF02982507.pdf

Punnett (1940) Notes on the D-chromosome of the sweet pea. J Genet 39: 301–308. https://link.springer.com/content/pdf/10.1007%2FBF02982844.pdf

Saito R, Fukuta N, Ohmiya A, Itoh Y, Ozeki Y, Kuchitsu K, Nakayama M (2006) Regulation of anthocyanin biosynthesis involved in the formation of marginal picotee petals in *Petunia*. Plant Sci 170(4):828–834. https://doi.org/10.1016/j.plantsci.2005.12.003

Saito R, Kuchitsu K, Ozeki Y, Nakayama M (2007) Spatiotemporal metabolic regulation of anthocyanin and related compounds during the development of marginal picotee petals in *Petunia hybrida* (Solanaceae). J Plant Res 120(4):563–568. https://doi.org/10.1007/s10265-007-0086-z

Sakamoto Y (1969) Flavones in green tea Part II. Identification of isovitexin and saponarin. Agric Biol Chem 33(6):959–961. https://www.jstage.jst.go.jp/article/bbb1961/33/6/33_6_959/_pdf

Shimizu-Yumoto H, Hayashi N, Ichimura K, Nakayama M (2012) Slantingly cross loading sample system enables simultaneous performance of separation and mixture to detect molecular interactions on thin-layer chromatography. J Chromatogr A 1245:183–189. https://doi.org/10.1016/j.chroma.2012.05.011

Spribille R, Forkmann G (1982) Chalcone synthesis and hydroxylation of flavonoids in 3′-position with enzyme preparations from flowers of *Dianthus caryophyllus* L. (carnation). Planta 155(2):176–182. https://doi.org/10.1007/BF00392549

Terahara N, Yamaguchi M (1986) HNMR spectral analysis of the malylated anthocyanins from *Dianthus*. Phytochemistry 25(12):2906–2907. https://doi.org/10.1016/S0031-9422(00)83769-3

Terahara N, Takeda K, Harborne JB, Self R, Yamaguchi M (1986) Anthocyanins acylated with malic acid in *Dianthus caryophyllus* and *D. deltoides*. Phytochemistry 25(7):1715–1717. https://doi.org/10.1016/S0031-9422(00)81242-X

Xie C, Veitch NC, Houghton PJ, Monique, Simmonds SJ (2003) Flavone *C*-glycosides from *Viola yedoensis* Makino. Chem Pharm Bull 51(10):1204–1207. https://www.jstage.jst.go.jp/article/cpb/51/10/51_10_1204/_pdf/-char/en

Yagishita Y, Hara Y, Nakayama M (2018) Heredity of flake- and stripe-variegated traits and their introduction into Japanese day-neutral winter-flowering sweet pea (*Lathyrus odoratus* L.) cultivars. Breed Sci 68:53–61. https://doi.org/10.1270/jsbbs.17079

Yoshida H, Itoh Y, Ozeki Y, Iwashina T, Yamaguchi M (2004) Variation in chalcononaringenin 2′-*O*-glucoside content in the petals of carnations (*Dianthus caryophyllus*) bearing yellow flowers. Sci Hort 99 (2):175–186. https://doi.org/10.1016/S0304-4238(03)00093-1

7 Carotenoid and Chlorophyll Accumulation in Flower Petals of Carnation

Akemi Ohmiya, Luna Iijima, and Sanae Kishimoto

Abstract

Carnation is one of the most important floricultural crops in the world. Over 20 wild species of *Dianthus* have been integrated during the long history of carnation breeding, and a wide range of petal colors, including red, yellow, orange, and white, have been developed. These flower colors are derived from quantitative and qualitative differences in flavonoid compounds. Wild *Dianthus* species expressing petal colors through carotenoids or chlorophylls have not been documented. In contrast, green-flowered and pale yellow-flowered carnation cultivars, which express their petal colors with these pigments, have been developed by conventional breeding. Such cultivars might be mutants that have lost the ability to avoid the accumulation of carotenoids and chlorophylls in the petals. In this section, based on our analysis of green- and pale yellow-flowered carnation cultivars, we discuss the possible mechanisms that regulate the accumulation of carotenoids and chlorophylls in carnation petals.

A. Ohmiya (✉) · S. Kishimoto
Institute of Vegetable and Floriculture Science, NARO, Fujimoto 2-1, Tsukuba 305-0852, Ibaraki, Japan
e-mail: ohmiya.akemi@gmail.com

L. Iijima
Department of Biotechnology, Tokyo University of Agriculture and Technology, Koganei 184-8588, Tokyo, Japan

7.1 Introduction

The major plant pigments responsible for flower color are flavonoids, carotenoids, chlorophylls, and betalains. Flavonoids and betalains are water-soluble pigments contained in the vacuole (Tanaka et al. 2008). Flavonoids consist of a large group of polyphenolic compounds, including colorless flavonols and flavones, and red and purple anthocyanins. Betalains are unique pigments, found exclusively in the Caryophyllales, imparting yellow, red, and purple colors. Carotenoids and chlorophylls are lipid-soluble pigments occurring in the plastids (Niyogi 2000; Li and Yuan 2013; Ohmiya 2013). Based on their structure and accumulated pigments, plastids can be categorized as proplastids, etioplasts, chloroplasts, chromoplasts, or amyloplasts (Li and Yuan 2013). Leaves accumulate substantial amounts of carotenoids in the chloroplasts, together with chlorophylls, because carotenoids play an essential role in photosynthesis (Hashimoto et al. 2016). In many plants, carotenoids are accumulated in the chromoplasts of fruits and flowers, responsible for yellow, orange to red colors (Li and Yuan 2013; Ohmiya 2013).

Plants belonging to the families Molluginaceae and Caryophyllaceae, in the core Caryophyllales, express their petal color through

T. Onozaki and M. Yagi (eds.), *The Carnation Genome*, Compendium of Plant Genomes,
https://doi.org/10.1007/978-981-15-8261-5_7

anthocyanins. In contrast, anthocyanins have never been detected in other families belonging to Caryophyllales (Bate-Smith 1962; Mabry 1964), which instead produce betalains. This suggests that anthocyanins and betalains are mutually exclusive pigments (Mabry 1964).

Over 20 wild species of *Dianthus*, belonging to the family Caryophyllaceae, have been used for breeding of carnation cultivars (Galbally and Galbally 1997). Petal colors of most ancestral species are pink. During the long history of carnation breeding, a wide range of petal colors, including red, yellow, orange, and white, have been developed. These diverse petal colors are derived from quantitative and qualitative differences in flavonoid compounds. Pink and red petals accumulate small and large amounts of anthocyanin, respectively. Yellow petal color is derived from chalcone, an intermediate product of anthocyanin (Itoh et al. 2000), and orange petal color is produced by a combination of red anthocyanin and yellow chalcone (Miyahara et al. 2018; see Chap. 8 in this book). Although white petals lack colored pigments, they contain substantial amounts of colorless flavonoids (Onozaki et al. 1999; Mato et al. 2000). Many reports regarding flavonoid compound accumulation in carnation petals have previously been published (see Chap. 6 in this book).

In addition to betalains, plants belonging to the genus *Dianthus* eliminate the accumulation of chlorophylls and carotenoids in petals, and no wild *Dianthus* species expressing their petal color with these pigments have been documented. In contrast, carnation cultivars with green flowers, accumulating chlorophylls and carotenoids in the chloroplasts of petals, have been developed by conventional breeding (Ohmiya et al. 2014). Furthermore, we recently discovered a carnation cultivar with pale yellow flowers, accumulating carotenoids in the chromoplasts (Iijima et al. 2020). These pale yellow- and green-flowered cultivars are considered to be mutants that have lost the ability to eliminate chlorophylls and carotenoids from the petals. However, little information is available about the mechanism that causes carotenoids and chlorophylls to accumulate in petals. In this section, based on our analyses of the green- and pale yellow-flowered carnation cultivars, we discuss the possible mechanism regulating the accumulation of these pigments in petals.

7.2 Carotenoids in Leaves and Petals

The green tissues of most plants show similar carotenoid profiles, i.e., carotenoids essential for photosynthesis, such as lutein, β-carotene, violaxanthin, neoxanthin, and zeaxanthin, are invariably found (Raju et al. 2007; Saini et al. 2015; Yuan et al. 2015). Carotenoids occur as chlorophyll-carotenoid-protein complexes in the chloroplast, and perform a photosynthetic function (Pogson and Albrecht 2011; Hashimoto et al. 2016). In flowers, carotenoids accumulate in the chromoplast (Vishnevetsky et al. 1999; Li and Yuan 2013). There is considerable diversity in the carotenoid profiles of petals of different plant species (Ohmiya 2011). For example, ray petals of chrysanthemum (*Chrysanthemum morifolium*) contain various types of isomers of lutein and lutein epoxides (Kishimoto et al. 2004), while the main carotenoids in petals of *Oncidium* are violaxanthin and neoxanthin (Hieber et al. 2006).

Carotenoid accumulation is closely associated with the differentiation of plastids during flower development (Sun et al. 2018). At early stages of development, petals display a pale green color, accumulating carotenoids and chlorophylls in the chloroplast. As the development progresses, a transition from chloroplasts to chromoplasts occurs, accompanied by changes in pigment composition (Egea et al. 2010). Chlorophyll content decreases and carotenoid composition changes from chloroplastic to chromoplastic (plant-specific), which are referred to as chloroplast-type and chromoplast-type carotenoids, respectively (Yamamizo et al. 2010). The formation of chromoplasts increases carotenoid storage capacity, and controls carotenoid accumulation in petals (Li and Yuan 2013).

Majority of carotenoids in petals are yellow xanthophylls (oxygenated carotenoids). The hydroxyl groups of most xanthophylls in petals are esterified with fatty acids, via acyl-CoA (Moehs et al. 2001; Yamamizo et al. 2010; Kishimoto et al. 2019), by the action of xanthophyll esterase (XES) (Ariizumi et al. 2014). Heterologous expression of *XES* genes leads to a significant increase in the carotenoid content and promotes chromoplast development in petals of petunia (*Petunia* × *hybrida*), suggesting that esterification is an important process for the sequestration of carotenoids into the chromoplast (Kishimoto et al. 2020).

7.3 Overview of Carotenoid Metabolism

7.3.1 Biosynthesis

Carotenoids are C40 carbohydrates belonging to the terpenoid compounds. Carotenoid biosynthesis begins with the formation of C5 building blocks, isopentenyl diphosphate (IPP), and its isomer dimethylallyl diphosphate (DMAPP), via the methylerythritol 4-phosphate (MEP) pathway in the plastids (Fig. 7.1) (for reviews, see Tanaka et al. 2008; Cazzonelli and Pogson 2010; Nisar et al. 2015). C20 geranylgeranyl diphosphate (GGPP) is formed from IPP and DMAPP by the action of GGPP synthase (GGPS). Two GGPP molecules are converted into the first C40 carotenoid, phytoene, by the action of phytoene synthase (PSY). Phytoene is then converted to lycopene by the addition of conjugated double bonds by phytoene desaturase (PDS) and ζ-carotene desaturase (ZDS), and the conversion of *cis*- to *trans*-configurations, by ζ-carotene isomerase (Z-ISO), and carotenoid isomerase (CRTISO). Cyclization of lycopene is a branch point of the carotenoid biosynthetic pathway. The formation of one β-ring and one ε-ring at either end, catalyzed by lycopene β-cyclase (LCYB) and lycopene ε-cyclase (LCYE), respectively, leads to α-carotene and its derivatives. The formation of two β-rings leads to β-carotene and its derivatives. Hydroxylation of the β-rings of β-carotene, catalyzed by a non-heme di-iron enzyme, β-ring hydroxylase (CHYB), yields zeaxanthin. Hydroxylation of the ε- and β-rings of α-carotene, catalyzed by the heme-containing cytochrome P450-type enzymes, CHYE/CYP97C and CHYB/CYP97A, respectively, yields lutein. Epoxidation of the β-rings of zeaxanthin, catalyzed by zeaxanthin epoxidase (ZEP), yields violaxanthin via a singly-epoxidized intermediate, antheraxanthin. Violaxanthin de-epoxidase (VDE) regenerates zeaxanthin from violaxanthin. Opening of one epoxide ring in violaxanthin by the action of neoxanthin synthase (NSY) yields neoxanthin.

7.3.2 Degradation

The steady-state level of carotenoids reflects the rates of biosynthesis and degradation. Carotenoid cleavage dioxygenases (CCDs) catalyze the oxidative cleavage of carotenoids and produce diverse apocarotenoid compounds that are involved in plant growth and reproduction (for reviews, see Ohmiya 2009; Hou et al. 2016). In *Arabidopsis*, the CCD enzyme family consists of nine members (Tan et al. 2003). Seven of these enzymes are involved in the synthesis of plant hormones. 9-*cis* epoxycarotenoid dioxygenases (NCED2, NCED3, NCED5, NCED6, and NCED9) cleave 9-*cis*-violaxanthin and 9-*cis*-neoxanthin to yield xanthoxin, a precursor of abscisic acid (Fig. 7.1) (Schwartz et al. 1997). CCD7 and CCD8 are involved in the synthesis of strigolactones from β-carotene (Alder et al. 2012). The remaining two CCDs (CCD1 and CCD4) contribute to carotenoid degradation in fruits and flowers. Some apocarotenoids produced by these enzymes provide unique aroma and color. For example, the red stigma of crocus (*Crocus sativus*) accumulates apocarotenoids, which are responsible for the red color (crocetin glycosides and picrocrocin) and aroma (safranal)

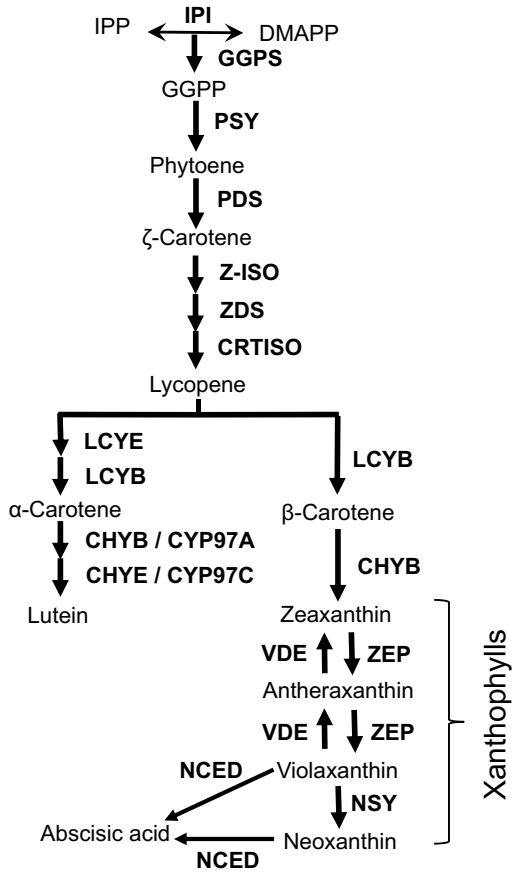

Fig. 7.1 Schematic representation of the carotenoid biosynthetic pathway in plants. IPP: isopentenyl diphosphate; IPI: IPP isomerase; GGPP: geranylgeranyl diphosphate; GGPS: GGDP synthase; PSY: phytoene synthase; PDS: phytoene desaturase; Z-ISO: ζ-carotene isomerase; ZDS: ζ-carotene desaturase; CRTISO: carotenoid isomerase; LCYE: lycopene ε-cyclase; LCYB: lycopene β-cyclase; CHYE: ε-ring hydroxylase; CHYB: β-ring hydroxylase, ZEP: zeaxanthin epoxidase; VDE: violaxanthin de-epoxidase; NSY: neoxanthin synthase; NCED: 9-*cis* epoxycarotenoid dioxygenase

of saffron (Winterhalter and Rouseff 2002). In chrysanthemum, lily (*Lilium brownii*), brassica (*Brassica napus*), petunia, azalea (*Rhododendron japonicum*), carotenoids synthesized in petals are degraded into colorless compounds by CCD4, resulting in white-colored petals (Ohmiya et al. 2006; Hai et al. 2012; Zhang et al. 2015; Ureshino et al. 2016; Kishimoto et al. 2018).

7.4 Yellow-Flowered Carnations

In the genus *Dianthus*, yellow flowers are rare, and found in only one wild species, i.e., *Dianthus knappii* (Pant.) Ascherson and Kanitz ex Borbas. The yellow coloration of *D. knappii* is derived from the high level of flavone and flavonols (Gatt et al. 1998), while in most carnation cultivars, yellow petal color is derived from chalcones. Itoh et al. (2000) reported that accumulation of chalcones is caused by disruption of a gene encoding chalcone isomerase. As no wild *Dianthus* species or carnation cultivars expressed their petal color through carotenoids, it seemed impossible to develop yellow-flowered carnation cultivars, accumulating carotenoids in petals, by conventional breeding. Interestingly, we recently discovered that a carnation cultivar, 'Club', accumulated carotenoids in petals (Iijima et al. 2020). There was no significant difference in the amount of flavonoids (including chalcone) in pale yellow petals of 'Club' and white petals of 'Siberia', indicating that 'Club' expressed its petal color with carotenoids. Carotenoid composition in petals of 'Club' was different from that in leaves, although the amount was extremely low [0.20 μg/g fresh weight (fw)] compared to that in leaves. Major carotenoids contained in the petals were (all-*E*)-neoxanthin, (all-*E*)-violaxanthin, and (all-*E*)-lutein. (9′*Z*)-neoxanthin, (9′*Z*)-violaxanthin, (all-*E*)-zeaxanthin, (all-*E*)-antheraxanthin, and β-carotene were also present as minor components (Fig. 7.2). In addition, some xanthophylls, particularly (9*Z*)-violaxanthin, were existed as esterified form. Transmission electron microscope observations revealed that the plastids in the petals possessed a chromoplastic structure, with several osmiophilic plastoglobules, and no granal stacking of thylakoid membranes. These results showed that petals of 'Club' accumulated petal-specific carotenoids in the chromoplasts. Therefore, it was expected that 'Club' would be a valuable parental cultivar for developing yellow-flowered carnation cultivars.

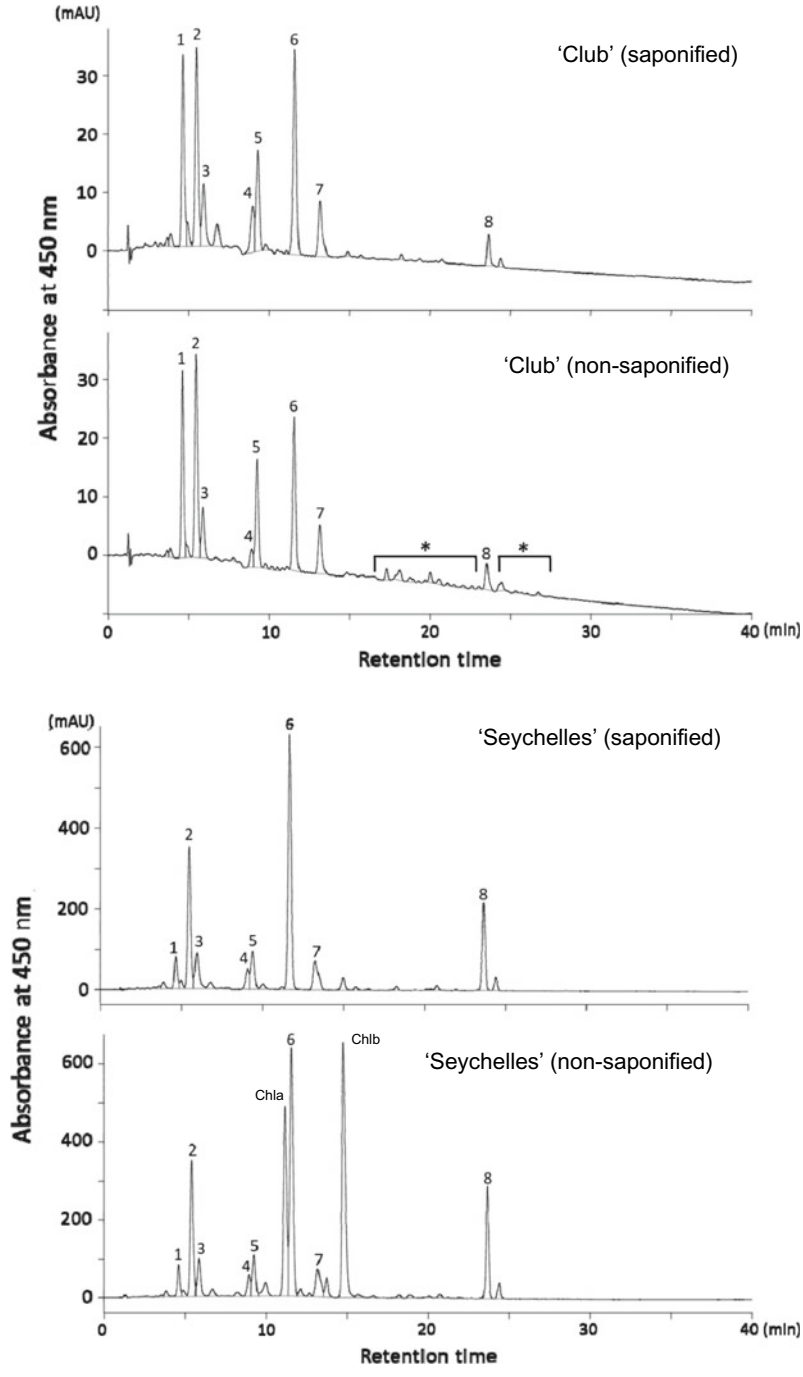

Fig. 7.2 HPLC chromatogram of carotenoid extracts from petals of 'Club' and 'Seychelles'. 1: (all-*E*)-neoxanthin; 2: (all-*E*)-violaxanthin; 3: (9′*Z*)-neoxanthin, 4: (9*Z*)-violaxanthin, 5: unknown; 6: (all-*E*)-lutein, 7: (all-*E*)-zeaxanthin + (all-*E*)-antheraxanthin, 8: β-carotene, Chla: chlorophyll *a*; Chlb: chlorophyll *b*; *: esterified xanthophylls

7.5 Carotenoid Metabolic Gene Expression in Petals of Carnation

To understand the mechanism underlying carotenoid accumulation in 'Club' petals, Iijima et al. (2020) compared the expression of genes related to carotenoid metabolism in 'Club', pink-flowered cultivar 'Elly', white-flowered cultivar 'Siberia', and green-flowered cultivar 'Seychelles'. Petals of 'Siberia' contained extremely low level of carotenoids (0.05 μg/gfw), while those of 'Seychelles' contained a substantial amount of carotenoids (3.25 μg/gfw), similar in composition to those of leaves (Fig. 7.2). 'Elly', which is a parental cultivar of 'Club', contained a similar amount of carotenoids to 'Club' (0.32 μg/gfw).

RNA sequencing analysis showed that there was no major difference in the expression of carotenogenic genes in petals of 'Club' and 'Elly': expression of most genes were lower than those of 'Siberia' and 'Seychelles' (Fig. 7.3). In 'Seychelles' petals, expression levels of *PSY1* and *LCYE* was remarkably higher, which was consistent with the results of our previous study (Ohmiya et al. 2013). Comparison of carotenogenic gene expressions of green and white petals and leaves in carnation revealed that most carotenogenic genes were expressed in white and green petals at a level similar to that in leaves, except *PSY1* and *LCYE*. Expression levels of *PSY1* and *LCYE* in white petals were very low, compared to those in leaves and green petals, and they decreased as petals matured, which was correlated with the carotenoid content. In many plants, PSY has been shown to be a key enzyme regulating carotenoid level in the tissue (Giuliano et al. 1993; Rodríguez-Villalón et al. 2009). LCYE also plays an important role in the synthesis of lutein, a major carotenoid contained in carnation petals. Cunningham et al. (1996) suggested that the apportioning of substrates into the pathways leading to α- and β-carotenes could be determined by the relative activities of LCYB and LCYE. We concluded that PSY and LCYE are key enzymes for carotenoid biosynthesis in carnation. Low expression levels of these key enzymes might cause low rate of carotenoid biosynthesis in petals of 'Club', 'Elly', and 'Siberia'.

In the HPLC analysis, peaks appeared at a retention time of approximately 17–28 min in the non-saponified samples but not in the saponified samples were esterified xanthophylls (Fig. 7.2). The esterification percentages of xanthophylls in petals of 'Club' and 'Elly' were 16.9% and 15.7%, respectively (Iijima et al. 2020), which were significantly higher than those observed in petals of 'Siberia' (8.1%) and 'Seychelles' (1.3%). Ariizumi et al. (2014) showed that disruption of *PALE YELLOW PETAL 1* (encoding XES) causes not only a loss of esterified xanthophylls, but also a drastic decrease in total carotenoid levels in tomato petals. This result indicates that esterification of xanthophylls is important for massive accumulation of carotenoids in petals. Deep yellow corollas of calibrachoa contain >200 μg/gfw carotenoids and >80% of them exist in esterified forms (Kishimoto et al. 2019). Esterification percentage in petals of 'Club' and 'Elly' was considerably less than that of calibrachoa. To increase the amount of carotenoids in petals of 'Club' and 'Elly', enhancement of XES activity might be necessary.

Among the carotenoid catabolic genes tested, a remarkable difference was observed in the *CCD4* expression (Iijima et al. 2020). Expression of *CCD4-1* and *CCD4-2* in 'Siberia' petals was more than 27and 20 times higher than in other cultivars, respectively. It has been reported in many plant species that CCD4 is responsible for the absence of carotenoids in petals (Ohmiya et al. 2006; Hai et al. 2012; Zhang et al. 2015; Ureshino et al. 2016; Kishimoto et al. 2018). Therefore, it is reasonable to consider that 'Siberia' petals have higher carotenoid degradation activity than other cultivars. As evident from the expression profiles of carotenogenic genes, the carotenoid biosynthetic activities of 'Siberia' petals are higher than those of 'Club' and 'Elly'. However, carotenoids synthesized in 'Siberia' petals might be degraded into colorless compounds, resulting in white petal color. In petals of 'Club' and 'Elly', a substantial amount

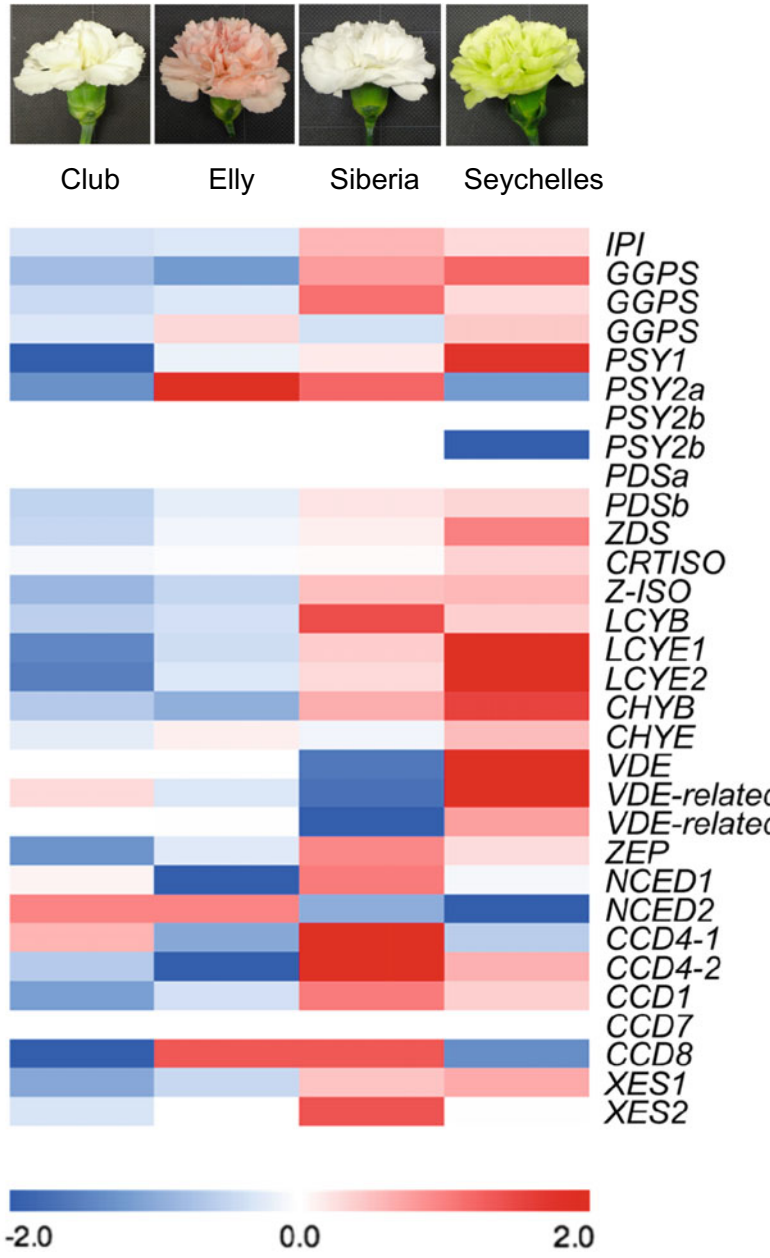

Fig. 7.3 RNA sequencing analysis of carotenoid-related genes in carnation petals. Expression values (TPM: transcripts per million) are log2 transformed and then median-centered by gene. The values are continuously mapped on the color scale provided at the bottom of the figure

of *CCD4* transcripts were detected, although at a level lower than that of 'Siberia'. We suggest that, to obtain cultivars with deep yellow flower color, selection of lines with lower *CCD4* expression is necessary.

Carotenoid accumulation in flowers is controlled by multiple factors, including biosynthesis, degradation, and plastid formation. There is an increasing evidence that each plant employs a different strategy to control carotenoid accumulation in flowers (Ohmiya 2013). High degradation activity is responsible for the lack of carotenoids in some plants. In chrysanthemum, both yellow and white petals express carotenoid biosynthetic genes at similar levels, whereas *CCD4a* is only expressed in white petals

(Ohmiya et al. 2006). In petunia, corollas of white-flowered cultivars express high levels of *CCD4a*, while those of pale yellow-flowered cultivars completely lack *CCD4* expression (Kishimoto et al. 2019). In case of Japanese morning glory (*Ipomoea nil*), expression levels of most carotenogenic genes functioning downstream of IPP isomerase (IPI) are extremely low in petals, suggesting that low level of carotenoid biosynthesis is the main reason for the absence of carotenoids (Yamamizo et al. 2010). In cauliflower (*Brassica oleracea*), absence of carotenoids in the white curd tissue (floral meristem) is attributed to a lack of their ability to differentiate proplastids into chromoplasts. The gain-of-function mutation in the *Orange* (*Or*) gene, a key component in chromoplast biogenesis, resulting in an orange pigmentation and a high level of β-carotene accumulation in curd tissues (Li et al. 2001; Paolillo et al. 2004).

Analysis of 'Club' and 'Elly' petals showed that carnation petals have an ability to generate chromoplasts and accumulate chromoplast-type carotenoids. However, the amount of carotenoids in petals of these cultivars are very small, compared to those in leaves and green petals. This is partly because they have lower biosynthetic activity and higher catabolic activity. Selection of lines with higher level of biosynthesis and/or lower level of degradation might aid in achieving higher carotenoid accumulation in carnation petals. 'Club' and 'Elly' will potentially help in developing carnation breeding strategies aimed at a wide range of flower colors.

7.6 Chlorophylls in Leaves and Petals

Chlorophylls are magnesium (Mg)-containing tetrapyrrole macromolecules responsible for green color in plants. As they play a central role in light harvesting and energy transduction in photosynthesis, mature leaves contain a substantial amount of chlorophylls (Niyogi 2000). Petals of many flowering plants contain chlorophylls during their early developmental stages (Pyke and Page 1998). The amount of chlorophylls decreases as petals develop, and petals of fully opened flowers accumulate only trace amounts. The absence of chlorophylls in petals is an important trait that enables flowers to be visually distinguished by pollinators against a background of green leaves, when the flowers are ready to be pollinated. Therefore, even if a mutation that results in green flowers occurs, such mutants may be eliminated from their natural habitat. In contrast, green-flowered mutants are preferentially selected and developed as cultivars in ornamental plant breeding. Hence, green-flowered cultivars are produced in many ornamental plants, including carnation.

7.7 Overview of Chlorophyll Metabolism

7.7.1 Biosynthesis

The chlorophyll biosynthesis pathway can be subdivided into four distinct parts (Fig. 7.4) (for reviews, see Eckhardt et al. 2004; Tanaka and Tanaka 2006; Masuda and Fujita 2008): (1) conversion of glutamyl-tRNA to 5-aminolevulinic acid (ALA), a precursor of tetrapyrrole compounds; (2) condensation of two molecules of ALA to form a pyrrole, porphobilinogen, and assembly of four molecules of porphobilinogen to form the first closed tetrapyrrole, uroporphyrinogen III; (3) formation of protoporphyrin IX via decarboxylation and oxidation reactions; (4) insertion of Mg^{2+} and phytol chain to form chlorophyll *a*. At least 15 enzymes are involved in the pathway, all of which have been identified and characterized.

7.7.2 Chlorophyll Cycle

In higher plants, the interconversion of chlorophyll *b* and *a*, termed as the "chlorophyll cycle", is known to occur (Fig. 7.4) (Tanaka et al. 1998). The chlorophyll cycle plays an important role in determining the balance of chlorophyll *a* and

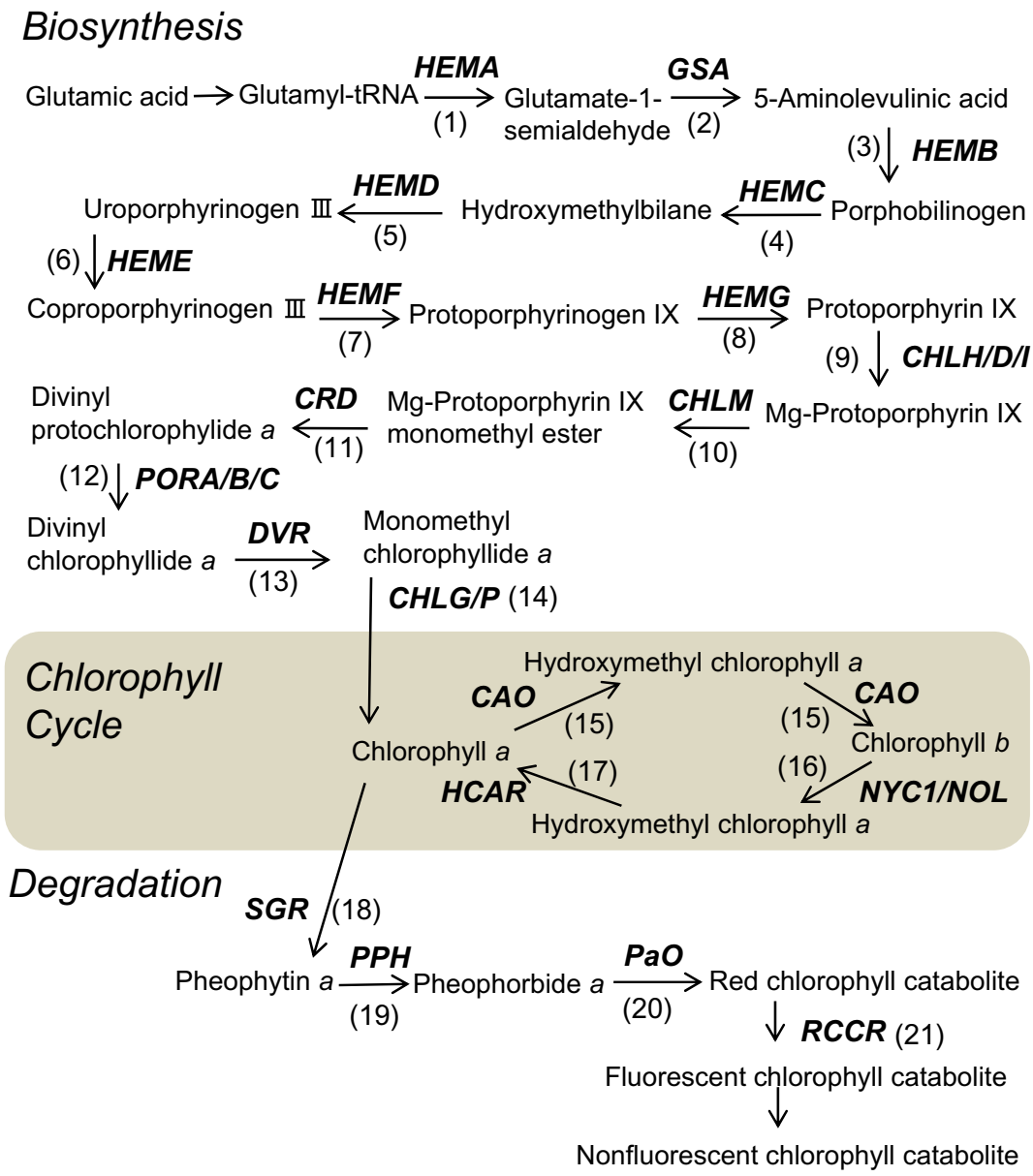

Fig. 7.4 Schematic representation of the chlorophyll metabolic pathway in plants. Genes (italicized) encode the following enzymes: (1) glutamyl-tRNA reductase; (2) glutamate-1-semialdehyde 2,1-aminotransferase; (3) 5-aminolevulinate dehydrogenase; (4) porphobilinogen deaminase; (5) uroporphyrinogen III synthase; (6) uroporphyrinogen III decarboxylase; (7) coproporphyrinogen III oxidase; (8) protoporphyrinogen oxidase; (9) Mg-chelatase; (10) Mg-protoporphyrin IX methyltransferase; (11) Mg-protoporphyrin IX monomethylester cyclase; (12) protochlorophyllide oxidoreductase; (13) divinyl chlorophyllide *a* 8-vinyl-reductase; (14) chlorophyll synthase; (15) chlorophyllide *a* oxygenase; (16) chlorophyll *b* reductase; (17) hydroxymethyl chlorophyll *a* reductase; (18) Mg-dechelatase; (19) pheophytinase; (20) pheophorbide *a* oxygenase; (21) red chlorophyll catabolite reductase

b. Chlorophyll *b* reductase, encoded by *NON-YELLOW COLORING 1* (*NYC1*) and *NYC1-like* (*NOL*) genes, catalyzes the conversion of chlorophyll *b* to 7-hydroxymethyl chlorophyll *a*, which is then converted into chlorophyll *a* by 7-hydroxymethyl-chlorophyll *a* reductase (HCAR). Chlorophyll *a* is reversibly converted to chlorophyll *b* by chlorophyllide *a* oxygenase (CAO), via 7-hydroxymethyl chlorophyll *a*.

7.7.3 Degradation

The chlorophyll degradation pathway is composed of a series of reactions that lead to the formation of non-fluorescent chlorophyll catabolites (Fig. 7.4) (for reviews, see Tanaka and Tanaka 2006; Hörtensteiner 2013). The initial step of this pathway is the removal of the central Mg atom from chlorophyll *a* by Mg-dechelatase, encoded by *Stay-Green* (*SGR*), to form pheophytin *a* (Shimoda et al. 2016). Pheophytinase (PPH) then catalyzes the removal of the phytol tail of pheophytin *a* to form pheophorbide *a*. Subsequently, the porphyrin macrocycle ring of pheophorbide *a* is opened by pheophorbide *a* oxygenase (PaO), to produce red chlorophyll catabolite (RCC). RCC is converted to non-fluorescent chlorophyll catabolites by the activity of RCC reductase (RCCR).

7.8 Chlorophyll Biosynthetic Gene Expression in Carnation Petals

A number of studies have reported about the genetic elements controlling chlorophyll accumulation in leaves. However, limited information is available about the mechanisms regulating chlorophyll accumulation in petals. To clarify the key factor that determines the chlorophyll content in carnation petals, we compared the expressions of chlorophyll metabolic genes in petals of red-flowered cultivar 'Francesco' (very low chlorophyll content), green-flowered cultivar 'Seychelles' (low chlorophyll content), and leaves (high chlorophyll content) (Ohmiya et al. 2014).

In petals of 'Francesco', the chlorophyll content decreased as petals matured, reaching extremely low levels at the later stages of development (Fig. 7.5). In petals of 'Seychelles', the chlorophyll content decreased from early to middle stages, and then increased at the late stage, suggesting that chlorophyll biosynthesis is active in the late stage of petal development. Chlorophyll content in 'Seychelles' petals at the late stage was about 7.9% of that in leaves.

Microarray analysis showed that expressions of most genes involved in chlorophyll biosynthesis were lower in 'Francesco' petals than in 'Seychelles' petals (Fig. 7.6). In particular, *HEMA1* (encoding glutamyl-tRNA reductase), *CHLH* and *CHLI* [encoding Mg-protoporphyrin IX chelatase (Mg-chelatase) subunits], and *CHLM* [encoding Mg-protoporphyrin IX methyltransferase (MgPMT)] exhibited extremely low expression in 'Francesco' petals. RT-qPCR analysis showed that expressions of *CHLH*, *CHLI*, and *CHLM* were closely associated with the change in chlorophyll content during petal development in 'Seychelles' petals, decreasing from early to middle stages and then increasing at the late stage. This result indicates that these genes are key factors involved in the greening of petals.

Expressions of selected genes in petals were further analyzed in five white-flowered cultivars ('White Sim', 'Byakko', 'Siberia', 'Shirayuki', and 'Delphi') and four green-flowered cultivars ('Prado Mint', 'Le France', 'Ice Tea', 'Martha Green') by RT-qPCR. *CHLH*, *CHLI*, and *CHLM* showed positive correlations with the chlorophyll content, with extremely low levels in white petals and substantial levels being expressed in green petals. There was a variability in the *HEMA1* expression, but no correlation with the chlorophyll content.

In chrysanthemum, the expression levels of chlorophyll biosynthetic genes were also compared between white- and green-flowered cultivars (Ohmiya et al. 2017). The expression of *HEMA1*, *CHLH*, *CRD*, and *PORC* tended to be lower in white petals than in green petals. In particular, *CRD* (encoding Mg-protoporphyrin IX monomethylester cyclase) expression was significantly lower in white petals of the five tested cultivars than in the green petals.

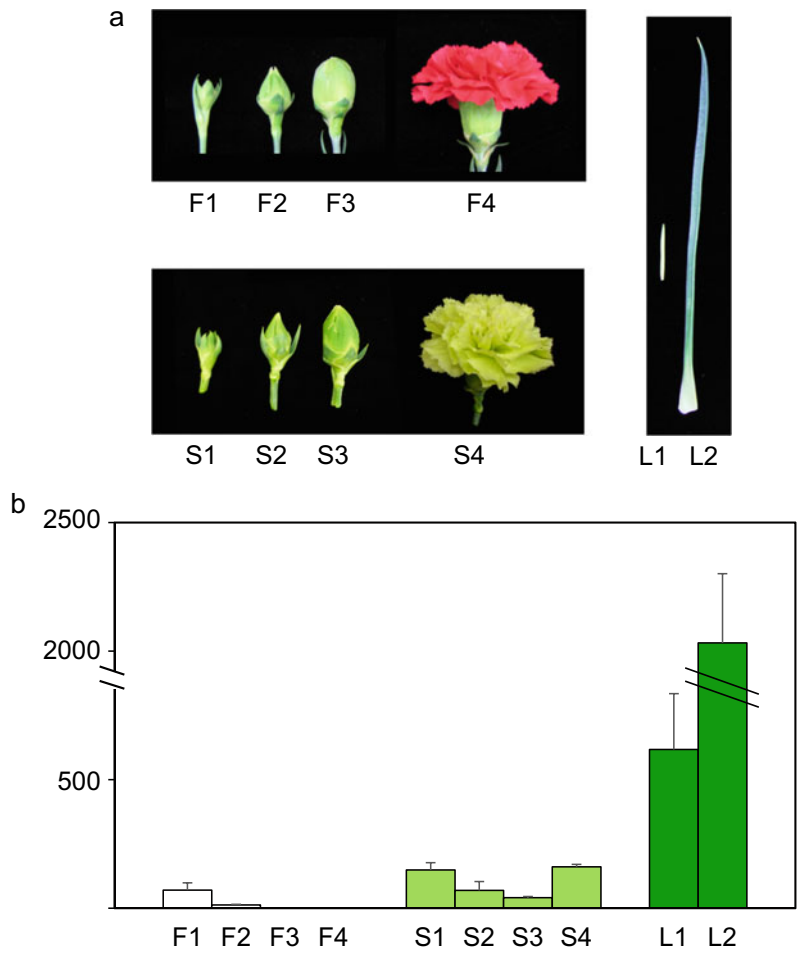

Fig. 7.5 **a** Photographs of carnation flowers and leaves used for chlorophyll analyses. **b** Chlorophyll content in petals and leaves of carnation. F1, F2, F3, and F4: Flowers of 'Francesco' at stages 1 to 4. S1, S2, S3, and S4: Flowers of 'Seychelles' at stages 1 to 4. L1 and L2: Young (L1) and mature (L2) leaves of 'Francesco'

Chlorophyll biosynthesis in leaves is strictly regulated and synchronously activated with the construction of the photosynthetic machinery, because of the phototoxic properties of chlorophylls and their intermediates (Tanaka et al. 2011). Indeed, genes encoding key enzymes of the chlorophyll biosynthesis pathway, including *HEMA1*, *CHLH*, *GENOME UNCOUPLED4* (*GUN4*, encoding an activator of Mg-chelatase), *CRD*, and *CAO* are coordinately up-regulated by light during photomorphogenesis (Matsumoto et al. 2004; Masuda and Fujita 2008). Similarly, expressions of a set of chlorophyll biosynthetic genes were up-regulated in green petals of both carnations and chrysanthemums, although expressions of different sets of genes were promoted between them (Ohmiya et al. 2014, 2017). In particular, the expression of *CHLH* was commonly accelerated in the green petals of these plants. Mg-chelatase (encoded by *CHLH*, *CHLI,* and *CHLD*) catalyzes the insertion of Mg^{2+} into protoporphyrin IX, a major step in the chlorophyll biosynthesis. Higher expression of *CHLH* in green petals suggests that green petals have higher chlorophyll biosynthesis activity than white petals.

7.9 Chlorophyll Catabolic Gene Expression in Carnation Petals

Drastic increase in chlorophyll degradation activity takes place at the onset of senescence in leaves, resulting in yellow coloration. Several types of mutants, exhibiting the stay-green

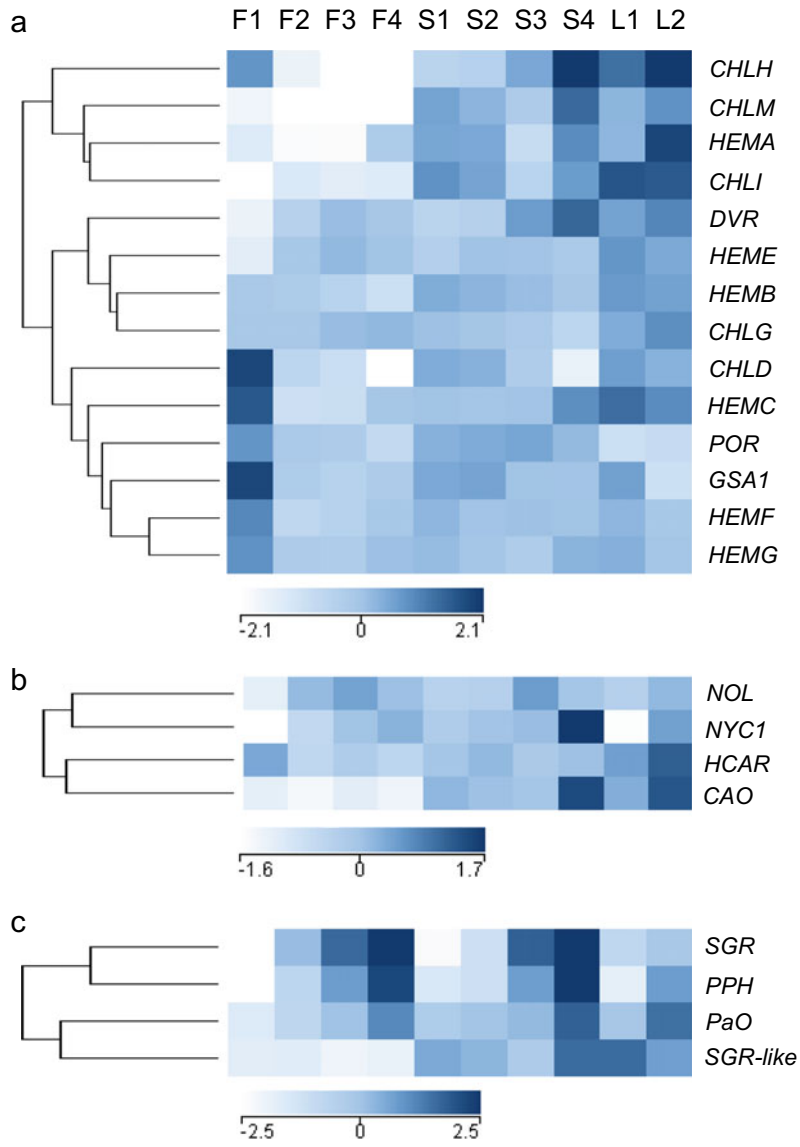

Fig. 7.6 Overview of expression profiles of genes related to **a** chlorophyll biosynthesis, **b** chlorophyll cycle, and **c** chlorophyll degradation in petals and leaves of carnation. Stages are designated as in Fig. 7.5. Custom oligonucleotide array was constructed, and microarray analysis was performed as previously described (Ohmiya et al. 2013). The microarray data were clustered with respect to genes using GeneSpring XII (Agilent), and dendrograms are shown on the left side of the heatmap. Color indicates normalized signal intensities as shown in the bar below the heatmap. Supplemental Fig. 3 in PLoS ONE (Ohmiya et al. 2014)

phenotype during leaf senescence, have been identified. Various stay-green genes, such as *SGR*, *NYC1*, *PaO*, and *PPH*, have been identified from the analyses of these mutants (for review, see Kusaba et al. 2013), all of which encode enzymes involved in chlorophyll degradation. Mutation in one of these genes suppresses chlorophyll degradation, consequently delaying the loss of chlorophylls during leaf senescence. In flowers, chlorophylls accumulate during early development, and disappear as petals mature. Chlorophyll degradation occurs at the premature stage, independent of petal senescence. It is of particular interest to determine if the accumulation of chlorophylls in pale green petals is caused by a loss of degradation activity, similar to the mechanism of the stay-green phenotype in leaves. Thus, we compared the expressions of chlorophyll catabolic genes in 'Francesco' and 'Seychelles'.

Microarray analysis showed that expressions of *PPH* and *SGR* increased as petals matured, in both 'Francesco' and 'Seychelles' (Fig. 7.6) (Ohmiya et al. 2014). At the late stage, the levels of *PPH*

and *SGR* transcripts were significantly higher in petals of both cultivars than in mature leaves of 'Francesco'. This suggests that petals of both cultivars have greater levels of chlorophyll degradation activity during development, and this activity is higher than in mature leaves. On comparing the expressions of catabolic genes in the petals of fully opened flowers of white- and green-flowered cultivars, we observed considerable variability in the expression levels of genes related to the chlorophyll cycle (*NYC1*, *NOL*, *CAO,* and *HCAR*) and chlorophyll degradation (*SGR*, *CLH*, *PPH*, and *PaO*) between the cultivars, but there was no significant correlation between transcript levels and the chlorophyll content (Ohmiya et al. 2014). This suggests that the difference in the chlorophyll levels of white and green petals is not caused by the different levels of catabolic activity.

It is worth noting that high expression of *SGR* in mature petals is commonly observed in carnation, chrysanthemum, and *Arabidopsis* (Ohmiya et al. 2014, 2017). *SGR* encodes an Mg-dechelatase which catalyzes the conversion of chlorophyll *a* to pheophytin *a*, the first and the most important step of chlorophyll degradation (Shimoda et al. 2016). Loss-of-function of SGR causes stay-green phenotypes of leaves in rice and *Arabidopsis* (Kusaba et al. 2007; Ren et al. 2007), and also in non-photosynthetic tissues, such as fruits of tomato, pepper, and kiwi, in which chlorophyll degradation normally occurs at the onset of fruit ripening (Barry et al. 2008; Pilkington et al. 2012). We assume that SGR is a key enzyme in chlorophyll degradation, and high level of *SGR* expression results in the absence or low levels of chlorophylls in flower petals.

Analysis of chlorophyll metabolic gene expressions suggested that, in white petals, lack of chlorophylls is caused by the low level of chlorophyll biosynthesis and high level of degradation activities. In green petals, the degradation activity was similar to that in white petals, but chlorophylls accumulated due to the higher biosynthesis activity at the late stage of development (Fig. 7.7). This hypothesis is supported by our crossing experiment (Ohmiya et al. 2014). Green petal color can be expected to be dominant over the white color if it is determined by chlorophyll biosynthesis ability. We performed crosses between white-flowered cultivar 'Shirayuki' (female) and green-flowered cultivar 'Seychelles' (male). All the F_1 progenies showed green petals, indicating that green petal color is dominant over white. These results indicate that green petal color of carnation is not a stay-green phenotype caused by deficiency of chlorophyll catabolic activity, rather it is caused by enhanced biosynthetic activity.

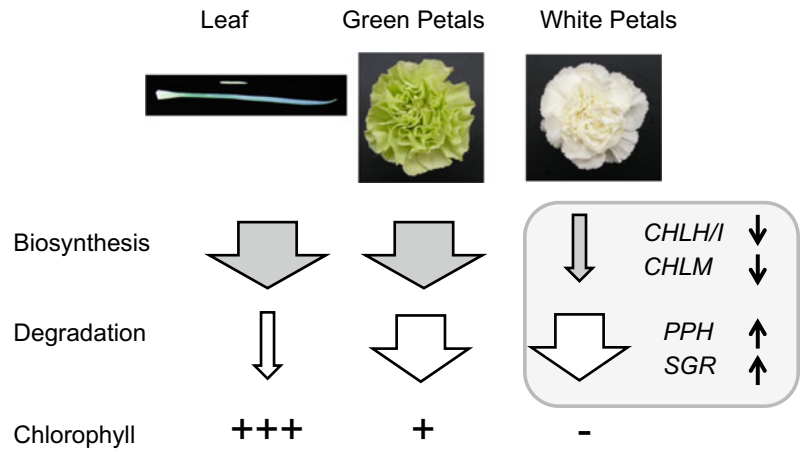

Fig. 7.7 Schematic representation of chlorophyll accumulation in carnation petals. Arrow width indicates the extent of activity of each pathway

7.10 Transcription Factors Involved in the Regulation of Chlorophyll Metabolic Pathway in Petals

From the analysis of chlorophyll metabolic gene expressions, we assume that, in petals, factor(s) that suppress chlorophyll biosynthesis (and/or enhance chlorophyll degradation) may exist, or factor(s) that enhance chlorophyll biosynthesis may be inactivated. Higher rate of chlorophyll biosynthesis in green petals might result from a loss or reduced activity of the suppressor, or greater activity of the activator. It is, therefore, of particular interest to determine how chlorophyll biosynthesis is regulated, and what transcription factors are involved in the process. However, little attention has been paid to this regulatory mechanism in flowers.

In chrysanthemum, several transcription factor genes, that are differentially expressed in the white and green petals and leaves, have been identified (Ohmiya et al. 2017). Of these, the expression of *CONSTANS-like 16* (*COL16*) was the most highly associated with the chlorophyll content of these tissues. Overexpression of *COL16* in petunia results in enhanced expression of chlorophyll biosynthetic genes, and produces green flowers (Ohmiya et al. 2018). These results suggest that COL16 is a strong candidate of positive regulator for chlorophyll biosynthesis in petals. Microarray analysis of carnation showed that expression of *COL16* was also associated with the chlorophyll content, and was higher in green petals than in non-green petals (our unpublished result). It is of particular interest to determine if COL16 also acts as a positive regulator of chlorophyll biosynthesis in carnation petals, in which case, *COL16* can be used as a marker gene for breeding green-flowered cultivars.

Chlorophyll biosynthesis requires a complex transcriptional network to manage the spatial and temporal regulation of chlorophyll accumulation in response to environmental and developmental stimuli. Multiple transcription factors, in addition to COL16, might be involved in the regulation of chlorophyll biosynthesis pathway. It would be interesting to know if COL16 affects chlorophyll biosynthesis directly, by binding to the promoters of biosynthesis enzymes, or indirectly, through the transcriptional network. Future studies should focus on direct targets of COL16, using a genome-wide ChiP-chip analysis of transcription factor-binding sites.

Higher chlorophyll catabolic gene expressions observed in carnation petals also led us to speculate that transcription factors that activate the pathway exist in petals. Manipulation of the chlorophyll catabolic pathway can also render the flowers greener. ANAC046 has been identified as a positive regulator of chlorophyll degradation in *Arabidopsis* leaves (Oda-Yamamizo et al. 2016). Introduction of a dominant negative (SRDX) *ANAC046* constructs into petunia, which causes loss-of-function of related transcription factors, resulted in down-regulation of chlorophyll catabolic genes. This suggests that common or closely related transcription factors that regulate chlorophyll degradation may exist in leaves and flowers (Oda-Yamamizo et al. 2017). In addition, suppression of chlorophyll catabolic genes resulted in accumulation of a higher level of chlorophylls in the corolla limbs, indicating that high level of chlorophyll catabolic gene expression is one of the reasons causing low levels or absence of chlorophylls in the petal. In carnation, involvement of the ANA046 ortholog in chlorophyll degradation in petals has not been elucidated, although genomic sequence closely related to *ANAC046* exists in the genome (https://carnation.kazusa.or.jp/).

7.11 Conclusion

Microarray analysis showed that the amounts of both carotenoids and chlorophylls in carnation petals are controlled at the transcriptional levels of the metabolic genes (Fig. 7.7). In leaves, strong candidates regulating the metabolic pathway of carotenoids and chlorophylls have been reported. However, we have limited knowledge about how the transcription of metabolic genes is controlled in petals and by what mechanism the

alteration of transcription, that leads to mutations expressing green and yellow colors, occurs. Identification of regulators will provide a deeper understanding of pigment metabolism and accumulation, as well as useful information for the development of molecular markers to accelerate carnation breeding.

References

Alder A, Jamil M, Marzorati M, Bruno M, Vermathen M, Bigler P, Ghisla S, Bouwmeester H, Beyer P, Al-Babili S (2012) The path from β-carotene to carlactone, a strigolactone-like plant hormone. Science 335:1348–1351

Ariizumi T, Kishimoto S, Kakami R, Maoka T, Hirakawa H, Suzuki Y, Ozeki Y, Shirasawa K, Bernillon S, Okabe Y, Asamizu E, Rothan C, Ohmiya A, Ezura H (2014) Identification of the carotenoid modifying gene *PALE YELLOW PETAL 1* as an essential factor in xanthophyll esterification and yellow flower pigmentation in tomato (*Solanum lycopersicum*). Plant J 79:453–465

Barry CS, McQuinn RP, Chung MY, Besuden A, Giovannoni JJ (2008) Amino acid substitutions in homologs of the STAY-GREEN protein are responsible for the green-flesh and chlorophyll retainer mutations of tomato and pepper. Plant Physiol 147:179–187

Bate-Smith E (1962) The phenolic constituents of plants and their taxonomic significance. Bot J Linn Soc 58:95–173

Cazzonelli C, Pogson BJ (2010) Source to sink: regulation of carotenoid biosynthesis in plants. Trends Plant Sci 15:266–274

Cunningham FX Jr, Pogson B, Sun Z, McDonald KA, DellaPenna D, Gantt E (1996) Functional analysis of the β and ε lycopene cyclase enzymes of Arabidopsis reveals a mechanism for control of cyclic carotenoid formation. Plant Cell 8:1613–1626

Eckhardt U, Grimm B, Hörtensteiner S (2004) Recent advances in chlorophyll biosynthesis and breakdown in higher plants. Plant Mol Biol 56:1–14

Egea I, Barsanb C, Bian W, Purgatto E, Latche A, Chervin C, Bouzayen M, Pech JC (2010) Chromoplast differentiation: current status and perspectives. Plant Cell Physiol 51:1601–1611

Galbally J, Galbally E (1997) Carnation and pinks for garden and greenhouse: their true history and complete cultivation. Timber Press, Portland, Oregon

Gatt MK, Hammett KRW, Markham KR, Murraya BG (1998) Yellow pinks: interspecific hybridization between *Dianthus plumarius* and related species with yellow flowers. Sci Hortic 77:207–218

Giuliano G, Bartley GE, Scolnik PA (1993) Regulation of carotenoid biosynthesis during tomato development. Plant Cell 5:379–387

Hai MTL, Masuda J, Miyajima I, Thien NQ, Mojtahedi N, Hiramatsu M, Kim J-H, Okubo H (2012) Involvement of carotenoid cleavage dioxygenase 4 gene in tepal color change in *Lilium brownii* var. *colchesteri*. J Japan Soc Hort Sci 81:366–373

Hashimoto H, Uragami C, Cogdell RJ (2016) Carotenoids and photosynthesis. Subcell Biochem 79:111–139

Hieber AD, Mudalige-Jayawickrama RG, Kuehnle AR (2006) Color genes in the orchid *Oncidium* Gower Ramsey: identification, expression, and potential genetic instability in an interspecific cross. Planta 223:521–531

Hörtensteiner S (2013) Update on the biochemistry of chlorophyll breakdown. Plant Mol Biol 82:505–517

Hou X, Rivers J, León P, McQuinn RP, Pogson BJ (2016) Synthesis and function of apocarotenoid signals in plants. Trends Plant Sci 21:792–803

Iijima L, Kishimoto S, Ohmiya A, Yagi M, Okamoto E, Miyahara T, Tsujimoto T, Ozeki Y, Uchiyama N, Hakamatsuka T, Kouno T, Cano EA, Shimizu M, Nishihara M (2020) Esterified carotenoids are synthesized in petals of carnation (*Dianthus caryophyllus*) and accumulate in differentiated chromoplasts. Sci Rep 10:15256

Itoh Y, Higeta D, Suzuki A, Yoshida H, Ozeki Y (2000) Excision of transposable elements from the chalcone isomerase and dihydroflavonol 4-reductase genes may contribute to the variegation of the yellow-flowered carnation (*Dianthus caryophyllus*). Plant Cell Physiol 43:578–585

Kishimoto S, Maoka T, Nakayama M, Ohmiya A (2004) Carotenoid composition in petals of chrysanthemum (*Dendranthema grandiflorum* (Ramat.) Kitamura). Phytochemistry 65:2781–2787

Kishimoto S, Oda-Yamamizo C, Ohmiya A (2018) Regulation of carotenoid pigmentation in corollas of petunia. Plant Mol Biol Rep 36:632–642

Kishimoto S, Oda-Yamamizo C, Ohmiya A (2019) Comparison of petunia and calibrachoa in carotenoid pigmentation of corollas. Breed Sci 69:117–126

Kishimoto S, Oda-Yamamizo C, Ohmiya A (2020) Heterologous expression of carotenoid esterase genes affects carotenoid accumulation in petunia corollas. Sci Rep 10:1299

Kusaba M, Ito H, Morita R, Iida S, Sato Y, Fujimoto M, Kawasaki S, Tanaka R, Hirochika H, Nishimura M, Tanaka A (2007) Rice NON-YELLOW COLORING1 is involved in light-harvesting complex II and grana degradation during leaf senescence. Plant Cell 19:1362–1375

Kusaba M, Tanaka A, Tanaka R (2013) Stay-green plants: what do they tell us about the molecular mechanism of leaf senescence. Photosynth Res 117:221–234

Li L, Paolillo DJ, Parthasarathy MV, DiMuzio EM, Garvin DF (2001) A novel gene mutation that confers abnormal patterns of β-carotene accumulation in cauliflower (*Brassica oleracea* var. *botrytis*). Plant J 26:59–67

Li L, Yuan H (2013) Chromoplast biogenesis and carotenoid accumulation. Arch Biochem Biophys 539:102–109

Mabry T (1964) The betacyanins, a new class of red violet pigments, and their phylogenetic significance. Roland Press, New York, NY, USA

Masuda T, Fujita Y (2008) Regulation and evolution of chlorophyll metabolism. Photochem Photobiol Sci 7:1131–1149

Mato M, Onozaki T, Ozeki Y, Higeta D, Itoh Y, Yoshimoto Y, Ikeda H, Yoshida H, Shibata M (2000) Flavonoid biosynthesis of white-flowered Sim carnations (*Dianthus caryophyllus*). Sci Hort 84: 333–347

Matsumoto F, Obayashi T, Sasaki-Sekimoto Y, Ohta H, Takamiya K, Masuda T (2004) Gene expression profiling of the tetrapyrrole metabolic pathway in Arabidopsis with a mini-array system. Plant Physiol 135:2379–2391

Miyahara T, Sugishita N, Ishida-Dei M, Okamoto E, Kouno T, Cano EA, Sasaki N, Watanabe A, Tasaki K, Nishihara M, Ozeki Y (2018) Carnation *I* locus contains two chalcone isomerase genes involved in orange flower coloration. Breed Sci 68:481–487

Moehs CP, Tian L, Osteryoung KW. DellaPenna D (2001) Analysis of carotenoid biosynthetic gene expression during marigold petal development. Plant Mol Biol 45:281–293

Nisar N, Li L, Lu S, Khin NC, Pogson BJ (2015) Carotenoid metabolism in plants. Mol Plant 8:68–82

Niyogi K (2000) Safety valves for photosynthesis. Curr Opin Plant Biol 3:455–460

Oda-Yamamizo C, Mitsuda N, Sakamoto S, Ogawa D, Ohme-Takagi M, Ohmiya A (2016) The NAC transcription factor ANAC046 is a positive regulator of chlorophyll degradation and senescence in Arabidopsis leaves. Sci Rep 6:23609

Oda-Yamamizo C, Mitsuda N, Ohmiya A (2017) Heterologous expression of chimeric repressor of Arabidopsis ANAC046 delays chlorophyll degradation in petunia flowers Plant Mol Biol Rep 35:611–618

Ohmiya A, Kishimoto S, Aida R, Yoshioka S, Sumitomo K (2006) Carotenoid cleavage dioxygenase (CmCCD4a) contributes to white color formation in chrysanthemum petals. Plant Physiol 142:1193–1201

Ohmiya A (2009) Carotenoid cleavage dioxygenases and their apocarotenoid products in plants. Plant Biotechnol 26:351–358

Ohmiya A (2011) Diversity of carotenoid composition in flower petals. Jpn Agric Res Q (JARQ) 45:163–171

Ohmiya A (2013) Qualitative and quantitative control of carotenoid accumulation in flower petals. Sci Hort 163:10–19

Ohmiya A, Tanase K, Hirashima M, Yamamizo C, Yagi M (2013) Analysis of carotenogenic gene expression in petals and leaves of carnation (*Dianthus caryophyllus* L.). Plant Breed 132:423–429

Ohmiya A, Hirashima M, Yagi M, Tanase K, Yamamizo C (2014) Identification of genes associated with chlorophyll accumulation in flower petals. PLoS ONE 9:e113738

Ohmiya A, Sasaki K, Nashima K, Oda-Yamamizo C, Hirashima M, Sumitomo K (2017) Transcriptome analysis in petals and leaves of chrysanthemums with different chlorophyll levels. BMC Plant Biol 17:202

Ohmiya A, Oda-Yamamizo C, Kishimoto S (2018) Overexpression of *CONSTANS-like16* enhances chlorophyll accumulation in petunia flowers. Plant Sci 280:90–96

Onozaki T, Mato M, Shibata M, Ikeda H (1999) Difference in flower color and pigment composition among white carnation (*Dianthus caryophyllus* L.) cultivars. Sci Hort 82:103–111

Paolillo DJ Jr, Garvin DF, Parthasarathy MV (2004) The chromoplasts of *Or* mutants of cauliflower (*Brassica oleracea* L. var. *botrytis*). Protoplasma 224:245–253

Pilkington SM, Montefiori M, Jameson PE, Allan AC (2012) The control of chlorophyll levels in maturing kiwifruit. Planta 236:1615–1628

Pogson BJ, Albrecht V (2011) Genetic dissection of chloroplast biogenesis and development: an overview. Plant Physiol 155:1545–1551

Pyke KA, Page AM (1998) Plastid ontogeny during petal development in Arabidopsis. Plant Physiol 116:797–803

Raju M, Varakumar S, Lakshminarayana R, Krishnakantha TP, Baskaran V (2007) Carotenoid composition and vitamin A activity of medicinally important green leafy vegetables. Food Chem 101:1598–1605

Ren G, An K, Liao Y, Zhou X, Cao Y, Zhao H, Ge X, Kuai B (2007) Identification of a novel chloroplast protein AtNYE1 regulating chlorophyll degradation during leaf senescence in Arabidopsis. Plant Physiol 144:1429–1441

Rodríguez-Villalón A, Gas E, Rodríguez-Concepción M (2009) Phytoene synthase activity controls the biosynthesis of carotenoids and the supply of their metabolic precursors in dark-grown Arabidopsis seedlings. Plant J 60:424–435

Saini RK, Nile SH, Park SW (2015) Carotenoid from fruits and vegetables: chemistry, analysis, occurrence, bioavailability and biological activities. Food Res Int 76:735–750

Schwartz SH, Tan BC, Gage DA, Zeevaart JA, McCarty DR (1997) Specific oxidative cleavage of carotenoids by VP14 of maize. Science 276:1872–1874

Shimoda Y, Ito H, Tanaka A (2016) Arabidopsis *STAY-GREEN*, Mendel's green cotyledon gene, encodes magnesium-dechelatase. Plant Cell 28:2147–2160

Sun T, Yuan H, Cao H, Yazdani M, Tadmor Y, Li L (2018) Carotenoid metabolism in plants: the role of plastids. Mol Plant 11:58–74

Tan BC, Joseph LM, Deng WT, Liu L, Li QB, Cline K, McCarty DR (2003) Molecular characterization of the Arabidopsis 9-*cis* epoxycarotenoid dioxygenase gene family. Plant J 35:44–56

Tanaka A, Ito H, Tanaka R, Tanaka NK, Yoshida K, Okada K (1998) Chlorophyll *a* oxygenase (CAO) is involved in chlorophyll *b* formation from chlorophyll *a*. Proc Natl Acad Sci USA 95:12719–12723

Tanaka A, Tanaka R (2006) Chlorophyll metabolism. Curr Opin Plant Biol 9:248–255

Tanaka R, Kobayashi K, Masuda T (2011) Tetrapyrrole metabolism in *Arabidopsis thaliana*. Arabidopsis Book 9: e0145

Tanaka Y, Sasaki N, Ohmiya A (2008) Plant pigments for coloration. Plant J (Special Issue) 54:733–749

Ureshino K, Nakayama M, Miyajima I (2016) Contribution made by the carotenoid cleavage dioxygenase 4 gene to yellow colour fade in azalea petals. Euphytica 207:401–417

Vishnevetsky M, Ovadis M, Vainstein A (1999) Carotenoid sequestration in plants: the role of carotenoid associated proteins. Trends Plant Sci 4:232–235

Winterhalter P, Rouseff RL (2002) Carotenoid-derived aroma compounds: an introduction. In: Winterhalter P, Rouseff RL (eds) Carotenoid derived aroma compounds, ACS Symposium Series vol 802. ACS, Washington, D.C. pp 1–17

Yamamizo C, Kishimoto S, Ohmiya A (2010) Carotenoid composition and carotenogenic gene expression during Ipomoea petal development. J Exp Bot 61: 709–719

Yuan H, Zhang J, Nageswaran D, Li L (2015) Carotenoid metabolism and regulation in horticultural crops. Hort Res 2:15036

Zhang B, Liu C, Wang Y, Yao X, Wang F, Wu J, King GJ, Liu K (2015) Disruption of a *CAROTENOID CLEAVAGE DIOXYGENASE 4* gene converts flower colour from white to yellow in *Brassica* species. New Phytol 206:1513–1526

8 Molecular Mechanisms of Carnation Flower Colors via Anthocyanin and Flavonoid Biosynthetic Pathways

Yoshihiro Ozeki, Luna Iijima, Kaoru Higuchi, Taira Miyahara, Nobuhiro Sasaki, Takashi Tsujimoto, Yutaka Abe, Yuki Matsuba, Yuzo Nishizaki, Akane Suzuki-Wagner, Jun Ogata, and Yoshio Itoh

Abstract

Anthocyanin synthesis is initiated by the phenylpropanoid pathway followed by aglycone synthesis; the products of synthesis are then modified with glucose and malate. Genes for the enzymes in the phenylpropanoid pathway consist of small gene families in Carnation database (DB) and particular gene (s) are expressed during anthocyanin and flavonol syntheses in petals. After phenylpropanoid metabolism, the enzymes chalcone synthase, chalcone isomerase, and flavanone 3-hydroxylase, which are categorized as early biosynthetic genes and consist of small gene families, supply intermediates for both anthocyanin and flavonol syntheses. The intermediates are catabolized by dihydroflavonol 4-reductase followed by anthocyanidin synthase; some intermediates are hydroxylated by flavonol 3′-hydroxylase; these three enzymes are encoded by genes categorized as late biosynthetic genes and consist of single genes in Carnation DB. Anthocyanidin is glucosylated by cytosolic UDP-glucose-dependent glucosyltransferase, a member of glycosyltransferase family 1, at the 3 position followed by transportation into vacuoles (or endoplasmic reticulum). Anthocyanin 3-*O*-glucoside is malylated by serine carboxypeptidase-like (SCPL) malyltransferase followed by glucosylation at the 5 position by a glycoside hydrolase family 1 (GH1) enzyme; both use acyl-glucose as a donor. Genes for these enzymes probably evolved from ancestral *SCPL* and *GH1* genes by local gene duplication associated with neofunctionalization and subfunctionalization.

Electronic supplementary material The online version of this chapter (https://doi.org/10.1007/978-981-15-8261-5_8) contains supplementary material, which is available to authorized users.

Y. Ozeki (✉) · L. Iijima · K. Higuchi · T. Miyahara · N. Sasaki · T. Tsujimoto · Y. Abe · Y. Matsuba · Y. Nishizaki · A. Suzuki-Wagner · J. Ogata · Y. Itoh
Department of Biotechnology and Life Science, Tokyo University of Agriculture and Technology, Koganei 184-8588, Tokyo, Japan
e-mail: ozeky@cc.tuat.ac.jp

T. Miyahara
Graduate School of Horticulture, Chiba University, Chiba 263-8522, Chiba, Japan

N. Sasaki
Department of Food and Life Sciences, Toyo University, Ora-gun 374-0193, Gunma, Japan

Y. Abe · Y. Nishizaki · J. Ogata
Division of Food Additives, Division of Pharmacognosy, Phytochemistry and Narcotics, National Institute of Health Sciences, Kawasaki 210-9501, Kanagawa, Japan

Y. Matsuba
North American Crop Protection Division, BASF, Research Triangle Park, Durham, NC 27709, USA

T. Onozaki and M. Yagi (eds.), *The Carnation Genome*, Compendium of Plant Genomes,
https://doi.org/10.1007/978-981-15-8261-5_8

8.1 Introduction

Carnations show wide color variations in their petals, including crimson, red, magenta, pink, orange, white, yellow, cream, and green (Supplemental Fig. 8.1A-H). Cyanic colors are produced by anthocyanins, yellows by chalcone, creams by flavonols, and green by chlorophyll (see Chaps. 6 and 7). In addition to petals with different monochromatic colors, the colors of flowers in some carnation varieties are expanded by variable intra-petal patterns of pale and dark colors (Supplemental Fig. 8.1I–P). Plant species within the order Caryophyllales, with the exception of the families Molluginaceae and Caryophyllaceae synthesize betalains; red coloration is produced by betacyanin and yellow from betaxanthin (Kay et al. 1981; Brockington et al. 2011). Carnations belong to the genus *Dianthus* (family Caryophyllaceae) and carry homologues of the genes that encode enzymes for betalain synthesis in their genomes (Yagi et al. 2014), but they do not function for betalain synthesis (Timoneda et al. 2019). Recently, Ohmiya and Kishimoto's group showed that carnations can have chloroplastic carotenoids in green-colored petals and also chromoplastic carotenoids in yellow-colored petals (Chap. 7).

Most carnation varieties are diploid and their flower colors are visible and distinguishable phenotypic traits that show Mendelian inheritance patterns. The excellent and pioneering genetic studies by Mehlquist over a half of century ago (Mehlquist 1940; Mehlquist and Geissmann 1947) identified *A*, *I*, and *S* genes (loci) responsible for red and yellow phenotypes. Advances in molecular biology have enabled specification of the genes that encode enzymes, transporters, and the transcription regulatory factors involved in anthocyanin and flavonoid biosynthetic pathways in plants; this increased knowledge has led to the elucidation of the coloring mechanisms in carnation flowers and has been exploited for traditional genetic breeding.

The enzymes involved in anthocyanin and flavonoid synthesis are illustrated in Fig. 8.1. They are involved in the three distinct pathways that modify phenylalanine derived from primary metabolism: the phenylpropanoid pathway to form 4-coumaroyl-CoA starting from phenylalanine; the anthocyanin/flavonoid pathway to form aglycones as lipophilic molecules; and the modification pathway in which sugar and acyl residues are attached to aglycones as hydrophilic molecules to be solubilized, compartmentalized, and accumulated in vacuoles.

Although the carnation genome project has provided considerable information on the genes encoding enzymes involved in anthocyanin and flavonoid synthetic pathways (Yagi et al. 2014), less detail understanding of the structures of these genes is available. We present the known detailed structures, using revised exon structures, for some of the genes in Supplemental Table 8.1.

Some genes are present in two different scaffolds in the Carnation database (Supplemental Table 8.2). There are two possible explanations for this: 'Francesco' is a heterozygous cultivar, so that one allele is located on a chromosome of the heterozygote that is found in two different sequence fragments, i.e., two different scaffolds; alternatively, a gene duplication event has occurred in the carnation genome. For *chalcone synthase* (*CHS*), *chalcone isomerase* (*CHI*), *malyl-glucose-dependent acyltransferase* (*AMalT*), and *acyl-glucose-dependent anthocyanin 5*-O-*glycosyltransferase* (*AA5GT*), duplicated genes were found in identical scaffolds (Figs. 8.3 and 8.4). In the following sections, we do not consider these possibilities to simplify the discussion.

8.2 Genes Encoding Enzymes in the Phenylpropanoid Pathway

In higher plants, the phenylpropanoid pathway plays multiple important roles in response to environmental cues and during plant development (Liang et al. 1989). The phenylpropanoid pathway synthesizes defense substances against abiotic and biotic stresses such as UV-irradiation, wounding, and elicitors after microbial attack, and expression of genes for enzymes involved in

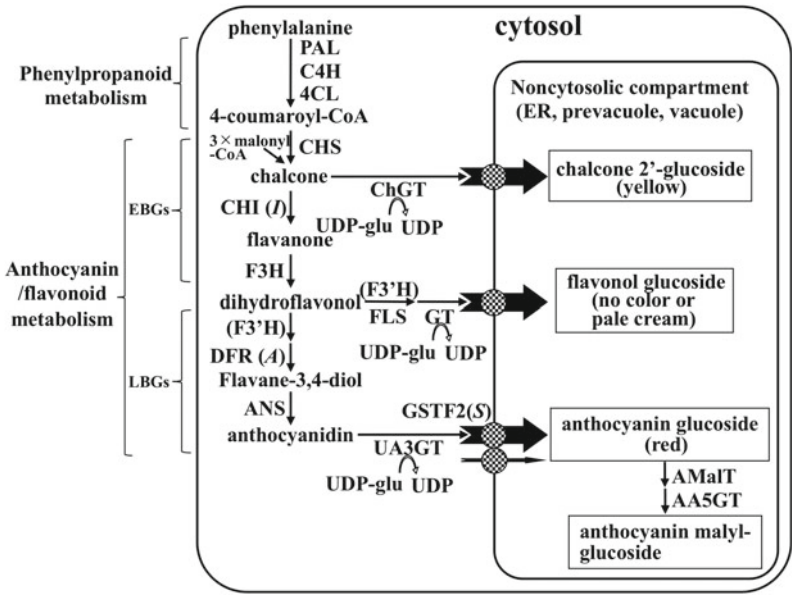

Fig. 8.1 Scheme of the anthocyanin/flavonoid biosynthetic pathway in carnations. PAL, phenylalanine ammonia-lyase; C4H, cinnamate 4-hydroxylase; 4CL, 4-coumarate:CoA ligase; CHS, chalcone synthase; CHI, chalcone isomerase; F3H, flavanone 3-hydroxylase; F3′H, flavonoid 3′-hydroxylase; DFR, dihydroflavonol 4-reductase; ANS, anthocyanidin synthase; FLS, flavonol synthase; UA3GT, UDP-glucose-dependent anthocyanin 3-*O*-glucosyltransferase; AMalT, malyl-glucose-dependent acyltransferase: AA5GT, acyl-glucose-dependent anthocyanin 5-*O*-glucosyltransferase; GT, glucosyltransferase; RT, rhamnosyltransferase

the synthesis of defense substances is induced by these cues. In addition, the spatiotemporal expression of these genes occurs in specific developmental tissues and organs during development, such as lignins, anthocyanins, and flavonoids.

In most plant species, phenylpropanoid pathway genes belong to small gene families (Fraser and Chapple 2011; Reinprecht et al. 2017); this is also the case for the carnation genome (Fig. 8.2). The carnation phenylalanine ammonia-lyase 1 gene (*DcaPAL1*) was first identified as PAL cDNA and its expression was observed to be high in petals and to increases during petal development concomitant with accumulation of anthocyanin; *DcaPAL1* expression is low in leaves, stems, and roots (Yoshimoto et al. 2000). Thus, *DcaPAL1* is expected to play an important role in anthocyanin synthesis, and may not have other functions in other tissues. It should be noted that *DcaPAL1* from scaffold7397 was highly expressed in both red and white flowers, but that *DcaPAL1* from scaffold829 was highly expressed in red petals but showed low expression in white petals (Supplemental Table 8.2). This observation suggests that scaffold829 *DcaPAL1* has a more important role in anthocyanin synthesis than that of scaffold7397; the latter might act in both anthocyanin and flavonol synthesis. Two other PAL cDNA sequences, *DcaPAL2* and *DcaPAL3*, were identified from stem tissue and deposited in the International Sequence Database Collaboration (INSDC), i.e., DDBJ/GenBank/EMBL databases. A homologous open reading frame (ORF) sequence corresponding to *DcaPAL2* (LC377189, FJ905296) was identified as *Dca13751* in scaffold829, but a stop codon was found in the second exon indicating that this gene might not encode an active enzyme protein. Another homologous nucleotide sequence for *DcPAL2* was found in scaffold10417, but sequence analysis programs using the carnation genome project database failed to identify any coding regions and did not assign a

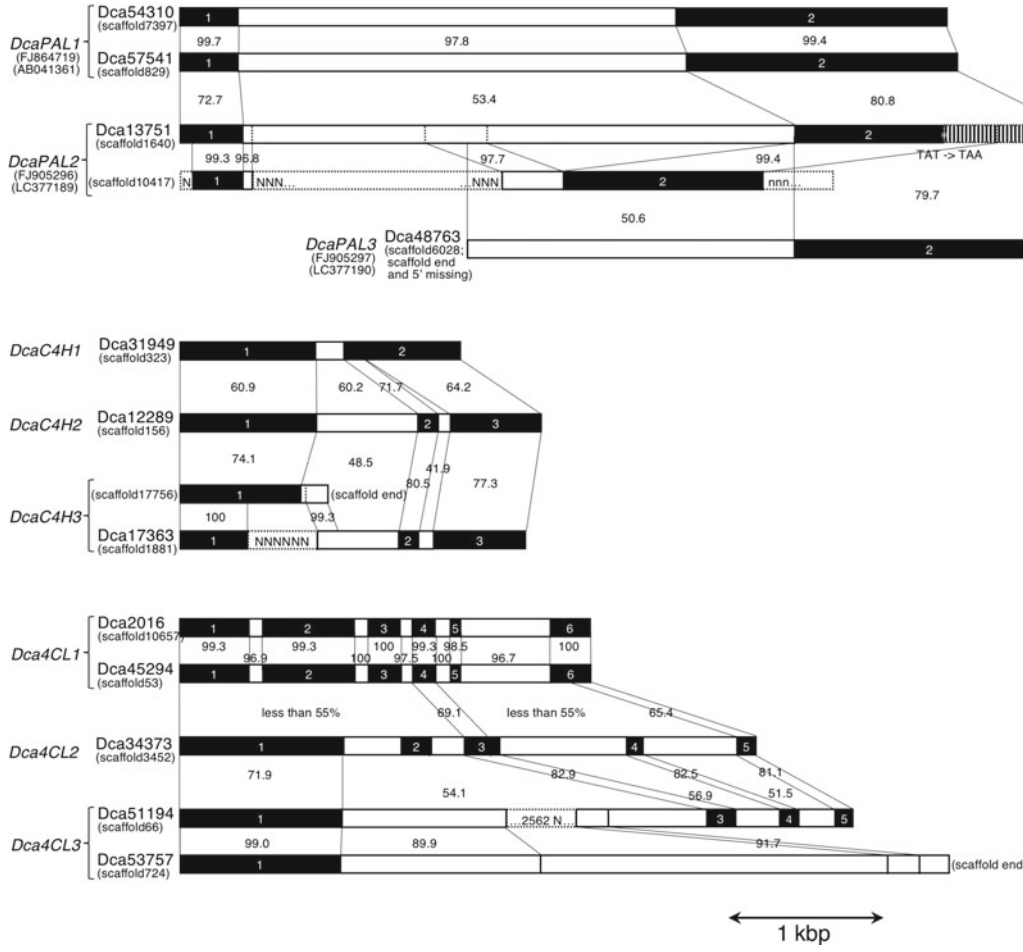

Fig. 8.2 Structures of carnation genes encoding enzymes involved in phenylpropanoid metabolism. Black and white bars indicate exon and intron regions, respectively. Numbers in black boxes show the ordinal numbers of exons. Numbers between regions of genes indicate percentage identity in nucleotide sequences in the corresponding regions of exons and introns of the genes. Dashed boxes with "N" show regions whose nucleotide sequence could not be determined by next-generation sequencing

Dca number because the partial ORF sequence of the first exon had lost the first methionine and could not be identified as a gene encoding a PAL enzyme. A partial sequence in scaffold10417 did not include a stop codon in the ORF sequence. These findings suggest that *DcPAL2* might be encoded in the gene identified in scaffold10417 of 'Francesco'. Complete sequences corresponding to *DcPAL3* cDNA (LC377190, FJ905297) could not be identified in Carnation DB. The 5′ end of scaffold6028 starts inside the first intron of *DcaPAL3* and nucleotide sequences corresponding to the upstream region of the first intron and the first exon of *DcaPAL3* have not been found in the Genome Assembly sequences of Carnation DB. Future studies to elucidate the fine detail of carnation genome nucleotide sequences will presumably identify the remaining region of *DcaPAL3*.

Three genes encoding cinnamate 4-hydroxylase (C4H) proteins were identified in Carnation DB (Fig. 8.2). *DcaC4H1* consists of two exons and one intron; *DcaC4H2* and *DcaC4H3* have three exons and two introns. Nucleotide sequence identity between these genes is less than 70%. The different exon–intron

structures and the low nucleotide sequence identity suggest that *DcaC4H1* might have arisen separately during evolution from the other two genes. Only *DcaC4H3*, from scaffold Dca17363, is expressed in petals of both red and white carnations (Supplemental Table 8.2). Although the complete nucleotide sequence of Dca17363 for *DcaC4H3* in Carnation DB has not been identified, part of *DcaC4H3* has been identified by BlastN analysis to Genome Assembly sequences in Carnation DB at the end of scaffold17756, which does not have a Dca number; this sequence was recognized as an un-transcribed sequence by Augustus and Augus-PASA. Further analyses of the fine genome sequence of carnations will no doubt determine whether *DcaC4H3* in scaffold17756 is an active or disrupted gene.

Over 40 years ago, three 4-coumarate:CoA ligase (4CL) proteins were found in cultured carrot cells; one of these was specifically expressed in carrot cells that synthesized anthocyanin (Heinzmann et al. 1977). In Arabidopsis, four 4CL isoforms have been identified, one of which, At4CL3, is involved in flavonoid synthesis (Ehlting et al. 1999; Hamberger and Hahlbrock 2004; Li et al. 2015; Leong and Last 2017). In carnation, three 4CL cDNAs have been identified and the corresponding genes located in Carnation DB (Fig. 8.2). *Dca4CL1* is composed of six exons and five introns, while *Dca4CL2* and *Dca4CL3* have five exons and four introns. The nucleotide sequences of *Dca4CL1* of Dca2016 in scaffold10657 and Dca45294 in scaffold53 showed high identity but had a low identity to *Dca4CL2* or *Dca4CL3*. These findings suggest that *Dca4CL1* and *Dca4CL2/Dca4CL3* may have arisen separately in evolution by gene duplication. The genome sequence for *Dca4CL3* is incomplete (Fig. 8.2). The nucleotide sequence in Carnation DB for the second exon of Dca51194 is unreadable and shown as N, while that of Dca53757 terminates at the end of scaffold724; the full-length cDNA has been isolated and the amino acid sequence has been confirmed (Supplemental Table 8.2). Expression of *Dca4CL3* is higher in both red and white carnations in all petal developmental stages (Supplemental Table 8.2), suggesting that *Dca4CL3* might be responsible for 4CL activity in both anthocyanin and flavonoid syntheses. Expression of *Dca4CL1* and *Dca4CL2* is low in petals, especially at later petal developmental stages; these genes may have other roles such as in lignin synthesis and defense substances against abiotic and biotic stresses.

The findings described above suggest that the *PAL*, *C4H,* and *4CL* genes involved in phenylpropanoid metabolism, namely *DcaPAL1*, *DcaC4H3*, and *Dca4CL3*, might have specifically evolved for anthocyanin synthesis and that the other members of their small gene families have gone down separate evolutionary paths to function in different spatiotemporal manners in the synthesis of other secondary metabolites for maintenance and protection of plants. It is possible that expression of *DcaPAL1*, *DcaC4H3*, and *Dca4CL3* may be regulated, in part, by the same system as the genes encoding enzymes involved in anthocyanin synthesis described in the following sections.

8.3 Genes for Enzymes Involved in Anthocyanin and Flavonoid Aglycone Synthetic Pathways

The ‘Francesco’ carnation genome harbors five genes for chalcone synthase (*CHS*) (Fig. 8.3). *DcaCHS1*, *DcaCHS2*, and *DcaCHS3* consist of two exons with a perfect ORF; however, *DcaCHS4* and *DcaCHS5* have a point mutation and an insertion sequence, respectively, that arose in a stop codon in the ORF sequence, and caused them to become pseudogenes. Scaffold1136 contains a cluster of three *CHS* genes: Dca3772 for *DcaCHS1*; Dca3769 for *DcaCHS3*; and Dca3771 for *DcaCHS4*. Dca3771 is in the opposite orientation to Dca3772 and Dca3769 (boxed panel in Fig. 8.3). This gene cluster might have been produced by a rearrangement occurring in the opposite direction during or after a duplication event rather than as simple gene duplication. The cDNA sequence of carnation *CHS* was deposited as Z67982 in INSDC and corresponds to *DcaCHS1* with a high transcripts per million (TPM) value in red and white petals

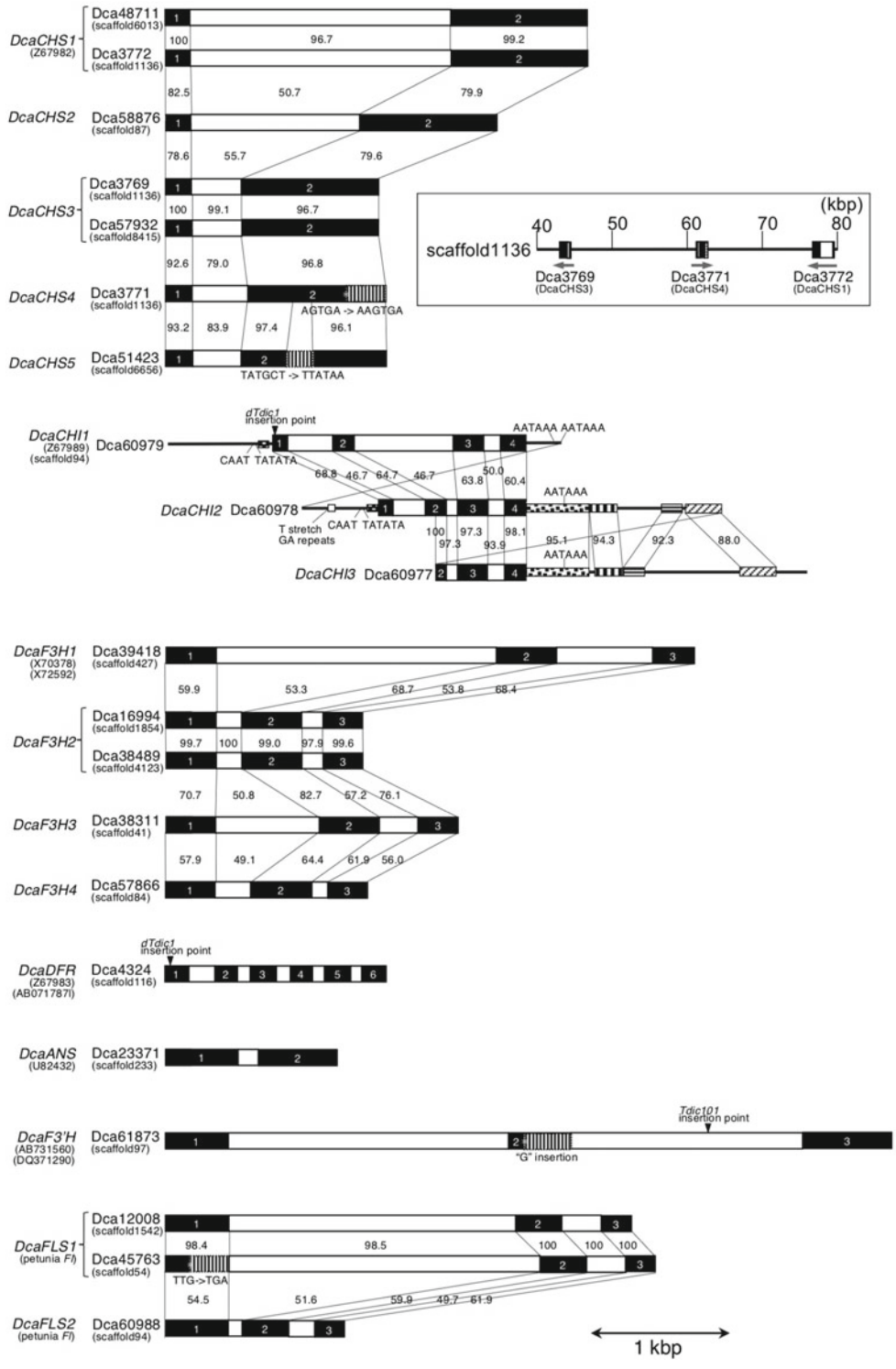

Fig. 8.3 Structures of carnation genes encoding enzymes for anthocyanidin and flavonol syntheses. The boxed figure shows the triplicated *CHS* genes found in scaffold1136, and arrows indicate the orientation of the genes

(Supplemental Table 8.2). Although the cDNA sequence corresponding to *DcaCHS2* has not been deposited in INSDC, the high expression of *DcaCHS2* in red petals at later petal developmental stages with a high level of anthocyanin synthesis, suggests that *DcaCHS2* might play an important role in anthocyanin synthesis rather than flavonol synthesis. Further details on *DcaCHI* genes are provided in Sect. 8.7.

The carnation genome harbors four *flavone 3-hydroxylase* (*F3H*) genes, namely *DcaF3H1*, *DcaF3H2*, *DcaF3H3*, and *DcaF3H4* (Fig. 8.3). Only *DcaF3H1* shows high expression in both red and white petals (Supplemental Table 8.2), suggesting that this gene may play an important role in both anthocyanin and flavonol syntheses. Repression of *DcaF3H1* activity results in the production of white or cream/pale pink flower phenotypes due to a lack of anthocyanin synthesis (Mato et al. 2000; Zuker et al. 2002; Goswami et al. 2018). Low levels of expression have been detected for *DcaF3H2*, *DcaF3H3*, and *DcaF3H4* suggesting these genes might be responsible for flavonoid synthesis in other tissues and organs.

CHS, *CHI*, and *F3H* genes are categorized as early anthocyanin biosynthetic genes (EBGs), whereas dihydroflavonol 4-reductase (*DFR*), anthocyanidin synthase (*ANS*), flavonoid 3′-hydroxylase (*F3′H*), and cytosolic UDP-sugar-dependent glycosyltransferase (UGTs) are grouped as late biosynthetic genes (LBGs) in dicot plants. The regulatory mechanisms of gene expression of EBGs differ from those of LBGs (Dubos et al. 2010; Petroni and Tonelli 2011; Goswami et al. 2018).

The LBGs *DFR*, *ANS*, and *F3′H* encode enzymes involved in later metabolic processes of anthocyanidin synthesis. These three LBG each have a single identified gene in the carnation genome (Fig. 8.3). A gene corresponding to *DFR* was identified by Mehlquist over 70 years ago as the *A* gene (Mehlquist 1940; Mehlquist and Geissman 1947); the activity of this enzyme is necessary to synthesize anthocyanin in red petals (Stich et al. 1992). Insertion of the DNA-type non-autonomous transposable element *dTdic1* into *DcaDFR* was found to disrupt its expression (Itoh et al. 2002). Movement of the insertion out of *DcaDFR* produced a variegated flower phenotype with red spots, flecks, and sectors on white petals (Supplemental Fig. 8.1O). Another DNA-type autonomous transposable element, *Tdic101*, is inserted into *DcaF3′H* in some carnation cultivars. Movement of *Tdic101* from *DcaF3′H* resulted in a variety of phenotypes with deep-red spots, flecks, and sectors on pale pink petals (Momose et al. 2013b).

Flavonol synthesis is mediated by enzymes encoded by two flavonol synthase (*FLS*) genes, *DcaFLS1* and *DcaFLS2*, in the carnation genome (Fig. 8.3). Many carnation cultivars have flavonols in both red and white petals (see Chap. 6), in which *DcaFLS1* for Dca12008, but not for Dca45763 having a point mutation to generate a stop codon in the first exon, might give FLS enzyme (Supplemental Table 8.2).

8.4 Genes Encoding Cytosolic Enzymes for UDP-Glucose-Dependent Glycosylation of Anthocyanins and Flavonols and for Transportation into Vacuoles

Anthocyanin and flavonol aglycones are lipophilic; if they were released into the cytosol without modification they would permeate plasma, endoplasmic, and tonoplast membranes and be disrupted. To prevent this, immediately after synthesis, anthocyanin and flavonol aglycones are modified to be hydrophilic by UDP-glucose-dependent glycosyltransferases (UGTs). Plants have many glycosyltransferases that can transfer sugar moieties to small molecules as acceptors; a wide range of endogenously synthesized small molecules can be modified, for example, secondary metabolites such as phenylpropanoids and flavonoids/anthocyanins; exogenous molecules can also be modified, for example, herbicides in the cytoplasm that may be detoxified or enclosed in a cellular compartment such as a vacuole. Glycosyltransferases are currently classified into 92 families, and family 1 glycosyltransferases (GT1) are characterized as

UGTs. Molecular biological analyses have shown that many plant species have more than 100 *UGT* genes; our current understanding of the genetics and biochemistry of plant UGTs can be found in a number of excellent reviews (Vogt and Jones 2000; Li et al. 2001; Bowles et al. 2006; Paquette et al. 2009; Yonekura-Sakakibara 2009; Yonekura-Sakakibara and Hanada 2011).

The Carnation DB contains 120 identified *GT1* genes (Yagi et al. 2014). Full-length cDNAs for UGTs have been isolated by degenerate PCR and recombinant proteins expressed in *Escherichia coli*; these proteins display flavonoid glucosyltransferase activity, and the cDNAs have been named *DicGT1* to *DicGT5* (Ogata et al. 2004). *DicGT1* is UDP-glucose-dependent *anthocyanin 3-O-glucosyltransgerase* (*UA3GT*) and forms anthocyanin 3-*O*-glucoside. Two corresponding genomic sequences, Dca47835 and Dca17573, have been identified in Carnation DB (Fig. 8.4). The recombinant protein translated from *DicGT4* shows high chalcone 2′-*O*-glucosyltransferase activity in vitro, whereas *DicGT5* has low activity; nevertheless, both can transfer a glucose molecule to kaempferol and quercetin at both the 3 and 7 positions and to apigenin and naringenin at the 7 position (Ogata et al. 2004). The recombinant proteins from *DicGT4* and *DicGT5* show similar catalytic activities to flavonoids, although they show only 30% similarities for their amino acid sequences. The genomic structures of these genes differ: *DicGT4* (Dca41029) is an intronless gene; *DicGT5* is composed of two exons in both Dca11979 and Dca46947 (Fig. 8.4). *DicGT2* and *DicGT3* do not show glucosyltransferase activity to anthocyanidins or to flavonoids (Ogata et al. 2004), suggesting that they do not act in the petals for flavonoid glucosylation but rather for glucosyl transfer to other substances. *DicGT2* does not have a Dca number as neither Augustus nor Augus-PASA recognized it as an intron-less transcribed gene, although the corresponding cDNA has been isolated (Ogata et al. 2004). Divergence in exon–intron organization has been reported for Arabidopsis UGTs. Almost half of the UGT genes have a single or few introns, similarly to *DicGT1*, *DicGT3*, and *DicGT5*, but intron-less UGT genes similar to *DicGT2* and *DicGT4* have also been identified in the Arabidopsis genome (Li et al. 2001; Paquette et al. 2009).

8.5 Transportation of Anthocyanin into Vacuoles as a Final Destination

Most secondary metabolites accumulate in vacuoles as a final destination, others in apoplasts; both vacuoles and apoplasts are inactive sites separated from cytosols. It is important that secondary metabolites are isolated from active proteins in the cytosol as some may be toxic for cytosolic activity. The transportation mechanism of anthocyanins is uncertain, as it is difficult to demonstrate biochemical evidence of transport activity. Glutathione *S*-transferases (GST) and multidrug and toxic compound extrusion (MATE)-type transporters are believed to play important roles in the transportation of anthocyanins into vacuoles (Marrs et al. 1995; Mueller et al. 2000; Zhao et al. 2009; Gomez et al. 2011; Sun et al. 2012; Pérez-Díaz et al. 2016; Luo et al. 2018; Jiang et al. 2019). The genome projects for many plant species have identified putative transporters. In Carnation DB, 84 and 25 homologues of GST and MATE, respectively, are present (Yagi et al. 2014). In carnations, the *S* gene was first identified by Mehlquist who reported that it regulated pale and dark red colors in petals (Mehlquist 1940; Mehlquist and Geissman 1947). The *ss* genotype was associated with lower anthocyanin accumulation producing pale pink colors compared to the *SS* or *S*- genotypes that showed dark red petal colors. A mutant of the *S* gene that showed variegation, s^{var}, had dark red spots, flecks, and sectors on pale pink petals (Supplemental Fig. 8.1P). In variegated colored mutants, one *GST* gene, *GSTF2* from Dca57804, is disrupted by the insertion of the DNA-type non-autonomous transposable element, *dTac1*, at the first intron (Fig. 8.4) (Sasaki et al. 2012; Momose et al. 2013a, b). When *dTac1* moves from *GSTF2*, the pale pink petal color reverts to dark red. Plants

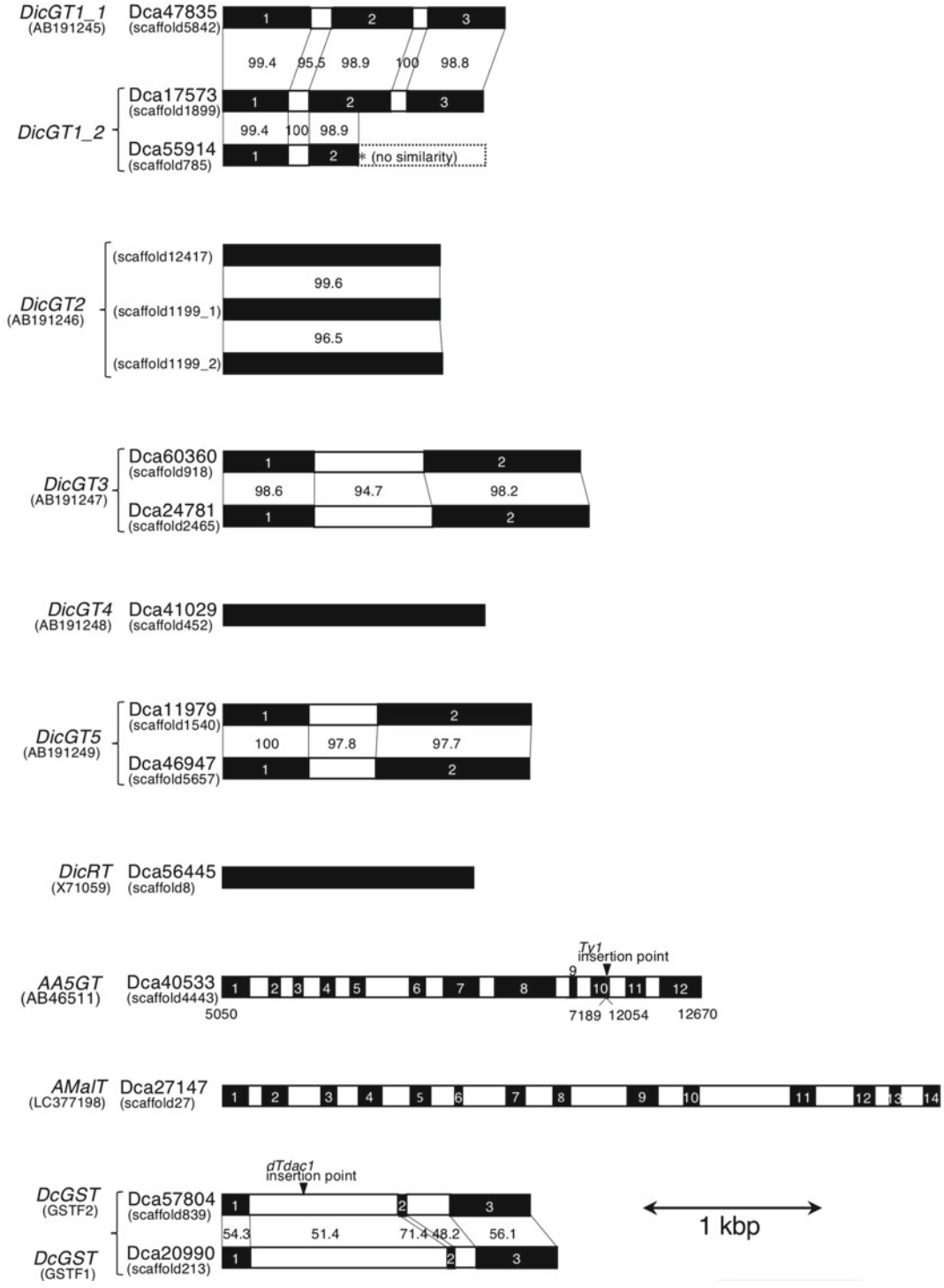

Fig. 8.4 Structures of carnation genes for glucosylation and malylation enzymes and glutathione *S*-transferases active in anthocyanin and flavonol syntheses

with the stable *ss* genotype have a two-nucleotide deletion in the ORF of *GSTF2* causing a frameshift mutation that blocks the synthesis of the active enzyme (Sasaki et al. 2012). The question arises of why pale-colored petals emerge since anthocyanin transportation and accumulation to the vacuoles should be depressed by disruption of *GSTF2*. One possibility is leaky transportation by other GST(s); although other GST(s) might be supposed to transport other low molecular weight substances with higher efficiency than anthocyanins to the vacuoles, they could transport anthocyanin with low efficiency, so that a limited amount of anthocyanin could be transported to and accumulate in vacuoles thereby producing pale pink petals.

8.6 Acylation and Glucosylation in Vacuoles Using Acyl-Glucose as Donors in Carnation Petals

Anthocyanidin aglycones are first modified by anthocyanin 3-*O*-glucosyltransferase and altered from lipophilic to hydrophilic molecules that can be transported into vacuoles. Carnation anthocyanins are characteristically further modified with a malyl residue onto the glucose at the 3 position, to form anthocyanin 3-*O*-malylglucoside (see Chap. 6). Two mechanisms for acyl-transfer to secondary metabolites have been identified: one is catalyzed by cytosolic enzymes belonging to the BAHD family [benzylalcohol *O*-acetyltransferase (BEAT), anthocyanin *O*-hydroxycinnamoyltransferase (AHCT), anthranilate *N*-hydroxycinnamoyl/benzoyltransferase (HCBT), and deacetylvindoline 4-*O*-acetyltransferase (DAT)] that use acyl-CoA as a donor molecule (St Pierre and De Luca 2000; D'Auria 2006; Luo et al. 2007); the other is by vacuolar enzymes belonging to the serine carboxypeptidase like (SCPL) family using acyl-glucose as a donor molecule (Mock and Strack 1993; Li and Steffens 2000; St Pierre and De Luca 2000; Steffens 2000; Milkowski and Strack 2004; Fraser et al. 2005; Stehle et al. 2009; Mugford and Milkowski 2012; Morghe and Last 2015). We showed that, in malyl acylation to anthocyanin 3-*O*-glucoside in carnations, malyl-glucose-dependent anthocyanin acyltransferase (AMalT) did not use malyl-CoA but malyl-glucose as a donor; this was the first report of aliphatic acyl-glucose-dependent acyltransferase activity on anthocyanin (Abe et al. 2008; Sasaki et al. 2013, 2014). *AMalT* cDNA was reported as LC377198 (Morimoto et al. 2019a) and corresponds to Dca27147 (Supplemental Table 8.3). A BlastP survey of Carnation DB using LC377198 ORF amino acid sequences identified several homologous sequences (Supplemental Table 8.3).

In Arabidopsis, the genes for several SCPL enzymes form a gene cluster generated by local gene duplication. On chromosome 2, 1-*O*-sinapoyl-β-glucose:L-malate sinapoyltransferase (SMT), 1-*O*-sinapoyl-β-glucose:anthocyanin sinapoyltransferase (SAT), 1-*O*-sinapoyl-β-glucose:1-*O*-sinapoyl-β-glucose sinapoyltransferase (SST), and two other SCPLs are tandemly located within a 30-kbp region, suggesting that, initially, *SCPL* genes might have arisen during evolution by gene duplication followed by neofunctionalization to gain acyltransferase activity and subfunctionalization to acquire different acyl acceptor preferences (Stehle et al. 2009). The carnation genome has not been evaluated to as fine a resolution as Arabidopsis and rice, nevertheless, pairs of tandemly duplicated SCPL genes within 20-kbp segments have been found (Supplemental Fig. 8.2). *AMalT* from Dca27147 is close to Dca27146 in scaffold27. Although the enzyme activity of Dca27146 is still unknown, the first gene duplication event involving *SCPL* genes might be followed by more duplications involving the gene pairs.

There has been considerable debate on the development of gene function from global gene duplication events such as chromosome or whole-genome duplication during evolution (Ohno 1970; Force et al. 1999; Sandve et al. 2018). Force et al. (1999) proposed that, in a global gene duplication event caused by chromosome or whole-genome duplication, neofunctionalization would produce new gene function in the duplicated genes, i.e., they would have different functions compared to the ancestral genes due to

alteration of gene architecture in their coding regions. By contrast, subfunctionalization would conserve gene function, i.e., the catalytic properties of an enzyme, but would alter gene expression properties by changes to their promoter and regulatory regions (Force et al. 1999). If these considerations on gene function changes after global gene duplication also apply to local tandem gene duplications in small regions of one chromosome, then the Dca27147 gene might have AMalT activity due to neofunctionalization. Further analyses of SCPL enzyme activities including that of Dca27146, and improving the resolution of the fine genomic sequence of carnations will provide fresh insights into the evolution of carnation SCPL enzymes by neofunctionalization and subfunctionalization. The evolution of *SCPL* genes was not only important for their roles in plant development but also for their activities against environmental stresses. Recent studies of Brassicaceae *SCPL* genes have shown that a duplication event of *SCPL* genes followed by neofunctionalization and subfunctionalization gave rise to the genes for flavonol-phenylacyltransferase which plays important roles in tolerance against UV irradiation (Tohge et al. 2016).

Mutant cultivars that synthesize and accumulate anthocyanin 3,5-*O*-diglucoside without malyl residues have been isolated after heavy ion irradiation (Chap. 9; Okamura et al. 2013). These cultivars accumulate anthocyanin 3,5-*O*-diglucoside in their vacuoles as anthocyanic vacuolar inclusions (AVIs). Heavy-ion beam irradiation does not induce point mutations in genes but causes deletions that remove significant genomic regions. This suggests that, in some AVI-forming mutants, the region including both Dca27147 and Dca27146 might be deleted. The function of Dca27146 is unknown but it does show high levels of expression in petals (Supplemental Table 8.2). Further analyses of these mutants will provide important information on the function of these genes.

Glucosylation at the 5 position of anthocyanin 3-*O*-glucoside has been reported to be mediated by UDP-glucose-dependent anthocyanin 5-glucosyltrasferase; in the rose, one UDP-glucose-dependent anthocyanin glucosyltransferase can mediate modification at the 5 position followed by 3 position glucosylation (Ogata et al. 2005). In carnations, cytosolic UDP-glucose-dependent anthocyanin 3-*O*-glucoside 5-glucosyltransferase does not catalyze this reaction; rather this is carried out by vacuolar acyl-glucose dependent anthocyanin 3-*O*-glucoside 5-glucosyltransferase (AA5GT) that belongs to the glycoside hydrolase family 1 (GH1) (Matsuba et al. 2010). This finding elucidated the mechanism of the glucosylation reaction at the 7 position of anthocyanins in blue flowers (Yoshida et al. 2009; Matsuba et al. 2010; Miyahara et al. 2012, 2014).

In Arabidopsis, AtBGLU10 is responsible for glucosylation of the final modification step of anthocyanin (Miyahara et al. 2013) and AtBGLU6 is responsible for glucosylation of flavonol; both enzymes belong to the GH1 family (Ishihara et al. 2016). The neofunctionalization and subfunctionalization processes after local gene duplication that gave rise to AA5GT activity in the GH1 family in the carnation genome are of interest; homologous sequences with more than 90% identity in ORF sequences have been found in the carnation genome (Supplemental Table 8.4). *AA5GT* was identified as AB507446 and AB646510 (Matsuba et al. 2010; Nishizaki et al. 2011), which correspond to Dca40534 in the 'Francesco' genome in which *Ty1dic1* is inserted (Nishizaki et al. 2011; Supplemental Fig. 8.3). Other pairs with similar sequences have been identified (Supplemental Fig. 8.3), and they are organized as dense gene clusters in small regions compared to *SCPL* genes (Supplemental Fig. 8.4). In scaffold4443, five *AA5GT* homologous sequences are located in a ca. 25-kbp region. Four of these sequences are in the same orientation, the other shows the opposite orientation. Local gene duplication events might have occurred in this region, to retain high nucleotide sequence similarity among the copies. However, Dca40534 is responsible for AA5GT activity because disruption by *Ty1dic1* prevents glucosylation of anthocyanin at the 5 position (Nishizaki et al. 2011). Other related sequences, e.g., Dca40533, Dca40535,

Dca11039, and Dca11040, are expressed in petals (Supplemental Table 8.2). Although Dca40533 was predicted to have 11 exons, the other sequences had 13 exons; Dca40533 is located at the end of scaffold4443, which could not yet be demonstrated as 13 exons in the front of scaffold4443. Genetic evidence indicates that *AA5GT* is a single gene in the carnation genome, suggesting that Dca40533 might not have AA5GT activity even if it does have two more exons. Homologous sequences to those in scaffold4443 are present in scaffold149 (Supplemental Fig. 8.4). These two scaffolds have almost the same gene architecture although scaffold149 contains one imperfectly duplicated gene fragment, Dca110XX (Supplemental Fig. 8.4), suggesting that the duplication event(s) producing the genes in scaffold4443 and scaffold149 might have been slightly different.

8.7 Acyanic Colors of Carnation—Yellow and Orange

Mehlquist demonstrated that yellow flower colors in carnation are regulated by a single gene locus that was named the *I* gene (Mehlquist 1940; Mehlquist and Geissman 1947). As described above, CHS first synthesizes chalcone as the C6–C3–C6 product; this synthesis is followed by isomerization by CHI to produce (2*S*)-naringenin. The yellow petal phenotype in *ii* genotype carnations indicates that these flowers accumulate chalcone 2′-*O*-glucoside (Harborne 1966; Forkmann and Dangelmayr 1980; Yoshida et al. 2004b). Thus, in the *ii* genotype, the anthocyanin synthesis pathway ceases at the CHI step, leading to the accumulation of chalcone 2′-*O*-glucoside. This blocking mechanism at the CHI step was confirmed by disruption of the *CHI* gene by the transposable element *dTdic1* (Larsen 1996; Itoh et al. 2002). Removal of *dTdic1* restores the ORF and activity of the enzyme. When the *DFR* gene is disrupted by the same *dTdic1* element as the *CHI* gene in yellow flower carnations, anthocyanin synthesis is repressed and white or cream colors due to flavonols are observed (Itoh et al. 2002).

Chalcone can form naringenin at a neutral pH in the cytosol. The chemical reaction forms (2*S*)- and (2*R*)-naringenin equally, while the CHI-mediated reaction forms only (2*S*)-naringenin. Other enzymes can utilize (2*S*)-naringenin, but (2*R*)-naringenin cannot be catalyzed by enzymes in the following steps of anthocyanin/flavonoid syntheses. Both (2*R*)-naringenin and (2*S*)-naringenin are lipophilic and can pass through tonoplast, endoplasmic, and plasma membranes to disrupt membrane structure and induce cell death. Therefore, prevention of (2*R*)-naringenin formation from chalcone is vital in vivo. To prevent this reaction, the 2′OH of chalcone is glucosylated by UDP-glucose-dependent glucosyltransferase (CHGT) that blocks the chemical circularizing reaction and forms a water-soluble and stable chalcone 2′-*O*-glucoside that produces yellow flower carnations (Ogata et al. 2004).

Although the above mechanism describes the generation of yellow flowers, it does not explain how orange flowers are produced. In orange-colored carnations, both red anthocyanin glucoside and yellow chalcone 2′-*O*-glucoside are accumulated in vacuoles of each cell, giving rise to an orange color (Fig. 8.5). This indicates that the metabolic pathways to anthocyanin glucoside and chalcone 2′-*O*-glucoside are not switched but that the pathway branches to produce both compounds. Data from the carnation genome project (Yagi et al. 2014) provide a clear idea of how to resolve this paradox; *CHI* genes designated as Dca60979, Dca60978, and Dca60977 were found in scaffold94 (Fig. 8.3). Both Dca60979 and Dca60978 encode a complete CHI ORF, whereas Dca60977 is disrupted because of loss of the first exon of the Dca60978 ORF. As described above, the *CHI* gene responsible for the *I* locus corresponds to Dca60979 and is disrupted by *dTdic1*, resulting in the generation of yellow flowers. In yellow carnations, a frameshift mutation in Dca60978 has occurred to give a stop codon in the ORF; by contrast, in orange carnations, at least one Dca60978 gene does not have the frameshift mutation but can be translated to give a CHI protein with enzyme activity (Miyahara et al. 2018). The estimated expression level of

Dca60978 is about 1/300th of that of Dca60979; the in vitro CHI enzyme activity encoded in the Dca60978 ORF is 1/10th that of Dca60979 (Miyahara et al. 2018). The small amounts of transcript and low catalytic activity for CHI derived from Dca60978 might result in incomplete catalysis from chalcone to (2*S*)-naringenin enabling other enzymes and transporters involved in anthocyanin synthesis to accumulate anthocyanins. The residual and excess chalcone molecules might be catalyzed by CHGT to chalcone 2′-*O*-glucoside followed by transportation into vacuoles. Some chalcone synthesized by CHS might be catalyzed to anthocyanin and the rest to chalcone 2′-*O*-glucoside both of which accumulate in vacuoles, resulting in the simultaneous presence and accumulation of both anthocyanin and chalcone 2′-*O*-glucoside, that is, red plus yellow color molecules to produce orange.

Our analyses indicated that local gene duplication of the *CHI* genes Dca60979 and Dca60978 gave high and low transcription activities but both translated proteins had an identical catalytic activity from chalcone to (2*S*)-naringenin (Miyahara et al. 2018). If the gene duplication concept of Force et al. (1999) is extended from the global genome level to the local level, local gene duplication events might have produced subfunctionalization in *CHI* genes causing an orange-colored phenotype in carnations. In the legume genome, neofunctionalization of a local tandem duplication of *CHI* genes was involved in the evolution of isoflavonoid synthesis. Four *CHI* genes were identified within a 15-kbp region of the *Lotus japonicus* genome; one *CHI* gene encoded an enzyme that catalyzed the step from chalcone to (2*S*)-naringenin, similarly to Dca60979 and Dca60978 of carnations, but two other *CHI* genes catalyzed the 6′-deoxychalcone to 5-deoxyflavanone and the 6′-hydroxychalcone to 5-hydroxyflavanone steps, which have essential roles in legume–microbe interactions (Shimada et al. 2003). Leguminous plants evolved sister CHI-like enzymes with different substrate preferences by local gene duplication and neofunctionalization.

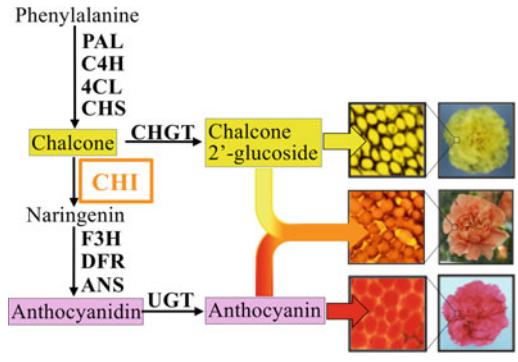

Fig. 8.5 Branching at CHI toward yellow-colored chalcone 2′-glucoside and red-colored anthocyanin to form a mixture of yellow and red pigments giving an orange color in carnation petals. The images on the left of the two panels of photographs show magnified observations of epidermal cells of yellow, orange, and red petals

8.8 Acyanic Flower Color—Pure and Paper White Color in Carnation

White carnations are important not only as ornamental flowers but also as ceremonial flowers. Although creamy white carnation flowers fulfil the former purpose, the later purpose requires pure or paper white-colored (completely colorless) carnation flowers. Many of the "white carnations" cultivars appear to have a pale cream color because they accumulate flavonols (see Chap. 7).

One problem that faces horticulturists cultivating white carnations is that some plants unexpectedly show either whole red or pink flowers or have red spots, flecks, and sectors on white petals (Totsuka et al. 2018). The presence of red spots, flecks, and sectors on a white background give severe problems for funerary events in Japan: white and red curtains are used in celebratory ceremonies, whereas white and black curtains are used for funerary ceremonies. White carnations with red spots and sectors are therefore inappropriate for the latter.

Several possible mechanisms may be responsible for the development of red spots, flecks, and sectors on white petals of carnations. The first is the movement of the transposable element

dTdic1 from *DFR* (Supplemental Fig. S1O) (Itoh et al. 2002). The second is a reduction in the transcription regulatory mechanisms controlling the expression of genes for enzymes involved in anthocyanin synthesis. LBGs are regulated by a triple complex of R2R3myb, basic helix-loop-helix (bHLH), and WD-40 (Dubos et al. 2010; Petroni and Tonelli 2011; Goswami et al. 2018). Our analyses have shown that a reduction in bHLH plays an important role in the repression of LBGs, resulting in reduced anthocyanin synthesis to generate white petals (Totsuka et al. 2018). If the reduction in bHLH is switched off by an as yet unknown mechanism, then red colors on white petals can emerge.

Red coloring on white petals is present in some vegetatively propagated carnation lines. Several flower color bud mutants have been isolated and some have been established as new horticultural cultivars (Mato et al. 2000, 2001; Morimoto et al. 2018, 2019a; Sugihara et al. 2019). The visible flower color phenotype in carnations is caused by the expression of genes involved in anthocyanin synthesis in petal epidermal cells, which are derived from the L1 layer cell lineage. Bud mutants bearing white flowers derived from cyanic flowered branches should contain epidermal cells in the L1 layer in which the gene(s) for enzymes involved in anthocyanin or chalcone syntheses are suppressed. Such mutations occur irrespective and independent of the cells in the L2 and/or 3 layers. In some white-colored carnations, mutation of genes related to anthocyanin synthesis occurs in L1 layer cells to produce a white petal phenotype; although L2 and/or 3 cell layers have the ability to express gene activity for anthocyanin synthesis this activity is suppressed by their developmental status. Such petals, therefore, consist of chimeric cell layers (Mehlquist et al. 1954; Farestveit 1969; Pereau-Leroy 1974). When such chimeric carnation petals are wounded, such as being bitten by thrips or by irradiation, L1 layer cells are damaged and die and the L2/3 cell layers inside the petals become the new petal surface and are used for renewal of the epidermis. The renewed epidermis consists of L2/3 cell layers in which the hidden potential of these cells can now be expressed and synthesis and accumulation of anthocyanin at the wound site is enabled (Sagawa and Mehlquist 1957; Samata et al. 1979; Johnson 1980; Yamaguchi 1989). This red coloring on white petals is an unavoidable aspect of vegetative asexual propagation of white-colored carnations derived from bud mutants (Yoshida et al. 2004a).

In order to avoid this pitfall and to obtain a purer white rather than creamy white, many white-flowered carnation cultivars have been established over a long period. Breeders have hybridized white carnation cultivars in which the genetic background is indistinguishable because the white phenotype is recessive and it is difficult to identify the responsible gene(s). A comprehensive analysis of the expression of genes involved in anthocyanin biosynthesis in 19 white cultivars revealed complex patterns of repression of these genes (Fig. 8.6). In some white flowers, expression of *DFR*, i.e., the *A* gene, is repressed (Mato et al. 2001), while in others it was expressed but produced white coloration. Many white cultivars showed loss of *ANS* and *GST* expression; however, these genes were expressed in other white cultivars (Fig. 8.6). These results show that the mechanisms for generating white carnations are complex. White carnations may have been generated by mutation of different genes in individual cultivars and were then selected and hybridized to other cultivars with a colorless phenotype without the use of any selectable color markers. Such blind hybridization may cause complexity and diversity for genotypic characterization of gene expression. Breeders may have expected to get a more stable colorless phenotype, and therefore hybridized several white cultivars with the view of stacking different genes for repression to obtain superior pure white offspring.

8.9 The Remaining Questions and Future Perspectives

The enzymes involved in anthocyanidin aglycone synthesis in carnation have been comprehensively identified and, in our recent studies, we

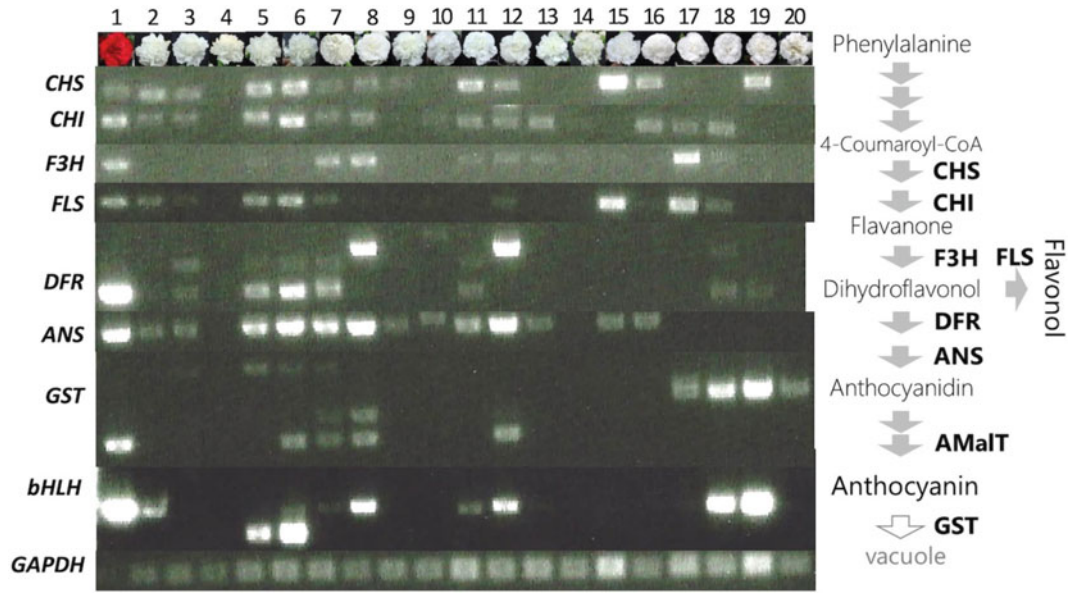

Fig. 8.6 Expression profiles of genes encoding enzymes and GST involved in anthocyanin and flavonol syntheses and for transportation into vacuoles in petals of white carnation cultivars. RNAs were prepared from petals of individual flowers followed by first-strand cDNA synthesis, and RT-PCR was performed with gene-specific primer sets using the cDNAs as templates. 1, Red Diamonds (red control); 2, Delphi; 3, Sorubik White Sca; 4, California White; 5, White Calypso; 6, Alaska; 7, 15F06; 8, 945-15; 9, White Sim; 10, Albivette; 11, Tobia; 12, Galaxy; 13, Linda S64; 14, U Conn White; 15, Kaly; 16, Shirayuki; 17, Tsubasa; 18, Mantova; 19, 15,036-080; 20, 15,010-059

have elucidated the modification steps with glucose and malate to anthocyanin 3-*O*-malylglucoside-5-*O*-glucoside. In vivo, red carnation petals accumulate anthocyanin 3-*O*, 5-*O*-cyclic malyl diglucoside (Chap. 6). The mechanism of this last reaction step, the ligation of a malyl residue onto the glucose at the 5 position to make a circularized molecule, remains unknown.

Mechanisms for the production of monochromatic color on petals have almost all been elucidated; however, those for the generation of bicolors have yet to be elucidated. Some spots, flecks, and sectors are the result of movement of DNA transposable elements (Itoh et al. 2002; Sasaki et al. 2012; Momose et al. 2013a, b). However, the mechanism producing picotee, bottom spots and stars (Fig. 6.7 in Chap. 6 and Supplemental Fig. 8.1I–N) remains unknown. It is possible this phenotype arises due to alteration of spatiotemporal regulation of gene expression for enzymes involved in anthocyanin synthesis. Gene silencing was suggested as a possible mechanism for petunia marginal white picotee flowers (Morita et al. 2012). A similar mechanism may occur in the marginal patterns of carnation petals. A recent study of the spatiotemporal expression of anthocyanin accumulation in *Dianthus* described anthesis in blooming flowers (Morimoto et al. 2019b). The spatiotemporal expression of genes for enzymes involved in anthocyanin synthesis will be studied to increase the diversity of flower coloring varieties.

The data collected in the genome projects of many plant species have revealed the importance of neofunctionalization and subfunctionalization after gene duplication in evolution to increase the diversity of plant secondary metabolites (Chae et al. 2014; Moghe and Last 2015; Tohge et al. 2016, 2018; Leong et al. 2019). These reports focused on divergent and novel secondary metabolites synthesized to play roles in the defense against abiotic stresses, such as UV

irradiation, and to drive off insects and animals. Only six major anthocyanidin molecules are synthesized, but more than 700 molecular species with different modifications have been reported. The diversity of anthocyanin molecules may have been generated, in part, by neofunctionalization and subfunctionalization after gene duplication; in addition to roles in plant defense, this large range of molecules may play important roles in the attraction of insects and birds as pollinators. They certainly attract human interest because of their contribution to the beauty of colorful horticultural flowers.

References

Abe Y, Tera M, Sasaki N, Okamura M, Umemoto N, Momose M, Kawahara N, Kamakura H, Goda Y, Nagasawa K, Ozeki Y (2008) Detection of 1-*O*-malylglucose: pelargonidin 3-*O*-glucose-6″-*O*-malyltransferase activity in carnation (*Dianthus caryophyllus*). Biochem Biophys Res Comm 373:473–477

Bowles D, Lim EK, Poppenberger B, Vaistij FE (2006) Glycosyltransferases of lipophilic small molecules. Annu Rev Plant Biol 57:567–597

Brockington SF, Walker RH, Glover BJ, Soltis PS, Soltis DE (2011) Complex pigment evolution in the Caryophyllales. New Phytol 190:854–864

Chae L, Kim T, Nilo-Poyanco R, Rhee SY (2014) Genomic signatures of specialized metabolism in plants. Science 344:510–513

D'Auria JC (2006) Acyltransferases in plants: a good time to be BAHD. Curr Opin Plant Biol 9:331–340

Dubos C, Stracke R, Grotewold E, Weisshaar B, Martin C, Lepiniec L (2010) MYB transcription factors in Arabidopsis. Trends Plant Sci 15:573–581

Ehlting J, Büttner D, Wang Q, Douglas CJ, Somssich IE, Kombrink E (1999) Three 4-coumarate:coenzyme A ligases in *Arabidopsis thaliana* represent two evolutionarily divergent classes in angiosperms. Plant J 19:9–20

Farestveit B (1969) Flower color chimeras in glasshouse carnations, *Dianthus caryophyllus* L. Yearb Roy Vet Agr Univ Copenhagen 19–33

Force A, Lynch M, Pickett FB, Amores A, Yan YL, Postlethwait J (1999) Preservation of duplicate genes by complementary, degenerative mutations. Genetics 151:1531–1545

Forkmann G, Dangelmayr B (1980) Genetic control of chalcone isomerase activity in flowers of *Dianthus caryophyllus*. Biochem Genet 18:519–527

Fraser CM, Chapple C (2011) The phenylpropanoid pathway in Arabidopsis. Arabidopsis Book 9:e0152

Fraser CM, Rider LW, Chapple C (2005) An expression and bioinformatics analysis of the Arabidopsis serine carboxypeptidase-like gene family. Plant Physiol 138:1136–1148

Gomez C, Conejero G, Torregrosa L, Cheynier V, Terrier N, Ageorges A (2011) *In vivo* grapevine anthocyanin transport involves vesicle-mediated trafficking and the contribution of anthoMATE transporters and GST. Plant J 67:960–970

Goswami G, Nath UK, Park JI, Hossain MR, Biswas MK, Kim HT, Kim HR, Nou IS (2018) Transcriptional regulation of anthocyanin biosynthesis in a high-anthocyanin resynthesized *Brassica napus* cultivar. J Biol Res (Thessalon) 26:19

Harborne JB (1966) Comparative biochemistry of flavonoids—I: Distribution of chalcone and aurone pigments in plants. Phytochemistry 5:111–115

Hamberger B, Hahlbrock K (2004) The 4-coumarate: CoA ligase gene family in *Arabidopsis thaliana* comprises one rare, sinapate-activating and three commonly occurring isoenzymes. Proc Natl Acad Sci USA 101:2209–2214

Heinzmann U, Seitz U, Seitz U (1977) Purification and substrate specificities of hydroxycinnamate: CoA ligase from anthocyanin-containing and anthocyanin-free carrot cells. Planta 135:313–318

Ishihara H, Tohge T, Viehöver P, Fernie AR, Weisshaar B, Stracke R (2016) Natural variation in flavonol accumulation in Arabidopsis is determined by the flavonol glucosyltransferase BGLU6. J Exp Bot 67:1505–1517

Itoh Y, Higeta D, Suzuki A, Yoshida H, Ozeki Y (2002) Excision of transposable elements from the chalcone isomerase and dihydroflavonol 4-reductase genes may contribute to the variegation of the yellow-flowered carnation (*Dianthus caryophyllus*). Plant Cell Physiol 43:578–585

Jiang S, Chen M, He N, Chen X, Wang N, Sun Q, Zhang T, Xu H, Fang H, Wang Y, Zhang Z, Wu S, Chen X (2019) MdGSTF6, activated by MdMYB1, plays an essential role in anthocyanin accumulation in apple. Hortic Res 6:40

Johnson RT (1980) Gamma irradiation and *in vitro* induced separation of chimeral genotypes in carnation. HortScience 15:605–606

Kay QON, Daoud HS, Striton CH (1981) Pigment distribution, light reflection and cell structure in petals. Bot J Linn Soc 83:57–83

Larsen ES (1996) Characterization of unstable anthocyanin loci in *Dianthus caryophyllus* L.: a new higher-plant transposable element system. PhD thesis of Stanford University, California

Leong BJ, Last RL (2017) Promiscuity, impersonation and accommodation: evolution of plant specialized metabolism. Curr Opin Struct Biol 47:105–112

Leong BJ, Lybrand DB, Lou YR, Fan P, Schilmiller AL, Last RL (2019) Evolution of metabolic novelty: a trichome-expressed invertase creates specialized metabolic diversity in wild tomato. Sci Adv 5:eaaw3754

Li Y, Baldauf S, Lim EK, Bowles DJ (2001) Phylogenetic analysis of the UDP-glycosyltransferase multigene family of *Arabidopsis thaliana*. J Biol Chem 276:4338–4343

Li Y, Kim JI, Pysh L, Chapple C (2015) Four isoforms of Arabidopsis 4-coumarate:CoA ligase have overlapping yet distinct roles in phenylpropanoid metabolism. Plant Physiol 169:2409–2421

Li AX, Steffens JC (2000) An acyltransferase catalyzing the formation of diacylglucose is a serine carboxypeptidase-like protein. Proc Natl Acad Sci USA 97:6209–6907

Liang XW, Dron M, Cramer CL, Dixon RA, Lamb CJ (1989) Differential regulation of phenylalanine ammonia-lyase genes during plant development and by environmental cues. J Biol Chem 264:14486–14492

Luo H, Dai C, Li Y, Feng J, Liu Z, Kang C (2018) Reduced Anthocyanins in Petioles codes for a GST anthocyanin transporter that is essential for the foliage and fruit coloration in strawberry. J Exp Bot 69:2595–2608

Luo J, Nishiyama Y, Fuell C, Taguchi G, Elliott K, Hill L, Tanaka Y, Kitayama M, Yamazaki M, Bailey P, Parr A, Michael AJ, Saito K, Martin C (2007) Convergent evolution in the BAHD family of acyl transferases: identification and characterization of anthocyanin acyl transferases from *Arabidopsis thaliana*. Plant J 50:678–695

Marrs KA, Alfenito MR, Lloyd AM, Walbot V (1995) A glutathione *S*-transferase involved in vacuolar transfer encoded by the maize gene *Bronze-2*. Nature 375:397

Mato M, Onozaki T, Ozeki Y, Higeta D, Itoh Y, Hisamatsu T, Yoshida H, Shibata M (2001) Flavonoid biosynthesis in pink-flowered cultivars derived from 'William Sim' carnation. (*Dianthus caryophyllus*). J Japan Soc Hortic Sci 70:315–319

Mato M, Onozaki T, Ozeki Y, Higeta D, Itoh Y, Yoshimoto Y, Ikeda H, Yoshida H, Shibata M (2000) Flavonoid biosynthesis of white-flowered Sim carnations (*Dianthus caryophyllus*). Sci Hortic 84:333–347

Matsuba Y, Sasaki N, Tera M, Okamura M, Abe Y, Okamoto E, Nakamura H, Funabashi H, Saito M, Matsuoka H, Nagasawa K, Ozeki Y (2010) A novel glucosylation reaction on anthocyanins catalyzed by acyl-glucose dependent glucosyltransferase in the petals of carnation and delphinium. Plant Cell 22:3374–3389

Mehlquist GAL (1940) Inheritance in the carnation, *Dianthus caryophyllus*. I. Inheritance of flower color. Proc Amer Soc Hort Sci 37:1019–1021

Mehlquist GAL, Geissman TA (1947) Inheritance in the carnation (*Dianthus caryophyllus*). III. Inheritance of flower color. Ann Miss Bot Gard 34:39–75

Mehlquist GAL, Ober D, Sagawa Y (1954) Somatic mutations in the carnation, *Dianthus caryophyllus* L. Proc Natl Acad Sci USA 40:432–436

Milkowski C, Strack D (2004) Serine carboxypeptidase-like acyltransferases. Phytochemistry 65:517–524

Miyahara T, Takahashi M, Ozeki Y, Sasaki N (2012) Isolation of an acyl-glucose-dependent anthocyanin 7-*O*-glucosyltransferase from the monocot *Agapanthus africanus*. J Plant Physiol 169:1321–1326

Miyahara T, Sakiyama R, Ozeki Y, Sasaki N (2013) Acyl-glucose-dependent glucosyltransferase catalyzes the final step of anthocyanin formation in *Arabidopsis*. J Plant Phyisiol 170:619–624

Miyahara T, Sugishita N, Ishida-Dei M, Okamoto E, Kouno T, Cano EA, Sasaki N, Watanabe A, Tasaki K, Nishihara M, Ozeki Y (2018) Carnation *I* locus has contains two chalcone isomerase genes involved in orange flower coloration. Breed Sci 68:481–487

Miyahara T, Tani T, Takahashi M, Nishizaki Y, Ozeki Y, Sasaki N (2014) Isolation of anthocyanin 7-*O*-glucosyltransferase from Canterbury bells (*Campanula medium*). Plant Biotechnol 31:555–559

Mock HP, Strack D (1993) Energetics of the uridine 5′-diphosphoglucose:hydroxycinnamic acid acyl-glucosyltransferase reaction. Phytochemistry 32:575–579

Moghe GD, Last RL (2015) Something old, something new: conserved enzymes and the evolution of novelty in plant specialized metabolism. Plant Physiol 169:1512–1523

Momose M, Itoh Y, Umemoto N, Nakayama M, Ozeki Y (2013a) Reverted glutathione *S*-transferase-like genes that influence flower color intensity of carnation (*Dianthus caryophyllus* L.) originated from excision of a transposable element. Breed Sci 63:435–440

Momose M, Nakayama M, Itoh Y, Umemoto N, Toguri T, Ozeki Y (2013b) An active *hAT* transposable element causing bud mutation of carnation by insertion into *flavonoid 3'-hydroxylase* gene. Mol Genet Genom 288:175–184

Morimoto H, Narumi-Kawasaki T, Takamura T, Fukai S (2018) Petal color characteristics of carnation mutative cultivars MINAMI series. Acta Hort 1208:7–12

Morimoto H, Narumi-Kawasaki T, Takamura T, Fukai S (2019a) Analysis of flower color variation in carnation (*Dianthus caryophyllus* L.) cultivars derived from continuous bud mutations. Hortic J 88:116–128

Morimoto H, Umakoshi K, Sugihara H, Narumi-Kawasaki T, Takamura T, Fukai S (2019b) Characteristics of delayed anthocyanin accumulation of *Dianthus* 'Colour Magician' after anthesis. Acta Hort 1263:207–214

Morita Y, Saito R, Ban Y, Tanikawa N, Kuchitsu K, Ando T, Yoshikawa M, Habu Y, Ozeki Y, Nakayama M (2012) Tandemly arranged *chalcone synthase A* genes contribute to the spatially regulated expression of siRNA and the natural bicolor floral phenotype in *Petunia hybrida*. Plant J 70:739–749

Mueller LA, Goodman CD, Silady RA, Walbot V (2000) AN9, a petunia glutathione *S*-transferase required for anthocyanin sequestration, is a flavonoid-binding protein. Plant Physiol 123:1561–1570

Mugford ST, Milkowski C (2012) Serine carboxypeptidase-like acyltransferases from plants. Methods Enzymol 516:279–297

Nishizaki Y, Matsuba Y, Okamoto E, Okamura M, Ozeki Y, Sasaki N (2011) Structure of the acyl-glucose-dependent anthocyanin 5-*O*-glucosyltransferase gene in carnations

and its disruption by transposable elements in some varieties. Mol Genet Genom 286:383–394

Ogata J, Itoh Y, Ishida M, Yoshida H, Ozeki Y (2004) Cloning and heterologous expression of a cDNA encoding flavonoid glucosyltransferases from *Dianthus caryophyllus*. Plant Biotechnol 21:367–375

Ogata J, Kanno Y, Itoh Y, Tsugawa H, Suzuki M (2005) Plant biochemistry: anthocyanin biosynthesis in roses. Nature 435:757–758

Ohno S (1970) Evolution by gene duplication. Springer-Verlag, New York

Okamura M, Nakayama M, Umemoto N, Cano EA, Hase Y, Nishizaki Y, Sasaki N, Ozeki Y (2013) Crossbreeding of a metallic color carnation and diversification of the peculiar coloration by ion-beam irradiation. Euphytica 191:45–56

Paquette SM, Jensen K, Bak S (2009) A web-based resource for the Arabidopsis P450, cytochromes b5, NADPH-cytochrome P450 reductases, and family 1 glycosyltransferases (https://www.P450.kvl.dk). Phytochemistry 70:1940–1947

Pereau-Leroy P, (1974) Genetic interaction between the tissues of carnation petals as periclinal chimeras. Radiat Bot 14:109–116

Pérez-Díaz R, Madrid-Espinoza J, Salinas-Cornejo J, González-Villanueva E, Ruiz-Lara S (2016) Differential roles for VviGST1, VviGST3, and VviGST4 in proanthocyanidin and anthocyanin transport in *Vitis vinifera*. Front Plant Sci 7:1166

Petroni K, Tonelli C (2011) Recent advances on the regulation of anthocyanin synthesis in reproductive organs. Plant Sci 181:219–229

Reinprecht Y, Perry GE, Pauls KP (2017) A comparison of phenylpropanoid pathway gene families in common bean. Focus on P450 and C4H genes. In: de la Vega MP, Santalla M, Marsolais F (eds) The Common Bean Genome. Compendium of Plant Genomes. Springer, Chem, pp 219–261

Sagawa Y, Mehlquist GAL (1957) The mechanism responsible for some X-ray induced changes in flower color of the carnation, *Dianthus caryophyllus*. Am J Bot 44:397–403

Samata Y, Tsuyuki Y, Inazu K, Iizuki K (1979) Induction of flower color changes in carnation (*Dianthus caryophyllus*) by gamma-ray irradiation, Bull Fac Agric Tamagawa Univ 29–41

Sandve SR, Rohlfs RV, Hvidsten TR (2018) Subfunctionalization versus neofunctionalization after whole-genome duplication. Nat Genet 50:908–909

Sasaki N, Matsuba Y, Abe Y, Okamura M, Momose M, Umemoto N, Nakayama M, Itoh Y, Ozeki Y (2013) Recent advances in understanding the anthocyanin modification steps in carnation flowers. Sci Hortic 163:37–45

Sasaki N, Nishizaki Y, Ozeki Y, Miyahara T (2014) The role of acyl-glucose in anthocyanin modifications. Molecules 19:18747–18766

Sasaki N, Nishizaki Y, Uchida Y, Wakamatsu E, Umemoto N, Momose M, Okamura M, Yoshida H, Yamaguchi M, Nakayama M, Ozeki Y, Itoh Y (2012) Identification of the *glutathione* S-*transferase* gene responsible for flower color intensity in carnations. Plant Biotechnol 29:223–227

Shimada N, Aoki T, Sato S, Nakamura Y, Tabata S, Ayabe S (2003) A cluster of genes encodes the two types of chalcone isomerase involved in the biosynthesis of general flavonoids and legume-specific 5-deoxy(iso)flavonoids in *Lotus japonicus*. Plant Physiol 131:941–951

St Pierre B, De Luca V (2000) Evolution of acyltransferase genes: origin and diversification of the BAHD superfamily of acyltransferases involved in secondary metabolism. In: Romeo JT, Ibrahim R, Varin L, De Luca V (eds) Recent advances in phytochemistry. Elsevier, Amsterdam, pp 285–315

Steffens JC (2000) Acyltransferases in protease's clothing. Plant Cell 12:1253–1256

Stehle F, Brandt W, Stubbs MT, Milkowski C, Strack D (2009) Sinapoyltransferases in the light of molecular evolution. Phytochemistry 70:1652–1662

Stich K, Eidenberger T, Wurst F, Forkmann G (1992) Enzymatic conversion of dihydroflavonols to flavan-3,4-diols using flower extracts of *Dianthus caryophyllus* L. (carnation). Planta 187:103–108

Sugihara H, Morimoto H, Narumi-Kawasaki T, Takamura T, Fukai S (2019) Characteristics of flower colour in the bud-mutated cultivars of the carnation Mini Tiara series. Acta Hort 1263:267–274

Sun Y, Li H, Huang JR (2012) Arabidopsis TT19 functions as a carrier to transport anthocyanin from the cytosol to tonoplasts. Mol Plant 5:387–400

Timoneda A, Feng T, Sheehan H, Walker-Hale N, Pucker B, Lopez-Nieves S, Guo R, Brockington S (2019) The evolution of betalain biosynthesis in Caryophyllales. New Phytol 224:71–85

Tohge T, de Souza LP, Fernie AR (2018) On the natural diversity of phenylacylated-flavonoid and their in planta function under conditions of stress. Phytochem Rev 17:279–290

Tohge T, Wendenburg R, Ishihara H, Nakabayashi R, Watanabe M, Sulpice R, Hoefgen R, Takayama H, Saito K, Stitt M, Fernie AR (2016) Characterization of a recently evolved flavonol-phenylacyltransferase gene provides signatures of natural light selection in Brassicaceae. Nat Commun 7:12399

Totsuka A, Okamoto E, Miyahara T, Kouno T, Cano EA, Sasaki N, Watanabe A, Tasaki K, Nishihara M, Ozeki Y (2018) Repressed expression of a gene for a basic helix-loop-helix protein causes a white flower phenotype in carnation. Breed Sci 68:139–143

Vogt T, Jones P (2000) Glycosyltransferases in plant natural product synthesis: characterization of a supergene family. Trends Plant Sci 5:380–386

Yagi M, Kosugi S, Hirakawa H, Ohmiya A, Tanase K, Harada T, Kishimoto K, Nakayama M, Ichimura K, Onozaki T, Yamaguchi H, Sasaki N, Miyahara T, Nishizaki Y, Ozeki Y, Nakamura N, Suzuki T, Tanaka Y, Sato S, Shirasawa K, Isobe S, Miyamura Y, Watanabe A, Nakayama S, Kishida Y, Kohara M, Tabata S (2014) Sequence analysis of the genome of

carnation (*Dianthus caryophyllus* L.). DNA Res 21:231–241

Yamaguchi M (1989) Basic studies on the flower color breeding of carnations (*Dianthus caryophyllus* L.). Bull Fac Hortic Minami Kyusyu Univ 19:1–75

Yonekura-Sakakibara K (2009) Functional genomics of family 1 glycosyltransferases in Arabidopsis. Plant Biotechnol 26:267–274

Yonekura-Sakakibara K, Hanada K (2011) An evolutionary view of functional diversity in family 1 glycosyltransferases. Plant J 66:182–193

Yoshida H, Akimoto H, Yamaguchi M, Shibata M, Habu Y, Iida S, Ozeki Y (2004a) Alteration of methylation profiles in distinct cell lineages of the layers during vegetative propagation in carnation (*Dianthus caryophyllus*). Euphytica 135:247–253

Yoshida H, Itoh Y, Iwashina T, Yamaguchi M, Ozeki Y (2004b) Differences in chalcononaringenin 2'-*O*-glucoside content in the petals of carnations (*Dianthus caryophyllus*) bearing yellow flowers. Sci Hortic 99:175–186

Yoshida K, Mori M, Kondo T (2009) Blue flower color development by anthocyanins: from chemical structure to cell physiology. Nat Prod Rep 26:884–915

Yoshimoto Y, Higeta D, Itoh Y, Yoshida H, Hasebe M, Ozeki Y (2000) Isolation and characterization of a cDNA for phenylalanine ammonia-lyase (PAL) from *Dianthus caryophyllus* (carnation). Plant Biotechnol 17:325–329

Zhao J, Huhman D, Shadle G, He XZ, Sumner LW, Tang Y, Dixon RA (2009) MATE2 mediates vacuolar sequestration of flavonoid glycosides and glycoside malonates in *Medicago truncatula*. Plant Cell 23:1536–1555

Zuker A, Tzfira T, Ben-Meir H, Ovadis M, Shklarman E, Itzhaki H, Forkmann G, Martens S, Neta-Sharir I, Weiss D, Vainstein A (2002) Modification of flower color and fragrance by antisense suppression of the *flavanone 3-hydroxylase* gene. Mol Breed 9:33–41

Advances in Mutation Technology to Create Novel Carnation Varieties

9

Masachika Okamura and Yoshihiro Hase

Abstract

Mutation breeding is advantageous and essential for carnation to extend the variation of genetic information and create novel traits. We have demonstrated that tissue culture combined with ion beam irradiation can create a wider spectrum in flower phenotype than that with gamma irradiation, which has been the most commonly used mutagen worldwide. We showed that chronic gamma irradiation also has the potential to generate a wide spectrum of flower color mutants comparable to ion beam irradiation. Furthermore, we found that non-acylated type anthocyanin is the key determinant in creating metallic coloration in carnation. We succeeded in diversifying the metallic coloration by ion beam irradiation. Through these studies, eight new varieties of carnation have been developed so far and sold worldwide for 8–15 years. Despite the relatively narrow genetic background of carnation, our research suggested that novel mutant varieties can be created by ion beam breeding system and also by finding key determinants that control flower phenotypes.

9.1 Introduction

Due to its wide range of flower colors and forms, its excellent storage quality and vase life, carnation (*Dianthus caryophyllus*) is one of the most valuable commercial flowers around the world. The global carnation market is maintained by the introduction of new varieties with improved characteristics through breeding. Since the genetic variability in carnation is relatively poor, the breeding potential for new flower colors is very limited. Carnation is a vegetatively propagated plant, which further reduces its genetic pool availability. In contrast, the heterozygous nature of carnation offers high mutation frequency. Thus, mutation breeding is advantageous and essential for carnation to extend the variation of genetic information and create novel traits in terms of growth, stem, flower shape and color.

Actually, majority of carnation varieties have been created by mutagenesis either spontaneously or intentionally (Mehlquist et al. 1954). For example, Sim carnations consisting of about 400 varieties are bud mutants originating from the variety 'William Sim' (Mato et al. 2000).

M. Okamura (✉)
Central Laboratories for Key Technologies, Kirin Company, Kanazawa-ku, Yokohama 234-0004, Kanagawa, Japan
e-mail: okamuragege@gmail.com

Y. Hase
Takasaki Advanced Radiation Research Institute, National Institutes for Quantum and Radiological Science and Technology (QST), Watanuki 1233, Takasaki, Gunma 370-1292, Japan
e-mail: hase.yoshihiro@qst.go.jp

T. Onozaki and M. Yagi (eds.), *The Carnation Genome*, Compendium of Plant Genomes,
https://doi.org/10.1007/978-981-15-8261-5_9

Another advantage of mutation induction in vegetatively propagated flowers is the ability to change one or a few characters of an otherwise outstanding variety without altering the remaining and often superior part of the genotypes (Broertjes 1968). This brings important advantages in flower production. Specifically, a series of varieties with various flower colors originating from one variety normally possess the same growth habit, stem, and foliage traits. This enables growers to produce flowers in various colors at low costs under the same cultivation conditions and management. These aspects of mutation breeding make this approach appealing for the improvement of traits and creation of novel colors in carnation.

Since the artificial mutation induction was demonstrated in maize with X-rays (Stadler 1928), a great deal of studies on the mutagenesis in plants by ionizing radiation have been carried out for both breeding and basic research. Mutation techniques by using ionizing radiations such as X-rays and gamma rays have successfully produced changes in phenotypic characters like color, shape, or size of flower and the like. Also, a number of promising mutants have been developed through in vitro mutagenesis combined with irradiation (Simard et al. 1992; Cassells et al. 1993). Somaclonal variation in the form of change in flower color, variegated leaves, floral, and leaf morphology have been reported in carnation (Hackett and Anderson 1967). It was found that ion beams show a high relative biological effectiveness (RBE) of growth inhibition, lethality, and so on as compared with low linear energy transfer (LET) radiation such as gamma rays, X-rays, and electrons (Blakely 1992). Ion beams deposit high energy densely and locally resulting in predominant induction of single- or double-strand DNA breaks with damaged end groups whose repair capacity is low (Goodhead 1995). Therefore, compared with low LET radiations, it is expected that ion beams are more effective in producing mutants.

In this chapter, we describe the establishment of ion beam irradiation method to create a wide variety of flower color and shape mutants, comparison of flowers obtained from ion beam method with those from acute and chronic gamma irradiations, creation and diversification of metallic color carnation by ion beam irradiation and their genetic analysis, as well as the commercialization and long-time stability of ion-beamed mutants.

9.2 Generation of a Wide Variety of Flower Color and Shape Mutants by Ion Beam Mutagenesis

Raising the effectiveness of mutation breeding requires the development of a novel approach. Ionizing radiation can be divided into two classes according to the linear energy transfer (LET), which represents the amount of energy that a particle or photon deposited to the irradiated material traversed per unit length. Low LET radiation such as gamma rays is the most commonly used mutagen in practical mutation breeding (FAO/IAEA Mutant Variety Database). Ion beams have also been known as high LET radiation; however, their extensive application for plant breeding has started in the 1990s (Tanaka et al. 1997; Hase et al. 2002; Shikazono et al. 2001). We have investigated the efficiency of ion beam irradiation in carnation for the induction of floral mutants. The biological effect and mutagenesis efficiency were compared with those of gamma rays. It was in 2002 that a series of variety was created and commercialized in carnation (Okamura et al. 2003).

9.2.1 Application of Ion Beams to Carnation

Spray carnation variety 'Vital' (cherry pink with serrated petals) was used for the experiment. Cultured leaf tissues were placed in Petri dishes containing Murashige and Skoog (MS) medium supplemented with 2 mg/l Zeatin, 30 g/l sucrose, and 7 g/l agar (MSZ medium). The samples were covered with sterilized Kapton film and irradiated with 18.3 MeV/u carbon ions (LET: 107 keV/μm) at the Takasaki Advanced

Radiation Research Institute (TARRI), National Institutes for Quantum and Radiological Science and Technology (QST) (formerly Japan Atomic Energy Research Institute (JAERI)). After irradiation, the leaf segments were transferred onto fresh MSZ medium in aseptic conditions and cultured in the growth room. The frequency of adventitious shoot regeneration was examined two months after irradiation. Regenerated plants were acclimatized in the greenhouse to investigate floral mutants. For comparison, leaf cultures were irradiated with gamma rays of 30-100 Gy/h for one hour at once using gamma ray (^{60}Co) irradiation facilities of TARRI, QST.

The shoot regeneration frequency decreased with increasing dose. The median regeneration dose (RD50) was estimated to be 15 Gy in carbon ion irradiation, while in gamma rays, RD50 was about 60 Gy. The RBE of 18.3 MeV/u carbon ions relative to gamma rays was estimated to be 4. Frequency of flower color and shape mutants around the median regeneration dose were 3.6% and 2.1–3.8% in carbon ions and gamma rays, respectively (Tables 9.1 and 9.2). The most striking thing was that the mutation spectrum of flower color and shape was wider in plants derived from carbon ion irradiation than those from gamma irradiation. The results strongly suggested that ion beams can induce a wider variety of mutants at lower doses compared to gamma rays.

9.2.2 Characteristics of the Mutants Obtained by Ion Beam Irradiation

Flower color mutants such as pink, light pink, and red were obtained by gamma irradiation, whereas the mutants obtained by carbon ion beam irradiation had a wider color spectrum such as pink, dark pink, light pink, salmon, red, yellow, complex, and striped types (Fig. 9.1). Furthermore, flower shape mutants such as round petals, Dianthus type, and rose type were obtained only from carbon ion irradiation (Fig. 9.2).

Table 9.1 Number of mutants in plants regenerated from leaf cultures irradiated with 18.3 MeV/u carbon ions

Dose (Gy)	Number of plants tested	Mutants in flower color and/or shape (No.)	Mutant frequency (%)
5	263	Round petals (2), Light pink (1)	1.1
10	284	Pink (1), Dark pink (1), Light pink (2), Salmon (2), Red (1), Striped type; pink and white (2), Dianthus type petals (2)	3.9
15	251	Pink (2), Pink/round petals (1), Yellow (1), Red (1), Red/round petals (1), Complex type; pink and white (2)	3.6
30	52	Striped type; pink and white (1), Cream (1)	3.8
Total	850	(24)	2.8

Table 9.2 Number of mutants in plants regenerated from leaf cultures irradiated with gamma rays

Dose (Gy)	Number of plants tested	Mutants in flower color and/or shape (No.)	Mutant frequency (%)
30	350	Pink (1), Minute striped (3)	1.1
50	426	Pink (2), Red (1), Minute striped (4), Round petals (2)	2.1
70	264	Pink (1), Light pink (2), Minute striped (7)	3.8
100	110	Red (1), Minute striped (2)	2.7
Total	1150	(26)	2.3

Fig. 9.1 Floral mutants obtained from carbon ion irradiation of carnation variety 'Vital'. Top (left to right): 'Vital' (cherry, serrated), red, dark pink, salmon. 2nd (left to right): bi-colored dark, yellow, striped, bi-colored light. 3rd (left to right): Dianthus type, light pink, round red, round pink. Bottom (left to right): pink, Dianthus type, Dianthus type/light pink, round type

Fig. 9.2 Flower shape mutants obtained by carbon ion irradiation of carnation variety 'Vital'. Top (left to right): 'Vital' (serrated), fewer petals, Dianthus type. Middle (left to right): round petals, smaller petals, Dianthus type. Bottom (left to right): round petals, less petals, Dianthus type

Fig. 9.3 Commercialization of carnation varieties bred by ion beam irradiation. **a** Carnation varieties Vital ion series produced by ion beam irradiation of 'Vital' (upper right): 'Red Vital' (upper left), 'Misty Pink Vital' (center), and 'Dark Pink Vital' (lower right). **b** Commercial production of 'Red Vital.' **c** Popular commercial variety 'Beam Cherry.'

Spray carnation variety 'Vital' has high productivity, long vase life, and resistance to Fusarium. Most of the mutants retained as much vigor as the parents. Red, dark pink, and bicolored mutants obtained from carbon ion irradiation were applied for registration with the Japanese Ministry of Agriculture, Forestry and Fisheries as 'Misty Pink Vital Ion,' 'Dark Pink Vital Ion,' and 'Red Vital.' A round petal mutant registered as 'Beam Cherry' not only retained the superior characteristics of the parent variety but also acquired stronger stem than the parent. These new varieties have been commercialized since the spring of 2002 and sold worldwide by Barberet & Blanc S. A. (Fig. 9.3).

These results indicate that ion beams can induce a wide variety of flower color and shape mutants and that the combined method of ion beam irradiation with tissue culture is useful to obtain commercial varieties in a short time (Okamura et al. 2003).

9.3 Mutagenic Effects of Acute and Chronic Gamma Irradiations on Flower Mutation

The ion beam irradiation could induce wide mutation spectrum as compared to gamma irradiation (acute irradiation with a relatively high dose rate). Another approach to induce mutations by gamma rays is chronic irradiation at relatively low dose rates. Since there was no data on the mutagenic effect of chronic gamma irradiation in carnation, we investigated the floral mutations induced by chronic gamma irradiation and compared the results with those obtained by the carbon ion and acute gamma irradiation.

9.3.1 Irradiation Effect of Chronic and Acute Gamma Irradiation

In this experiment, 'Star,' a standard type variety with orange fancy flowers (orange flowers accompanied with red flecks and sectors), was used. Nodes with axillary buds of the aseptic cultured plants were excised from the in vitro plants and placed in a Petri dish containing MS medium supplemented with 0.1 mg/l NAA and 0.1 mg/l BA, 30 g/l sucrose and 7 g/l agar (MSNB medium). The samples covered with sterilized Kapton film were irradiated with 26.7 MeV/u carbons (LET: 87 keV/μm) at TARRI, QST. The irradiated nodes with buds were cultured in vitro till they grow into plants. The plant was then acclimatized in the greenhouse and pinched. The axillary shoots obtained from these pinched plants were then used for flowering tests to investigate floral mutation. In vitro plants were used for chronic and acute gamma irradiation. For chronic gamma irradiation, samples were exposed to the ^{60}Co source at the Institute of Radiation Breeding (IRB), the National Agriculture and Food Research

Organization (NARO). The samples were in a gamma room with lighting (16 h of light: 8 h of dark) at 18–20 °C and irradiated with a dose rate of 0.5 Gy/h for 20 h every other day during the 20-day period, resulting in a total dose of 100 Gy. For acute gamma irradiation, samples were irradiated with 30–100 Gy at once within one hour.

The relationship between irradiation dose and growth rate (fresh weight of a shoot grown 3 weeks after irradiation) was investigated for each axillary bud from the irradiated nodes. The chronic irradiation with 100 Gy in total had little influence on shoot growth as compared to the control. D50, which is the dose required to reduce the weight of the fresh shoot to 50% of the control, was 17 Gy and 60 Gy for carbon ion beams and acute gamma rays, respectively. Thus, the RBE of 26.7 MeV/u carbon ions was estimated to be 3.5 times higher than acute gamma rays (Okamura et al. 2006a).

9.3.2 Floral Mutants: Mutation Rates and Spectra

In the ion beam irradiation, flower color mutants such as dark orange, light orange, salmon, and yellow were obtained. In addition, white mutant with red stripes (referred to as 'striped' in Figs. 9.4 and 9.5) emerged. Striped type mutants emerged at higher frequency in ion-beamed plants than in plants irradiated with chronic gamma rays. Also, flower shape or size mutants such as round petals, smaller and larger flowers emerged. Flower color mutants induced by acute gamma rays included dark orange, light orange, and salmon. A range of floral color mutation was wider in ion beam irradiation than acute gamma ray irradiation. In chronic gamma ray irradiation, flower color mutants such as dark orange, light orange, salmon, and yellow were obtained (Fig. 9.4). Floral mutants obtained from ion beam, acute gamma ray, and chronic gamma irradiations are summarized in Fig. 9.5. The range of flower color mutation was wider in chronic gamma irradiation than in acute gamma irradiation.

9.3.3 Genetic Background of the Yellow Mutants

Yellow and orange flower color in carnation results from the accumulation of chalcone 2′-glucoside. Production of this pigment needs the

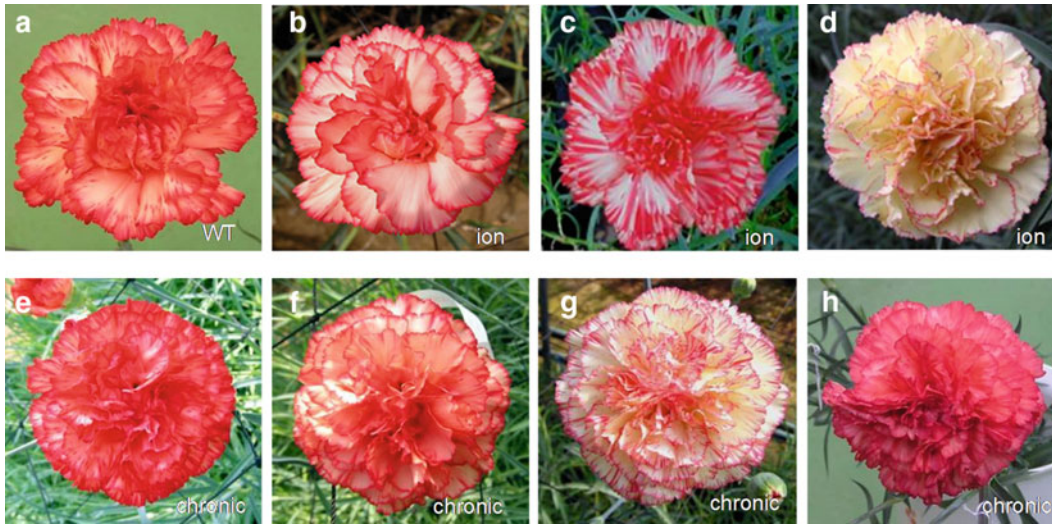

Fig. 9.4 Flower of 'Star' (**a**) and representative mutants obtained from irradiation with ion beams (**b**–**d**) and those with chronic gamma rays (**e**–**h**). **b** Light orange, **c** Striped, **d** Yellow, **e** Dark orange, **f** Light orange, **g** Yellow, and **h** Salmon

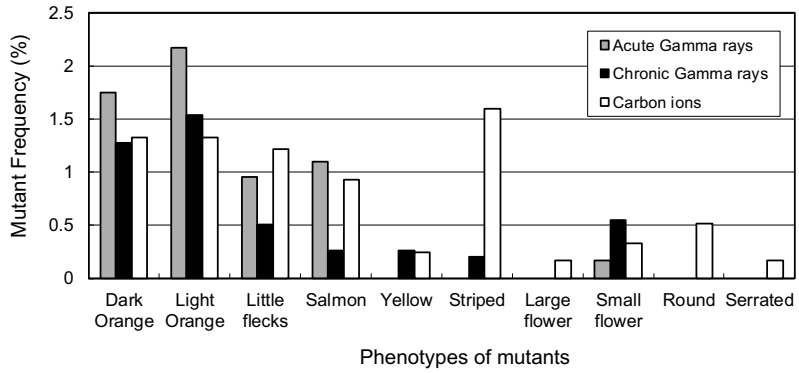

Fig. 9.5 Frequencies (%) of floral color and shape mutants of carnation variety 'Star' by acute gamma ray (gray bars), chronic gamma ray (black bars) and ion beam (white bars) irradiations: Mutation spectrum was wider in plants irradiated with chronic gamma rays or ion beams compared to those irradiated with acute gamma rays. Yellow color and striped color emerged in both ion beam and chronic gamma irradiations, but not in acute gamma irradiation

disruption of chalcone isomerase (CHI) activity. In addition, dihydroflavonol 4-reductase (DFR) needs to be defective in order to produce yellow flowers (Fig. 9.6). As described above, the variety 'Star' has variegated flowers having red flecks and sectors on orange background. Mutant flowers with yellow background were obtained only through ion beam and chronic gamma irradiation (Fig. 9.7). In order to examine the genetic background of the yellow mutants, the genes encoding CHI and DFR were analyzed.

A class II transposable element named dTdic1 was found through a study of variegated flowers (Itoh et al. 2002). It was suggested that, in a yellow-flowered carnation having white sectors, both *CHI* and *DFR* genes were homozygously

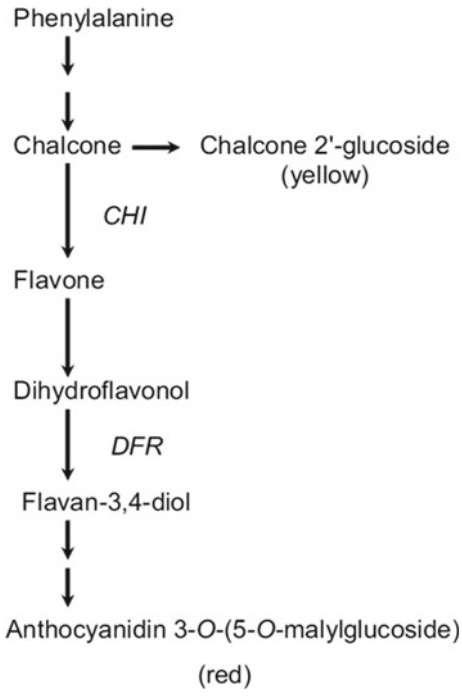

Fig. 9.6 A schematic pathway of anthocyanin and flavonoid biogenesis in carnation. *CHI* chalcone isomerase, *DFR* dihydroflavonol 4-reductase

Fig. 9.7 Flower appearance of 'Star' (upper), and gamma-irradiated mutant (lower left) and ion beamed mutant (lower right)

disrupted by dTdic1, and the occasional excision of dTdic1 from *CHI* causes white sectors on a yellow background.

Since only L1 layer (the outermost layer) is responsible for pigment accumulation in carnation, periclinal chimeras are sometimes involved in back mutation (Sagawa and Mehlquist 1957). Therefore, for PCR analysis of the *CHI* and *DFR* genes, the L1 layer of flower petals was used to extract DNA so as to eliminate the inconsistency between phenotype and genotype due to periclinal chimeras. Both 'Star' and the yellow mutants were homozygous for defective *CHI* allele caused by dTdic1. On the other hand, 'Star' was heterozygous in *DFR* locus; one allele is a functional wild type *DFR* allele, while the other is a dTdic1-disrupted *DFR* allele. PCR analysis suggested that, in both yellow mutants from ion beam and chronic gamma irradiation, the wild-type *DFR* allele was disrupted (Fig. 9.8), i.e., the yellow mutants had no functional *DFR*. This suggests that the wild type *DFR* gene was disrupted in the L1 layer by irradiation, which resulted in a yellow background instead of the original orange background (Okamura et al. 2006b).

These results indicate that chronic gamma irradiation is more effective in mutation generation than acute gamma irradiation, and that chronic gamma irradiation has a potential to generate a wide spectrum of flower color mutants comparable to that of ion beam irradiation. In addition, the genetic background elucidated above well corresponds to the biosynthetic pathway of the pigment, suggesting that the difference in mutation spectrum is caused by the difference in mutagenesis efficiency.

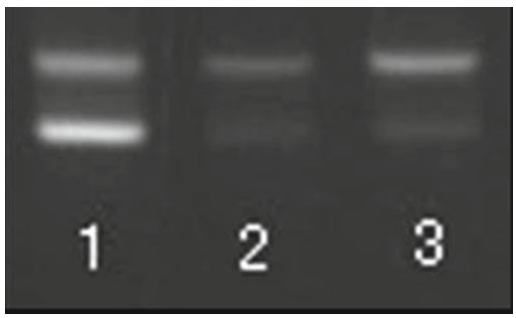

Fig. 9.8 Molecular analysis of *DFR* alleles. 1: 'Star,' 2: a yellow mutant obtained by chronic gamma irradiation; 3: a yellow mutant obtained by carbon ion irradiation. An upper band indicates inactive *DFR* gene disrupted by dTdic1 transposable element and a lower band indicates functional wild-type *DFR* allele. Pale lower bands in lanes 2 and 3 are due to the contamination of L2 layer tissues that inevitably attach to the L1 layer tissue samples

9.4 Crossbreeding of a Metallic Color Carnation and Diversification of the Peculiar Coloration by Ion Beam Irradiation

Carnations have basic colors consisting of cyanic and non-cyanic molecules. Anthocyanins are responsible for the cyanic colors such as pink, red, and purple, chalcone is responsible for yellow color, and chlorophyll is responsible for green color. There are also orange or brown colors achieved by a combination of the pigments mentioned above. Thus, it is generally believed that all possible types of colors are already in the market.

Four major anthocyanins are known in carnation: pelargonidin 3-malylglucoside (Pg3MG), cyanidin 3-malylglucoside (Cy3MG), pelargonidin 3,5-cyclicmalyldiglucoside (Pg3,5cMdG), and cyanidin 3,5-cyclicmalyldiglucoside (Cy3,5cMdG). All of these anthocyanins are glycosylated and are normally acylated by malic acid (Bloor 1998; Nakayama et al. 2000). Each carnation variety has a specific anthocyanin as its major anthocyanin; carnation varieties having anthocyanins Pg3MG, Cy3MG, Pg3,5cMdG, or Cy3,5cMdG are generally red, dark red, pink, or purple, respectively. The structural simplicity of anthocyanin constituents makes it laborious to produce novel flower colors in carnation. The fact that wild *Dianthus* species and their relatives have the same anthocyanins as those found in carnation varieties increases the difficulty in enriching flower color variation by crossing carnation varieties with wild *Dianthus* species and relatives.

Some carnation varieties are known to display dusky and metallic flower colors (defined

herein as peculiar colors) when their petal epidermal cells contain anthocyanin inclusions in vacuoles. Pigment inclusions were investigated in several flower species and referred to as anthocyanic vacuolar inclusions or AVIs (Markham et al. 2000). However, information on the relationship between AVIs and peculiar colors is limited (Morita et al. 2005; Zhang et al. 2006). In addition, there are very few kinds of peculiar color phenotypes in carnation. Therefore, we focused on diversifying peculiar colors in an attempt to create a variety of novel colors in carnation.

Firstly, we revealed the inheritance pattern of the peculiar flower color and to breed a line displaying a novel metallic appearance and a more glittering purple color than any other existing varieties. Subsequently, we tried to diversify metallic color by changing the structure and composition of the line through ion beam irradiation. Also, we investigated the relationship between peculiar colors, constituents of anthocyanins and related compounds, the genes, and characteristics of AVIs involved in the color expression (Okamura et al. 2013).

9.4.1 Heredity of the Peculiar Color Phenotype and Linkage with the Presence of AVIs

Among our carnation collections, we found several varieties and breeding lines that have dusky purple flowers (similar to 'Nazareno' in Fig. 9.9a). Microscopic observation revealed that all of the peculiar color lines had AVIs in their petal epidermal cells (similar to 'Nazareno' in Fig. 9.9b). To examine the hereditary pattern of the peculiar color phenotype, we selected two normal pink color lines '07MC4' and '04MC1' without AVIs in petal epidermal cells (similar to 'Beam Cherry' in Fig. 9.9) that previously segregated peculiar color by self-pollination, hereinafter referred to as peculiar color segregators, and conducted reciprocal crosses. The segregation ratio of normal color to peculiar color individuals in the cross between the two peculiar color segregators turned out to be close to 3:1. In addition, the segregation ratio of normal to peculiar in the cross between the peculiar color segregator and peculiar color line was close to 1:1. These results indicate that the expression of the peculiar color phenotype is controlled by a single recessive allele.

9.4.2 Anthocyanin Composition of the Peculiar Color Line

To gain more insight into the expression of the peculiar color phenotype, we analyzed the anthocyanins of the several varieties and breeding lines. Normal color carnations 'Beam Cherry,' '07MC4' and '04MC1' had Pg3,5cMdG, and 'Red Vital' had Pg3MG as their major anthocyanin (Table 9.3, Fig. 9.9c). Peculiar color carnations, '01MA1' and 'Nazareno' had pelargonidin 3,5-diglucoside (Pg3,5dG) as their major anthocyanin. Major anthocyanins of all the normal color lines were anthocyanins acylated by malate, whereas the anthocyanins of all the peculiar color lines were non-acylated anthocyanins (Table 9.3). The result suggested that the non-acylated type anthocyanin may play an essential role in AVIs formation.

9.4.3 Diversification of Metallic Color by Ion Beam Irradiation

From the peculiar color plants obtained by the cross '07MC4' × '04MC1', we selected an individual with the most metallic, bluish-purple flower. Stability of the unique flower color was confirmed after vegetative propagation and then we designated the individual as 'Line A' (Fig. 9.10a). We further tried to diversify the metallic flower color by the ion beam irradiation. Petal segments of 'Line A' were irradiated with 26.7 MeV/u carbon ions and cultured in vitro to obtain regenerated plants. Flowers of the regenerated plants were examined in greenhouses. The frequency of occurrence of flower color mutants increased as the irradiation dose increased (Table 9.4). Among a variety of mutants obtained, we finally selected three mutants displaying the most metallic colors and named them

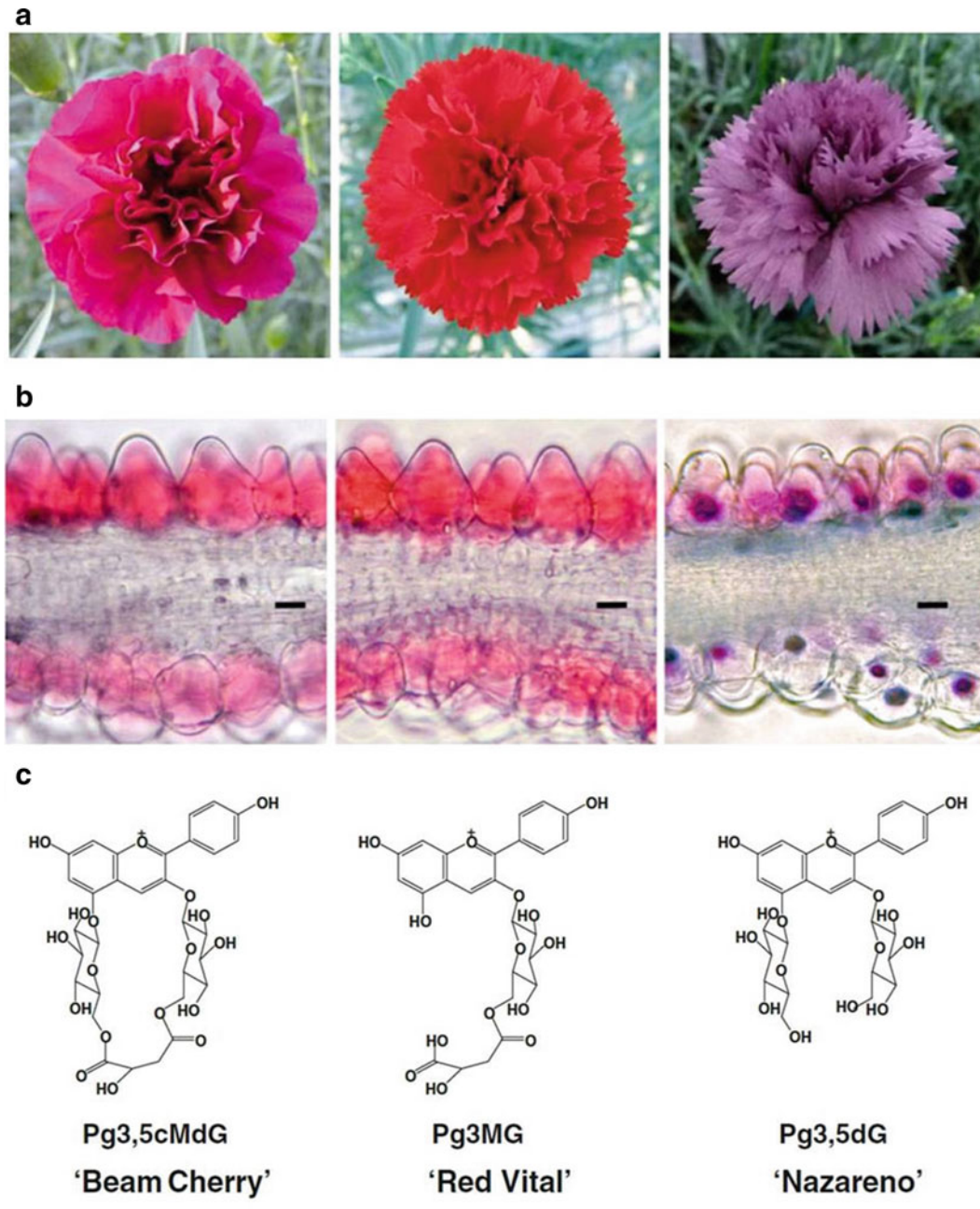

Fig. 9.9 Flower morphologies and anthocyanin structures in carnation varieties. Flower phenotypes (**a**), microscopic photographs of transverse cross sections of petal epidermal cells (**b**), and the structures of anthocyanins (**c**) of varieties (left to right), 'Beam Cherry' (pink, no AVIs), 'Red Vital' (red, no AVIs), and 'Nazareno' (dusky purple, AVIs rich). Scale bars in microscopic photographs indicate 30 μm

'Line B' (metallic reddish purple), 'Line C' (metallic crimson) and 'Line D' (metallic red), respectively (Fig. 9.10a).

The major anthocyanins and related compounds of 'Lines A–D' were analyzed using HPLC. The dominant anthocyanin of 'Line A'

Table 9.3 Flower colors and major anthocyanins of normal and peculiar color type carnation lines used in this study

Carnation line	Flower color	Anthocyanin
(Normal color type)		
'Beam Cherry'	Pink	Pg3,5cMdG
'Red Vital'	Red	Pg3MG
'04MC1'	Pink	Pg3,5cMdG
'07MC4'	Pink	Pg3,5cMdG
'06MP1'	Pink	Pg3,5cMdG
(Peculiar color type)		
'01MA1'	Dusky Purple	Pg3,5dG
'Nazareno'	Dusky Purple	Pg3,5dG

Note Five randomly selected peculiar color individuals segregating from the cross '07MC4' × '04MC1' predominantly contained Pg3,5dG, a non-acylated anthocyanin, whereas five normal color individuals predominantly contained Pg3,5cMdG, an acylated anthocyanin

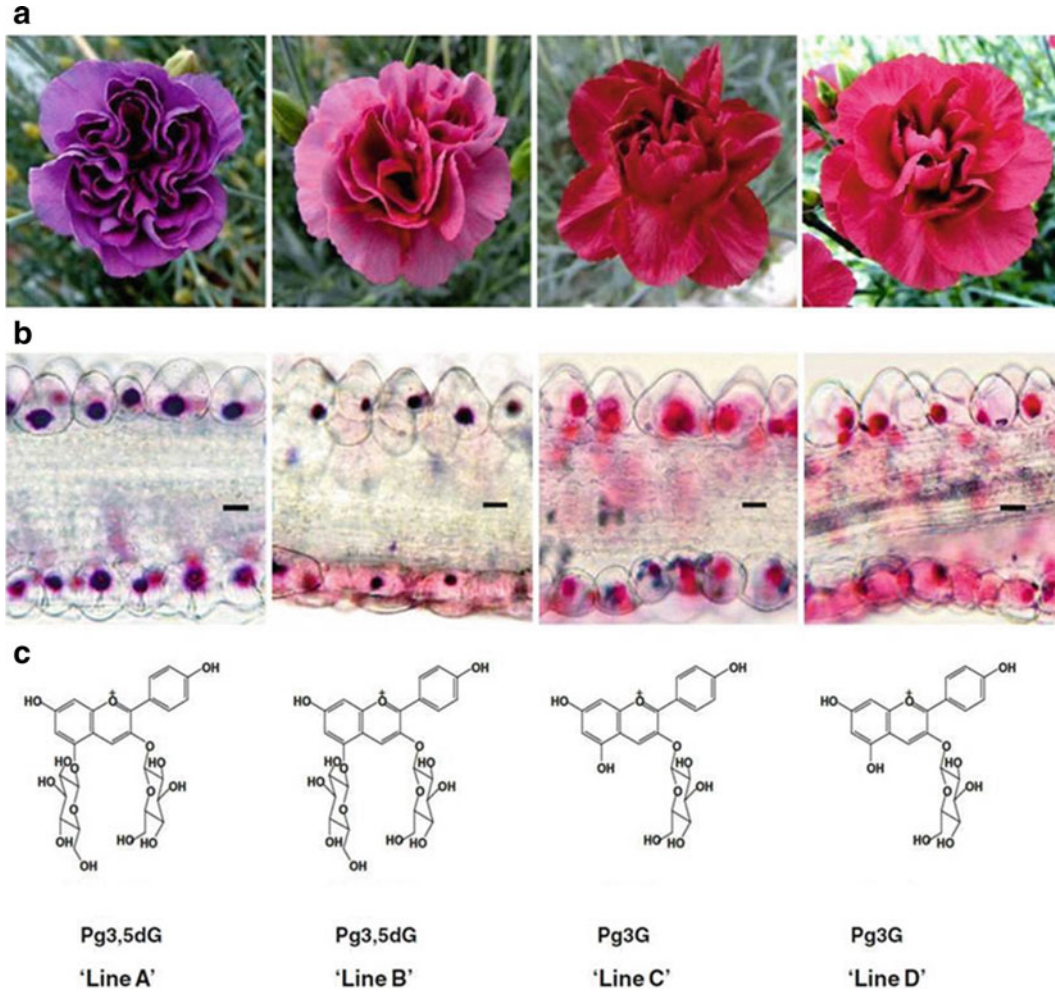

Fig. 9.10 Flower phenotypes (**a**), microscopic photographs of transverse cross sections of petal epidermal cells (**b**), and the structures of anthocyanins (**c**) of carnation breeding lines; (left to right), 'Line A' (metallic bluish purple, AVIs rich), 'Line B' (metallic reddish purple, AVIs average), 'Line C' (metallic crimson, AVIs rich) and 'Line D' (metallic red, AVIs average). Scale bars in microscopic photographs indicate 30 μm

Table 9.4 Flower color mutants induced by carbon ion irradiation on metallic bluish-purple breeding line 'Line A'

Dose (Gy)	Number of regenerated plants examined	Number of flower color mutants				Frequency of flower color mutants (%)[b]
		Metallic reddish purple	Metallic crimson	Metallic red	Others[a] (Pink, Violet)	
0	50	0	0	0	0	0.0
7	160	3	0	0	2	3.1
15	145	4	2	2	2	6.2
20	141	4	3	2	3	8.5

[a]Others consisted of one Pink and one Slightly Metallic Pink from a 20 Gy irradiation and five Dusky Violet mutants
[b]The percentage of mutants was calculated as the number of flower color mutants relative to the total number of plants examined

and 'Line B' was Pg3,5dG, whereas that of 'Line C' and 'Line D' was pelargonidin 3-glucoside (Pg3G) (Fig. 9.10c). Anthocyanin concentration was compared between the lines containing the same anthocyanin. The concentration of 'Line B' was about 68% of 'Line A,' and that of 'Line D' was about 86% of 'Line C.' Major flavonoids of 'Lines A–D' were the same, namely kaempferol 3-(6″-rhamnosyl-sophoroside) and kaempferol 3-sophoroside.

9.4.4 Characteristics of AVIs in the Metallic Color Lines

Petal epidermal cells of the four metallic color lines, 'Lines A–D,' were microscopically observed to investigate the characteristics of AVIs (Fig. 9.10b). All four of the metallic color lines have AVIs throughout the epidermal cells on the petal adaxial side. The color of vacuolar sap on the adaxial side of petal epidermal cells is much lighter in the four metallic color lines than that of typical dusky purple types such as 'Nazareno,' and the AVIs of the four metallic color lines are highly condensed. The water-clear area of the epidermal cells serves like a diamond that reflects a lot of light, resulting in a glittering appearance of the metallic color lines. In addition, differences in the number of anthocyanin inclusions on the abaxial side were observed for mutants containing the same anthocyanin (Fig. 9.10), a phenomenon that affects shade and hue as well. That is, in the petal epidermal cells on the abaxial side, the level of pigment inclusion is much lower and the color of the vacuolar sap is much deeper in 'Lines B and D' compared with those of 'Lines A and C.' Unique, blue inclusions were observed in most of the abaxial epidermal cells of 'Line C' (Fig. 9.10b).

9.4.5 Genetic Basis of the Peculiar Color Lines

The enzyme catalyzing the addition of malate to the anthocyanin glycoside moiety in carnation is anthocyanin malyltransferase (AMalT) (Abe et al. 2008). Due to the fact that the expression of the peculiar color phenotype is controlled by a single recessive allele and that anthocyanins of all the peculiar color lines were non-acylated anthocyanins, *AMalT* is considered the key gene for the peculiar color. Carnation is known to have a single copy of the *AMalT* gene (Umemoto et al. 2009). In addition, since the major anthocyanin of 'Lines C and D' obtained from ion beam irradiation was Pg3G, these two lines are believed to have lost anthocyanin 5-O-glucosyltransferase (AA5GT) activity. AA5GT catalyzes the glycosylation of Pg3G into Pg3,5dG (Matsuba et al. 2010). We analyzed the expression of *AMalT* and *AA5GT* genes in the metallic color lines. Transcripts for *AMalT* were detected in 'Beam Cherry,' whereas *AMalT* transcripts were not detected in any of the four metallic color lines (Fig. 9.11a). Although *AA5GT* gene transcripts were detected in both

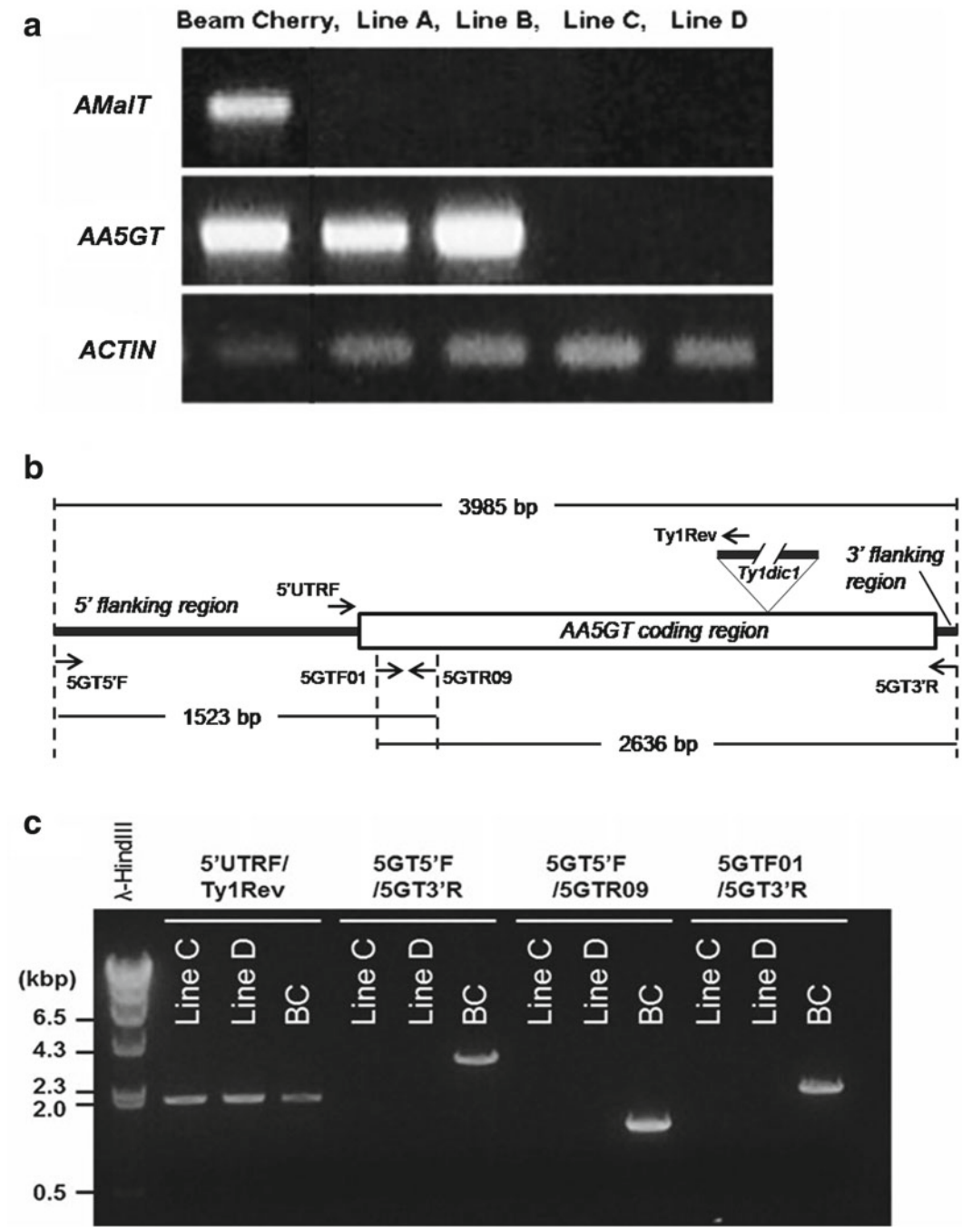

Fig. 9.11 Analysis of *AA5GT* and *AMalT* genes in glittering carnation lines and 'Beam Cherry'. **a** RT-PCR analysis of *AA5GT* and *AMalT* in a carnation variety and breeding lines: (left to right) 'Beam Cherry' (pink, no AVIs), 'Line A' (metallic bluish purple, AVIs rich), 'Line B' (metallic reddish purple, AVIs average), 'Line C' (metallic crimson, AVIs rich), and 'Line D' (metallic red, AVIs average). **b** Primer positions used for the genomic PCR for amplification of *AA5GT* genomic region. *Ty1dic1* is a transposon that inactivates *AA5GT* by inserting into the exon 10. **c** Genomic PCR analysis using the genomic DNA extracted from 'Line C,' 'Line D,' and 'Beam Cherry (BC)' with the primer sets indicated above

'Line A' and 'Line B,' no transcripts of the gene were detected in 'Line C' or 'Line D,' suggesting that *AA5GT* gene mutation took place in 'Lines C and D.' These results correspond well with the anthocyanin present in each line. The results also verify the correlation between the lack of AMalT activity and AVIs.

We carried out genomic PCR analysis to clarify what type of mutation has been generated in 'Lines C and D.' There are instances that *AA5GT* is inactivated by transposon insertion to produce red flowers with an anthocyanin Pg3MG, and the inactivated *AA5GT* is designated as *AA5GT/Ty1dic1* (Nishizaki et al. 2011). Genomic PCR using the primer set 5′UTRF and Ty1Rev, which was designed to detect specifically the *AA5GT/Ty1dic1*, amplified the product with expected length in both 'Line C' and 'Line D,' as well as in the control 'Beam Cherry' (Fig. 9.11b, c). Three primer sets that amplify the coding region and 5′ and 3′ flanking region detected the expected length amplicons in 'Beam Cherry,' but not in 'Lines C and D' (Fig. 9.11c). These results suggest that 'Line A,' the parent of 'Lines C and D,' is heterozygous for this locus with *AA5GT/Ty1dic1* and that a large disruption including the whole healthy *AA5GT* region is responsible for the lack of glucose moiety at the 5-position, which was caused presumably by ion beam irradiation.

The mechanism causing the metallic color lines is rationally explained as follows: (1) by making an intentional cross to produce homozygous *AMalT*-deficient alleles, a peculiar color population was obtained that contained AVIs due to the accumulation of non-acylated anthocyanins; from the peculiar color population, a line was selected that had a novel metallic appearance caused by high levels of anthocyanin condensation on the adaxial surface of petal epidermal cells; (2) a new hue, a reddish metallic color, due to structural alteration of anthocyanin glycosylation resulted from the inactivation of the *AA5GT* gene by ion beam irradiation; and (3) a new tone, a light metallic color, related to the reduction in condensation level of anthocyanins on the abaxial surface of epidermal cells resulted from mutagenesis by ion beam breeding.

Our result supports the concept that inactivation of the single-copy *AMalT* gene causes the accumulation of non-acylated anthocyanins, thereby resulting in the peculiar coloration of carnation. Since we have developed a variety of metallic colors using this concept, the gene *AMalT* is to be called the 'metallic color gene' in carnation.

9.5 Conclusion and Perspectives

We have established a system to create mutants by combining tissue culture with ion beam irradiation. We succeeded in developing the world's first carnation variety series with a wide variety of floral color and shape while retaining the parent's superior characteristics including disease resistance, long vase life, and so on. This has become a pioneering research of ion beam breeding method which continues developing remarkably even now. Up to now, eight varieties of carnation have been created by the ion beam breeding system and sold worldwide for 8–15 years depending on varieties. Their economic effect at the wholesale price in total has amounted up to more than 100 million USD. In addition, characteristics of all the eight varieties remain stable. These facts demonstrated the important features of ion beam breeding system: (1) higher mutation rates which enable to create superior varieties from a smaller number of individuals in a relatively narrow test field, (2) a wide spectrum of mutation which enables to acquire novel mutants, and (3) a fewer mutation sites in a desirable mutant which enable to minimize the number of accompanying undesirable mutations.

The development of mutant varieties using ion beams has been reported in many ornamental plants thus far, and some species have been used to investigate the process of mutagenesis (Yamaguchi 2018). Also, in chrysanthemum, flower color mutants were obtained at a higher frequency from cultured petals than from cultured leaves, both of which were irradiated with ion beams (Okamura et al. 2015). Similarly, compared with mock-treated petunia seedlings, those

treated with sucrose (to stimulate color pigment biosynthesis) yielded a higher frequency of flower color mutants after ion beam irradiation (Hase et al. 2010). In addition, it was demonstrated that the physiological status of plant tissue greatly affects the frequency and types of mutations induced by high-LET radiation at the molecular level (Hase et al. 2018). These findings are highly relevant for developing more efficient mutation breeding strategies to control the direction of mutation and also for understanding the molecular mechanism of mutagenesis by ionizing radiation.

Compared to acute gamma ray irradiation, the floral mutation spectrum was wider in chronic gamma ray irradiation. This suggests that novel mutants such as yellow, which had not been obtained in acute irradiation due to lethality, become obtainable by chronic irradiation. Due to its high-dosage, acute irradiation would cause a larger number of DNA damages in a cell per unit time than chronic irradiation (Sparrow et al. 1961). Thus, it is possible that, compared to chronic irradiation, cells irradiated with acute gamma rays are more likely to become lethal before genes responsible for a rare mutant are disrupted. In contrast, a new type of mutated cells might survive in chronic irradiation, while the number of disrupted genes per cell remains small.

Carnation has a long history of breeding and a vast diversity of cultivated varieties have been produced. Every possible variation in color is said to have been bred, and materials to create novel colors have been exhausted. However, we succeeded in creating a peculiar colored carnation with a highly metallic appearance. Diversifying the metallic color variation by a combination of crossbreeding and ion beam breeding provided a breakthrough to address this problem. The efficiency and effectiveness of ion beam breeding were verified in that metallic color mutants with superior characteristics were induced at higher rates than those previously reported (Okamura et al. 2003 and 2012). The whole gene region deletion in the metallic color mutants induced by ion beam irradiation directly lead to solid mutants. These results suggest a potential to a more effective mutation breeding in carnation.

Acknowledgements The authors thank Momose M, Umemoto N, Yasuno N, Ohtsuka M, Onishi N, Yamaguchi Y, Morishita T, Tanaka A, Shikazono N, Nakayama M, Sasaki N, and Ozeki Y for their assistance. A part of this study was supported by a grant for the Research and Development Program for New Bio-industry Initiatives from Bio-oriented Technology Research Advancement Institution, Japan.

References

Abe Y, Tera M, Sasaki N, Okamura M, Umemoto N, Momose M, Kawahara N, Kamakura H, Goda Y, Nagasawa K, Ozeki Y (2008) Detection of 1-*O*-malylglucose: pelargonidin 3-*O*-glucose-6″-*O*-malyltransferase activity in carnation (*Dianthus caryophyllus*). Biochem Biophys Res Comm 373:473–477. https://doi.org/10.1016/j.bbrc.2008.04.153

Blakely EA (1992) Cell inactivation by heavy charged particles. Radiat Environ Biophys 31:181–196

Bloor SJ (1998) A macrocyclic anthocyanin from red/mauve carnation flowers. Phytochemistry 49:225–228. https://doi.org/10.1016/S0031-9422(97)01051-0

Broertjes C (1968) Mutation breeding of vegetatively propagated crops. In: Fifth congress European association for research on plant breeding, Milan, pp 139–165

Cassells AC, Walsh C, Periappuram C (1993) Diplontic selection as a positive factor in determining the fitness of mutants of *Dianthus* 'Mystere' derived from x-irradiation of nodes in *in vitro* culture. Euphytica 70:167–174

FAO/IAEA Mutant Variety Database. https://mvd.iaea.org

Goodhead DT (1995) Molecular and cell models of biological effects of heavy ion radiation. Radiat Environ Biophys 34:67–72

Hackett WP, Anderson JM (1967) Aseptic multiplication and maintenance of differentiated carnation shoot tissue derived from shoot apices. Proc Amer Soc Hort Sci 90:365–369

Hase Y, Yamaguchi M, Inoue M, Tanaka A (2002) Reduction of survival and induction of chromosome aberrations in tobacco irradiated by carbon ions with different linear energy transfers. Int J Radiat Biol 78:799–806. https://doi.org/10.1080/09553000210152971

Hase Y, Okamura M, Takeshita D, Narumi I, Tanaka A (2010) Efficient induction of flower-color mutants by ion beam irradiation in petunia seedlings treated with high sucrose concentration. Plant Biotechnol 27:99–103. https://doi.org/10.5511/plantbiotechnology.27.99

Hase Y, Satoh K, Kitamura S, Oono Y (2018) Physiological status of plant tissue affects the frequency and types of mutations induced by carbon-ion irradiation in Arabidopsis. Sci Rep 8:1394. https://doi.org/10.1038/s41598-018-19278-1

Itoh Y, Higeta D, Suzuki A, Yoshida H, Ozeki Y (2002) Excision of transposable elements from the chalcone

isomerase and dihydroflavonol 4-reductase genes may contribute to the variegation of the yellow-flowered carnation (*Dianthus caryophyllus*). Plant Cell Physiol 43:578–585

Markham KR, Gould KS, Winefield CS, Mitchell KA, Bloor SJ, Boase MR (2000) Anthocyanin vacuolar inclusions–their nature and significance in flower colouration. Phytochemistry 55:327–336. https://doi.org/10.1016/S0031-9422(00)00246-6

Mato M, Onozaki T, Ozeki Y, Higeta D, Itoh Y, Yoshimoto Y, Ikeda H, Yoshida H, Shibata M (2000) Flavonoid biosynthesis in white-flowered Sim carnations (*Dianthus caryophyllus*). Sci Hortic 84:333–347. https://doi.org/10.1016/S0304-4238(99)00140-5

Matsuba Y, Sasaki N, Tera M, Okamura M, Abe Y, Okamoto E, Nakamura H, Funabashi H, Takatsu M, Saito M, Matsuoka H, Nagasawa K, Ozeki Y (2010) A novel glucosylation reaction on anthocyanis catalyzed by acyl-glucose dependent glucosyltransferase in the petals of carnation and delphinium. Plant Cell 22:3374–3389. https://doi.org/10.1105/tpc.110.077487

Mehlquist GA, Ober D, Sagawa Y (1954) Somatic mutations in the carnation, *Dianthus caryophyllus* L. Proc Natl Acad Sci USA 40:432–436

Morita Y, Hoshino A, Kikuchi Y, Okuhara H, Ono E, Tanaka Y, Fukui Y, Saito N, Nitasaka E, Noguchi H, Iida S (2005) Japanese morning glory *dusky* mutants displaying reddish-brown or purplish-gray flowers are deficient in a novel glycosylation enzyme for anthocyanin biosynthesis, UDP-glucose:anthocyanidin 3-*O*-glucoside-2″-*O*-glucosyltransferase, due to 4-bp insertions in the gene. Plant J 42:353–363. https://doi.org/10.1111/j.1365-313X.2005.02383.x

Nakayama M, Koshioka M, Yoshida H, Kan Y, Fukui Y, Koike A, Yamaguchi M (2000) Cyclic malyl anthocyanins in *Dianthus caryophyllus*. Phytochemistry 55:937–939. https://doi.org/10.1016/S0031-9422(00)00263-6

Nishizaki Y, Matsuba Y, Okamoto E, Okamura M, Ozeki Y, Sasaki N (2011) Structure of the acyl-glucose-dependent anthocyanin 5-*O*-glucosyltransferase gene in carnations and its disruption by transposable elements in some varieties. Mol Genet Genomics 286:383–394. https://doi.org/10.1007/s00438-011-0655-7

Okamura M, Yasuno N, Ohtsuka M, Tanaka A, Shikazono N, Hase Y (2003) Wide variety of flower-color and -shape mutants regenerated from leaf cultures irradiated with ion beams. Nucl Instrum Methods Phys Res B 206:574–578. https://doi.org/10.1016/S0168-583X(03)00835-8

Okamura M, Momose M, Umemoto N, Toguri T, Tanaka A, Hase Y, Yamaguchi Y, Morishita T (2006a) Flower breeding by quantum beam technology and their commercialization. In: Abstract, 27th international horticultural congress and exhibition (IHC 2006), pp 321–322

Okamura M, Tanaka A, Momose M, Umemoto N, da Silva JAT, Toguri T (2006b) Advances of mutagenesis in flowers and their industrialization. In: da Silva JAT (ed) Floriculture, ornamental and plant biotechnology, vol 1. Global Science Books, Isleworth, Middlesex, UK, pp 619–628

Okamura M, Umemoto N, Onishi N (2012) Breeding glittering carnations by an efficient mutagenesis system. Plant Biotechnol 29:209–214. https://doi.org/10.5511/plantbiotechnology.12.0104a

Okamura M, Nakayama M, Umemoto N, Cano EA, Hase Y, Nishizaki Y, Sasaki N, Ozeki Y (2013) Crossbreeding of a metallic color carnation and diversification of the peculiar coloration by ion-beam irradiation. Euphytica 191:45–56. https://doi.org/10.1007/s10681-012-0859-x

Okamura M, Hase Y, Furusawa Y, Tanaka A (2015) Tissue-dependent somaclonal mutation frequencies and spectra enhanced by ion beam irradiation in chrysanthemum. Euphytica 202:333–343. https://doi.org/10.1007/s10681-014-1220-3

Sagawa Y, Mehlquist GAL (1957) The mechanism responsible for some X-ray induced changes in flower color of the carnation, *Dianthus caryophyllus*. Am J Botany 44:397–403

Shikazono N, Tanaka A, Watanabe H, Tano S (2001) Rearrangement of the DNA in carbon ion-induced mutants of *Arabidopsis thaliana*. Genetics 157:379–387

Simard MH, Michaux-Ferriere N, Silvy A (1992) Variants of carnation (*Dianthus caryophylus* L.) obtained by organogenesis from irradiated petals. Plant Cell Tissue Organ Cult 29:37–42

Sparrow AH, Cuany RL, Miksche JP, Schairer LA (1961) Some factors affecting the responses of plants to acute and chronic radiation exposures. Radiat Bot 1:10–34

Stadler LJ (1928) Mutations in barley induced by X-rays and radium. Science 68:186–187

Tanaka A, Shikazono N, Yokota Y, Watanabe H, Tano S (1997) Effects of heavy ions on the germination and survival of *Arabidopsis thaliana*. Int J Radiat Biol 71:121–127

Umemoto N, Abe Y, Cano EA, Okamura M, Sasaki N, Yoshida S, Ozeki Y (2009) Carnation serine carboxypeptidase-like acyltransferase is important for anthocyanin malyltransferase activity and formation of anthocyanic vacuolar inclusions. In: 5th international workshop on anthocyanins 2009 in Japan, p 115

Yamaguchi H (2018) Mutation breeding of ornamental plants using ion beams. Breed Sci 68:71–78. https://doi.org/10.1270/jsbbs.17086

Zhang H, Wang L, Deroles S, Bennett R, Davies K (2006) New insight into the structure and formation of anthocyanic vacuolar inclusions in flower petals. BMC Plant Biol 6:29. https://doi.org/10.1186/1471-2229-6-29

Development of Violet Transgenic Carnations and Analysis of Inserted Transgenes

10

Noriko Nakamura, Takamasa Suzuki, Yukiko Shinbo, Steve Chandler, and Yoshikazu Tanaka

Abstract

The pink, red and magenta colors in carnation flowers are due to the accumulation of pelargonidin and cyanidin-based anthocyanins. Carnations lack violet/blue flowers due to an absence of delphinidin-based anthocyanins, which are the dominant anthocyanins in most species having violet or blue flowers. The deficiency of delphinidin is attributed to the lack of the *flavonoid 3',5'-hydroxylase* (*F3'5'H*) gene in carnation, the key gene for biosynthesis of delphinidin. Transgenic violet flower carnation varieties were generated by successful introduction and expression of a heterologous F3′5′H. Coexpression of a specific flavonoid biosynthesis gene or suppression of an endogenous gene involved in flavonoid biosynthesis was shown to enhance delphinidin accumulation. Some of the resultant transgenic carnation varieties have been commercialized in the USA, EU, Japan and other countries after obtaining the required permissions to release genetically modified organisms. Extensive molecular analysis of transgenic carnation is required by EU regulatory authorities and to a lesser extent in Japan. The analysis shows that the transgenic events often contain multiple transgenes and sometimes rearranged and/or partial T-DNA regions.

10.1 Introduction

The flavonoid biosynthetic pathway is generally well conserved among plants (Tanaka et al. 2008). Though successful modification of flower color by genetic engineering of the pathway (especially toward blue) has been reported in many plant species (Nishihara and Nakatsuka 2011; Tanaka and Brugliera 2013; Noda 2018; Okitsu et al. 2018), carnation is the species where most commercial progress has been made to date. Carnation is one of the most popular cut flower ornamentals with red, pink or magenta flowers available due to the accumulation of pelargonidin and cyanidin-based anthocyanins. Copigments, usually flavonols, also affect carnation flower color (Nakayama 2020; Ozeki 2020). However, carnation flowers lack a blue hue due to a deficiency of delphinidin-based anthocyanins. Delphinidin-based anthocyanins are typically

N. Nakamura · Y. Shinbo · Y. Tanaka (✉)
Suntory Global Innovation Center Ltd, Seika-dai, Seika-cho, Soraku-gun, Kyoto 619-0284, Japan
e-mail: Yoshikazu_Tanaka@suntory.co.jp

T. Suzuki
Department of Biological Chemistry, College of Bioscience and Biotechnology, Chubu University, 1200 Matsumoto-cho, Kasugai 487-8501, Aichi, Japan

S. Chandler
School of Applied Sciences, Royal Melbourne Institute of Technology, RMIT University, Bundoora, VIC 3083, Australia

T. Onozaki and M. Yagi (eds.), *The Carnation Genome*, Compendium of Plant Genomes,
https://doi.org/10.1007/978-981-15-8261-5_10

found in violet and blue flowers such as petunia, pansy and gentian. Flavonoid 3′,5′-hydroxylase (F3′5′H) is the key enzyme for delphinidin biosynthesis (Fig. 10.1) and the lack of delphinidin-based anthocyanin in carnation and *Dianthus* is attributed to lack of *F3′5′H* gene. *F3′5′H* genes, first isolated from petunia and then many species, have been used to engineer blue flowers in plants such as carnation, rose and chrysanthemum (Tanaka and Brugliera 2013). *F3′5′H* gene was introduced to carnation via *Agrobacterium*-mediated transformation to generate transgenics with novel blue hue flowers. Coexpression of an additional flavonoid gene or suppression of an endogenous gene was in some cases necessary for exclusive delphinidin accumulation and significant color change toward blue. The transgenic violet carnations (Fig. 10.2) have been marketed worldwide for more than 20 years. In this chapter, we will describe the development and commercialization of the violet carnations and present the results of extensive analysis of the introduced transgenes.

10.2 Development of Violet Carnations

10.2.1 Key Success Factors to Develop and Commercialize Transgenic Plants

Since the development and commercialization of genetically modified plants including violet carnation have been reviewed (Nishihara and Nakatsuka 2011; Tanaka and Brugliera 2013; Chandler and Tanaka 2018), we briefly describe the tactics necessary to generate transgenic plants suitable for commercialization here. Critical factors and/or steps are:

(i) Isolation of a key gene to confer a novel character to a host plant (a *F3′5′H* gene in the case of generating blue flowers). Since many useful genes have been isolated from various plant species, this step is not rate limiting.

(ii) Establishment of an efficient transformation protocol for a target species (carnation, Lu et al. 1991). Since the effectiveness of the transgene varies between transgenic events to a great extent, it is necessary to generate many transgenic plants to obtain an event with desired phenotypes. This step still requires laborious optimization of tissue culture protocols (Chandler and Tanaka 2018) and some plant species/varieties are recalcitrant to transformation.

(iii) Optimization of transgene expression. Expression of a transgene is commonly regulated by a promoter sequence. Both constitutive and tissue-specific promoters can be used. It is not always easy to predict which promoter will work most satisfactorily in a target species. It may also be necessary to modify competing biosynthetic pathway(s) using RNAi or genome editing, an example of which will be described below.

(iv) Choosing a commercially viable variety with the proper genetic background for phenotypic modification is also important.

10.2.2 Engineering the Carnation Flavonoid Biosynthetic Pathway to Alter Flower Color

The generation of transgenic violet carnations has been previously reported in detail (Tanaka and Brugliera 2013). Overexpression of petunia *F3′5′H* cDNA in a carnation line accumulating pelargonidin resulted in a mixture of pelargonidin and delphinidin in flowers, with a marginal shift toward blue. The mixture of pelargonidin and delphinidin was due to competition of the introduced F3′5′H with endogenous biosynthetic enzymes such as flavonoid 3′-hydroxylase, flavonol synthase and dihydroflavonol 4-reductase (DFR) (Fig. 10.1). It is noteworthy that some plant species such as petunia contain DFR which efficiently catalyzes dihydromyricetin and not

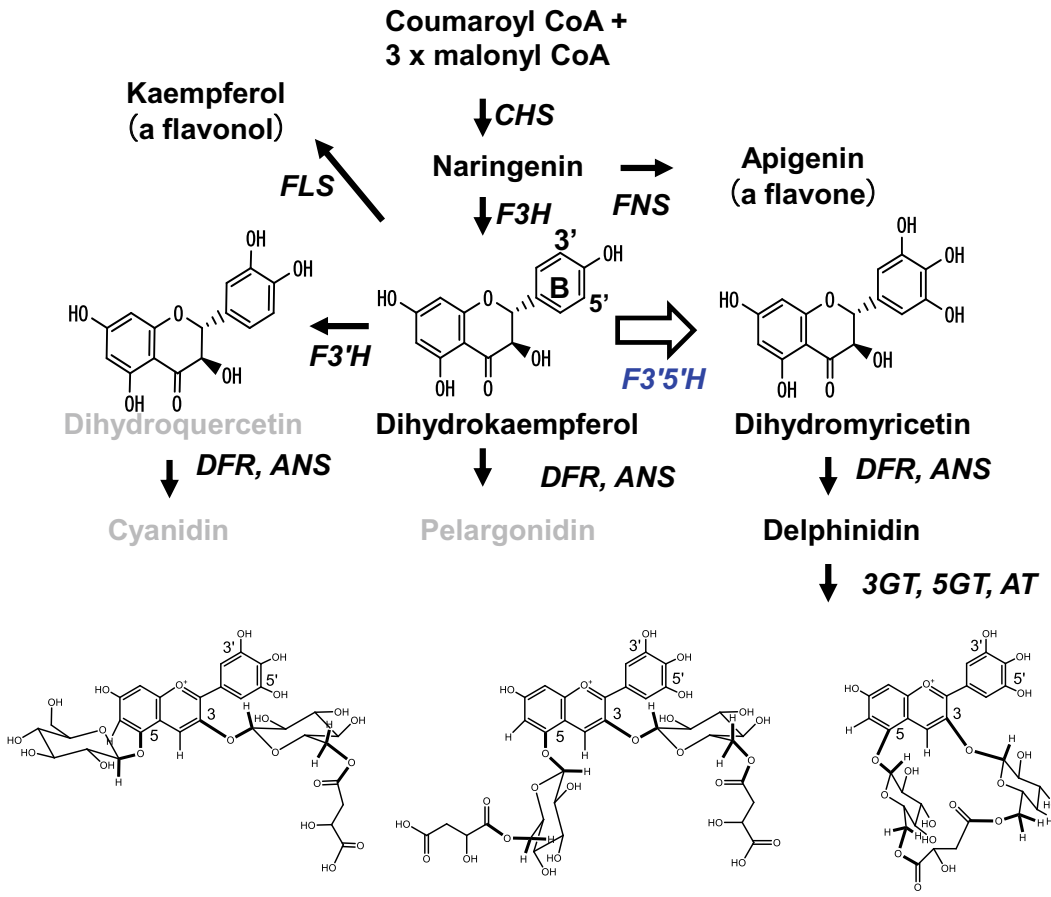

Fig. 10.1 Flavonoid biosynthetic pathway focusing on carnation. The pathway leading to anthocyanins in carnation. The transgenic carnations expressing heterologous flavonoid 3′,5′-hydroxylase (F3′5′H) gene mainly accumulate three delphinidin-derived anthocyanins (Fukui et al. 2003). See Chapter 8 for details. CHS, chalcone synthase; CHI, chalcone isomerase; F3H, flavanone 3-hydroxylase; F3′H, flavonoid 3′-hydroxylase; DFR, dihydroflavonol 4-reductase; ANS, anthocyanidin synthase; 3GT, UDP-glucose: anthocyanidin 3-*O*-glucosyltransferase; 5GT, malyl glucose-dependent anthocyanin 5-glucosyltransferase; AT, malyl glucose-dependent anthocyanin acyltransferase; FLS, flavonol synthase; FNS, flavone synthase (Most carnation varieties do not have FNS)

dihydrokaempferol, which is the reason why petunia does not accumulate pelargonidin and thus does not have brick red/orange flowers (Meyer et al. 1987). Petunia *DFR* is therefore a suitable gene for accumulation of delphinidin-based anthocyanins in transgenic plants.

To avoid the competition described above, white carnation varieties deficient in *DFR* gene were chosen as hosts. Two binary vectors (pCGP1470 and pCGP1991, Fig. 10.3) containing a pansy or petunia *F3′5′H* gene and a petunia *DFR* gene were constructed. In pCGP1470, petunia *F3′5′H* and petunia *DFR* cDNAs are under the control of a petal specific snapdragon chalcone synthase promoter and a constitutive promoter (Mac1 promoter) respectively, while pCGP1991 contains pansy *F3′5′H* cDNA under the control of the snapdragon chalcone synthase promoter and petunia *DFR* genomic DNA including the promoter, coding region with introns and terminator (Fig. 10.3).

A white midi (single-flowered, dwarf carnation varieties developed by Mediterranean breeders for high productivity) variety, deficient

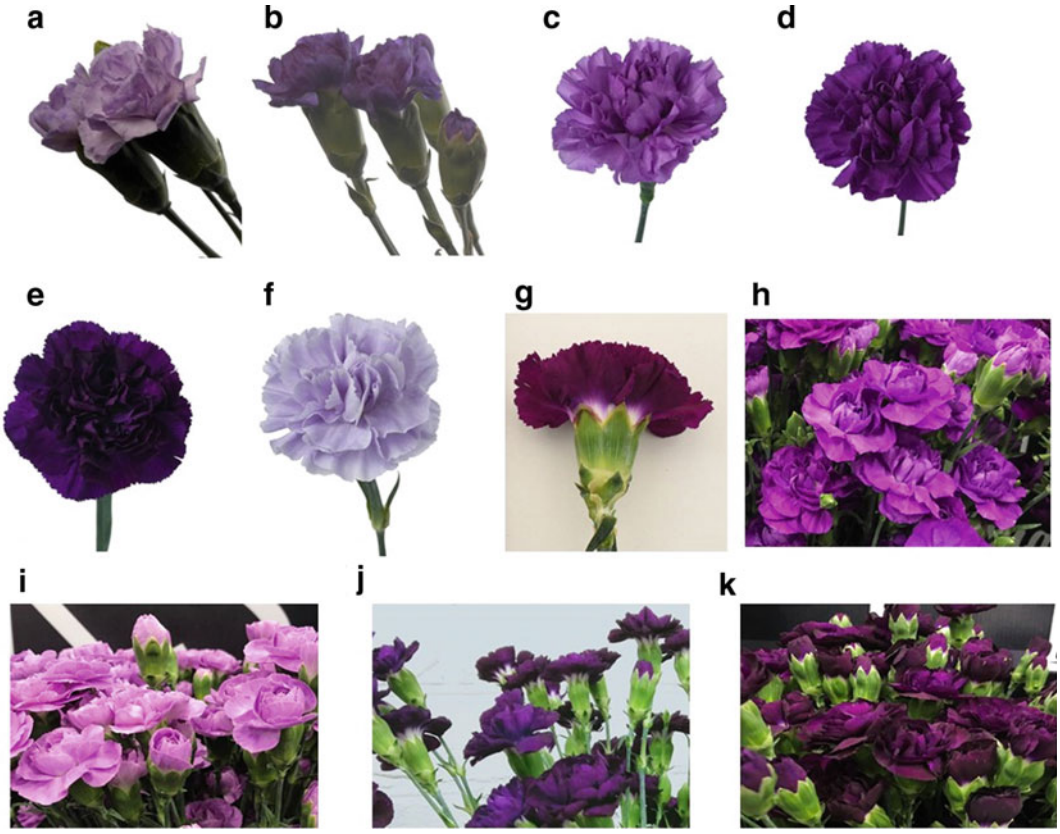

Fig. 10.2 Transgenic carnation varieties. **a** 'Moondust,' **b** 'Moonshadow,' **c** 'Moonlite,' **d** 'Moonshade,' **e** 'Moonvista,' **f** 'Moonaqua,' **g** 'Moontea,' **h** 'Moonberry,' **i** 'Moonpearl,' **j** 'Moonvelvet,' **k** 'Moonique'

in *DFR* gene, was transformed with *Agrobacterium* harboring pCGP1470. The resultant transgenic plants exhibited pale violet flowers exclusively accumulating delphinidin-based anthocyanins ('Moondust' OECD unique identifier FLO-Ø7442-5, Fig. 10.2a). This result indicated that coexpression of heterologous F3′5′H and DFR efficiently directed the carnation flavonoid biosynthetic pathway toward delphinidin. A selected line was commercialized with the brand name of 'Moondust' in 1996 in Australia followed by the USA and Japan. This was the first commercialization of a transgenic ornamental plant. The same midi host was also transformed with *Agrobacterium* harboring pCGP1991 to result in a variety with darker violet-colored flowers 'Moonshadow' (OECD unique identifier FLO-11363–2, Fig. 10.2b).

The standard-type white carnation variety 'Cream Cinderella,' deficient in *DFR* gene, was transformed with pCGP1470 to yield violet-flower transgenic lines having a range of anthocyanin amounts and color intensities. Such phenotypical variation is common in plant transformation experiments. Currently, two lines from the transgenic plants are commercialized; 'Moonlite' (OECD unique identifier FLO-4Ø644-6, Fig. 10.2c) and 'Moonshade' (OECD unique identifier FLO-4Ø619-8, Fig. 10.2d).

The introduction of pCGP1991 to the same host also yielded violet flower color modified carnations. The flower color in transgenics produced using this transformation vector tends to be darker than those with pCGP1470 and one of the darkest lines was selected for commercialization ('Moonvista'; OECD unique identifier FLO-4Ø685-2,

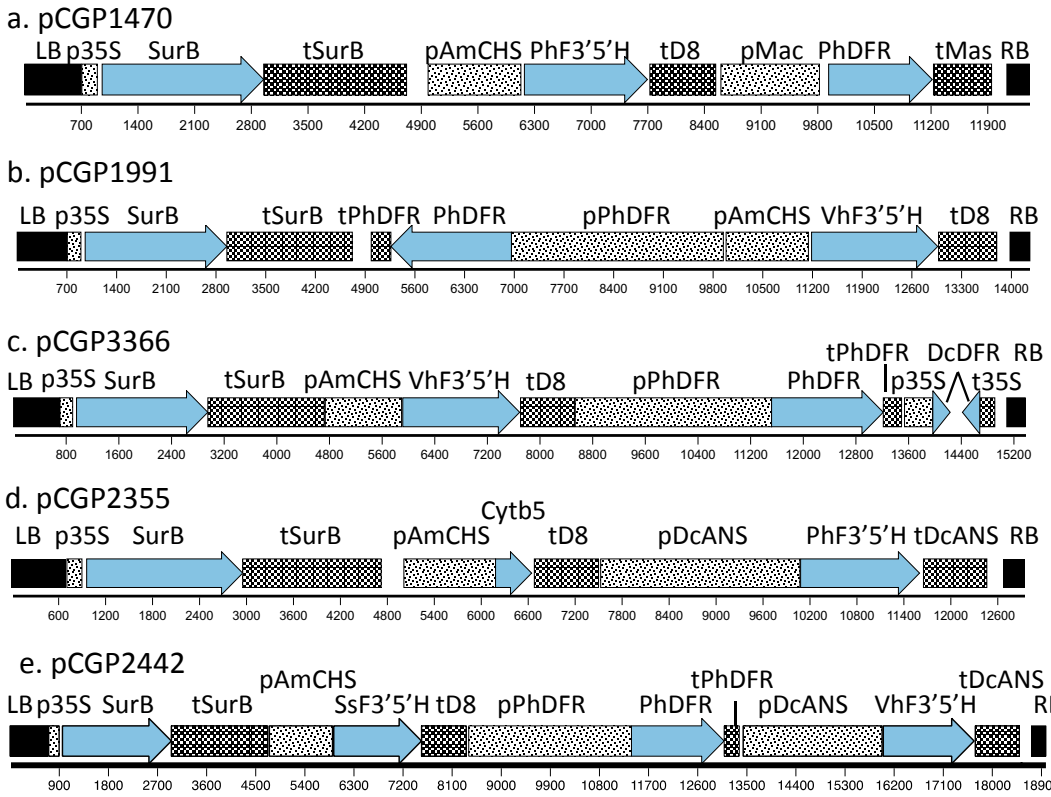

Fig. 10.3 T-DNA regions of the binary vectors. Coding sequences are shown in blue and left border (LB) and right border (RB) are shown in black. p35S, cauliflower mosaic virus 35S promoter; *SurB,* a tobacco acetolactate synthase gene conferring herbicide resistance to plants; tSurB, tobacco *SurB* terminator; pAmCHS, *Antirrhinum majus CHS* promoter; PhF3′5′H, *Petunia hybrida flavonoid 3′,5′-hydroxylase* cDNA; tD8, petunia lipid transfer protein gene terminator; pMac, *Mac1* promoter; PhDFR in pCGP1470, petunia *dihydroflavonol 4-reductase* cDNA; tMas, *Agrobacterium* manopine synthase terminator; pPhDFR, petunia *DFR* promoter; PhDFR, petunia genomic *DFR* including introns; tPhDFR, petunia *DFR* terminator; VhF3′5′H, viola *F3′5′H*cDNA; DcDFR, carnation *DFR*c DNA; Cytb5, petunia cytochrome *b5*; pDcANS, carnation *ANS* promoter; tDcANS, carnation *ANS* terminator; SsF3′5′H, *Salvia sp. F3′5′H* cDNA

Fig. 10.2e). Interestingly, a pale color line was also obtained and commercialized ('Moonaqua'; OECD unique identifier FLO-4Ø689-6, Fig. 10.2f). It is also interesting that 'Moonshadow' has bluer flowers than the lines derived from 'Cream Cinderella' although all the transgenic plants mainly accumulate delphinidin 3,5-diglucoside modified with malyl group in the flowers. The blueness in flowers of 'Moonshadow' is due to the presence of flavone *C*-glucoside (apigenin 6-*C*-glucosyl-7-*O*-glucoside-6‴-malyl ester). This compound is present in the host flowers and plays a role as a copigment, causing bathochromic shift (bluer and darker color) (Fukui et al. 2003). In later experiments, the pink-flower colored variety Cinderella was used as a host and transformed with pCGP1991. The resultant transgenic variety 'Moontea' (OECD unique identifier SHD-27531–4, Fig. 10.2g) is slightly redder than 'Moonshade' but has been successfully commercialized.

In 1998, transcribing double-strand RNA (RNA interference (RNAi)) was shown to efficiently down-regulate a target sequence in plants (Waterhouse et al. 1998). Down-regulation of endogenous DFR was achieved in carnation using this technology. A binary vector pCGP3366 (Fig. 10.3c) containing a cassette transcribing carnation *DFR* double-strand RNA

in addition to the cassettes in pCGP1991 was used to transform the spray-type variety 'Cerise Westpearl' (CWP). While the flowers of the host were pink (pelargonidin), the flowers of the transgenic lines were a range of purple/violet shades. Two lines, 'Moonberry' (OECD unique identifier IFD-25958–3, Fig. 10.2h) and 'Moonpearl' (OECD unique identifier IFD-25947–1, Fig. 10.2i) were selected for commercialization. Successful artificial down-regulation of endogenous DFR indicates that varieties of carnation other than *DFR* mutants can be utilized as hosts to generate transgenic lines with violet flowers.

An alternative tactic to change the pathway to delphinidin is to enhance the efficiency of F3′5′H activity. Again, using CWP as a host, additional expression of a petunia cytochrome $b_5$to transfer electrons to F3′5′H (pCGP2355, Fig. 10.3d) resulted in the darkest purple color flowered transgenic event among Moon carnations, 'Moonvelvet' (OECD unique identifier IFD-26407–2, Fig. 10.2j). Expression of two *F3′5′H* genes (pCGP2442; pansy and salvia *F3′5′H*) in the host 'Kortina Chanel' resulted in production of the transgenic line 'Moonique' (OECD unique identifier IFD-19907- 9, Fig. 10.2k) with similar, but slightly redder, dark-colored flowers.

10.3 Analysis of Transgenes in Violet Carnations

Transfer of T (transfer)-DNA to plants via *Agrobacterium* has been widely used to generate transgenic plants. T-DNA is segmented by two similar 25 bp sequences, the right (RB) and left (LB) borders. The RB is an essential cis-acting sequence for transfer and the LB defines the end of the transfer (De Buck et al. 1999). Some transgenic plants contain a single and clean integration of T-DNA in their genome while some contain multiple T-DNAs sometimes accompanied with end-to-end ligation of RB sequence (De Buck et al. 1999). Simple single-copy integration is desirable for stable gene expression since plural integrations or rearranged integrations may trigger gene silencing or recombination. Although there is variation in transgene expression, it has been shown in *Arabidopsis* that a single copy insertion gave similar level of gene expression regardless of integration site in the genome (Nagaya et al. 2005). Furthermore, since some regulatory authorities require complete sequence analysis of the transgenes and their flanking sequences, a transgenic plant having a single copy insertion is more desirable, as molecular analysis is much easier than for events with multiple inserts. It also reasonable to choose a transgenic line that does not include integrated sequences derived from the vector backbone (absence of vector DNA is often referred as "clean integration"). Integration of vector sequences is common in transgenic plants as shown by example in *Medicago sativa* (Nicolia et al. 2017).

In parallel with phenotypic selection, we carried out Southern analysis of some transgenic carnation varieties to identify copy number (summarized in Table 10.1). Extensive analysis revealed that some transgenic carnation varieties have complicated integrations, which will be described here.

When a transgenic carnation contains one or two transgenes with a simple integration pattern, conventional inverse PCR using genomic DNA and/or construction of a genomic library successfully provided integration data. It is not so easy to analyze transgenic lines with multiple integrations with complicated integration patterns. Analysis of 'Moondust,' 'Moonshade,' 'Moonpearl' and 'Moonique' are not complete. The information on the genome structure of carnation (Yagi et al. 2014) and the carnation database (https://carnation.kazusa.or.jp/) helped to obtain flanking sequences around the integrated transgenes (Table 10.1). Flanking sequences are necessary because possible open reading frames generated by integration of T-DNA need to be subjected to in silico allergen analysis for the EU regulatory authorities.

Short transformation vector sequence from outside of T-DNA region is sometimes integrated into the carnation genome. Trial and long-term production data show that this is not detrimental to growth or health of the transgenic carnation

Table 10.1 Summary of the transgenic carnation varieties

Variety name	Vector	Host (color)	Locus	Scaffold number 5′ side	3′ side
Moondust	pCGP1470	Unesco (white)	N. D		
Moonshadow	pCGP1991	Unesco (white)	Locus 1	3386	3386
			Locus 2	25,239	6190
			Locus 3	1542	2542
Moonlite	pCGP1470	Cream Cinderella (white)	Locus 1	3618	3618
			Locus 2	8	8
Moonshade	pCGP1470	Cream Cinderella (white)	N. D		
Moonvista	pCGP1991	Cream Cinderella (white)	Locus 1	-	69
			Locus 2	516	516
			Locus 3	83	83
			Locus 4	1366, 741	–
Moonaqua	pCGP1991	Cream Cinderella (white)	Locus 1	36,879 83	680
			Locus 2	337	337
			Locus 3	759	759
Moontea	pCGP1991	Cinderella (pink)	Locus 1	1330	1330
Moonberry	pCGP3366	Cerise Westpearl (pink)	Locus 1	169	169
Moonpearl	pCGP3366	Cerise Westpearl (pink)	N. D		
Moonvelvet	pCGP2355	Cerise Westpearl (pink)	Locus 1	127	1563
Moonique	pCGP2442	Kortina Chanel (pink)	N. D		

N. D., Not determined; –, not identified. Scaffold numbers are based on Yagi et al. 2014 and the carnation database (https://carnation.kazusa.or.jp/)

and bioinformatic analysis indicates no new ORFs are generated as a result of these integrations. Extra-T-DNA integration of the antibiotic-resistant gene (in this case, tetracycline-resistant gene) used as a bacterial selection marker would not be acceptable from a regulatory point of view and molecular analysis has shown this has not occurred in any of the transgenic varieties where integration has been fully analyzed.

10.4 'Moonshadow' FLO-11363–2

'Moonshadow' contains three loci having complicated transgene insertion patterns (Fig. 10.4). The first locus contains two expression cassettes of F3′5′H and two RB sequences. The locus is in Scaffold 3386. It also contained two unknown sequences, one of which turned out to be from Scaffold 3386 and the other of which is unidentified. These results indicate T-DNA can be integrated via complex rearrangement. Both locus 2 and locus 3 contain two intact expression units of *F3′5′H* and *DFR* cDNA. High transgene expression associated with such multiple integrations of F3′5′H and DFR may contribute to the high anthocyanin content and dark flower color of 'Moonshadow.' The 5′-flanking sequence of Locus 2 matched Scaffold 25,239 while the 3′-flanking sequence matched Scaffold 6190. Both flanking sequences of Locus 3 matched Scaffold 1542.

10.5 'Moonlite' FLO-40644–6

'Moonlite' has two integrations, one contains the full T-DNA region and an additional sequence of the binary vector and the other is a partial sequence derived from the right border side of

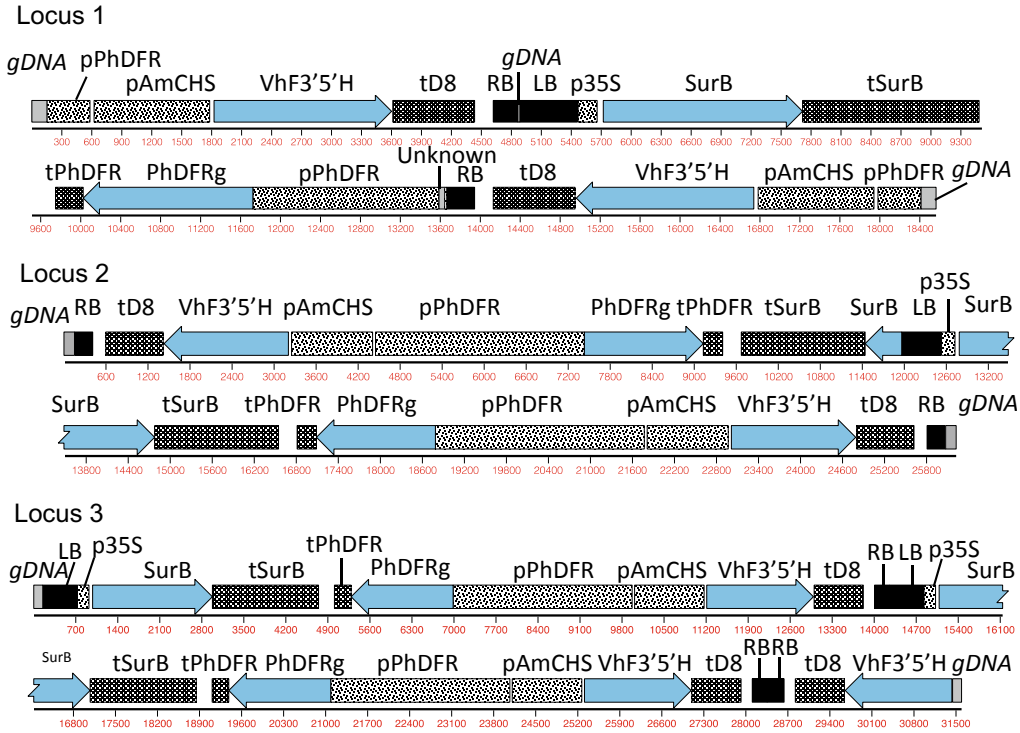

Fig. 10.4 The structures of the inserted transgenes in the 'Moonshadow' genome gDNA, carnation genome

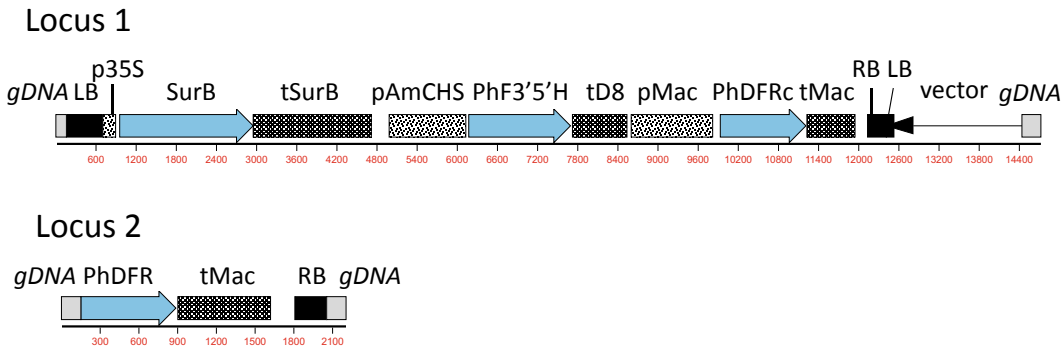

Fig. 10.5 The structures of the inserted transgenes in the 'Moonlite' genome

the T-DNA (Fig. 10.5). The two integrations are in Scaffold 3618 and Scaffold 8.

10.6 'Moonvista' FLO-40685–2

The initial southern blot analysis indicated that 'Moonvista' contained two copies of LB, two copies of *SurB*, one copy of petunia *DFR*, three copies of pansy *F3′5′H* and four RB sequences. Genomic library screening and inverse PCR showed there to be two integration sites (Locus 1 and Locus 2). Locus 1 contained one copy of the full T-DNA sequence and a partial *F3′5′H* expression unit. Its 5′ flanking sequence did not match any known genome scaffold sequences while the 3′ flanking sequence had high

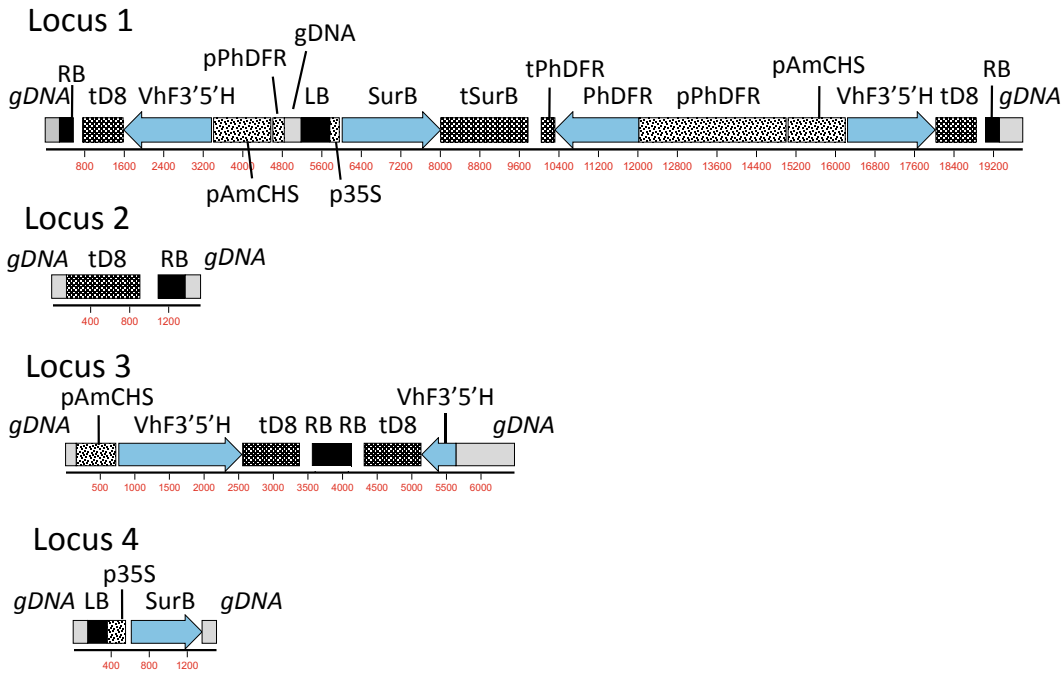

Fig. 10.6 The structures of the inserted transgenes in the 'Moonvista' genome

homology to Scaffold 69. Locus 2 (in Scaffold 516) contains a partial T-DNA containing the D8 terminator and RB sequences (Fig. 10.6). As the sequence information for Locus 1 and Locus 2 did not match with the copy numbers predicted by the Southern analysis, we analyzed the genome again with a next-generation sequencer. Mate-pair libraries (3 and 10 kb) were sequenced with a HiSeq2000 sequencer (Illumina) following which the reads containing T-DNA sequences were collected and assembled. The mate-pair reads having T-DNA sequences at both ends were regarded to be derived from the internal integrated T-DNA sequences while those having T-DNA sequences at one end and unknown sequences at the other ends were regarded to span integrated T-DNA and carnation genome sequence. The analysis identified flanking sequences, which matched Locus 1 and Locus 2 and another short integration locus not detected with Southern analysis, Locus 4. The 5′ flanking sequence of this locus matched Scaffolds 1366 and 741 while the 3′ flanking sequence did not match any of the scaffolds in the carnation genome sequence. Our experience with the analysis of this event shows that Southern analysis may not be an appropriate method for comprehensive analysis of transgene integration.

Another locus (Locus 3) also not inferred from Southern analysis was also found in 'Moonvista.' Two assembles containing the T-DNA sequence, which did not match Locus 1, 2 and 4 were obtained. They only had one flanking sequence (which matched Scaffold 83) which suggested that the two assembles are nascent. Developing a sequence analysis program making use of 1.4 billion reads revealed the complete structure of Locus 3 (Fig. 10.6). Locus 3 contains long inverted repeats consisting of *F3′5′H*, *tD8* and RB. Such inverted repeats were assumed to hamper sequence analysis by inverse PCR and library construction.

10.7 'Moonaqua' FLO-40689–6

'Moonaqua' contains three integration sites. Locus 1 (the 5′ flanking sequence matched with Scaffold 36,879 and 83 and the 3′ flanking sequence with Scaffold 680) contains the full T-

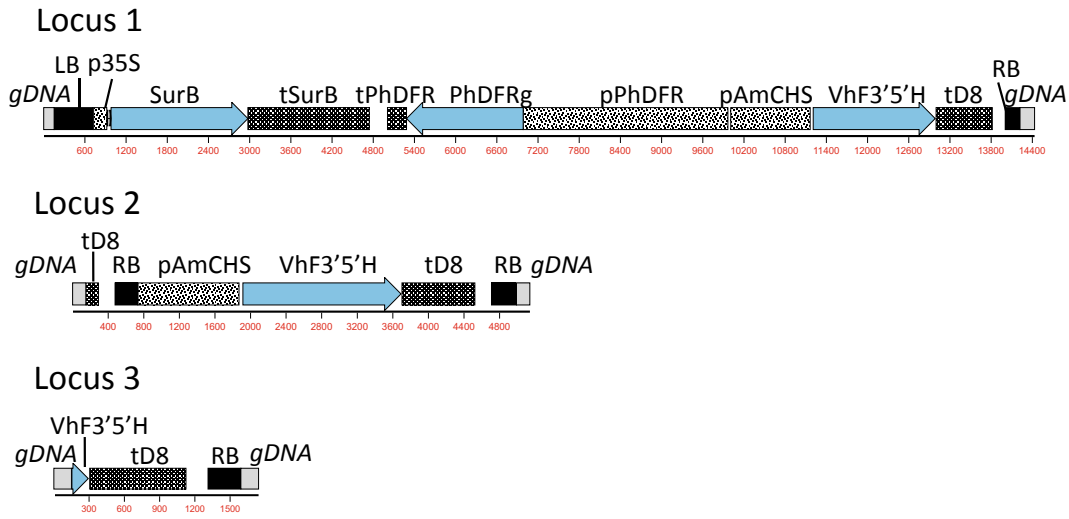

Fig. 10.7 The structures of the inserted transgenes in the 'Moonaqua' genome

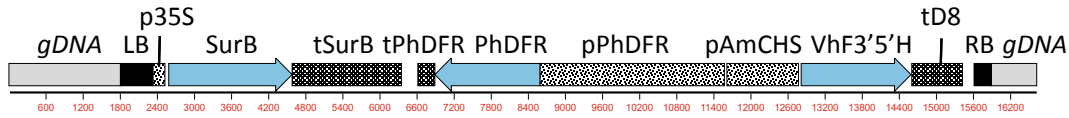

Fig. 10.8 The structure of the inserted transgenes in the 'Moontea' genome

DNA sequence. Locus 2 (in Scaffold 337) has only a *F3'5'H* expression unit with RB sequences in both ends. Locus 3 (in Scaffold 759) contains a partial expression unit of *F3'5'H* close to the right border (Fig. 10.7). Flowers of the variety 'Moonaqua' accumulated the lowest concentration of anthocyanin of any transgenic carnation variety generated using the transformation vectors pCGP1470 or pCGP1991 (Tanaka and Brugliera 2013). It is possible that the multiple integrations in this event interfere with efficient transgene expression.

10.8 'Moontea' SHD-27531–4

The pink variety 'Cinderella' was transformed with *Agrobacterium* containing pCGP1991 and transgenic lines with a reddish–bluish flower color were obtained. To avoid analytical complexity examples of which are outlined above, 'Moontea' was selected for commercialization after screening and confirmation that the event had a single, clean, transgene integration (Fig. 10.8). In 'Moontea,' the transgene insertion is on Scaffold 1330.

10.9 'Moonberry' IFD-25958–3 and 'Moonvelvet' IFD-26407–2

Southern analysis of these lines indicated that they both contain a single insert in their genomes. Amplification of the relevant sequences by PCR and inverse PCR and subsequent Sanger sequencing by primer walking also revealed that they both contain an intact T-DNA sequence, without extra sequences from the transformation vector (Fig. 10.9). Bioinformatic analysis of flanking sequences showed that the integration in 'Moonberry' is in Scaffold 169 of the carnation genome. The 5′ flanking sequence at the integration site for 'Moonvelvet' matched Scaffold

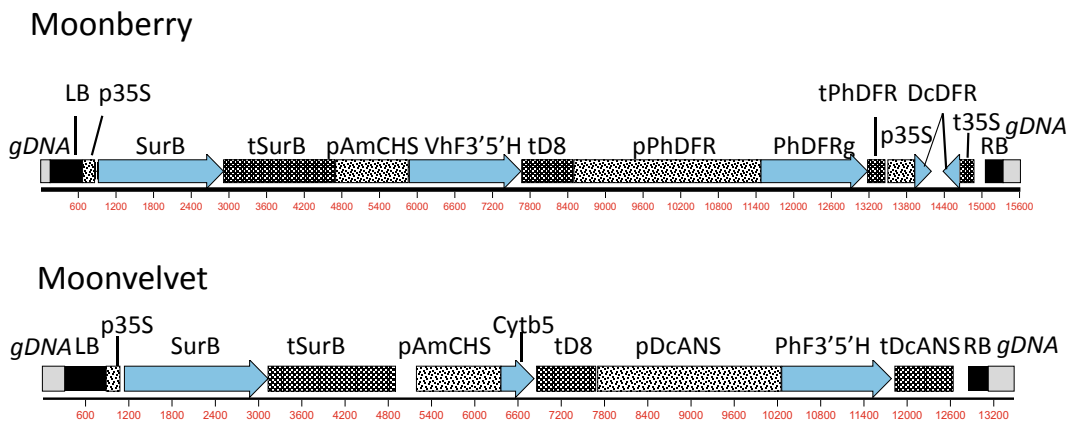

Fig. 10.9 The structures of the inserted transgenes in the 'Moonberry' and 'Moonvelvet' genomes

127 and the 3′ flanking sequence matched Scaffold 1563.

10.10 Concluding Remarks

As outlined in this chapter, transgenic carnation varieties with novel color have been developed by engineering the production of delphinidin-based anthocyanins in flowers. Several varieties have now been available for more than 20 years. Modification of multiple varieties, in different hosts, has been successfully achieved, which makes flower color manipulation in carnation an example of a genetic modification that can be reliably applied across several parental backgrounds. Because it is a vegetatively propagated plant, the commercialization history of transgenic carnation is a unique case for genetically modified plants and is also the only ornamental GMO with such a long timeline of commercialization.

Molecular analysis of the different transgenic carnation varieties confirmed that integration pattern of transgenes cannot be predicted after transformation. The first transgenic varieties to be developed, relatively early in the history of the technology and before it was decided to screen for single clean, integration events, usually had multiple insertion sites with incomplete insertions and rearrangements. There was no correlation between the number of insertion sites or amount of transgene rearrangement and the level of anthocyanin accumulation. All the transgenic carnation varieties have been stable and have retained their characteristic phenotype, measured by the delphinidin concentration in flowers. This observation shows that phenotypic stability in carnation is not a function of the complexity of transgene integration.

The complexity of transgene integration does, however, come at the cost of elaborate, time-consuming molecular analysis for regulatory approval and in practice, it is a sensible product development policy to screen for single integration.

References

Chandler SF, Tanaka Y (2018) Transgenic Research in Floricultural Crops. In: Rout RG, Peter KV (eds) Genetic Engineering of Horticultural Crops. Academic Press, pp 121–136

De Buck S, Jacobs A, Van Montagu M, Depicker A (1999) The DNA sequences of T-DNA junctions suggest that complex T-DNA loci are formed by a recombination process resembling T-DNA integration. Plant J 20:295–304

Fukui Y, Tanaka Y, Kusumi T, Iwashita T, Nomoto K (2003) A rationale for the shift in colour towards blue in transgenic carnation flowers expressing the flavonoid 3′,5′-hydroxylase gene. Phytochemistry 63:15–23

Lu CY, Nugent G, Wardley-Richardson T, Chandler SF, Young R, Dalling MJ (1991) *Agrobacterium*-mediated transformation of carnation (*Dianthus caryophyllus* L.). Nat Biotechnol 9:864–868

Meyer P, Heidemann I, Forkmann G, Saedler H (1987) A new petunia flower colour generated by

transformation of a mutant with a maize gene. Nature 330:677–678

Nagaya S, Kato K, Ninomiya Y, Horie R, Sekine M, Yoshida K, Shinmyo A (2005) Expression of randomly integrated single complete copy transgenes does not vary in *Arabidopsis thaliana*. Plant Cell Physiol 46:438–444

Nicolia A, Ferradini N, Veronesi F, Rosellini D (2017) An insight into T-DNA integration events in *Medicago sativa*. Int J Mol Sci 18:1951

Nishihara M, Nakatsuka T (2011) Genetic engineering of flavonoid pigments to modify flower color in floricultural plants. Biotechnol Lett 33:433–441

Nakayama M (2020) Flower pigments responsible for cyanic, yellow, and pale-yellow coloration of carnation. In: Yagi M, Onozaki T (eds) The Carnation Genome, Springer, pp 61–79

Noda N (2018) Recent advances in the research and development of blue flowers. Breed Sci 68:79–87

Okitsu N, Noda N, Chandler S, Tanaka Y (2018) Flower color and its engineering by genetic modification. In: Huylenbroeck JV (ed) Ornamental Crops. Handbook of Plant Breeding, vol 11, Springer, Switzerland, pp 29–62

Ozeki Y (2020) Molecular mechanisms of carnation flower colors by anthocyanin and flavonoid biosynthetic pathways. In: Yagi M, Onozaki T (eds) The Carnation Genome, Springer, pp 99–117

Tanaka Y, Brugliera F (2013) Flower colour and cytochromes P450. Phil Trans R Soc B 368 (1612):20120432

Tanaka Y, Sasaki N, Ohmiya A (2008) Plant pigments for coloration: Anthocyanins, betalains and carotenoids. Plant J 54:733–749

Yagi M, Kosugi S, Hirakawa H, Ohmiya A, Tanase K, Harada T, Kishimoto K, Nakayama M, Ichimura K, Onozaki T, Yamaguchi H, Sasaki N, Miyahara T, Nishizaki Y, Ozeki Y, Nakamura N, Suzuki T, Tanaka Y, Sato S, Shirasawa K, Isobe S, Miyamura Y, Watanabe A, Nakayama S, Kishida Y, Kohara M, Tabata S (2014) Sequence analysis of the genome of carnation (*Dianthus caryophyllus* L.). DNA Res 21:231–241

Waterhouse PM, Graham MW, Wang M-B (1998) Virus resistance and gene silencing in plants can be induced by simultaneous expression of sense and antisense RNA. Proc Natl Acad Sci USA 95:13959–13964

The Characteristics of Flower Scents in Carnations

11

Kyutaro Kishimoto

Abstract

Benzenoid aromatic compounds are the most important scent components of *Dianthus*, although some wild *Dianthus* species also produce terpenoids and fatty acid derivatives as principal scent components, and thereby having diverse scents. The scent of *Dianthus* carnations is described as spicy and is generally ascribed to eugenol. Our research shows lower diversity of carnation scents than wild *Dianthus* scents and differing main scent types among cultivars for cut and potted flowers. We also found that scents of most of the current cultivars for cut flowers were not spicy and had fruity notes derived from methyl benzoate. In addition, scent emissions decreased sharply after harvesting, and were almost absent after a few days. In this chapter, we describe the chemistry of scents from the current carnation cultivars. In plants, methyl benzoate is usually synthesized from benzoic acid by benzoic acid carboxyl methyltransferases (BAMT). Hence, the corresponding gene *BAMT* is considered important for scent biosynthesis in carnations. From nucleotide sequence analyses of the carnation genome, more than 10 candidate *BAMT* genes were found. We describe the characteristics of this gene and its homologs in the second half of this chapter.

11.1 Introduction

In reviews of fragrance-related publications, it is clear that the scent of carnations (*Dianthus caryophyllus* L.) has long been used as a fragrance (Anonis 1985; Ghozland and Fernandez 2010). Moreover, perfumes that imitate carnation scents are widely marketed on the internet. But the real scent of fresh carnation flowers may be familiar to few people. In our questionnaire survey of about 1,000 ordinary people in Japan, less than 8% could recall the actual scent of carnations (Kishimoto et al. 2012), whereas 20, 70, and 66% of people claimed familiarity with the scents of chrysanthemums, roses, and lilies, respectively. Hence, although carnations are widely perceived as aromatic flowers in books and other literature, few Japanese people have experienced the scent of carnations.

The carnation scent is described as spicy and similar to that of cloves (Ghozland and Fernandez 2010), and the benzenoid aromatic compound eugenol is identified as a major source of this scent (Clery et al. 1999). Therefore, to experience the scent of carnations described in the literature, one merely needs to open the lid of a clove bottle and smell the spicy fragrance of

K. Kishimoto (✉)
Institute of Vegetable and Floriculture Science, NARO, 2-1 Fujimoto, Tsukuba 305-0852, Ibaraki, Japan
e-mail: cucumber@affrc.go.jp

T. Onozaki and M. Yagi (eds.), *The Carnation Genome*, Compendium of Plant Genomes,
https://doi.org/10.1007/978-981-15-8261-5_11

eugenol. At the florist, carnations are available as red, white, yellow, green, and brown flowers that have been produced by traditional breeding, and blue flowers that were developed through genetic engineering (Fukui et al. 2003). With knowledge of the scent of eugenol, one could ask whether the scents of these flowers are as diverse as their colors, and whether the spicy scent of cloves is present?

In this chapter, we summarize the scent characteristics of currently marketed carnations.

11.2 Scent Diversity in Carnations

Carnations are flowers of the *Dianthus* family, which originate from an evolutionary hot spot on the Mediterranean coast (Valente et al. 2010). In this region, wild *Dianthus* species have adapted to dryness (Valente et al. 2010) and the rich variety of scents from wild *Dianthus* reflects species diversity in the genus.

11.2.1 Wild Dianthus Scents

The scents of many wild *Dianthus* species are thought to originate from benzenoid aromatic compounds such as isoeugenol, methyl salicylate, methyl benzoate, and benzyl benzoate (Kishimoto et al. 2011, 2013). These benzenoids are synthesized from sugar metabolites of glycolysis and the pentose phosphate cycle (Fig. 11.1). These substrates are converted to phenylpropanoid/benzenoids via the shikimate pathway (Fig. 11.1; Muhlemann et al. 2014). Methyl salicylate is generally used as a fragrance in foods and beverages (Burdock 2010). Moreover, because this compound has anti-inflammatory activities, it is frequently used as a medicine. The scent of methyl salicylate is often perceived as sweet or medicinal (Burdock 2010; Clery et al. 1999). For many Japanese, this scent is that of poultice, yet in the USA, this scent is commonly associated with root beer. The scent of methyl benzoate is described as fruity or floral (Burdock 2010). It is also the main component of the sweet scent of petunia (*Petunia hybrida*) and snapdragon (*Antirrhinum majus*; Negre et al. 2003). Benzyl benzoate also has a pleasant scent and is used in perfumes (Burdock 2010). Various other scent compounds have been detected in wild *Dianthus*, and most are fragrant benzenoids (Kishimoto 2012; Kishimoto et al. 2011).

The fatty acid derivatives (*Z*)-3-hexenol and (*Z*)-3-hexenyl acetate are principal scents in several minor wild *Dianthus* species (Kishimoto et al. 2011). These compounds are synthesized via the hydroperoxide lyase pathway of oxylipin metabolism and are often called green leaf volatiles (Matsui 2006). (*Z*)-3-hexenol smells of chopped leaves and the scent of (*Z*)-3-hexenyl acetate is described as green and fruity with a floral note that is reminiscent of banana (Burdock 2010).

Dianthus superbus flowers are widely distributed from Europe to the Far East and their scents, which are based on terpenoids (Galbally and Galbally 1997; Kishimoto et al. 2011), reportedly increase at night (Erhardt 1991). This feature is considered suitable for nocturnal pollinators (Erhardt 1991). The major scent component β-caryophyllene is a bicyclic sesquiterpene that sits among essential oils of various herbs (Alma et al. 2007; Calvo-Irabien et al. 2009), and its relaxing odor is often described as woody, spicy, dry, or camphoraceous, with a citrus background (Burdock 2010). Another major component, (*E*)-β-ocimene, is found in various flowers and fruits, and is experienced as a warm herbaceous odor or a woody odor with a floral scent (Burdock 2010). Like benzenoids, these terpenoids are products of sugar metabolism. Recent studies show that monoterpenes and sesquiterpenes are mainly synthesized by plastidial methylerythritol phosphate and cytosolic mevalonate (MVA) pathways, respectively (Muhlemann et al. 2014).

Although exceptions have been described, groups of plants generally use the same biosynthetic pathways to produce scents. For example,

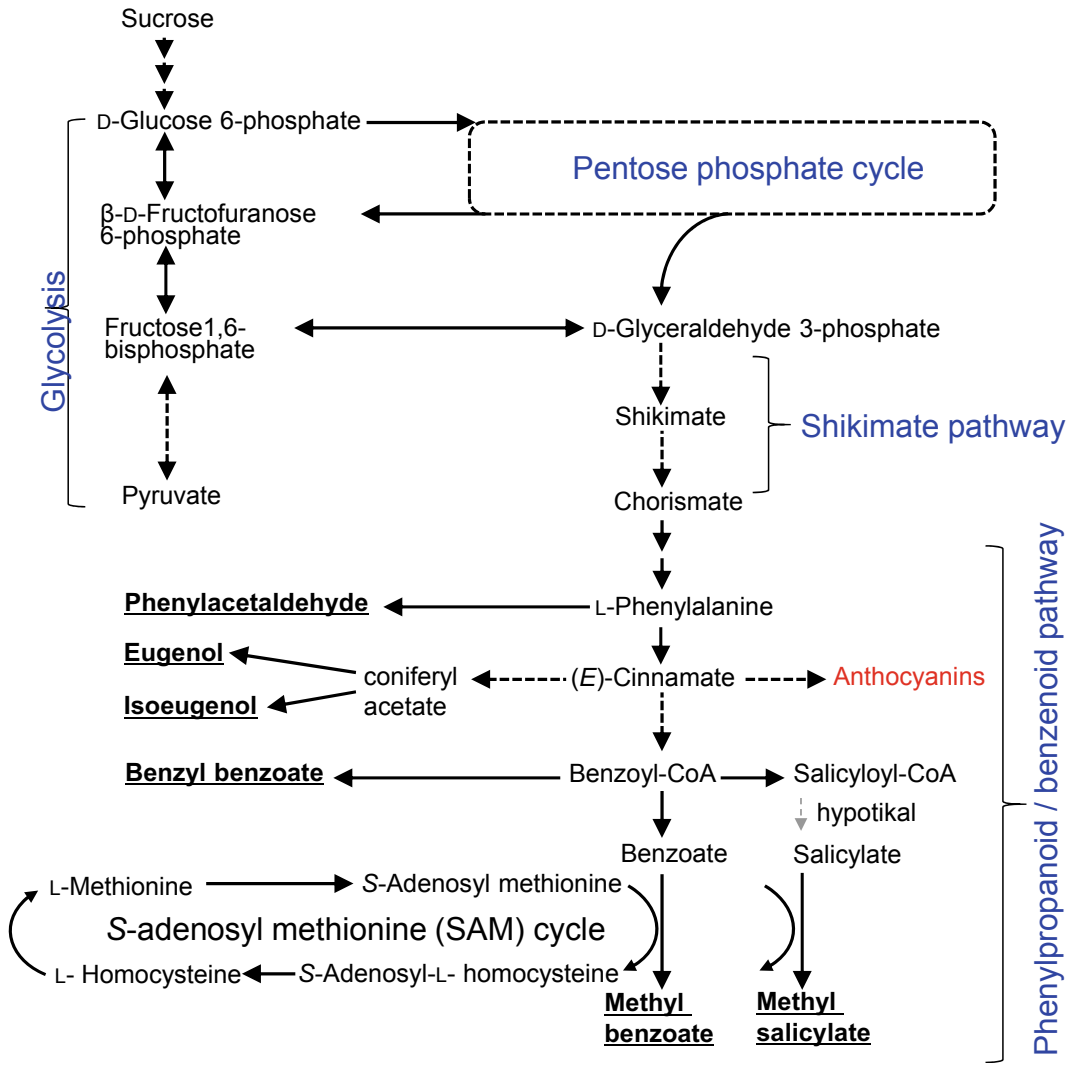

Fig. 11.1 Biosynthetic pathway for benzenoid aromatic compounds; benzenoid aromatic compounds are principal scent components of most *Dianthus* species and are synthesized in the phenylpropanoid/benzenoid biosynthetic pathway via the shikimate pathway. Solid and dotted arrows indicate single and multiple catalytic processes, respectively. Underlined and red letters indicate scent and color components, respectively. Blue letters indicate the names of biosynthesis pathways

Petunia and *Chrysanthemum* are excellent sources of benzenoids and terpenoids, respectively (Kondo et al. 2006; Sun et al. 2015). Among scent compounds of *Dianthus*, aromatic benzenoids do not always play greater roles than fatty acid derivatives and terpenoids. Hence, the primary metabolic pathways of dominant scents differ between species, leading to diverse scents of *Dianthus* flowers.

11.2.2 Carnation Scents

Marketed carnations can be red, white, yellow, pink, orange, green, purple, brown, or blue. This color diversity is likely comparable to or greater than that of wild *Dianthus* species. To clarify the diversity of carnation scents, we investigated emitted volatiles of 25 carnation cultivars for cut flowers in Japan (Kishimoto et al. 2019).

Cultivars were randomly selected and their shapes included standard and spray types. In all cultivars, the main scent components were aromatic benzenoids, as indicated by the typical scent compositions shown in Fig. 11.2 (Upper panel). The dominant scent component of 21 cultivars (84%) was methyl benzoate, which produces a fruity odor. The common cultivar Francesco was also classified into this type, but only one cultivar carried the spicy scent of eugenol. The principal scents in the other three cultivars were weak-scent benzenoids, such as benzyl benzoate and benzyl alcohol. We also collected cultivars that were deliberately considered to have characteristic scents. Their principal scents were eugenol or benzyl benzoate and no carnation cultivars had dominant fatty acid derivative or terpenoid scents (Kishimoto et al. 2019). Hence, most carnations in Japan have fruity scents derived from methyl benzoate and sometimes have the spicy scent of eugenol or the weak floral scent of benzyl benzoate.

Clery et al. (1999) compared the emitted scents from traditional carnation cultivars (registered before 1970) and modern cultivars (registered after 1994) and suggested that modern cultivars have lost the spicy fragrance of eugenol. Although their sample numbers were small, the results of this European study indicated that methyl benzoate is the major scent component of modern carnation cultivars, as described for carnations in Japan.

The diversity of carnation scents is much less than that of wild *Dianthus*. In a review of floral fragrance, Vainstein et al. (2001) suggested that modern cultivars have been unintentionally selected against fragrance, reflecting the negative correlation between longevity and fragrance. However, no positive or negative correlations between types of scent and floral longevity have been reported for carnations.

A relationship between the scents of volatile benzenoids and anthocyanin-derived color was previously reported in carnations. In their study, Zuker et al. (2002) suppressed the anthocyanin biosynthesis gene for flavanone 3-hydroxylase using antisense technology, and observed petal color changes from red to white and increased production of volatile benzenoids. Hence, color- and scent-biosynthetic pathways may compete in carnation flowers. Accordingly, biosynthetic processes for these phenotypes generally overlap in plants (Fig. 11.1), suggesting that the selection of darker colored flowers that are rich in anthocyanins will favor the loss of fragrant strains. In contrast, our transcriptome analysis showed that expression periods of anthocyanin- and scent-biosynthetic genes do not overlap at the carnation flowering stage (unpublished data). Similar pattern of gene expression was also observed in *Petunia hybrida* flowers (Verdonk et al. 2005). This strongly suggests that the processes of developing color and scent do not overlap during flower development. Thus, the phenomenon described by Zuker et al. (2002) may be unique to transgenic carnations.

In carnations, wilt (*Fusarium oxysporum* f. sp. *dianthi*)-resistant cultivars of the Mediterranean-type were rapidly distributed during the 1980s (Onozaki 2018, Yagi et al. 2014b). Perhaps methyl benzoate was the dominant scent component of this variety. In any case, why current carnation scents differ from those described in books about perfume is an interesting theme of carnation research.

Most scents of cut carnation flowers that are sold at florists are fruity and are derived from methyl benzoate. However, we found that carnation scents are lost rapidly after harvest (Kishimoto et al. 2019), with scent emissions from cut flowers decreasing by 15%–50% over the 2 days after harvest (Fig. 11.2 lower panel). In addition, we compared sensory tests for the carnation scent in 80 subjects and quantitatively investigated scent emissions over time (Kishimoto et al. 2019). For the average subject scent emissions from most cut flowers decreased to almost undetectable levels within a few days (Fig. 11.2 lower panel; Kishimoto et al. 2019). Hence, carnations at florists are almost unscented. Our transcriptome analyses of Francesco flowers showed rapid decreases in expression levels of several scent-related genes after cutting of the flowers (unpublished data), suggesting that rapid declines in scents of cut flowers are in part related to gene expression levels. Commercial

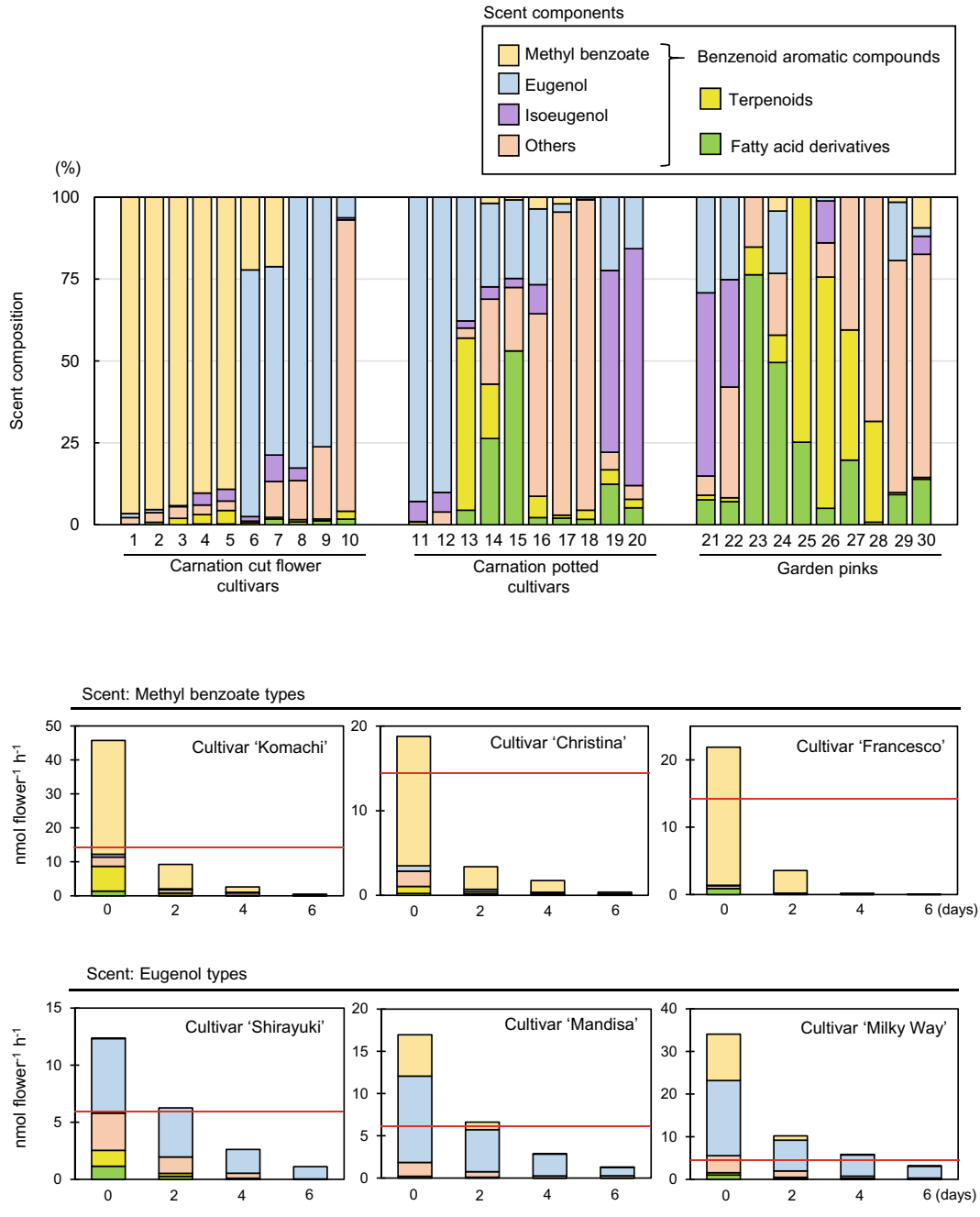
Scent components
Methyl benzoate
Eugenol
Isoeugenol
Others
Benzenoid aromatic compounds
Terpenoids
Fatty acid derivatives
(%)
Scent composition
100
75
50
25
0
1 2 3 4 5 6 7 8 9 10
Carnation cut flower cultivars
11 12 13 14 15 16 17 18 19 20
Carnation potted cultivars
21 22 23 24 25 26 27 28 29 30
Garden pinks
Scent: Methyl benzoate types
nmol flower⁻¹ h⁻¹
Cultivar 'Komachi'
Cultivar 'Christina'
Cultivar 'Francesco'
0 2 4 6 (days)
Scent: Eugenol types
Cultivar 'Shirayuki'
Cultivar 'Mandisa'
Cultivar 'Milky Way'

Fig. 11.2 Scent components of carnations and changes in relative emissions; upper panel, comparison of scent compositions between carnations and garden pinks; emitted scent compounds from flowers were collected using a dynamic headspace method with a Tenax TA column (Oka et al. 1999). The collected scent compounds were analyzed using gas chromatography–mass spectroscopy (GC–MS) and were identified and quantified using corresponding standards. The graphs show the ratios (%) of each scent component relative to total emissions (nmol flower^{-1} h^{-1}). Cultivar names: Komachi C10 (1), Francesco (2), Komachi (3), Chiquita (4), Christina (5), Mandisa (6), Milky Way (7), Shirayuki (8), Across (9), Siberia (10), Precious (11), Fosset Red (12), Rafale (13), Cheerful (14), Orfica (15), Milky Salmon Pink (16), Shantery (17), Memorial White (18), Bambino (19), Magical White (20), Raspberry Thunder (21), Coconut Sunday (22), Diana Crimson Picoty (23), Matsuzaka Nadeshiko (24), Dynasty Red (25), Supra Purple (26), Telstar Orchid (27), Telstar Burgundy (28), Kaori (29), Saint First (30). Lower panel; changes in emission quantities and compositions of scents in carnation cut flowers from the day of harvesting until 6 days later; intensities of flower scents were evaluated by 80 subjects as very scented, scented, slightly scented, or unscented. Red lines indicate boundaries at which more than 70% of subjects gave the positive evaluations "very scented" or "scented". This figure is a modification of a figure published by Kishimoto et al. (2019)

cut carnations are generally treated with ethylene inhibitors such as silver thiosulfate (STS) to suppress flower senescence. Yet, it was confirmed that this treatment was not the cause of scent reductions (Kishimoto et al. 2019).

After harvesting of carnation flowers, eugenol-type scents were shown to last longer than those of methyl benzoate (Fig. 11.2 lower panel). Accordingly, the aroma threshold of eugenol was shown to be lower than that of methyl benzoate in humans. Moreover, eugenol-type scents decreased more slowly than those of methyl benzoate (Fig. 11.2 lower panel). Nonetheless, for use as aromatic cultivars, improved persistence of scents is required. If you come across a fragrant carnation cut flower, I strongly encourage you to look up the cultivar name, because it is a very valuable experience.

Carnation scents are lost during processing into cut flowers, but remain present in potted flowers. Accordingly, no aromatic carnation cultivars for cut flowers are known, whereas several potted carnations are sold as aromatic cultivars in Japan. We investigated the scent compositions of 25 potted carnation cultivars (Kishimoto et al. 2015), as presented in Fig. 11.2 (upper panel). Sensory tests of the scents of these cultivars were also performed previously (Kishimoto et al. 2015). These studies show that some cultivars produce eugenol and isoeugenol as principal scent components and are sufficiently scented for sensual uses. Isoeugenol scents were also preferred by subjects, and 13%–32% of them identified the scent as a vanilla-like fragrance. The chemical structures of isoeugenol and vanillin, which has the fragrance of vanilla, are very similar, and isoeugenol is often used as a precursor for vanillin synthesis (Priefert et al. 2001). In fragrance-related books, the isoeugenol scent is described as spicy (Burdock 2010), but people who are accustomed to the scent of vanillin may recognize it as vanilla.

In our investigations, benzenoid aromatic compounds such as eugenol, isoeugenol, benzyl benzoate, phenylacetaldehyde, or methyl salicylate and terpenoids such as β-caryophyllene or nerolidol were detected as major scent components in the pot cultivars (Kishimoto et al. 2015). Figure 11.2 shows some of the results (upper panel). Scents based on eugenol or benzyl benzoate were also found in the cut flower cultivars but these findings were rare (Kishimoto et al. 2019). Other scent compounds were also detected in cut flower cultivars but were not the principal components (Kishimoto et al. 2019). On the other hand, methyl benzoate, which is the most principal scent of cut flower cultivars, was a minor component in pot cultivars (Kishimoto et al. 2015; Fig. 11.2 upper panel). Hence, differing scents of cut flower cultivars and pot cultivars of carnations may reflect different genetic backgrounds.

We also investigated scent emissions from horticultural *Dianthus* cultivars other than carnations, such as garden pinks (Kishimoto et al. 2015; Fig. 11.3). These flowers better resemble their wild ancestor species than carnations, and their scent components were clearly more diverse than those of carnations. Among randomly selected cultivars of garden pinks, we found

flowers with benzenoids, terpenoids, and fatty acid derivatives as principal scent components (Fig. 11.2 upper panel). These data suggest that the diversity of scents from wild species is preserved in garden pinks.

Our research shows that carnation scents are less diverse than those of wild *Dianthus*. Therefore, we explored the possibility of introducing new scents into carnations by crossing with wild species. The wild species *Dianthus superbus* var. *longicalycinus* has high terpenoids, β-caryophyllene, and β-ocimene contents (Kishimoto et al. 2011). After interspecific mating between this wild species and a carnation species lacking terpenoids, these terpenoids were acquired as principal scent components in F_1 hybrids (Kishimoto et al. 2013). Additionally, the benzenoids eugenol, benzyl alcohol, methyl *o*-anisate, and methyl salicylate were acquired by interspecific hybrids between carnations and the fragrant wild species, and their scents were perceptible (Kishimoto et al. 2013). Hence, it is possible to breed scents of various benzenoids and terpenoids into carnations.

11.2.3 Scent-Biosynthetic Genes in Current Cultivars

As described above, benzenoid aromatic compounds are the most important sources of scent in *Dianthus* (Kishimoto and Yagi (2015); Kishimoto et al. 2011, 2015, 2019), and methyl benzoate is the most common and principal scent component in current carnation cultivars for cut flowers (Kishimoto et al. 2019). The scent of Francesco is also typical of current cultivars, and about 90% of the emitted scent is due to methyl benzoate (Fig. 11.2 upper panel). In plants, methyl benzoate is commonly synthesized from benzoic acid by BAMT (Fig. 11.1). In this catalytic process, a methyl group is supplied from the *S*-adenosyl-L-methionine (SAM) cycle (Fig. 11.1). Generally, methylation of carboxyl groups reduces the boiling points of target compounds, leading to improved transpiration efficiencies. Therefore, this methylation reaction is one of the most important processes for the production of flower scents. Salicylic acid carboxyl methyltransferases (SAMTs) and jasmonic

Fig. 11.3 Garden pink flowers; scent compositions of these flowers are shown in Fig. 11.2

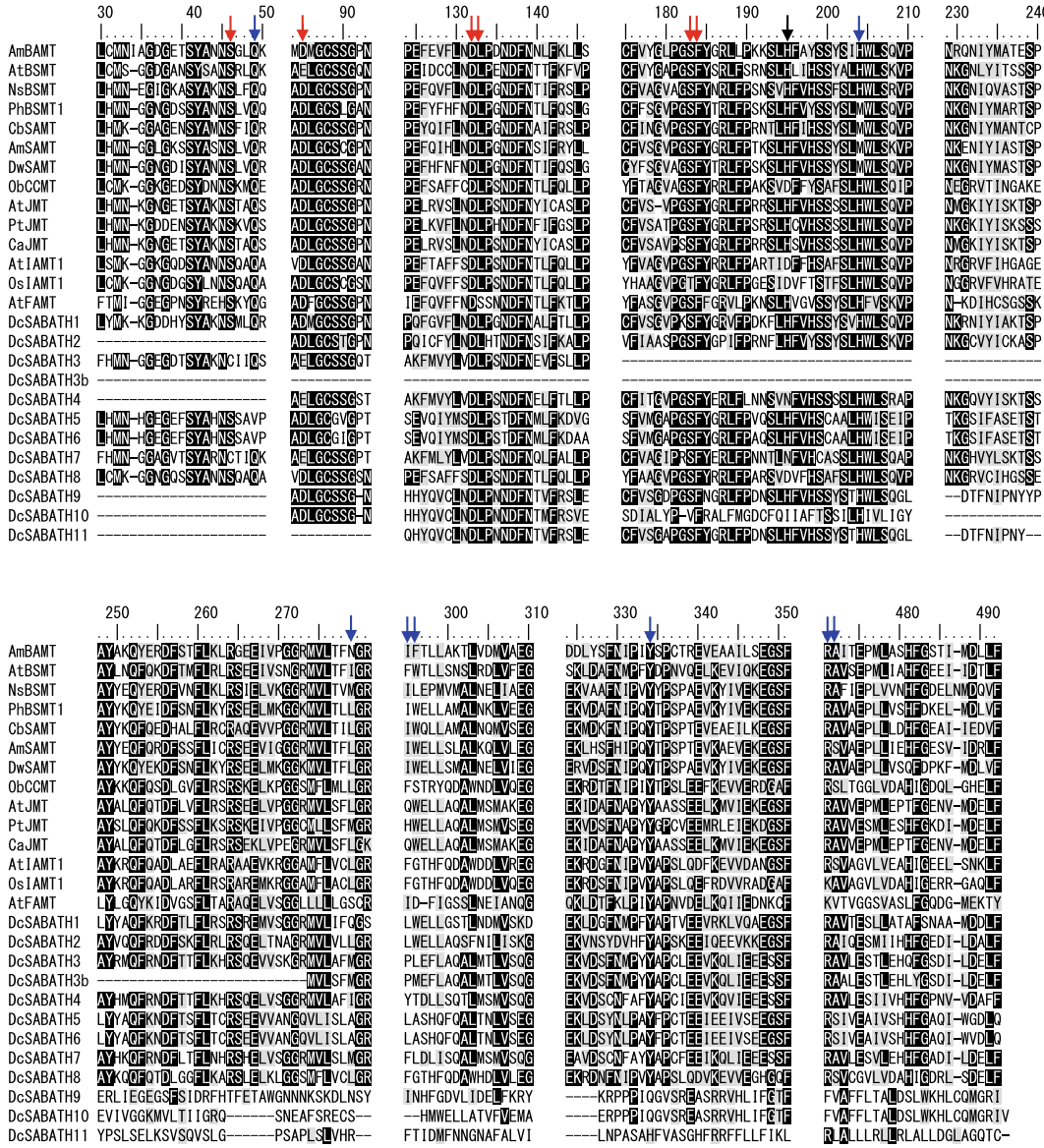

Fig. 11.4 Comparisons of common motifs between *S*-adenosyl-L-methionine-dependent benzoic acid/salicylic acid carboxyl methyltransferases (SABATHs) of *Dianthus caryophyllus* (DcSABATHs) and other plant SABATH family proteins; AmBAMT, *Antirrhinum majus* benzoic acid carboxyl methyltransferase (AAF98284); AtBSMT, *Arabidopsis thaliana* benzoic acid/salicylic acid methyltransferase (AAY25461); NsBSMT, *Nicotiana suaveolens* BSMT (CAF31508); PhBSMT1, *Petunia hybrida* BSMT1 (AAO45012); CbSAMT, *Clarkia breweri* salicylic acid methyltransferase (AAF00108); AmSAMT, *A. majus* SAMT (AAN40745); DwSAMT, *Datura wrightii* SAMT (ABO71015); ObCCMT1, *Ocimum basilicum* cinnamate/*p*-coumarate methyltransferase (ABV91100); AtJMT, *A. thaliana* jasmonic acid methyltransferase (AAG23343); PtJMT, *Populus trichocarpa* JMT (AGR50489); CaJMT, *Capsicum annuum* JMT (ABB02661); AtIAMT1, *A. thaliana* indole acetic acid methyltransferase 1 (BAD43349); OsIAMT1, *Oryza sativa* IAMT1 (ABZ04474); CaCAS1, *Coffea arabica* caffeine synthase 1 (BAC43760);CsTCS1, *Camellia sinensis* theobromine and caffeine synthase 1(BAB12278). The black arrow indicates the position related to substrate specificity for benzoic acid. Red arrows indicate *S*-adenosyl-L-methionine binding residues. Blue arrows indicate residues that interact with carboxyl moieties of salicylic acid or indole-3-acetate

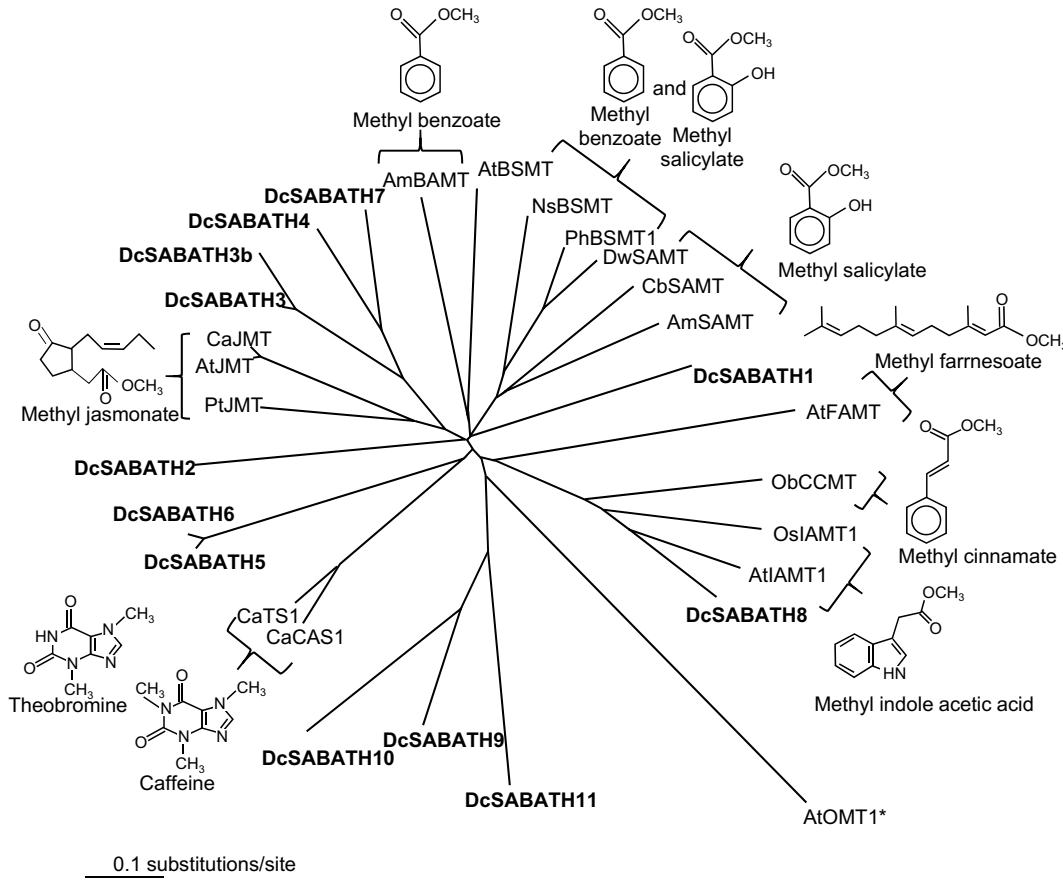

Fig. 11.5 Phylogenetic relationships between known *S*-sdenosyl-L-methionine (SAM)-dependent benzoic acid/salicylic acid carboxyl methyltransferases (SABATHs) and SABATHs from *Dianthus caryophyllus* (DcSABATHs); AmBAMT, *Antirrhinum majus* benzoic acid methyltransferase (AAF98284); AtBSMT, *Arabidopsis thaliana* benzoic acid/salicylic acid methyltransferase (AAY25461); NsBSMT, *Nicotiana suaveolens* BSMT (CAF31508); PhBSMT1, *Petunia hybrida* BSMT1 (AAO45012); CbSAMT, *Clarkia breweri* salicylic acid methyltransferase (AAF00108); AmSAMT, *A. majus* SAMT (AAN40745); DwSAMT, *Datura wrightii* SAMT (ABO71015); AtJMT, *A. thaliana* jasmonic acid methyltransferase (AAG23343); CaJMT, *Capsicum annuum* JMT (ABB02661); PtJMT, *Populus trichocarpa* JMT (AGR50489); AtIAMT1, *A. thaliana* indole acetic acid methyltransferase 1 (BAD43349); OsIAMT1, *Oryza sativa* IAMT1 (ABZ04474); ObCCMT1, *Ocimum basilicum* cinnamate/*p*-coumarate methyltransferase (ABV91100); CaCAS1, Coffea arabica caffeine synthase 1 (BAC43760); CsTCS1, *Camellia sinensis* theobromine and caffeine synthase 1 (BAB12278). **Arabidopsis thaliana O*-methyl transferase1 (AtOMT1) is not a SABATH family member. This figure is a modification of a figure published by Yagi et al. (2014a)

acid carboxyl methyltransferases (JMTs) are known as similar enzymes (Ross et al. 1999; Seo et al. 2001). These SAM-dependent methyltransferases are collectively referred to as the SABATH family (D'Auria et al. 2003) and are found only in the plant kingdom. They also lack significant sequence similarity with other methyltransferases (Wang et al. 2017). We previously identified 11 primary sequence structures (*DcSABATH1-11*) that were similar to SABATH, and these were candidate *BAMT* genes in the Francesco genome (Yagi et al. 2014a). Yet it remains unclear which DcSABATHs contribute to carnation scents. Figure 11.4 shows the amino acid sequences of DcSABATHs and known SABATHs in flowering plants. The 204th amino acid residue is notable in these SABATHs (black arrow in Fig. 11.4), because substrate specificity

for benzoic acid, a precursor of methyl benzoate, is dramatically improved by substituting the amino acid at this position with histidine (black arrow in Fig. 11.4; Barkman et al. 2007). Because many DcSABATHs retain this histidine, they are expected to synthesize methyl benzoate preferentially over other methylated volatiles. Yet about half of the known DcSABATHs lack the amino acid residues that are important for binding to SAM (red arrows in Fig. 11.4). Hence, these DcSABATHs may not function as BAMT.

In phylogenetic analyses, most DcSABATHs are dissimilar to known BAMT (Fig. 11.5), in part because known SABATHs are derived from plants other than Caryophyllales. Many members of the BAMT subfamily can methylate both salicylic acid and benzoic acid, and therefore have weak substrate specificities (Fig. 11.5; Barkman et al. 2007; Negre et al. 2003). Moreover, many DcSABATHs have retained the target site of the salicylic acid carboxyl group (blue arrows in Fig. 11.4). Comparisons of DcSABATHs, which produce almost no methyl salicylate, with SABTHs of wild *Dianthus*, which are rich in methyl salicylate, may reveal substrate specificities of the SABTH family. We believe that sequence analysis of the Francesco genome (Yagi et al. 2014a) has led the way for further research on scent biosynthesis-related genes in carnation.

References

Alma MH, Ertaş M, Nitz S et al (2007) Chemical composition and content of essential oil from the bud of cultivated Turkish clove (*Syzygium aromaticum* L.). BioResources 2:265–269

Anonis DP (1985) The application of carnation in perfumery. Flav Fragr J 1:9–15

Barkman TJ, Martins TR, Sutton E et al (2007) Positive selection for single amino acid change promotes substrate discrimination of a plant volatile-producing enzyme. Mol Biol Evol 24:1320–1329

Burdock GH (2010) Fenaroli's handbook of flavor ingredients six edition. CRC Press

Clery RA, Owen NE, Chambers SF (1999) An investigation into the scent of carnations. J Essent Oil Res 11:355–359

Calvo-Irabien LM, Yam-Puc JA, Dzib G et al (2009) Effect of postharvest drying on the composition of mexican oregano (*Lippia graveolens*) essential oil. J Herb Spice Med Plant 15:281–287

D'Auria JC, Chen F Pichersky E (2003) Recent Advances in Phytochemistry, Elsevier Science Ltd, pp 253–283

Erhardt A (1991) Pollination of *Dianthus superbus* L. Flora 185:99–106

Fukui Y, Tanaka Y, Kusumi T et al (2003) A rationale for the shift in colour towards blue in transgenic carnation flowers expressing the flavonoid 3',5'-hydroxylase gene. Phytochemistry 6:15–23

Galbally J, Galbally E (1997) Carnation and pinks for garden and greenhouse. Timber Press

Ghozland F, Fernandez X (2010) L' herbier parfumé : histoires humaines des plantes à parfum. Editions Plume De Carotte

Kishimoto K (2012) Characteristics of floral scent components in *Dianthus*. SHOKUCHO (Japan Association for Advancement of Phyto-Regulators Journal) 46:291–299 (In Japanese)

Kishimoto KI, K, Yagi M. (2015) Features of the scent of carnation cultivars for cut flowers in *Dianthus*. Horticultural Research (Supplement) 14:127 (In Japanese)

Kishimoto K, Inamoto K, Ymaguchi H et al (2019) Component analysis and sensory evaluation of scent emitted from cut carnation flowers. Bull NARO Veg & Flor Sci 3:29–40 (In Japanese with English summary)

Kishimoto K, Nakayma M, Yagi M et al (2011) Evaluation of wild *Dianthus* species as genetic resources for fragrant carnation breeding based on their floral scent composition. J Japan Soc Hort Sci 80:175–181

Kishimoto K, Taiki K, Onozaki T et al (2015) Analysis and sensory evaluation of emitted scent compounds of pot carnation flowers. Bull Natl Inst Flor Sci 15:1–13 ((In Japanese with English summary))

Kishimoto K, Yagi M, Onozaki T et al (2013) Analysis of scents emitted from flowers of interspecific hybrids between carnation and fragrant wild *Dianthus* species. J Japan Soc Hort Sci 82:145–153

Kondo M, Oyama-Okubo N, Ando T (2006) Floral scent diversity is differently expressed in emitted and endogenous components in *Petunia axillaris* lines. Ann Bot 98:1253–1259

Matsui K (2006) Green leaf volatiles: hydroperoxide lyase pathway of oxylipin metabolism. Curr Opin Plant Biol 9:274–280

Muhlemann JK, Klempien A, Dudareva N (2014) Floral volatiles: from biosynthesis to function. Plant Cell Environ 37:1936–1949

Negre F, Kish CM, Boatright J et al (2003) Regulation of methyl benzoate emission after pollination in snapdragon and petunia flowers. Plant Cell 15:2992–3006

Oka N, Ohnishi H, Hatano T et al. (1999) Aroma evolution during flower opening in *Rosa damascena* Mill. Z Naturforsch 54c:889–895

Onozaki T (2018) Dianthus. In: Van Huylenbroeck J (ed) Ornamental Crops. Springer Nature Germany, pp 349–381

Priefert H, Rabenhorst J, Steinbüchel A (2001) Biotechnological production of vanillin. Appl Microbiol Biotechnol 569:296–314

Ross JR, Nam KH, D'Auria JC et al (1999) *S*-Adenosyl-L-methionine: salicylic acid carboxyl methyltransferase, an enzyme involved in floral scent production and plant defense, represents a new class of plant methyltransferases. Arch Biochem Biophys 367:9–16

Seo HS, Song JT, Cheong JJ et al (2001) Jasmonic acid carboxyl methyltransferase: a key enzyme for jasmonate-regulated plant responses. Proc Natl Acad Sci USA 98:4788–4793

Sun H, Zhang T, Fan Q et al (2015) Identification of floral scent in chrysanthemum cultivars and wild relatives by gas chromatography-mass spectrometry. Molecules 20:5346–5359

Vainstein A, Lewinsohn E, Pichersky E, Weiss D (2001) Floral fragrance. New inroads into an old commodity. Plant Physiol 127:1383–1389

Valente LM, Savolainen V, Vargas P (2010) Unparalleled rates of species diversification in Europe. Proc Biol Sci 277:1489–1496

Verdonk JC, Haring MA, van Tunen AJ et al (2005) ODORANT1 regulates fragrance biosynthesis in petunia flowers. Plant Cell 17:1612–1624

Wang B, Wang S, Wang Z (2017) Genome-wide comprehensive analysis the molecular phylogenetic evaluation and tissue-specific expression of SABATH gene family in *Salvia miltiorrhiza*. Genes 8:365

Yagi M, Kosugi S, Hirakawa H et al (2014) Sequence analysis of the genome of carnation (*Dianthus caryophyllus* L.). DNA Res 21:231–241

Yagi M, Yamamoto T, Isobe S et al (2014) Identification of tightly linked SSR markers for flower type in carnation (*Dianthus caryophyllus* L.). Euphytica 198:175–183

Zuker A, Tzfira T, Ben-Meir H, Ovadis M, Shklarman E, Itzhaki H, Forkmann G, Martens S, Neta-Sharir I, Weiss D Vainstein A (2002) Modification of flower color and fragrance by antisense suppression of the flavanone 3-hydroxylase gene. Mol Breeed 9:33–41

12 Breeding of Interspecific Hybridization Among Carnation (*Dianthus caryophyllus* L.), *Dianthus japonicus* Thunb., and *Dianthus* × *isensis* Hirahata *et* Kitam.

Mikio Nimura

Abstract

Interspecific hybridization is one of the most important strategies used for creating variations in ornamental plants because it has the potential to combine useful traits, such as favorable morphology, disease resistance, and some environmental tolerances, of both parents that could not be achieved by crossing within a single species. Because carnation (*Dianthus caryophyllus* L.) cannot tolerate hot and humid climates (e.g., hot summers in Japan), the quality and yield of cut flowers decrease under these conditions. Therefore, for stable and quality carnation production in Japan and elsewhere, it is important to breed cultivars with heat tolerance and early flowering. Herein, two indigenous species to Japan, *Dianthus japonicus* Thunb. and *Dianthus* × *isensis* Hirahata *et* Kitam., were cross-hybridized with carnation to introduce useful traits of these two species into carnation. On reciprocal interspecific hybridization between carnation and *D. japonicus*, hybrid plants were obtained only when carnation was used as the seed parent. Although hybrid plants rarely obtained were sterile, they successfully restored fertility by producing amphidiploids through artificial chromosome-doubling treatment. When reciprocal interspecific crosses were employed between carnation and *D.* × *isensis*, fertile hybrid plants were obtained in both cross-directions. Because these two types of interspecific hybrids exhibited useful traits of the donor species, they will be efficiently used as valuable germplasm for further carnation breeding.

Abbreviations

CC	Genome constitution of *Dianthus caryophyllus* L.
JJ	Genome constitution of *Dianthus japonicus* Thunb.
II	Genome constitution of *Dianthus* × *isensis* Hirahata *et* Kitam.

M. Nimura (✉)
Aichi Agricultural Research Center, Sagamine, Yazako, Nagakute City, Aichi Prefecture 480–1193, Aichi, Japan
e-mail: mikio_nimura@pref.aichi.lg.jp

T. Onozaki and M. Yagi (eds.), *The Carnation Genome*, Compendium of Plant Genomes,
https://doi.org/10.1007/978-981-15-8261-5_12

12.1 Introduction

Carnation (*Dianthus caryophyllus* L.) is one of the major floricultural crops in Japan and worldwide. It is a member of the family Caryophyllaceae and belongs to the genus *Dianthus*. The original species of *D. caryophyllus* L. was probably native to Mediterranean areas, and most of the carnation cultivars have been bred in Europe and the USA, which have a relatively cool climate.

As a result, most cultivars do not have tolerance to hot and humid climate and tend to grow unfavorably in the hot, humid summer of Japan, which results in various disease problems and production of lower-quality cut flowers. To increase the yield and quality of cut flowers, carnation should be cultivated to produce flowers before the hot summer arrives. To circumvent these problems, and to achieve more stable carnation production in Japan, it is important to breed cultivars with both heat tolerance and early flowering traits.

In plant breeding, interspecific hybrids have been produced among various species for the creation of novel genetic variability in the crops or for introgression of agriculturally useful traits from alien species into cultivated species. However, interspecific hybrid formation between distantly related species is commonly difficult because of cross incompatibility expressed as inhibition of pollen tube growth, failure of fertilization, abortion of early hybrid embryo, production of sterile seed, and lethal hybrid formation at the seedling stage. The embryo rescue technique using in vitro culture is an excellent tool for surmounting several lethal stages. With this technique, various cultivars have been produced via wide hybridization in several ornamental crops such as lilies (Asano 1980, 1982, 1984).

Interspecific hybridization is one of the most important strategies used for producing variations in ornamental crop breeding. Interspecific hybrids have the potential to show hybrid vigor and to combine the traits that in general do not occur within a single species (Volker and Orme 1988). Moreover, interspecific or intergeneric hybrids have the enormous potential to extend not only their qualitative but also their quantitative traits, such as the type of flower, plant morphology, environmental adaptation abilities, and flower vase life. Although natural hybrids may occasionally be produced between species whose flowering time overlaps, pre- and post- fertilization barriers hinder the formation of these hybrids.

There have been several reports on interspecific hybridization in the genus *Dianthus*, such as crosses of carnation with *Dianthus superbus* L. (Kanda 1992), crosses among 22 species of *Dianthus* (Ohtsuka et al. 1995), acquisition of hybrids between carnation and *Dianthus capitatus* Bald. Ex DC. (Onozaki et al. 1998), somatic hybridization through protoplast fusion between *Dianthus chinensis* L. and *Dianthus barbatus* L. (Nakano and Mii 1993a), and between carnation and *D. chinensis* (Nakano and Mii 1993b). However, only a few trials that focus on introducing the superior traits of other *Dianthus* species into carnation have so far been conducted.

Dianthus japonicus Thunb., a perennial species native to Japan, is characterized by easy seed propagation, a fasciculate cyme with many small flowers, an upright robust stem, broad and thick evergreen foliage with a developed cuticle, and high heat tolerance (Ito et al. 1994). It is also resistant to carnation bacterial wilt (Kagito and Tsuchiya 1968). Because of these valuable characteristics, *D. japonicus* is now expected to be used as breeding material for carnation, despite the fact that it has a different morphology and ecology from carnation, as well as several characteristics—such as easy seed set, season flowering (midsummer to autumn flowering), and single type of flower—that are considered to be undesirable for carnation breeding.

Dianthus × *isensis* Hirahata *et* Kitam., one of the classical, floricultural crops in Japan, is considered to be a hybrid between *D. chinensis* L. and *D. superbus* var. *longicalycinus* (Maxim.) F.N. Williams produced in the nineteenth century (Ito et al. 1994). *D.* × *isensis* is characterized by

a unique flower shape, with curled, hung-down fimbriate petals, a narrow leaf lamina with a gray-green or bright-green color, a narrow stem nearly 30 cm in height, and a branching habit at the base of the stem. In addition, it has very early and perpetual flowering traits and is easy to reproduce via seed and vegetative propagation (Ito et al. 1994).

12.2 Carnation × *D. Japonicus*

Reciprocal interspecific crosses were carried out as 12 combinations between six lines of carnation and one line of *D. japonicus* (Nimura et al. 2003). When six lines of carnation were used as maternal parents, the interspecific hybrids were obtained only when one line of carnation, '98sp1651' was used as the seed parent, whereas seedlings obtained from other combinations yielded maternal-type progeny. One possible reason for this difference in hybrid productivity in reciprocal interspecific crosses might be that '98sp1651' has an effective genetic background for producing the hybrids. When the other carnation lines were used as maternal parents, most ovules died within 3 weeks after pollination. To rescue the abortive embryos, embryo culture was also carried out before the death of ovules in the crosses with some carnation lines as maternal parents, and the obtained putative interspecific hybrids were evaluated by morphological characters. Therefore, it is possible that the development of hybrid embryos was inhibited by some physiological factors possessed by most carnation lines used as maternal parents.

Another possible reason for the difference in hybrid production in the reciprocal interspecific crosses might be that the combination between the hybrid nuclear genome and '98sp1651' cytoplasmic genome allowed for the survival of the hybrid embryo or for the development of endosperm. In the present study, it was considered that nuclear–cytoplasmic interaction might result in the stunted development of the endosperm when *D. japonicus* was used as the maternal parent. In reciprocal interspecific crosses, direction of the crossing alters the genome composition of endosperm in the hybrid seeds because of the fusion between two genomes derived from the seed parent and one genome from the pollen parent at the double fertilization event. It is also possible that *D. japonicus* does not support the growth of hybrid embryo nutritionally when it is used as the maternal parent. In these two possible cases, it might be possible to produce interspecific hybrids by examining the timing of hybrid embryo rescue culture and/or culture medium constitution. However, if abortion of the hybrid embryo is caused by the influence of the cytoplasmic gene, it might be extremely difficult to obtain a hybrid.

The nuclear DNA content of the parental plants determined using flow cytometry were 1.48 pg in carnation and 2.57 pg in *D. japonicus*, and *D. japonicus* had about 1.7 times larger DNA content than carnation. Because the hybrid was expected to have an intermediate DNA content of the parents, the value of DNA content was used as an indicator for detecting the true intermediate hybrids. Consequently, 12 out of 25 progenies obtained from the cross of carnation line '98sp1651' with pollen of *D. japonicus* had an expected DNA content of 2.03 pg, which was intermediate to the parents. However, the DNA contents of 13 other progenies and a total of 167 progenies derived from other carnation lines used as the seed parent were 1.48 pg, which was the same as that of carnation. On the other hand, the DNA contents of six progenies obtained by culturing 2380 ovules, derived from the crosses using *D. japonicus* as a seed parent, showed the same DNA content as *D. japonicus* (Table 12.1).

Random amplified polymorphic DNA (RAPD) analysis was conducted on the putative hybrids to detect the specific marker of *D. japonicus* used as the pollen parent. All of the 12 progenies obtained from the carnation line '98sp1651,' which had already shown an intermediate DNA content of the two parental species, had specific bands from pollen parent *D. japonicus* 'HAMA 1.' These DNA fragments were not detected in the 13 progenies that had not shown the hybrid nature by flow cytometry.

In the present study, approximately half of the progenies obtained from '98sp1651' and all those

Table 12.1 Flow cytometric analysis of the DNA content of progenies in reciprocal interspecific crosses between *Dianthus caryophyllus* and *D. japonicus*

Female	Male	No. of progenies	DNA content		
			caryophyllus-like	Intermediate	*japonicus*-like
D. japonicus × *D. caryophyllus*					
HAMA1	98sp1441	4	0	0	4
	98sp1651	–	–	–	–
	98sp1960	–	–	–	–
	98spLPB	–	–	–	–
	99sp367-11	–	–	–	–
	99sp594-16	2	0	0	2
D. caryophyllus × *D. japonicus*					
98sp1441	HAMA1	104	104	0	0
98sp1651		25	13	12	0
98sp1960		3	3	0	0
98spLPB		4	4	0	0
99sp367-11		53	53	0	0
99sp594-16		3	3	0	0

obtained from the other lines of carnation used as the maternal parents showed very similar morphologies to maternal carnation plants that showed no evidence of hybrid nature by DNA analysis. However, some of the carnation-like progenies showed stunted growth or death, and others showed different color and morphology of flowers from those of the mother carnation plants. In barley (*Hordeum vulgare*), it is known that haploid is efficiently produced by crossing with *Hordeum bulbosum*, a wild relative species, because of the selective elimination of *H. bulbosum* chromosomes at the early stage of embryo development (Kasha and Kao 1970). Furthermore, it has been reported in carnation that doubled haploids were obtained by inducing pseudogamy via pollinating with X-ray-irradiated pollen (Sato et al. 2000). These results may suggest that the carnation-like progenies obtained in the present study are doubled haploid. Because cross-fertilization is general in carnation, it is possible that recessive lethal or unfavorable genes heterozygously possessed by carnation were expressed in these doubled haploids, which resulted in the death or growth depression of plants. Because progenies from '98sp1651' showed a segregation ratio of approximately 1 hybrid: 1 carnation-like plant, hybrid-type progenies were considered to be produced by the effect of a few genes that act to prevent the elimination of alien chromosomes, that is, those of *D. japonicus*. However, these possibilities need to be clarified in further studies.

All 12 interspecific hybrids obtained from the cross using '98sp1651' had an intermediate flower size between carnation and *D. japonicus* and a uniform flower color of reddish purple. The hybrids also had a *D. japonicus*-like fasciculate cymose inflorescence but had fewer flowers, like carnation. The shape of their leaves rather resembled that of carnation, but was broader. Most of the hybrids that were planted in late January flowered from June 10 to July 17. Among the 12 hybrids, 7 had double flowers and 5 showed single flowers. Although three out of five single-flowered hybrids had fully developed anthers, they did not dehisce and contained only a few pollen grains, which had an abnormal shape. When carnation or the hybrid plants were pollinated with these abnormal pollen grains, no

Fig. 12.1 Characteristics of the hybrids obtained from the cross between *D. caryophyllus* and *D. japonicus*. **a** Flowering plant of *D. caryophyllus* '98sp1651' (left), hybrid '43B' (center), and *D. japonicas* 'HAMA1' (right). **b** Flower variations in the interspecific hybrids

seed was produced. On the other hand, the remaining two single-flowered hybrids as well as seven double-flowered hybrids had no anthers (Fig. 12.1). In cutting propagation using lateral buds, all 12 hybrids showed high-rooting ability compared with carnation. All hybrids had stronger stems and showed more vigorous growth compared with carnation in the summer season.

The six progenies obtained by ovule culture of *D. japonicus* × *D. caryophyllus* grew normally and showed almost the same morphology as *D. japonicus* in terms of leaf shape, which is round, wide, and thick. These results supported those obtained on nuclear DNA contents using flow cytometry (Table 12.1).

However, the hybrids had several undesirable characters such as fewer flowers per stem and segregation of single-flowered individuals. To remove these undesirable characters, it is necessary to backcross the hybrids with carnation. By culturing more immature embryos, it might be possible to obtain more hybrids from various genotypes of carnation as the maternal parents.

It is difficult to use the hybrids obtained in this study as the pollen parent or as the seed parent for further breeding because of complete sterility. To restore fertility, it is necessary to produce an amphidiploid using artificial chromosome-doubling. After amphidiploids have been successfully produced, they will be efficiently used

for introducing desirable characters of *D. japonicus*—such as broad leaf, strong stem, heat tolerance, and disease resistance—into carnation.

12.3 Artificial Chromosome-Doubling and Fertile Amphidiploid Induction

Both greenhouse and in vitro-grown plants of one hybrid line between carnation and *D. japonicus*, '47B,' which displayed a double flower, were used for the artificial chromosome-doubling treatment with colchicine or amiprophos-methyl (APM) (Nimura et al. 2006b). Colchicine dropping treatments onto the shoot tips of the greenhouse-grown interspecific hybrid plants yielded one amphidiploid (4.7%) at a concentration of 2000 mgL^{-1} for 1 day, and two amphidiploids (6.6%) at a concentration of 1000 mgL^{-1} for 5 days. Moreover, one octoploid hybrid (4.7%) was induced via treatment with 2000 mgL^{-1} for 1 day. The survival rate of the shoot tips after the colchicine treatment ranged from 40 to 70% depending on the concentration and the duration of the treatment (Table 12.2). In general, a higher concentration and longer duration of treatment reduced the survival of shoot tips, which resulted in failure to induce shoots at the node. Moreover, a higher concentration and longer duration of treatment increased the number of mixoploid shoots consisting of diploid shoots with tetraploid or hyperploid cells as well as tetraploid ones with octoploid cells.

In vitro shaking culture of the hybrid shoots led to the production of one tetraploid (5%) via the application of APM at 5–10 mgL^{-1}. With APM treatment, the survival rate of hybrid shoots was 100% at 5 and 10 mgL^{-1} but this figure drastically reduced to 20% at 20 mgL^{-1}, whereas those with colchicine treatment were 67% at 500 mgL^{-1} and 30% at 1000 mgL^{-1}. Many mixoploids were obtained by in vitro shaking culture compared with the dropping treatment of intact plants grown in the greenhouse (Tables 12.2 and 12.3). Three months after the chromosome-doubling treatment, the plants obtained from axillary buds were classified into six types according to the ploidy level (as shown in Fig. 12.2): diploid (**a**), tetraploid (**d**), octoploid (**f**) and mixoploids (**b**, **c**, **e**). Results of the flow cytometric analysis conducted after 1 year showed that all mixoploids showing the **b** type (73 plants) and **c** type (11 plants) reverted to diploid plants. The plants considered to be tetraploid (9 plants) or mixoploid showing the **e** type pattern (4 plants) were confirmed to be tetraploid (13 plants), whereas those considered to be diploid and octoploid in the first year did not show any change in ploidy levels.

Table 12.2 Effects of colchicine dropping treatment for apical meristem on the survival rate and induction of polyploids in F1 hybrid of *Dianthus caryophyllus* × *D. japonicus*

Treatment		No. of shoots treated	No. of shoots that survived (%)[a]	DNA C-values (min – max)					
Concentration ($mg\ L^{-1}$)	Duration (days)			Diploid	Tetraploid	Octoploid	Mixoploid		
				2C-4C	4C-8C	8C-16C	2C-8C	2C-16C	4C-16C
0	1	20	20 (100)	20					
500	1	20	14 (70)	12			2		
1000	1	17	10 (59)	6			4		
2000	1	21	13 (62)	4	1	1	4	1	2
0	5	20	20 (100)	20					
500	5	28	19 (68)	7			12		
1000	5	30	14 (47)	2	2		8	2	
2000	5	32	13 (40)	2	3		5	3	

[a]Recorded at 3 months after treatment

Table 12.3 Effect of in vitro colchicine or amiprophos-methyl treatment for 24 h on the survival rate and induction of polyploids in F1 hybrid of *Dianthus caryophyllus* × *D. japonicus*

Plant materials	Treatment		No. of shoots treated	No. of shoots that survived (%)[a]	DNA C-values (min – max)					
					Diploid	Tetraploid	Octoploid	Mixoploid		
	Antimitotic agents	Concentration (mg L^{-1})			2C-4C	4C-8C	8C-16C	2C-8C	2C-16C	4C-16C
F1 hybrid '47B'	Cholchicine	0	30	30 (100)	30					
		500	30	20 (67)	12	1		7		
		1000	30	9 (39)	4			4	1	
	Amiprophos-methyl	0	20	20 (100)	20					
		5	20	20 (100)	6	1		12		1
		10	20	20 (100)	2	1		14	2	1
		20	20	4 (20)	1			1	2	
Carnation '98sp1651'	Cholchicine	0	30	30 (100)	30					
		500	30	10 (33)		2		7		1
		1000	30	8 (27)		1		5		2
	Amiprophos-methyl	0	20	20 (100)	20					
		5	20	20 (100)	11			9		
		10	20	20 (100)	3	3		10	2	2
		20	20	10 (50)	2			3	5	

[a]Recorded at 3 months after treatment

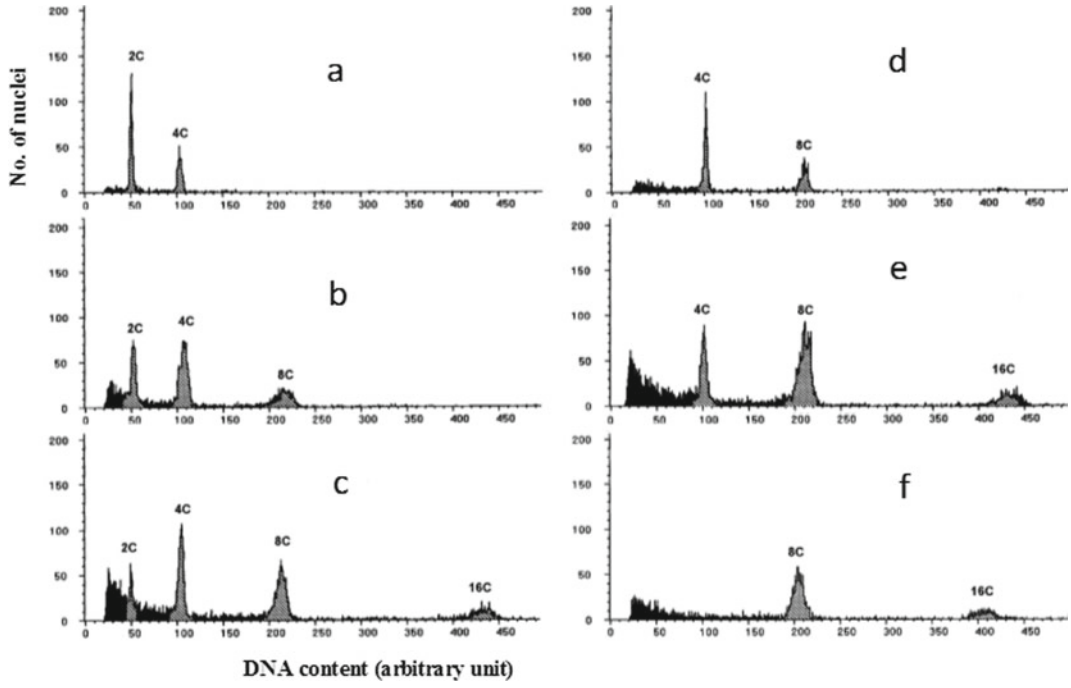

Fig. 12.2 Flow cytometric types of the plantlets obtained from artificial chromosome-doubling in F1 hybrid '47B' of *D. caryophyllus* × *D. japonicus*. **a** No treatment or 2C-4C, **b** 2C-8C, **c** 2C-16C, **d** 4C-8C, **e** 4C-16C, and **f** 8C-16C

Dropping was performed onto naked shoot tips after the removal of immature nonexpanded leaves. Although amphidiploids could be induced with this method, it was necessary to treat many plants as target material because of the low efficiency of the production of plants with chromosome-doubling, as well as to supply a large area for maintaining the treated plants. Furthermore, it takes a long time to propagate a sufficient number of amphidiploid plants necessary for testing the field performance of amphidiploids. Therefore, it was also evaluated using the in vitro treatment, which requires neither a field for cultivation nor many experimental plant materials, and the amphidiploids could be rapidly micropropagated by continuing in vitro culture.

In carnation, tetraploids have already been produced by artificial chromosome-doubling with in vitro dropping treatment of colchicine onto shoot tips of excised lateral buds (Yamaguchi and Kakei 1985). In the present study, therefore, carnation was used as control plant material in addition to the interspecific hybrid with the use of in vitro shaking culture treatment. Moreover, in addition to colchicine, APM was evaluated because it was recognized as a more efficient agent and a less toxic substance than colchicine (Sri Ramuluet al. 1991). In the present study, the use of APM was found to be effective in inducing chromosome-doubling of the hybrids at low concentrations (5 or 10 mgL^{-1}) without showing any toxic effect. The yield of the tetraploids in carnation was higher than that in the interspecific hybrid, and the maximum yield of tetraploids (25%) was obtained by in vitro shaking culture in 1/2 MS liquid medium containing APM at 10 mgL^{-1}. Therefore, it was concluded that 10 mgL^{-1} was the optimum concentration for inducing chromosome-doubling without causing damage to the explants in the APM treatment. As no apparent differences in morphological and physiological characters were observed among all 13 amphidiploid plants, it was assumed that differences in the concentration of APM did not affect the nature of the resulting amphidiploids in the present study.

A total of 13 completely nonchimeric amphidiploid plants were obtained from the interspecific hybrid '47B,' 1 year after the chromosome-doubling treatments, regardless of differences in treatment conditions. These amphidiploids showed larger values in various morphological characters—including the diameter of stems, leaves, and flowers, and the number of petals per flower—than the original diploid hybrids. Moreover, the amphidiploid hybrids produced fertile pollen grains, and their guard cells were larger than those of diploid hybrids. No significant morphological differences were found among the 13 amphidiploids. However, in mixoploids (shown in histogram **b** or **c** in Fig. 12.2), the leaves and flowers were larger than those of the diploids, although the number of petals per flower was the same as that of diploids. Moreover, the size of the guard cells of mixoploids was almost the same as that of diploids.

Progeny plants were successfully obtained by selfing of the amphidiploid hybrid. When the amphidiploid hybrid was backcrossed with the pollen of carnation and *D. japonicus*, respectively, germinable seeds were produced from the former but not from the latter. The seedlings obtained from the backcross with carnation grew normally, and were confirmed to be triploid based on flow cytometric analysis. The results of the flow cytometric analysis were also confirmed on the basis of counting of the chromosome number in the root-tip cells of the hybrid, the parental plants, and the presumed amphidiploid. Both parental species and the hybrid showed the same diploid chromosome number ($2n = 2x = 30$), whereas in the presumed amphidiploid, a tetraploid chromosome number ($2n = 4x = 60$) was obtained, as expected. Moreover, the presumed octoploid plant showed an octoploid chromosome number ($2n = 8x = 120$).

Because the amphidiploids obtained in the present study displayed several desirable characters of *D. japonicus*, such as vigorous growth in summer, an upright robust stem, and broad leaves, they are expected to be used for the breeding of carnation.

12.4 *D. Japonicus* × *Dianthus* × *isensis*

Reciprocal interspecific hybridization was conducted as four combinations between one line of *D. japonicus* and two lines of *D.* × *isensis* (Nimura et al. 2006a). At attempt was made to cross the resulting interspecific hybrid with carnation. In cross combinations using two different *D.* × *isensis* lines as maternal parents, seeds were obtained only when 'ISE 1' was crossed with the pollen of *D. japonicus*. The number of seeds obtained from each ovary varied, and the average number was 17.3, which was less than that obtained from the intraspecific cross of *D.* × *isensis* or *D. japonicas* (approximately 30–100 seeds). A total of 53 seeds were thus obtained. Among the 48 seeds (91%) that germinated, 46 seedlings grew into plants and bloomed.

Only one line of *D.* × *isensis* showed cross-compatibility with *D. japonicus*. Similarly, in interspecific hybridization between carnation and *D. japonicas* as the male donor parent, hybrids were obtained in only one out of six lines of carnation used as female parents. These results suggest that broad intraspecific variations exist in the ability to cross with other *Dianthus* species. It is therefore important to select genotypes with a wide and high ability to cross with other species of particular target species.

Flowers on one branch of each of the two hybrids that flowered in late May were larger than the others, and their stems were thicker. The anthers of these large flowers dehisced and contained many pollen grains that were found to be fertile because of their morphology and their ability to be stained with acetocarmine (Fig. 12.3).

Usually, it is difficult or impossible to use interspecific hybrids directly as breeding material because of sterility. In most cases, disturbance of normal chromosome segregation during meiosis results in the formation of gametes with an unbalanced chromosome constitution, which eventually causes sterility (van Tuyl and Lim 2003). Therefore, it is necessary to restore

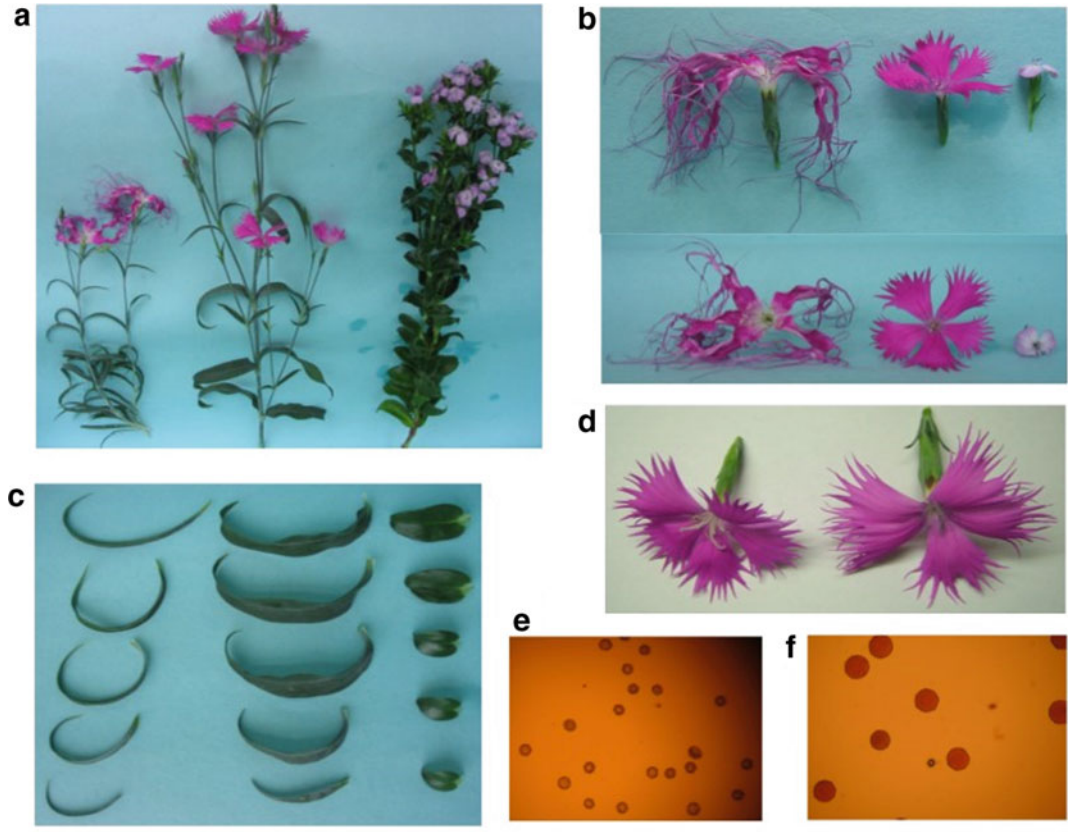

Fig. 12.3 Characteristics of hybrids obtained from a cross between *D.* × *isensis* and *D. japonicus*. **a** Flowering plants of *D.* × *isensis* (left), the hybrid (center), and *D. japonicus* (right). **b** Flowers of the parental species, *D.* × *isensis* (left), *D. japonicus* (right), and the hybrid (center). **c** Leaves of *D.* × *isensis* (left), the hybrid (center), and *D. japonicus* (right). **d** Flowers of the "normal" hybrid (left) and the amphidiploid created by natural chromosome-doubling (right). **e** Pollen of the "normal" hybrid. **f** Pollen of the amphidiploid hybrid produced by natural chromosome-doubling

fertility by inducing amphidiploidy through artificial chromosome-doubling with the use of colchicine or other chemicals with mitotic inhibitor activity once a hybrid has been successfully obtained.

In the present study, however, spontaneous chromosome-doubling was confirmed in one branch in two out of 46 interspecific hybrids of *Dianthus*, and thus it seems that this is not exactly a rare occurrence. Tetraploid branches might have arisen through the formation of a chimera in the original hybrid tissues (allodiploid), with natural chromosome-doubled tissues (amphidiploid or allotetraploid). As amphidiploids usually restore fertility because of normal chromosome pairing at meiosis, the next generation can be successfully obtained via self-pollination. As natural chromosome-doubling is considered to play an important role in plant evolution and speciation because of the acquisition of fertility, it is possible that some species with high ploidy levels in the genus *Dianthus* have evolved through natural chromosome-doubling.

D. × *isensis* is considered to be a hybrid between *D. chinensis* L. and *D. superbus* var. *longicalycinus* (Maxim.) F. N. Williams (Ito et al. 1994). Although no tetraploid has been reported in *D.* × *isensis*, there are several tetraploid varieties of *D. chinensis*, and among its interspecific hybrids is "Daimonji," a hybrid with carnation (Ito et al.

1994). In the present study, two interspecific hybrids underwent natural chromosome-doubling, and it is possible that somatic cell-doubling occurs relatively frequently in this interspecific hybrid combination. On the other hand, natural chromosome-doubling was not observed in interspecific hybrids between carnation and *D. japonicus* as the pollen parent. Moreover, tetraploids could not easily be obtained by applying artificial chromosome-doubling treatments to the interspecific hybrids obtained in this study. Therefore, it is possible that *D. chinensis* has a "genetic factor," which might exist in the line of *D.* × *isensis* used here. Because *D.* × *isensis* could have passed this "genetic factor" to its interspecific hybrids with *D. japonicus*, natural chromosome-doubling might have occurred in some of the hybrids. The relatively low frequency (2/46) of hybrids showing spontaneous chromosome-doubling suggests limited expression of the putative "genetic factor." More recent results of reverse crosses showed that all of the progeny were diploid, and no natural chromosome-doubling was observed in these plants, suggesting the possibility of maternal inheritance of this "genetic factor.".

Hybrids obtained from a cross between *D.* × *isensis* (♀) and *D. japonicus* (♂) displayed an intermediate leaf width and flower-size morphology compared with the parents. Favorable *D. japonicus* characters such as its strong stem, multiflorous character, and larger leaf width were also transmitted successfully to all 46 hybrids. Moreover, all hybrids showed more vigorous growth compared with *D.* × *isensis* during summer and were easy to propagate vegetatively by cuttings. As the hybrids had the single-flower character inherited from both parents, the tetraploid hybrid (single-flowered plant) was crossed with a double-flowered diploid carnation, which resulted in 18 progenies consisting of 14 double-flowered plants and four single-flowered ones. A similar segregation pattern was also obtained in my preliminary study on carnation, in which a cross between double- and single- flowered plants yielded both double- and single- flowered progeny.

The amphidiploids (tetraploids) obtained in the present study could produce triploid progeny via reciprocal crossing with a diploid carnation, and the triploid progeny then produced few seeds when crossed with pollen from a diploid carnation. As fewer than 20 of the seeds from such a triploid × diploid cross germinated successfully, the seedlings with aneuploidic DNA contents might be used for further breeding via recurrent backcrossing with diploid carnation. It might also be possible to obtain fertile tetraploid progeny by crossing the amphidiploids with a tetraploid carnation, which could be produced via artificial chromosome-doubling to introduce the desirable characters of *D. japonicus* (broad leaf, strong stem, and heat tolerance) and *D.* × *isensis* (early flowering and unique petal shape) into carnation.

12.5 Natural and Artificial Chromosome-Doubling in Interspecific Hybrids

Interspecific hybrids produced by the cross between species with different genomes are usually sterile because of the abnormal segregation of chromosomes at meiosis I. However, amphidiploids obtained by chromosome doubling of such an interspecific hybrid were able to have their fertility restored because of the acquisition of a complete diploid set of chromosomes derived from each ancestral species. Because interspecific hybrids obtained from carnation × *D. japonicus* were completely sterile, artificial chromosome-doubling was attempted to restore the fertility of the hybrids. Consequently, an efficient artificial doubling method was established for both interspecific hybrids and carnation, and amphidiploid of the interspecific hybrid and autotetraploid of the carnation were successfully obtained. Chromosome-doubling is known to be induced by inhibition of spindle fiber formation during mitosis, which results in the formation of cells with restituted nucleus. Spontaneous chromosome-doubling is also known to occasionally occur during growth; in fact, this was observed in two hybrid plants between *D.* × *isensis* and *D. japonicus*. In these plants, chimera with a tetraploid branch was induced by natural chromosome-doubling. Complete

amphidiploids were obtained by selfing of the fertile flowers on the tetraploid branch of the chimeric plant (Nimura et al. 2006a).

Amphidiploids are usually obtained from the interspecific hybrid via artificial chromosome-doubling of somatic cells as described above. Amphidiploids are also produced by fertilization of unreduced gametes and by interspecific crossing between the tetraploids produced from diploid parents. The occurrence of amphidiploids in nature is induced by interspecific hybridization followed by chromosome-doubling, which is known to have played an important role in the speciation and evolution of *Triticum*, *Brassica*, *Nicotiana*, and others. Triticale was obtained via interspecific hybridization between *Triticum durum* and *Secale cereale*, which is an example of artificial production of amphidiploid (Stace 1987). In Japan, a vegetable crop of *Brassica napus* "Hakuran" ($2n = 4x = 38$, AACC) was produced from the cross between *Brassica rapa* ($2n = 2x = 20$, AA) and *Brassica oleracea* ($2n = 2x = 18$, CC) (Nishi 1980). In ornamentals, interspecific hybrids have been produced in various crops such as *Lilium* (Asano 1982; van Tuyl et al. 2000, 2002), *Cyclamen* (Ishizaka and Uematsu 1994), and *Iris* (Yabuya 1985). Because the amphidiploid exhibits traits from both parents including numerous undesirable ones, it is usually necessary to cross these hybrids with some cultivars for further improvement.

12.6 Carnation × *Dianthus* × *isensis*

Reciprocal interspecific crosses were carried out in 14 combinations between one line of *D.* × *isensis* and seven lines of carnation (Nimura et al. 2006c). When the carnation was crossed with the pollen of *D.* × *isensis*, the number of seeds obtained from each ovary varied, and the average was 6.7 seeds. Of the seven carnation lines used as the maternal parent, germinated seeds were obtained from four lines. In total, 79 seedlings grew normally after germination. When *D.* × *isensis* was used as the maternal parent, most crosses produced sterile seeds, and fertile seeds were obtained from the pollination of only two carnation lines. Thus, a total of only five seedlings were obtained. In the present study, six out of 14 cross combinations in reciprocal interspecific crosses between carnation and *D.* × *isensis* yielded progeny plants.

In contrast to the results obtained with interspecific hybridization between carnation and *D. japonicus*, hybrid plants were obtained more efficiently in the present interspecific cross combination irrespective of the direction of the cross. Moreover, because the hybrids were fertile like the diploids, they can be used as breeding material without the need for artificial chromosome-doubling.

Among the 79 progenies obtained from crosses where carnation was used as the maternal parent, 30 had the expected intermediate DNA content between the parents. However, the remaining 49 progenies had the same DNA content as carnation. Meanwhile, three out of five progenies from crosses of *D.* × *isensis* as maternal parent had the expected intermediate DNA content between the parents. In the remaining two progenies, one had the triploid hybrid DNA content (2.74 pg) corresponding to the sum of two genomes of *D.* × *isensis* and one genome of carnation, whereas the other had the same content as *D.* × *isensis*.

Based on the results of flow cytometric analysis, RAPD analysis was carried out on the putative hybrids obtained from the crosses of carnation as maternal parent and three out of five progenies from the crosses of *D.* × *isensis* as maternal parent. The hybrids had specific marker bands from both parents. Moreover, these RAPD bands were also present in the presumed triploid hybrid. The results of flow cytometric analysis were further confirmed by counting chromosome numbers in the root-tip cells of the presumed diploid hybrids, the presumed triploid hybrid, and the parental plants. Both parental species and the presumed diploid hybrids had the same diploid chromosome number ($2n = 2x = 30$), whereas the presumed triploid hybrid had the expected chromosome number of triploid ($2n = 3x = 45$).

When *D.* × *isensis* was pollinated using carnation '01sp48H18A' pollen, both diploid

hybrids (IC genome) and a triploid hybrid (IIC genome) with two genomes of *D.* × *isensis* and one genome of carnation were obtained. The triploid hybrid could be formed via fertilization of an unreduced diploid egg of *D.* × *isensis* by normal carnation pollen, as observed in previous studies on *Cyclamen* (Takamura and Miyajima 1996, 1999) and *Primula* (Kato and Mii 2000).

The 30 progenies derived from crosses of carnation × *D.* × *isensis*, which showed hybrid nature by flow cytometric and RAPD analyses, had roughly the intermediate morphology of both parents, whereas the other 49 seedlings showed carnation-like morphology and looked similar to the respective line of carnation used as maternal parent. On the other hand, three out of five progenies from crosses of *D.* × *isensis* used as maternal parent showed the intermediate morphology of both parents, whereas one out of the remaining two progenies was a triploid hybrid and had single flowers with larger petals compared with diploid hybrids (Fig. 12.4). However, another one of the progenies had a *D.* × *isensis*-like morphology.

All 33 interspecific diploid hybrids thus obtained had an intermediate flower size between that of carnation and *D.* × *isensis*, and the flower colors varied from purple-pink to purple-red. In addition, the hybrids had flower petals with deep serrations, which gave a different impression from that of traditional carnations. However, the hybrids had a carnation-like inflorescence and were taller than *D.* × *isensis*. The leaf shape of the hybrids resembled that of carnation, but was more curled (Fig. 12.5a, c). The hybrids showed early flowering and bloomed from the end of May until the middle of June, whereas carnation-like progenies flowered in July or later. The hybrids were separated into two groups according to their flower types: 15 double-flowered plants and 18 single-flowered plants. The anthers of the diploid hybrids dehisced normally and contained many fertile pollen grains with a normal morphology, which were stainable with acetocarmine. Accordingly, plants of the second filial (F2) generation were obtained by selfing of the diploid hybrid flowers, which set seeds normally. Moreover, in propagation by cutting using lateral shoots, all hybrids had a high rooting ability, comparable to that of carnation, and almost all cuttings were rooted successfully.

The hybrids obtained by reciprocal crosses between carnation and *D.* × *isensis* showed an intermediate morphology between the parents in terms of leaf width and flower size. As a result, several favorable characters of *D.* × *isensis*, such as early flowering and large flowers with deep sinuses, were successfully transmitted to the hybrids. Moreover, the hybrids showed a branching habit at the base of the stem, and were easy to propagate by cutting. However, the F1 hybrids had several undesirable characters such as thinner stems and leaves compared with carnation and segregation of single-flowered individuals. By using an embryo rescue technique, it might be possible to obtain more hybrids from

Fig. 12.4 Flowers of the hybrids obtained from the cross between *D.* × *isensis* and *D. caryophyllus*. The diploid hybrid with double flower 'IC-1' (left), the diploid hybrid with single flower 'IC-2' (center), and the triploid hybrid with single flower 'IIC-1' (right). Bar = 30 mm

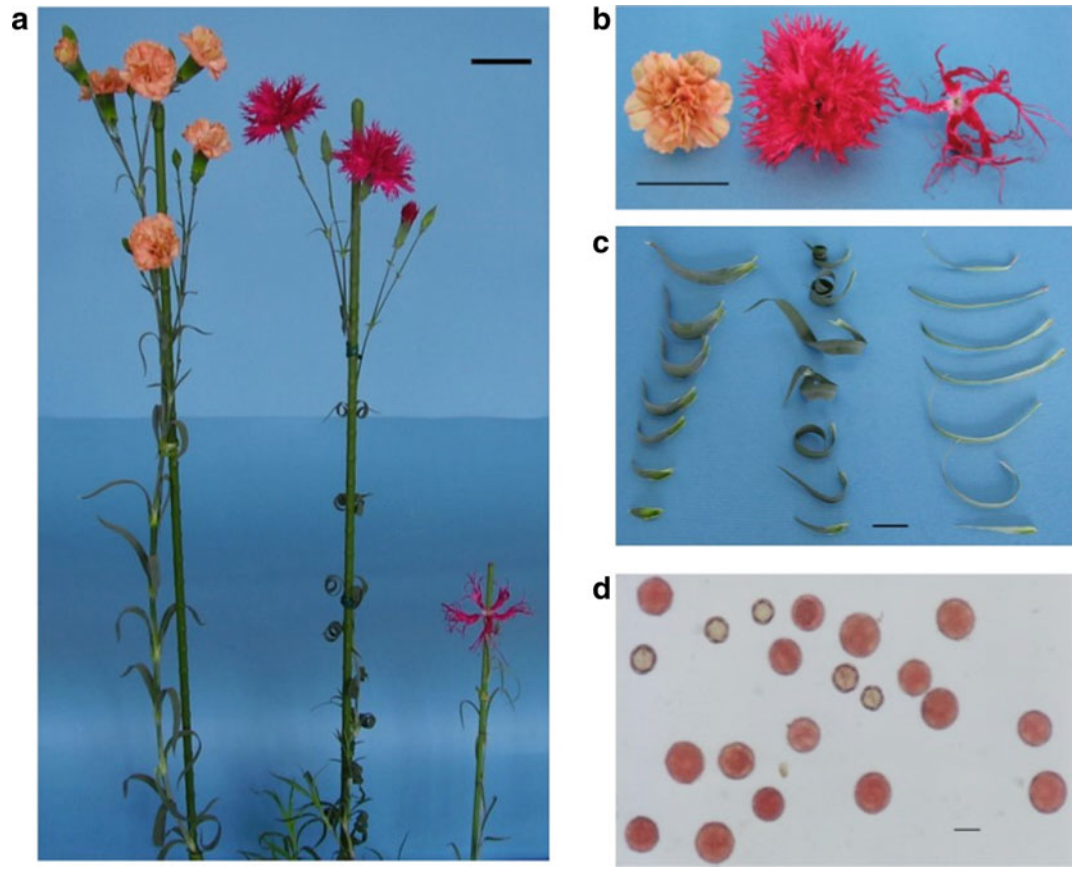

Fig. 12.5 Characteristics of the diploid hybrid obtained from the cross between *D. caryophyllus* and *D.* × *isensis*. **a** Flowering plant of *D. caryophyllus* '98sp1651' (left), the diploid hybrid 'CI-1' (center), and *D.* × *isensis* 'ISE1' (right). **b** Flowers of the parental species and the hybrid, *D. caryophyllus* '98sp1651' (left), the diploid hybrid 'CI-1' (center), and *D.* × *isensis* 'ISE1' (right). **c** Leaves of *D. caryophyllus* '98sp1651' (left), the diploid hybrid 'CI-1' (center), and *D.* × *isensis* 'ISE1' (right). **d** Fertile pollen of the interspecific diploid hybrid. Bars: **a** 50 mm; **b** 40 mm; **c** 30 mm; **d** 50 μm

various genotypes of carnation as maternal parents. In this study, only one triploid interspecific hybrid, which was an allotriploid ($2n = 3x = 45$) with two genomes of *D.* × *isensis* and one genome of carnation, was obtained. Allotriploidy has been used efficiently to produce alien monosomic addition lines through backcrossing with the diploid genome donor in various crosses such as alliums (Shigyo et al. 1996) and wheat (Taketa and Takeda 2001; Taketa 2003). Therefore, the production of alien monosomic addition lines of *D.* × *isensis* with an extra chromosome from carnation using the same procedure may also be expected.

12.7 Nondiploid Hybrid Formation by Unreduced Gametes

Triploid hybrid was produced when *D.* × *isensis* was pollinated with carnation. Assessment of relative DNA contents by flow cytometric analysis revealed that this triploid hybrid had two genomes of *D.* × *isensis* and one genome of carnation. Therefore, it is considered that *D.* × *isensis* used as maternal parent produced unreduced female gamete. Unreduced gamete formation is a consequence of failure in meiosis. Although gametes (e.g., pollen and embryo sac)

should be normally haploid, failure in meiosis sometimes occurs and produces the so-called "unreduced gametes" or "2n gametes," which have somatic chromosome number. Unreduced gametes are produced by either nonreductional segregation of homologous chromosomes at first meiotic division or nonequational segregation of sister chromatid at the second division. Moreover, in either interspecific hybrids or intergeneric hybrids, there are some cases in which a restored nucleus is produced owing to insufficient or lack of chromosome pairing at first meiotic division. There are some cases in which the restored nucleus is induced owing to failure in meiosis attributed to environmental factors such as low temperature and chemicals (Ramanna and Jacobsen 2003). If these fertile gametes are fertilized, polyploids will be formed (van Tuyl and Lim 2003; Lim et al. 2004; Hayashi et al. 2007; Nimura et al. 2008). In general, triploids are sterile and of little interest in breeding. However, in vegetatively propagated ornamentals such as *Alstroemeria* and lily, the triploid is preferred over diploids and tetraploids. Triploids have been used successfully used as parents in planned crossings to produce various ploidy levels in *Lilium* (Lim et al. 2003). An interesting feature of triploids is that it is sometimes possible to generate progenies with near-diploid (circa diploid) and near-tetraploid chromosome constitutions by making the crosses as female parents with diploid and tetraploid, respectively. The progeny with a near-diploid constitution is potentially useful for breeding at the diploid level as demonstrated in the analytical breeding of potato and other polyploid crops.

12.8 Relationship Among *D. caryophyllus*, *D. japonicus*, and *D.* × *isensis*

Relationship among the different taxa has formerly been examined through similarity of morphological traits, mode of reproduction, cross-compatibility, geographical distribution, etc. In addition, information on DNA sequence similarity or DNA mutation similarity has recently been incorporated to clarify the relationships based on the progress in molecular evolutionary research.

Results on the cross-compatibility among *D. caryophyllus*, *D. japonicus*, and *D.* × *isensis* (Fig. 12.6) show that there is some reproductive isolation between carnation and *D. japonicus* because crossing of *D. japonicus* (♀) × carnation (♂) was incompatible. Moreover, although hybrids were obtained from the opposite crossing, they were sterile and their reproductive ability was almost lost. Reproductive isolation was also found between *D. japonicus* and *D.* × *isensis*. Although interspecific hybrids were obtained in both directions of reciprocal crossing, all hybrids were sterile. In contrast, interspecific hybrids between carnation and *D.* × *isensis* were easily obtained in both directions of reciprocal crossing, and they produced F2 progeny by self-pollination. Therefore, these two species might have closely related genomes to each other and might have almost no reproductive isolation. Accordingly, interspecific hybrids between these two species will be useful for diploid-level carnation breeding.

The sequence analysis of chloroplast DNA has been effectively utilized for phylogenetic study in various taxonomic groups such as several genera that belong to Rosaceae (Potter et al. 2002; Wu et al. 2002; Shaw and Small 2004; Ohta et al. 2006) and Japanese rice populations (Ishikawa et al. 2002). The reference genome sequence of carnation was reported by Yagi et al. (2014), and the chloroplast genome was also determined by Li et al. (2019). In the future, it is expected that DNA level analysis will be enforced in clarifying relationships among the three *Dianthus* species used in the present study.

12.9 Conclusions

D. japonicus Thunb., which is a perennial species native to Japan with a high tolerance for heat, and *D.* × *isensis* Hirahata *et* Kitam., which is a hybrid species indigenous to Japan with very early flowering trait, were used to introduce these useful traits into carnation (*D. caryophyllus* L.).

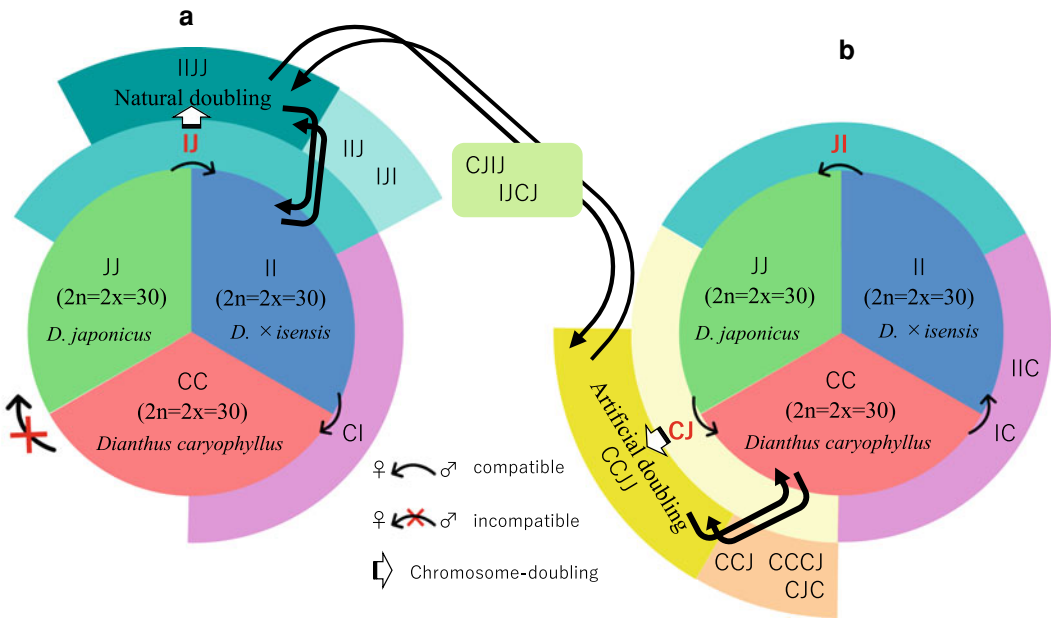

Fig. 12.6 Cross-compatibility and hybrid fertility among *D.caryophyllus*, *D. japonicus,* and *D.* × *isensis.* **a** Clockwise crosses: II was crossed with the pollen of JJ, CC was crossed with the pollen of II, and JJ was crossed with the pollen of CC. **b** Counter-clockwise crosses: JJ was crossed with the pollen of II, CC was crossed with the pollen of JJ, II was crossed with the pollen of CC

First, when reciprocal crosses were carried out between six lines of *D. caryophyllus* and *D. japonicus*, interspecific hybrids were obtained only when carnation was used as seed parent, and genotypic differences in crossability were found among carnation genotypes. Because the interspecific hybrid obtained from this cross combination was sterile, an attempt was made to establish an efficient method of artificial chromosome-doubling and thereby obtain fertile amphidiploids. Next, reciprocal interspecific crosses were carried out between *D.* × *isensis* and *D. japonicus*, which resulted in the successful production of interspecific hybrids irrespective of cross direction. Although all hybrids were sterile, fertile amphidiploids were obtained via occurrence of spontaneous chromosome-doubling in some hybrid plants produced from the cross in which *D.* × *isensis* was used as seed parent. Interspecific hybrids were also successfully obtained between *D.* × *isensis* and carnation irrespective of the cross direction. Furthermore, F2 progeny was directly obtained from the diploid hybrids without producing amphidiploids, suggesting that they might have closely related genomes to each other.

References

Asano Y (1980) Studies on crosses between distantly related species of lilies III. New hybrids obtained through embryo culture. J Japan Soc Hort Sci 47:401–414

Asano Y (1982) Chromosome association and pollen fertility in some interspecific hybrids of *Lilium*. Euphytica 31:121–128

Asano Y (1984) Fertility of a hybrid between distantly related species in *Lilium*. Cytologia 49:447–456

Hayashi M, Kato J, Ohashi H, Mii M (2007) Variation of ploidy level in inter-section hybrids obtained by reciprocal crosses between tetraploid *Primura denticulata* (2n = 4x = 44) and diploid *P. rosea* (2n = 2x = 22). J Hort Sci Biotechnol 82:5–10

Ishikawa R, Sato Y-I, Tang T, Nakamura I (2002) Different maternal origins of Japanese lowland and upland rice populations. Theor Appl Genet 104:976–980

Ishizaka H, Uematsu J (1994) Amphidiploids between *Cyclamen persicum* Mill. and *C. hederifolium* Aiton.

induced through colchicine treatment of ovules in vitro and plants. Breed Sci 44:161–166

Ito A, Takeda K, Tsukamoto Y, Tomino K (1994) Dianthus. In: Tsukamoto Y (ed) The grand dictionary of horticulture, vol 2. Shogakukan Ltd, Tokyo Japan, pp 1671–1678

Kagito N, Tsuchiya Y (1968) Outbreak and protection of carnation bacterial wilt. Shokubutsu Boeki (Japan) 22:67–70

Kanda M (1992) Ovule culture for hybridization between Carnation and species of the genus *Dianthus*. J JapanSoc Hort Sci 61(Suppl. 2):464–465

Kasha KJ, Kao KN (1970) High-frequency haploid production in barley (*Hordeum vulgare* L.). Nature 225:874–876

Kato J, Mii M (2000) Differences in ploidy levels of interspecific hybrids obtained by reciprocal crosses between *Primura sieboldii* and *P. kisoana*. Theor Appl Genet 101:690–696

Li G, Tembrock LR, Wu Z, Liu F (2019) Complete chloroplast genome of carnation (Caryophyllaceae: *Dianthus caryophyllus* L.). Mitochondrial DNA Part B 4:1463–1464

Lim KB, Ramanna MS, Jacobsen E, van Tuyl JM (2003) Evaluation of BC2 progenies derived from 3x–2x and 3x–4x crosses of *Lilium* hybrids: a GISH analysis. Theor Appl Genet 106:568–574

Lim KB, Shen TM, Rodrigo BG, Ramanna MS, Van Tuyl JM (2004) Occurrence of SDR 2N-gametes in *Lilium* hybrids. Breed Sci 54:13–18

Nakano M, Mii M (1993a) Somatic hybridization between *Dianthus chinensis* and *D. barbatus* through protoplast fusion. Theor Appl Genet 86:1–5

Nakano M, Mii M (1993b) Interspecific somatic hybridization in *Dianthus*: selection of somatic hybrids by the use of iodoacetamide inactivation and regeneration ability. Plant Sci 88:203–208

Nimura M, Kato J, Mii M, Morioka K (2003) Unilateral compatibility and genotypic difference in crossability in interspecific hybridization between *Dianthus caryophyllus* L. and *D. japonicus* Thunb. Theor Appl Genet 106:1164–1170

Nimura M, Kato J, Mii M, Katoh T (2006a) Amphidiploids produced by natural chromosome-doubling in inter-specific hybrids between *Dianthus* × *isensis* Hirahata *et* Kitam. and *D. japonicus* Thunb. J Hort Sci Biotechnol 81:72–77

Nimura M, Kato J, Horaguchi H, Mii M, Sakai K, Katoh T (2006b) Induction of fertile amphidiploids by artificial chromosome-doubling in interspecific hybrid between *Dianthus caryophyllus* L. and *D. japonicus* Thunb. Breed Sci 56:303–310

Nimura M, Kato J, Mii M (2006c) Interspecific hybrid production by reciprocal crosses between *Dianthus caryophyllus* L. and *Dianthus* × *isensis* Hirahata *et* Kitam. J Hort Sci Biotechnol 81:995–1001

Nimura M, Kato J, Mii M, Ohishi K (2008) Cross-compatibility and the polyploidy of progenies in reciprocal backcrosses between diploid carnation (*Dianthus caryophyllus* L.) and its amphidiploid with *Dianthus japonicus* Thunb. Sci Hort 115:183–189

Nishi S (1980) Differentiation of Brassica crops in Asia and the breeding of 'HAKURAN' a newly synthesized leafy vegetable. In: Tsunoda S, Hinata K, Gomez-Campo C (eds) Brassica crops and wild allies. Japanese Scientific Societies Press, Tokyo, pp 133–150

Ohta S, Osumi S, Katsuki T, Nakamura I, Yamamoto T, Sato Y (2006) Genetic characterization of flowering cherries (*Prunus* subgenus *Cerasus*) using rp116-rp114 spacer sequences of chloroplast DNA. J Japan Soc Hort Sci 75:72–78

Ohtsuka H, Horiuchi M, Inaba Z, Wakasawa H, Fukushima T (1995) Interspecific hybrids between carnation and dianthus species by using embryo culture and their characteristics. Bull Shizuoka Agric Exp Stn 40:27–38

Onozaki T, Ikeda H, Yamaguchi T, Himeno M (1998) Introduction of bacterial wilt (*Pseudomonas caryophylli*) resistance in *Dianthus* wild species to carnation. Acta Hort 454:127–132

Potter D, Gao F, Bortiri PE, Oh SH, Baggett S (2002) Phylogenetic relationships in *Rosaceae* inferred from chloroplast matK and trnL-trnF nucleotide sequence data. Plant Syst Evol 231:77–89

Ramanna MS, Jacobsen E (2003) Relevance of sexual polyploidization for crop improvement—a review. Euphytica 133:3–18

Sato S, Katoh N, Yoshida H, Iwai S, Hagimori S (2000) Production of doubled haploid plants of carnation (*Dianthus caryophyllus* L.) by pseudo fertilized ovule culture. Sci Hort 83:301–310

Shaw J, Small R (2004) Addressing the '"hardest puzzle in American pomology"' Phylogeny of Prunus sect. *Prunocerasus* (*Rosaceae*) based on seven noncoding chloroplast DNA regions. Am J Botany 91:985–996

Shigyo M, Tashiro Y, Isshiki S, Miyazaki S (1996) Establishment of a series of alien monosomic addition lines of Japanese bunching onion (*Allium fistulosum*L.) with extra chromosome from shallot (*A. cepa* L. Aggregatum group). Genes Genet Syst 71:363–371

Sri Ramulu K, Verhoeven HA, Dijkhuis P (1991) Mitotic blocking, micronucleation, and chromosome doubling by oryzalin, amiprophos-methyl, and colchicine in potato. Protoplasma 160:65–73

Stace CA (1987) Triticale: a case of nomenclatural mistreatment. Taxon 1:445–452

Takamura T, Miyajima I (1996) Cross-combination and the ploidy of progenies in crosses between diploid and tetraploid Cyclamen (*Cyclamen persicum* Mill.). J Japan Soc Hort Sci 64:883–889

Takamura T, Miyajima I (1999) Varietal and individual differences in cross-compatibility in the 2x × 4x crosses of cyclamen (*Cyclamen persicum* Mill.). J Japan Soc Hort Sci 68:55–60

Taketa S, Takeda K (2001) Production and characterization of a complete set of wheat-wild barley (*Hordeum vulgare* ssp. spontaneum) chromosome addition lines. Breed Sci 51:199–206

Taketa S (2003) Cytogenetic studies on wheat-barley intergeneric hybridization and the phylogeny of the genus *Hordeum*. Breed Res (Japan) 5:109–116

van Tuyl JM, van Dijken A, Chi HS, Lim KB, Villemoes S, van Kronenburg BCE (2000) Breakthrough in interspecific hybridization of lily. Acta Hort 508:83–88

van Tuyl JM, Maas IWGM, Lim KB (2002) Introgression in interspecific hybrids of lily. Acta Hort 570:213–218

van Tuyl JM, Lim KB (2003) Interspecific hybridization and polyploidisation as tools in ornamental plant breeding. Acta Hort 612:13–22

Volker PW, Orme RK (1988) Provenance trials of *Eucalyptus globules* and related species in Tasmania. Australian Forestry 51:257–265

Wu S, Ueda Y, He H, Nishihara S, Matsumoto S (2002) Phylogenetic analysis of Japanese *Rosa* species using matK sequences. Breed Sci 50:275–281

Yabuya T (1985) Amphidiploids between *Iris laevigata* Fisch. and *I. ensata* Thunb. induced through *in vitro* culture of embryos treated with colchicine. Japan J Breed 35:136–144

Yagi M, Kosugi S, Hirakawa H et al (2014) Sequence analysis of the genome of carnation (*Dianthus caryophyllus* L.). DNA Res 21:231–241

Yamaguchi M, Kakei M (1985) Study in polyploidy breeding of carnation. I. Tetraploid production by colchicine treatment. J Japan Soc Hort Sci 54 (Suppl. 2):354–355

Carnation (*Dianthus caryophyllus*) Cultivars Developed for Aichi Prefecture

13

Makiko Hotta

Abstract

Aichi Prefecture is the second-largest producer of carnations in Japan. At the Aichi Agricultural Research Center (AARC), nine unique cultivars have been developed with the goal of achieving brand recognition for locally cultivated spray-type carnations. In particular, the cultivar "Kane Ainou 1-go," which was developed in cooperation with the National Agriculture and Food Research Organization (NARO), has an extremely long vase life of 19.2–21.3 days and high annual yields. Furthermore, due to its hard stems, high-quality cut flowers can be obtained as early as autumn. This cultivar has desirable characteristics, such as large pink flowers and thick stems, and is an example of the outstanding qualities for which the AARC carnation breeding program strives to become known.

13.1 Introduction

Forty-two million carnation stems were produced within Aichi Prefecture in 2017, making it the second-largest producer of carnations in Japan (Ministry of Agriculture, Forestry and Fisheries Statistics, 2019). Commercial cultivars, such as the "candle series," developed by Chotaro Inagaki, the first chairman of the Aichi Flower Growers Associations' Carnation Section Breeding Club, are popular with growers. Various locations within the prefecture are becoming significant production areas, particularly Nishio City, and growers depend on the availability of high-quality cultivars.

Currently, commercial growers are not conducting their own breeding programs. However, we introduced many cultivars and lines they have grown up so far as crossing parents in 1994. In cooperation with the Aichi Flower Growers Associations' Carnation Section Breeding Club, the Aichi Agricultural Research Center (AARC) has concentrated breeding efforts in carnation cultivar development, more so than public laboratories. This focused effort has resulted in the development of highly marketable cultivars that are being registered under the Plant Variety Protection and Seed Act and cultivated throughout production areas of Aichi Prefecture.

The main cultivars are described below. All of the following flowers are "spray-type" cultivars. And all crossing parents of them were bred in the AARC.

(1) Ayers Rock

"Ayers Rock" was obtained by the crossing between "97sp150" (♀) having pale yellow-green flower, and "97sp191" (♂) having bright red flower (Nimura et al. 2002). This has double

M. Hotta (✉)
Aichi Agricultural Research Center, 1-1 Sagamine Yazako Aichi, Nagakute, Aichi, Japan
e-mail: makiko_hotta@pref.aichi.lg.jp

T. Onozaki and M. Yagi (eds.), *The Carnation Genome*, Compendium of Plant Genomes,
https://doi.org/10.1007/978-981-15-8261-5_13

middle flowers with vivid yellowish-red streak color on yellowish-pink ground color of both side of petals. After flowering, the color changes gradually and the ground color of petals become light orange after 1 week. Earliness of the flowering is a little late, but the cut flower yield is same/above the existing varieties. The spray formation is well ordered and the stem is strong enough though a little thin.

An application to register "Ayers Rock" was submitted in 2002. This variety was registered (No.13486) in 2005.

(2) First Love

"First Love" was obtained by the crossing between "99sp450-5" (♀) having vibrant purple-red flower, and "00sp99C50A" (♂) having purple-pink flower. With vibrant purple-red borders along with its white petals, this is a cultivar with beautiful colors. This cultivar has thick stems, grows well, has a sense of volume from its many florets, is of high quality, and is highly productive. Moreover, this is a mid- to late-blooming cultivar, suitable for shipping from December to May.

An application to register "First Love" was submitted in 2007. This variety was registered (No.20110) in 2010.

(3) Kane Aichi 7-go

"Kane Aichi 7-go" was obtained by the crossing between "05sp111A90A" (♀) having red flower bordered with white, and "05sp40I6A" (♂) having pale yellow-green flower bordered with vibrant purple-red (Kume et al. 2015). The flowers are a "pink-beige" caused by mixing pink with greenish-yellow, and when viewing them, the pink color in the outer petals gradually dims as the beige color grows more intense, eventually changing into greenish-yellow. This cultivar grows well on a firm stem that is difficult to break. The flowers are large, and each stem produces a relatively high number of flowers. Because the peduncles are long, this cultivar is well suited for flower arrangements using snapped-off lateral stems. This cultivar is high quality. It is a mid- to late-blooming species, and it is suitable for shipping from late November to June.

An application to register "Kane Aichi 7-go" was submitted in 2013. This variety was registered (No. 24851) in 2016.

(4) Kane Aichi 8-go

"Kane Aichi 8-go" was obtained by the crossing between "Art16" (♀) having white flower, and "Kane Aichi 5-go" (♂) having bright yellow-green flower (Hattori et al. 2011; Matsuno et al. 2015). The flowers are "yellow-green," and the stems have good extensibility, allowing sufficient plant height from the first flower. Flower diameters are large, and many flowers are produced per stem. It has an average yield, but the quality rate is somewhat high. This is a mid- to late-blooming cultivar, and it is suitable for shipping from early December to June.

An application to register "Kane Aichi 8-go" was submitted in 2014. This variety was registered (No. 25863) in 2017.

As described above, the majority of cultivars produced are mid- to late-blooming cultivars. The first mid- to late-blooming cultivars of the Aichi Prefecture cropping type are harvested from mid to late November, which allows for flowers with firmer stems to be harvested later when the temperature begins to fall.

13.2 Carnation Production, Consumer Trends, and Joint Research with NARO

The domestic volume of carnations in circulation is approximately 600 million flowers at present. However, domestic production has been steadily decreasing, with current production on equaling about half the amount produced in 1995, leading to an increase in imports of cut flowers to compensate for the reduction in domestic production (Figs. 13.1 and 13.2).

One of the causes of this decline is the domestic production off-season. Domestic carnation cultivation can be broadly broken into the "Southwest Warm District Cropping Type" production areas,

Fig.1 Original carnation cultivars of Aichi prefecture

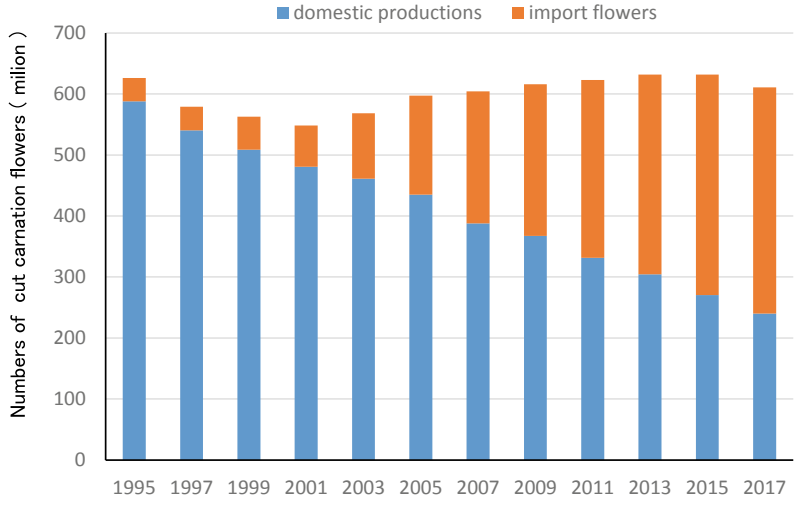

Fig.2 Changes of domestic volume of carnations in circulation in Japan

such as those found in Aichi Prefecture, Chiba Prefecture, and Hyogo Prefecture, which ship flowers roughly from November to June, and the "Cold District Cropping Type" production areas, such as those found in Nagano Prefecture and Hokkaido, which ship flowers roughly from June to October.

It is difficult to ship high-quality cut flowers with firm stems from the "Southwest Warm District Cropping Type" production areas during the "Cold District Cropping Type" production areas' fall off-season from October through early November, when shipments typically decrease. Due to climate change, years with intense, lingering summer heat are becoming more common making the development of high-quality cultivars with firm stems in October that are ready to ship during the off-season even more difficult.

Furthermore, another factor responsible for the increase in imported cut flowers is that postharvest temperature of imported cut flowers is carefully managed, maintaining the long vase life desired by consumers. Currently, people in the Japanese flower industry are searching for ways to increase vase life of domestically produced flowers as well as how to integrate flower production, distribution, and retail.

In order to respond to these issues from the perspective of cultivar development in Aichi Prefecture, the AARC conducted joint research with the NARO Institute of Floricultural Science (Currently: Institute of Vegetable and Floriculture Science, NARO), which developed the standard-type carnation cultivars "Miracle Rouge" and "Miracle Symphony" (Onozaki et al. 2006a), both of which have extremely long vase lives. The goal of the breeding program was to create a spray-type cultivar with a long vase life.

13.3 "Kane Ainou 1-go" Development and Characteristics

(1) Development History

Line 108–44, which is a standard-type cultivar developed by NARO, has a desirable long vase life (Onozaki et al. 2006b), and it was cross-bred with various spray-type carnations in 2006 and 2009. After several cycles of selfing to produce inbred lines, line 10sp1-6 was selected based on yield, vase life, and cut flower quality, which included flower color and size parameters. From 2012 onward, experimental cultivation of line 10sp1-6 was conducted in various production areas throughout Aichi Prefecture, and in February 2015, it was shipped to 11 floriculture wholesalers nationwide. The wholesalers were asked to complete a survey evaluating their marketability. Because of their large, voluminous flowers, it was rated highly and judged to have practical use as a new cultivar. In 2015, it was named "Kane Ainou 1-go," and in 2018 the variety was registered. Furthermore, the cultivation of this cultivar utilized the National Agriculture and Food Research Organization's project.

(2) Growth/Bloom Characteristics

Carnations come in many colors, but the majority of spray-type carnations produced is pink. "Kane Ainou 1-go" has light pink flowers (JHS 0402), fulfills several production requirements and has widely spreading blooms.

Quality standards for spray-type carnations are generally as follows: cut flower length of 60 cm, droop degree (the degree of droop of the tip when supported horizontally at 45 cm from the cut flower head) of 10° or less, and four or more colored flowers.

"Kane Ainou 1-go" was compared with cultivars "Chicas" and "Silhouette," which are popular in Aichi Prefecture due to their marketability as practical use cultivars. "Kane Ainou 1-go" had equal or greater stem thickness, flower diameter, and number of petals. Although "Kane Ainou 1-go" had a shorter plant height and fewer colored flowers than the control cultivars, their length and number were adequate to provide sufficient quality. The Fall 2015 survey found a droop degree of less than 10°, flower diameter of 56.5 mm, 39.7 flower petals, and 4.6 colored flowers. Furthermore, because "Kane Ainou 1-go" has few lateral stems, it can be considered a labor-saving cultivar due to its reduced need for bud picking.

This cultivar blooms in early October, and it is classified as an early bloomer. The end-of-year yield was higher than the control cultivars at more than 3.0 flowers per stock, and the annual yield (until May 8) was also higher than the control cultivars at 6.5 flowers (Table 13.1).

(3) Vase Life

Because spray carnations have multiple flowers per stem, vase life is determined via two categories: "flower head vase life," which tests the first lateral stem flower head after the peduncle is cut at 5 cm, and "cut flower vase life," in which the entire flower is tested. Flower head vase life tests were conducted three times under the same conditions from 2014 to 2015. These evaluations showed a stable vase life of 19.2–21.3 days. This vase life was three times that of 'Silhouette' and "Chicas," which had a vase life of 6.2–7.9 days. Given the common production conditions of all three cultivars, the vase life of "Kane Ainou 1-go" is a trait inherited from the 108–44 parent. The vase life of the breeding material line 108–44 is 19.1–23.6 days (at 23 °C or lower), and its long vase life was successfully bred into "Kane Ainou 1-go."

Carnations are highly sensitive to ethylene (Woltering and van Doorn 1988), and one week postharvest, flowers typically begin to wilt due to ethylene production (Halevy and Mayak 1981). "Silhouette" and "Chicas" flowers, much like other popular cultivars, wilt approximately 1 week after harvesting. The color of "Kane Ainou 1-go" will fade, but the flower petals do not wilt. Instead, the flower petals lose tension, and the edges turn brown (Fig. 13.3).

Fig.3 Kane Ainou 1-go

The cut flower vase life was tested twice in 2015, and all flowers had a shorter vase life at 14.5–15.3 days than flower head vase life. However, this was still nearly twice as long as the vase life of "Silhouette" and "Chicas" of 6.4–8.2 days. The shortened cut flower vase life of "Kane Ainou 1-go" compared with the flower head vase life was likely caused by the deterioration of the water balance (water uptake vs transpiration) in the cut flowers. The cut flower vase life and flower head vase life of the control cultivars were roughly the same, making early wilting most likely due to ethylene rather than the deterioration of the water balance.

When exposed to 10μL/L of exogenous ethylene, "Kane Ainou 1-go" responded in 3.9 h, compared with 4.0 and 4.5 h for "Silhouette" and "Chicas," respectively, indicating all it has approximately the same sensitivity as the control cultivars. In addition, ethylene production during natural senescence was below the detection limit

Table 13.1 Seasonal yield changes (number of cut flowers/plant) of carnation cultivars Kane Ainou 1-go, Silhouette, and Chicas

	2015			2016					
	October	November	December	January	February	March	April	May	Total
Kane Ainou 1-go	1.1	1.0	0.9	0.6	0.8	0.8	0.9	0.3	6.5
Silhouette	0.1	0.7	1.0	0.7	0.7	0.5	0.9	0.2	4.7
Chicas	0.0	0.4	0.9	0.8	0.7	0.5	0.9	0.3	4.6
Plants were planted on June 19, 2015									
Data were collected until May 8, 2016									

in "Kane Ainou 1-go," which is significantly lower than that of "Silhouette" and "Chicas," at 66.7 nL/g FW/h and 27.8 nL/g FW/h, respectively. Following these evaluations, it became clear that the long vase life of "Kane Ainou 1-go," much like line 108–44, is caused by its particularly low ethylene production at senescence.

In general, carnations are treated with a solution of the ethylene inhibitor silver thiosulfate (STS) at production sites in order to increase their cut flower vase life. Accordingly, we investigated the influence of STS upon vase life. The cut flower vase life of "Silhouette" and "Chicas," was extended by 4 days when treated with the ethylene inhibitor STS. However, when "Kane Ainou 1-go" was treated with STS, no significant difference was found in vase life compared with untreated areas (Fig. 13.4). The same results were found for the flower head vase life. As stated above, "Kane Ainou 1-go" produces very little ethylene during senescence, which is thought to be the reason that no significant changes were seen following the application of the ethylene inhibitor. In spite of this, the untreated "Kane Ainou 1-go" cut flower vase life was 14.5 days, which is clearly longer than the STS-treated control cultivar vase life of 10.1–11.0 days (Figs. 13.4 and 13.5).

Overall, "Kane Ainou 1-go" is a pink spray-type cultivar that produces very little ethylene at senescence and has an extremely long vase life. Its end-of-year yield is high because it blooms early, and it produces high-quality cut flowers that can be collected during the fall off-season for domestic carnation production due to its hard stems. This combination of desirable traits makes it a cultivar that can fill a gap in the production cycle and be sought after by growers and consumers alike.

13.4 Conclusion

We were able to develop "Kane Ainou 1-go," a "groundbreaking" new cultivar that is licensed by three seed and nursery companies (as of August 2019), and there are plans to distribute it across Japan. Moreover, the abundant colors of carnations available are likely sustaining their high consumption. According to the "Latest Trends in Flower Distribution," which collected data from more than 20 wholesale companies, even the high-revenue cultivars only had a market share of 3.2–3.9% in 2007, 2009, and 2011. In the future,

Fig.4 Variation in the vase life of (Left) "Kane Ainou 1-go" and (Right) "Chicas" at 0, 8, and 20 days after harvest. The flowers were held in distilled water under standard conditions (25°C, 12-hphotoperiod, 60% RH)

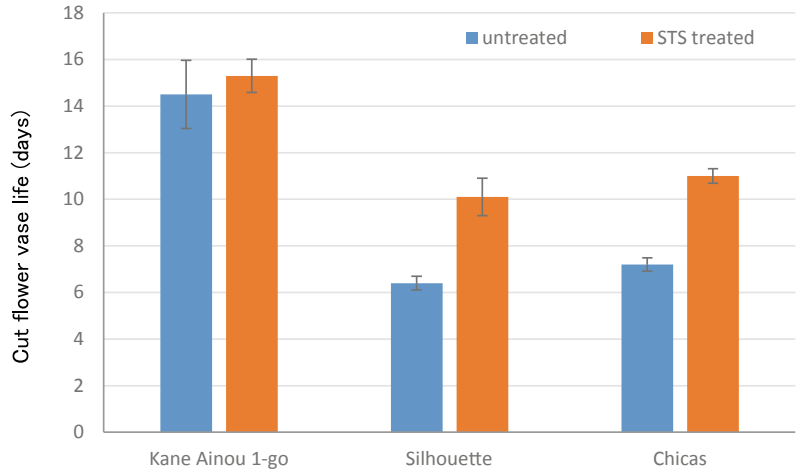

Fig.5 Effects of silver thiosulfate (STS) upon cut flower vase life measured in days of three carnation cultivars, Kane Ainou 1-go, Silhouette, and Chicas under standard conditions (25°C, 12-hphotoperiod, 60% RH). Values of vase life are the means ±SE of the data for 10 flowers

through developing cultivars in a wider variety of colors and the desirable properties, the AARC may likely 1 day reach its goal of being synonymous with high quality, spray-type carnations with a large repertoire of cultivars that will suit the needs of growers in the Aichi Prefecture.

References

Halevy AH, Mayak S (1981) Senescence and postharvest physiology of cut flowers, part 2. Hort Rev 3:59–143

Hattori H, Nimura M, Inubushi K, Okumura Y, Ohishi K (2011) Breeding of 'Kāne Aichi 4-Go' and 'Kāne Aichi 5-go': New Cultivarsof Spray Carnation. Res Bull Aichi Agric Res Ctr 43:55–63 ((In Japanese with English abstract))

Hotta M, Hattori H, Hirano T, Kume T, Okumura Y, Inubushi K, Inayoshi Y, Ninura M, Matsuno J, Onozaki T, Yagi M, Yamaguchi H, Yamaguchi N (2016) Breeding and characteristics of spray-type carnation 'Kane Ainou 1-go' with long vase life. Res Bull Aichi Agric Res Ctr 48:63–71 ((In Japanese with English abstract))

Kume T, Hattori H, Ohishi K, Hirano T, Okumura Y, Inubushi K, Inayoshi Y, Nimura M, Yamaguchi N (2015) Breeding and characteristics of spray-type carnation 'Kane Aichi 7-go.' Res Bull Aichi Agric Res Ctr 47:139–142 ((In Japanese))

Matsuno J, Hattori H, Hirano T, Ohishi K, Kume T, Inayoshi Y, Okumura Y, Inubushi K, Yamaguchi N (2015) Breeding and characteristics of spray-type carnation 'Kane Aichi 8-go' with yellow-green flower. Res Bull Aichi Agric Res Ctr 47:143–146 (In Japanese)

Nimura M, Sakai K, Morioka K (2002) Carnation New Cultiver "Carne Aichi 1-go" Having Earth-colored Flowers. Res. Bull. Aichi Agric. Res. Ctr. 34:157–161 (In Japanese with English abstract)

Onozaki T, Ikeda H, Shibata M, Tanikawa N, Yagi M, Yamaguchi T, Amano M (2006) Breeding and characteristics of carnation Norin No. 1 'Miracle Rouge' and No. 2 'Miracle Symphony' with long vase life. Bull Natl Inst Flor Sci 5:1–16 (In Japanese with English abstract)

Onozaki T, Tanikawa N, Yagi M, Ikeda H, Sumimoto K, Shibata M (2006) Breeding of carnations (Dianthus caryophyllus L.) for long vase life and rapid decrease in ethylene sensitivity of flowers after anthesis. J Japan SocHortSci 75:256–263

Woltering EJ, van Doorn WG (1988) Role of ethylene in senescence of petals-morphological and taxonomical relationships. J Exp Bot 39:1605–1616